Fine-grained Haptics: Sensing and Actuating Haptic Primary Colours *(force, vibration, and temperature)*

Alexander Co Abad

School of Mathematics, Computer Science and Engineering

Liverpool Hope University

A thesis submitted for the degree of

Doctor of Philosophy - Computer Science and Informatics

January 2023

I dedicate this thesis to
my loving wife Soledad
and to my son Lucas Alejandro.

DECLARATION

I hereby declare that the contents of this thesis are my original work and have not been submitted in whole or in part for consideration for any other degree or qualification at this or any other university. With the exception of those instances when it is clearly stated in the text, everything in this thesis is the result of my own work. Some parts of this thesis have been published in articles listed in the contributed papers section. This thesis contains fewer than 65,000 words including appendices, bibliography, footnotes, tables and equations and has fewer than 150 figures.

Alexander Co Abad
January 2023

Acknowledgements

Personal

I would like to give my heartfelt thanks to my research supervisor, Dr. Anuradha Ranasinghe, who made this work possible. Thank you for all your advice, constructive criticism, patience, and guidance throughout my Ph.D. study. I would also like to give thanks to my director of studies, Prof. David Reid, who directed the flow of my research. Thank you for all the technical insights, feedback, and suggestions. I am grateful to the thesis review panel, independent chair: Dr. Stephe Harrop, external examiner: Prof. Kaspar Althoefer, and internal examiner: Dr. Emanuele Secco for accepting to be my examiners and for all the insightful comments and suggestions. I would like to thank Prof. Raouf Naguib and Dr. Ogbonnaya Anicho, my close friends at LHU, who helped me a lot during my stay at the university. I would also like to thank Prof. Altulya Nagar, Pro-Vice-Chancellor for Research, and all the academic and management personnel of LHU who supported me during my schooling.

I would like to give special thanks to my loving wife, Soledad, and my son, Lucas Alejandro for all the love, inspiration, and support, and to my whole family for their continuous support and understanding. Your inspiration and prayers helped me a lot and sustained me this far.

Finally, I would like to thank the Almighty God for all the graces He has given me, and to the Blessed Mother Mary for her constant intercession.

Institutional

I would like to thank the Department of Science and Technology - Engineering Research and Development for Technology (DOST-ERDT) and Mme. Maillefer Study Program of De La Salle University, Manila, Philippines for the PhD scholarship given to me.

Abstract

This thesis discusses the development of a multimodal, fine-grained visual-haptic system for teleoperation and robotic applications. This system is primarily composed of two complementary components: an input device known as the HaptiTemp sensor (combines "Haptics" and "Temperature"), which is a novel thermosensitive GelSight-like sensor, and an output device, an untethered multimodal fine-grained haptic glove.

The HaptiTemp sensor is a visuotactile sensor that can sense haptic primary colours known as *force, vibration, and temperature*. It has novel switchable UV markers that can be made visible using UV LEDs. The switchable markers feature is a real novelty of the HaptiTemp because it can be used in the analysis of tactile information from gel deformation without impairing the ability to classify or recognise images. The use of switchable markers in the HaptiTemp sensor is the solution to the trade-off between marker density and capturing high-resolution images using one sensor. The HaptiTemp sensor can measure vibrations by counting the number of blobs or pulses detected per unit time using a blob detection algorithm. For the first time, temperature detection was incorporated into a GelSight-like sensor, making the HaptiTemp sensor a haptic primary colours sensor. The HaptiTemp sensor can also do rapid temperature sensing with a 643 ms response time for the 31°C to 50°C temperature range. This fast temperature response of the HaptiTemp sensor is comparable to the withdrawal reflex response in humans. This is the first time a sensor can trigger a sensory impulse that can mimic a human reflex in the robotic community. The HaptiTemp sensor can also do simultaneous temperature sensing and image classification using a machine vision camera—the OpenMV Cam H7 Plus. This capability of simultaneous sensing and image classification has not been reported or demonstrated by any tactile sensor. The HaptiTemp sensor can be used in teleoperation because it can communicate or transmit tactile analysis and image classification results using wireless communication. The HaptiTemp sensor is the closest thing to the human skin in tactile sensing, tactile pattern recognition, and rapid temperature response.

In order to feel what the HaptiTemp sensor is touching from a distance, a corresponding output device, an untethered multimodal haptic hand wearable, is developed to actuate the haptic primary colours sensed by the HaptiTemp sensor.

This wearable can communicate wirelessly and has fine-grained cutaneous feedback to feel the edges or surfaces of the tactile images captured by the HaptiTemp sensor. This untethered multimodal haptic hand wearable has gradient kinesthetic force feedback that can restrict finger movements based on the force estimated by the HaptiTemp sensor. A retractable string from an ID badge holder equipped with mini-servos that control the stiffness of the wire is attached to each fingertip to restrict finger movements. Vibrations detected by the HaptiTemp sensor can be actuated by the tapping motion of the tactile pins or by a buzzing minivibration motor. There is also a tiny annular Peltier device, or ThermoElectric Generator (TEG), with a mini-vibration motor, forming thermo-vibro feedback in the palm area that can be activated by a 'hot' or 'cold' signal from the HaptiTemp sensor. The haptic primary colours can also be embedded in a VR environment that can be actuated by the multimodal hand wearable. A VR application was developed to demonstrate rapid tactile actuation of edges, allowing the user to feel the contours of virtual objects. Collision detection scripts were embedded to activate the corresponding actuator in the multimodal haptic hand wearable whenever the tactile matrix simulator or hand avatar in VR collides with a virtual object. The TEG also gets warm or cold depending on the virtual object the participant has touched. Tests were conducted to explore virtual objects in 2D and 3D environments using Leap Motion control and a VR headset (Oculus Quest 2).

Moreover, a fine-grained cutaneous feedback was developed to feel the edges or surfaces of a tactile image, such as the tactile images captured by the HaptiTemp sensor, or actuate tactile patterns in 2D or 3D virtual objects. The prototype is like an exoskeleton glove with 16 tactile actuators (tactors) on each fingertip, 80 tactile pins in total, made from commercially available P20 Braille cells. Each tactor can be controlled individually to enable the user to feel the edges or surfaces of images, such as the high-resolution tactile images captured by the HaptiTemp sensor. This hand wearable can be used to enhance the immersive experience in a virtual reality environment. The tactors can be actuated in a tapping manner, creating a distinct form of vibration feedback as compared to the buzzing vibration produced by a mini-vibration motor. The tactile pin height can also be varied, creating a gradient of pressure on the fingertip.

Finally, the integration of the high-resolution HaptiTemp sensor, and the untethered multimodal, fine-grained haptic hand wearable is presented, forming a visuotactile system for sensing and actuating haptic primary colours. Force, vibration, and temperature sensing tests with corresponding force, vibration, and temperature actuating tests have demonstrated a unified visual-haptic system. Aside from sensing and actuating haptic primary colours, touching the edges or surfaces of the tactile images captured by the HaptiTemp sensor was carried out using the fine-grained cutaneous feedback of the haptic hand wearable.

Contents

List of Figures

List of Abbreviations

AI . . . . . Artificial Intelligence

AR . . . . . Augmented Reality

BRDF . . . . . Bidirectional Reflectance Distribution Function

BRISK . . . . Binary Robust Invariant Scalable Keypoints

CCD . . . . . Charge-Coupled Device

CNN . . . . . Convolutional Neural Network

DSP . . . . . Digital Signal Processing

ERM . . . . . Eccentric Rotating Mass

GPIO . . . . . General Purpose Input/Output

GUI . . . . . Graphical User Interface

HCI . . . . . Human-Computer Interaction

HPC . . . . . Haptic Primary Colours

HSV . . . . . Hue Saturation Value

IDE . . . . . Integrated Development Environment

IEEE . . . . . Institute of Electrical and Electronics Engineers

IoT . . . . . Internet of Things

LBP . . . . . Local Binary Patterns

LED . . . . . Light Emitting Diode

LRA . . . . . Linear Resonant Actuator

LK . . . . . Lucas-Kanade

OpenCV . . . Open source Computer Vision library

OpenMV . . . Open source Machine Vision library

OpTaCon . . . Optical Tactile Conversion

PID . . . . . Proportional Integral Derivative

PWM . . . . . Pulse Width Modulation

RANSAC . . . RANdom SAmple Consensus

RGB . . . . . Red, Green, Blue

ROI . . . . . Region Of Interest

SMA . . . . . Smart Memory Alloy

SMP . . . . . Shape Memory Polymer

SVM . . . . . Support Vector Machine

TEG . . . . . ThermoElectric Generator

TIR . . . . . Total Internal Reflection

UV . . . . . Ultra Violet

VR . . . . . Virtual Reality

XR . . . . . eXtended Reality

1 Introduction

1.1 Abstract

Psychologists estimate that 80% of the information humans obtain from the environment is through vision [1]. Even data-sets in training Artificial Intelligence (A.I.) algorithms are biased towards images or visual data. However, touch is how we first communicate as babies and it is fundamental to human well-being [2]. According to Bresciani et al., touch has a stronger influence on vision than vision on touch, and touch is more reliable than vision [3]. We often touch the things we see because we know that looks can be deceiving. The sense of touch makes as grounded with reality. In general, the term "touch" is used interchangeably with the term "haptics". In a strict sense, haptics combines two senses: touch and kinesthetics. It has also been reported that when visual perception is impaired, haptic perception is the natural recourse [4]. But if vision is not impaired, haptics can complement human vision that may enhance perception as we explore and navigate the world.

In contrast with vision, touch or haptic information comes to us through direct contact with the object of interest. Touch information can go further beyond the reach of the hand if it is combined with vision. By experience, we associate touch information, such as softness or hardness, roughness or smoothness, with the things we see based on the object's appearance and the effects of light and shadow. For

example, a shiny object is often thought as having a smooth surface. We often approximate the touch information of the things we see until we touch the object directly. In line with the combination of touch and vision, this thesis focuses on developing devices that combine vision and haptics with applications in sensing and actuating haptic primary colours *(force, vibration, and temperature)*. Like an event-based camera that mimics the functionality of a real eye, this thesis aims to create the equivalent for visuotactile system; a mechanism that can detect tactile parameters such as force, vibration, and temperature, and recognise or classify objects based on texture or shape. This visuotactile sensor combines information from both vision and touch. Moreover, this thesis aims to develop an untethered multimodal fine-grained haptic hand wearable with haptic primary colours feedback that enables the user to feel haptic primary colours and tactile parameters, such as the edges, surface, and shapes of a 2D image, or touch all the sides or contours of a 3D virtual object. Furthermore, this thesis integrates the visuotactile sensor and haptic hand wearable to form a visual-haptic system.

1.2 Background

Humans can construct representations of the world by detecting different stimuli from their environment through their sensory receptors and converting them into neural signals [5, 6]. Through the invention of the mirror, humans could see their reflections and the other things beyond their line of sight by simply changing the angle or the position of the mirror. Moreover, with the invention of optical lenses, humans have expanded their vision to see things that the naked eye cannot see. The lenses in the telescope make far objects appear nearer, while lenses in the microscope make small things bigger. Through optical lenses, humans extended the range and magnification of human vision.

With the invention of the camera and an optical display counterpart, humans could capture photos and videos that can be easily stored, processed, replicated, and transmitted to different places.

The visual image with embedded tactile and temperature information is then used to actuate a corresponding tactile display that recreates the tactile and temperature parameters detected by the sensor to enable the user to feel the image seen by the user.

Different sensors are available to sense tactile forces, vibration, and temperature, but there is no unified solution to mimic the human skin. This thesis presents a unified, monolithic sensor capable of detecting haptic primary colours *(force, vibration, and temperature)* and can do object classification using tactile images. The sensor is like a flexible mirror that projects tactile images that a camera can capture on the other side. The information can be processed in real-time, stored for future processing, or transmitted to other locations by converting tactile and temperature data into a visual domain using a digital camera. In order to feel things out of reach, a tactile image and temperature data must be used to actuate a corresponding tactile display and a ThermoElectric Generator (TEG), respectively. This thesis presents an untethered multimodal fine-grained haptic hand wearable to actuate the tactile and temperature data for the user to feel the remote object contacted by the monolithic visuotactile sensor.

The term *fine-grained* is defined in this thesis as *multi-point or multi-contact* and synonymous to the term *high-resolution*. Both the sensor and the actuator developed in this thesis can be considered as fine-grained because they are multi-point or multi-contact haptic devices.

The combination of a visuotactile sensor and an untethered multimodal fine-grained haptic wearable forms a visuotactile system that has a multitude of uses, for example, in telerobotics, telemedicine, and VR/XR.

1.2.1 Visuotactile Sensing

Visuotactile sensation and perception research dates back to the 18th century [7] and has grown into a multidisciplinary field of study by psychologists and philosophers, as well as technologists, engineers, and roboticists in the areas of haptics, robotics, and machine vision [1, 4, 7].

A visuotactile sensor can help us recognise material by the image of its texture and tactile information. The visuotactile sensor developed in this thesis is like a real fingertip that can sense shape, texture, force, vibration, and temperature. It has a machine vision camera for stand-alone tactile image recognition or classification and tactile sensing.

This visuotactile GelSight-like sensor is portable or can be fitted on a robotic manipulator. Advances in visual machine learning have relied on both hardware acceleration and distributed computation. For the same reasoning, a visuotactile sensor with an independent built-in machine learning capability is also desirable. A finger with a little mind on its own help alleviate processing bottlenecks.

The counterpart of a visuotactile sensor is a visuotactile display, or tactile-augmented visual system. This thesis uses the terms "tactile matrix actuators" and "tactile displays" interchangeably. In robotics, a visuotactile display can give the human controller a better sense of what the robot is touching. Combining vision and haptics can improve our perception of reality, and robotic sensing and manipulation. For example, a fingertip tactile display that can help the user feel the edges of an image captured by a sensor is useful in telerobotics and teleoperation.

1.2.2 Haptic Primary Colours

Like the visible light that has many colours are processed and reduced by the eye's Red, Green, and Blue (RGB) cone receptors [8], as shown in Figure 1.1, Tachi et al. theorised in 2013 that haptics, can also be reduced to three components, namely: force, vibration, and temperature. These three components were named as the Haptic Primary Colours (HPC) and they corresponds to tactile and thermal receptors in the skin [9, 10], namely: 1) Meissner's corpuscles, 2) Ruffini endings, 3) Merkel cells, 4) Pacinian corpuscles, 5) warmth receptors (free nerve endings), 6) cold receptors (free nerve endings), and 7) pain receptors (free nerve endings) [10]. The HPC theory is a general theory that combines the tactile primary colour model presented by Kajimoto et al. in 2004 [11] as shown in Figure 1.2 with the temperature sensing. In the tactile primary colours model, only three haptic

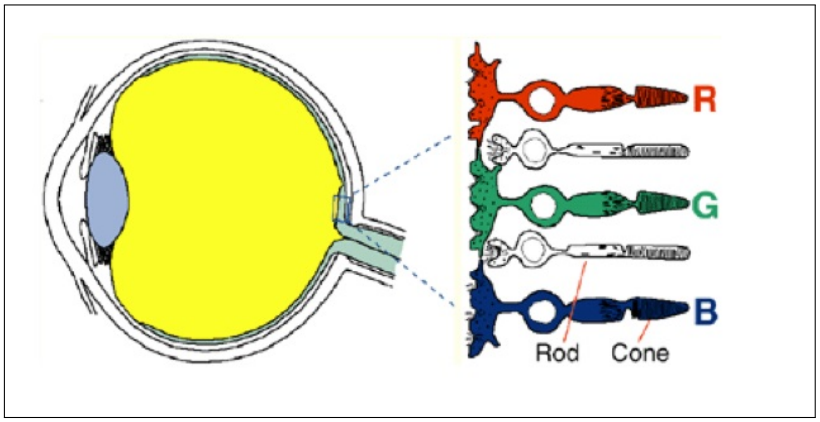

Figure 1.1: The colour receptors in the eye, known as "cones", detects red, green, and blue colours of the visible spectrum of light. [8]

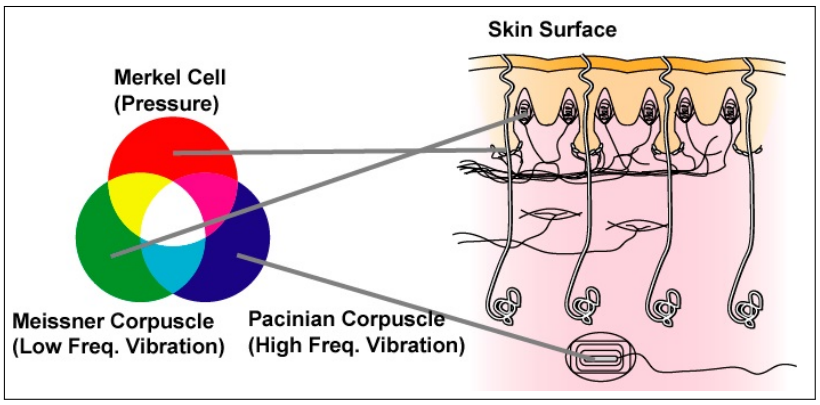

Figure 1.2: The tactile primary colours model by Kajimoto et al. [11]

.

receptors were considered, namely: Merkel cells for pressure, Meissner corpuscles for low-frequency vibrations, and Pacinian corpuscle for high-frequency vibrations, while in the haptic primary colour model, as shown in Figure 1.3, the Ruffini endings for tangential force, and the nerve endings for cold, warm, and pain were taken into account. The illustration of HPC theory in Figure 1.3 shows how the three bases in physical space (force, vibration, and temperature) are detected by the physiological mechano and thermo receptors to produce the haptic perceptions in psychological space (hardness/softness, roughness/smoothness, dryness/wetness, cold/warm, and painful/itchy).

The whole haptic primary colours system diagram is shown in Figure 1.4. At the sensor side, the contacted object's force, vibration, and temperature parameters are detected, processed, and transferred to a computer or Digital Signal Processing

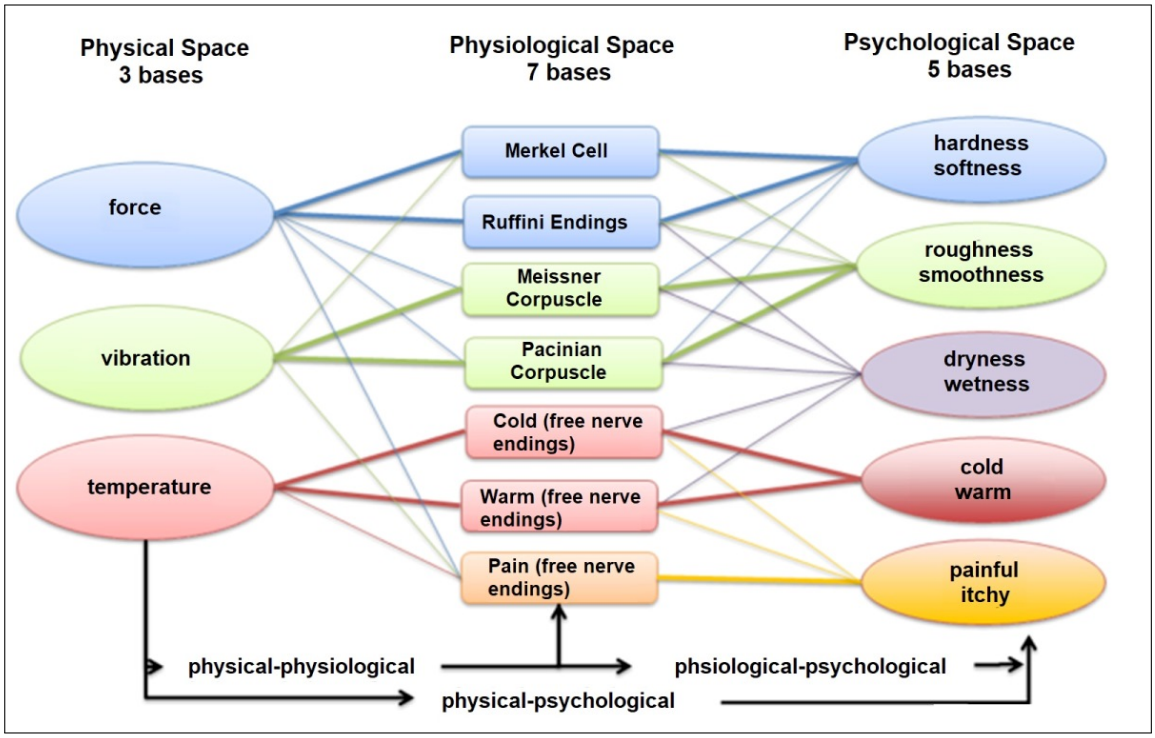

Figure 1.3: The haptic primary colour model by Tachi et al. [10]

.

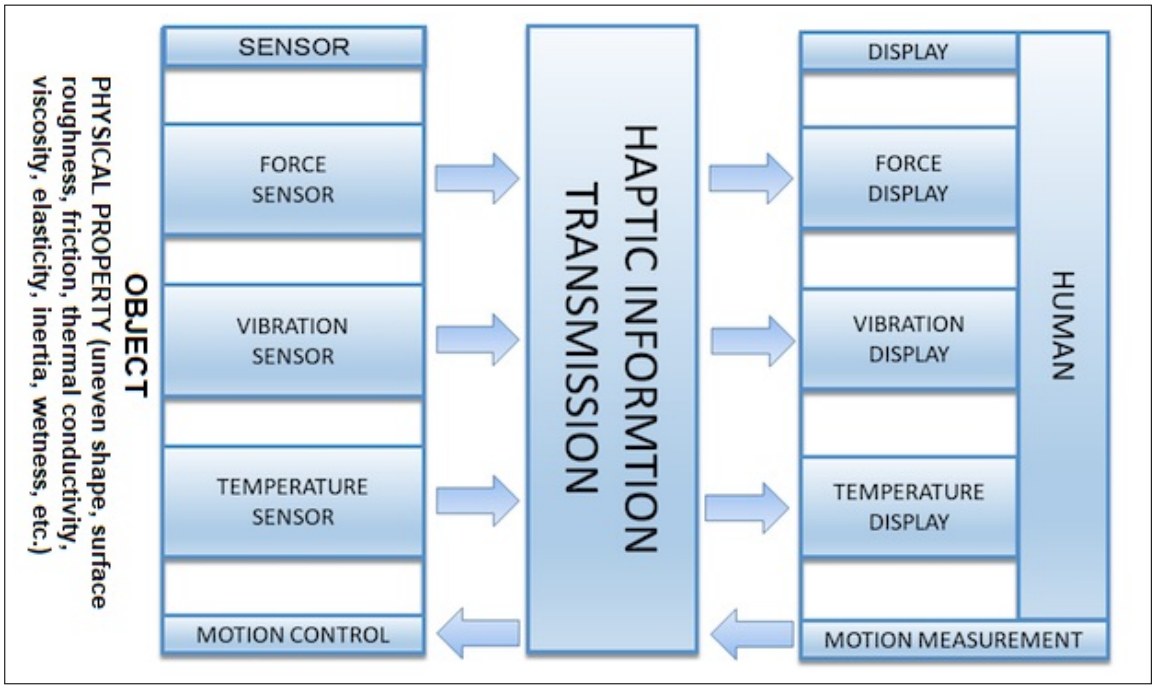

Figure 1.4: Illustration of HPC sensing, transmission, and reception.[10]

.

(DSP) device. A haptic primary colours display is needed to perceive the haptic primary colours detected by the sensor. This display actuates the force, vibration, and temperature parameters detected by the sensor so that humans can perceive the haptic parameters of the contacted object by the sensor. According to Tachi et al. [10], the measurement system, transmission, and presentation based on the principle of haptic primary colours can be illustrated as shown in Figure 1.4. They said that generally, human cutaneous receptors only sense force (skin deformation), vibration, and temperature change, which occur in contact with the physical body when the person touches an object.

1.2.3 Kinesthetic and Cutaneous Feedback

In the past two decades, researchers in psychophysics, experimental psychology, mechanical design, electronics, automation, and computer science have rapidly increased their multidisciplinary study of haptics [12].

Haptics is considered a perceptual system with cutaneous and kinesthetic subsystems, which generally involve active manual exploration. The general block diagram of haptics is shown in Figure 1.5. Vision is for spatial information, and haptics is effective at processing an object's material characteristics [12]. Sreelakshmi and Subash published a thorough analysis of haptics and its applicability to various fields in 2017. They listed haptic technology applications such as vision substitution, virtual education, haptics in the automotive industry, arts and design, medicine, holography, biometrics, and e-commerce [13]. They also listed five common haptic devices, including Novint Falcon, Haptic Knobs, Haptic Paddles, Force Feedback Gaming Joysticks, and SensAble's Omni Phantom. A more recent application-based review of haptics technology was published in 2021 by Giri et al. They classified the application of haptic devices based on construction, functionality, and significant limitations related to haptics technology [14]. They presented a list of haptic devices that are commercially available and are being used in telerobotics, telemedicine, and Virtual Reality (VR) applications.

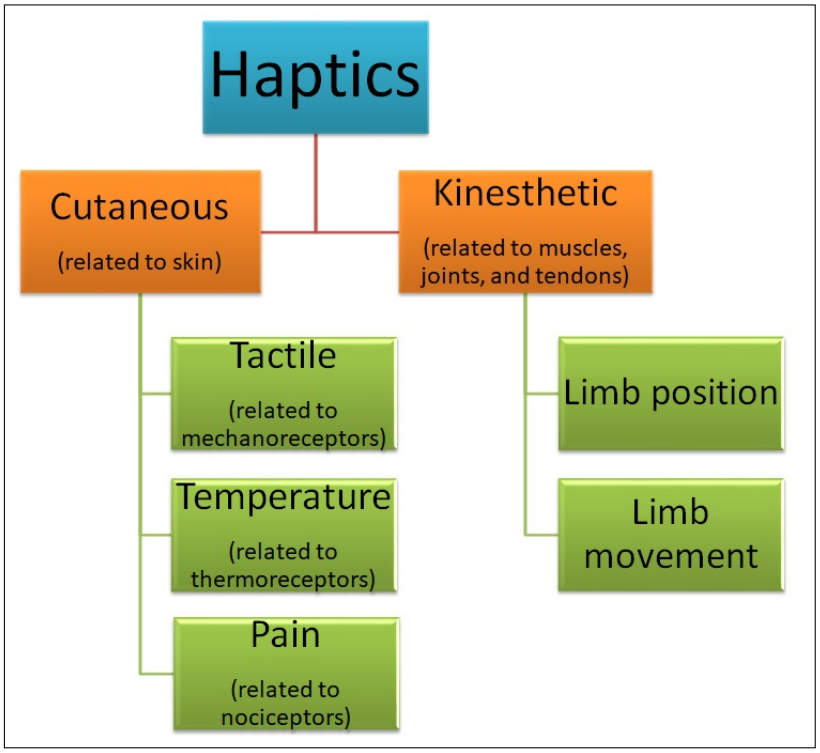

Figure 1.5: Haptics block diagram based on [12]

.

Kinesthetic and cutaneous feedback are the main topics of study in application-based haptics technology. Kinesthetic feedback, commonly known as proprioception, is the knowledge or sense of touch produced from muscle tensions with the aid of sensory receptors, according to Giri et al. [14]. The applied forces in the muscles and joints and the position and speed of adjacent body components are all factors in kinesthetic feedback [15]. On the other hand, cutaneous feedback, commonly referred to as tactile feedback, describes the data gathered from multiple mechanoreceptors on the skin [14] that allow people to distinguish an object's characteristics such as shape, edges, and texture [16].

Haptic devices can be either input (haptic sensors) or output devices (haptic actuators or haptic displays). Rapid advancements have been made in haptic device research and development to make it easier to interact with virtual reality (VR) items or remote settings and to improve the immersive experience [17, 18, 19, 20]. The success of spatial computing, which promotes cooperation, communication, and integration between humans and robots, is significantly influenced by naturalistic

interaction with a real or virtual environment [17, 20]. Comfort and wearability are key considerations when designing haptic devices. Wearability can be defined as the combination of weight, functionality, form-factor, and ergonomics [17, 18]. Kinesthetic, cutaneous, or a combination of cutaneous and kinesthetic feedback are all possible types of haptic feedback for wearables [12, 17, 18].

This thesis focuses on the development of a thermosensitive GelSight-like visuotactile sensor and untethered multimodal hand wearable with haptic primary colours *(force, vibration, and temperature)* and fine-grained cutaneous feedback that can be used in telerobotics and eXtended Reality (XR) applications, such as VR, Augmented Reality (AR), and Mixed Reality (MR).

1.3 Motivation

This thesis focuses on following research questions:

1. Can we make a unified haptic sensor capable of sensing haptic primary colours *(force, vibration, temperature)* and can capture high-resolution tactile images for texture classification?

2. Can we make an untethered multimodal hand wearable with haptic primary colours and fine-grained cutaneous feedback?

3. Can we integrate 1. and 2. wirelessly to produce a unified visual-haptic sensing and actuating system for teleoperation and virtual reality?

There are many issues in the world of image processing, such as occlusion, specularity, and shadow [21]. Some information is being lost because of these issues. For instance, textile recognition using image processing alone finds it difficult to analyse weave patterns when the cloth has designs or imprints. The design images on the fabric occlude the weave pattern needed to classify the textile. Moreover, getting a photo of a shiny metallic coin is challenging without proper lighting. The specularity or bright spot on metallic objects poses a problem for image recognition because we cannot clearly see the bright spot's details. Poor lighting condition

also creates a shadow that might be considered noise that affects image processing. Occlusion, specularity, and shadow issues are commonly encountered by people working in the world of photography, visual advertisements, and computer vision.

A low-cost, high-resolution GelSight-like visuotactile sensor with uniform lighting in capturing tactile images capable of material recognition and sensing force, vibration, and temperature is a very good solution to the issues related to occlusion, specularity, and shadow. This sensor can be used in telerobotics applications. Moreover, an untethered fine-grained hand wearable with a 4x4 fingertip tactile matrix display on each fingertip can give rich tactile feedback that may enhance our viewing and immersive experience in teleoperations and Virtual Reality (VR) applications. The combination of a high-resolution visual-haptic sensor and fine-grained haptic hand wearable could enhance our immersive experience in exploring the world around us and the virtual world.

1.4 Scope and Delimitation

The visuotactile sensor in this thesis, known as HaptiTemp, is made from a commercially available cosmetic silicone sponge painted with thermochromic pigments. By using commercially available clear silicone as the gel material for the HaptiTemp sensor, the complicated process and long hours of creating a clear silicone gel have been skipped. Though the HaptiTemp sensor is based on GelSight sensor technology, this thesis focused only on haptic sensing and tactile image classification without 3D image reconstruction. The applied force by the contacted object on the HaptiTemp sensor is displayed as variations in the vector field arrows produced by the Lucas-Kanade (LK) algorithm using the OpenCV library. There is no absolute force measurement done in this thesis.

On the other hand, the untethered fine-grained haptic wearable fingertip tactile matrix display was made from commercially available Metec P20 Braille cells controlled individually using a small microcontroller Arduino Nano 33 IoT. The haptic wearable was tested with human participants in conjunction with Leap

Motion Controller and Oculus Quest 2 VR headset, but the tactile pin movement is only in binary (fully up or fully down) motion.

1.5 Aims and Objectives

- **Aim**

This thesis aims to develop high-resolution input and output visuotactile interfaces. A low-cost GelSight-like visuotactile sensor with tactile and temperature sensing capability is developed as an input interface. This sensor has a machine vision camera for on-board tactile sensing and image recognition. On the other hand, the output visuotactile interface is an untethered, fine-grained haptic hand wearable with cutaneous and kinesthetic feedback. This hand wearable is coupled to a visual display or VR headset.

- **Objectives**

1. To develop a low-cost visuotactile GelSight-like sensor capable of sensing haptic primary colours (force, vibration, and temperature) and can do tactile image recognition or classification.

2. To develop an untethered multimodal fine-grained haptic hand wearable with haptic primary colours *(force, vibration, and temperature)* and fine-grained cutaneous feedback. This wearable can be used to feel the surfaces and edges of an image captured by the visuotactile sensor or can be used to explore the surfaces or contours of 2D and 3D virtual objects in a VR environment.

3. To integrate the low-cost thermosensitive GelSight-like visuotactile sensor and untethered multimodal hand wearable with haptic primary colours *(force, vibration, and temperature)* and fine-grained cutaneous feedback to form a visuotactile system for sensing and actuating haptic primary colours.

1.6 Contributions

The contributions of this thesis are as follows:

1. A novel unified visuotactile haptic primary colours *(force, vibration, and temperature)* sensor is developed in this thesis. This sensor is based on GelSight sensor technology and is named as the HaptiTemp sensor. A unified stand-alone solution is presented in this thesis using a machine vision camera OpenMV Cam H7 Plus for onboard tactile image recognition. Using the WiFi module connected to the HaptiTemp sensor's machine vision camera, the whole sensor can send tactile images, real-time videos, and real-time data wirelessly. The HaptiTemp sensor can do simultaneous temperature sensing and image classification. This novel capability has not been reported in any literature.

2. The HaptiTemp sensor has a novel switchable UltraViolet (UV) markers in the reflective coating helped to create a unified visuotactile sensor that can be used for tactile image recognition and tactile forces analysis using one elastomeric slab. The UV markers can be turned on using UV LEDs during tactile forces analysis because these UV markers can be clearly tracked using an optical flow algorithm and vector arrows to visualise slip, shear, and torsion inferred from gel deformation. The UV markers can be made invisible by turning off the UV LEDs when doing tactile image recognition. UV markers mitigate the negative effects of permanent markers that may hide some important image features that might be helpful for object classification through image processing, especially if these markers are bigger than the image features.

3. The HaptiTemp sensor has a novel thermosensitive reflective layer that can detect temperature and capture high-resolution tactile images—the first of its kind in any GelSight-like sensor. The HaptiTemp sensor has a similar structure as the GelSight sensor, but the reflective layer is made from different layers of thermochromic pigments with different colours and temperature

thresholds. This thermosensitive reflective coating on top of the UV markers makes it possible for the GelSight-like sensor to detect not only force and vibration but also temperature.

4. The HaptiTemp sensor can rapidly detect temperature change (19°C/s). A response time of 643 ms for the cold-to-hot and hot-to-cold that covers 31°C to 50°C was recorded. This is unique in providing a system that parallels the withdrawal reflex of the human autonomic system to extreme heat. This is the first time a sensor can trigger a sensory impulse like a withdrawal reflex of humans in the robotic community.

5. The development of an untethered fine-grained exoskeleton haptic hand wearable consists of five 4x4 miniaturised fingertip actuators, 80 in total, to convey cutaneous feedback. The prototype is portable, modular, and can be wirelessly connected using classic Bluetooth or WiFi. The components for the prototype are commercially available, and the software application was developed using open-source software. The wearable haptic device has a maximum power consumption of 830 mW and a total weight of 204 g. The prototype can be used to scan a binary image or detect the edges of an image by using the Canny edge detection algorithm. Moreover, it can be fed with predetermined patterns such as the Braille patterns or tapping patterns. This would be useful to enhance multimodal perception in minimally invasive surgeries. Since the current trend focuses on kinesthetic feedback studies, the wearable would add more subtle information to the surgeon, similar to open surgeries.

6. The untethered fine-grained exoskeleton haptic hand wearable was tested with human participants and can be integrated with hand tracking devices such as Leap Motion Controller and Oculus Quest 2 VR headset to scan and feel the contours of a 2D or 3D VR object. Participants felt basic texture information such as a sphere, edge, and corner of the cube on the 3D screen when they wore the Oculus Quest 2 VR headset.

7. An untethered multimodal haptic hand wearable was also developed with force, vibration, and temperature feedback. It is made from low-cost and commercial off-the-shelf components. A 26 mm annular Peltier element with a 10 mm hole is coupled to an 8 mm mini disc vibration motor, forming thermo-vibrotactile feedback for the user. All the other fingertips have an 8 mm disc vibration motor strapped on them using Velcro. Moreover, kinesthetic feedback extracted from a retractable ID badge holder with a small solenoid stopper is used as force feedback that restricts the fingers' movement. Hand and finger tracking is done using Leap Motion Controller interfaced to a virtual setup with different geometric figures developed using Unity software.

1.7 Contributed Papers

Journal:

- **A. C. Abad**, D. Reid and A. Ranasinghe, "A Novel Untethered Hand Wearable with Fine-Grained Cutaneous Haptic Feedback." MDPI Sensors Journal. 2022; 22(5):1924; `https://doi.org/10.3390/s22051924.`

- **A. C. Abad**, D. Reid and A. Ranasinghe, "HaptiTemp: A Next-Generation Thermosensitive GelSight-like Visuotactile Sensor," in IEEE Sensors Journal, DOI: 10.1109/JSEN.2021.3135941

- **A. C. Abad** and A. Ranasinghe, "Visuotactile Sensors with Emphasis on GelSight Sensor: A Review", IEEE Sensors Journal, Volume 20, Issue 14, 09 March 2020, DOI: 10.1109/JSEN.2020.2979662

Conference:

- **A. C. Abad**, M. Ormazabal, D. Reid and A. Ranasinghe, "Pilot Study: A Visuotactile Haptic Primary Colors Sensor," 2021 IEEE Sensors, 2021, pp. 1-4, doi: 10.1109/SENSORS47087.2021.9639848.

- **A. C. Abad**, M. Ormazabal, D. Reid and A. Ranasinghe, "An Untethered Multimodal Haptic Hand Wearable," 2021 IEEE Sensors, 2021, pp. 1-4, doi: 10.1109/SENSORS47087.2021.9639526.

- **A. C. Abad**, D. Swarup, D. Reid, and A. Ranasinghe, "4x4 Fingertip Tactile Matrix Actuator with Edge Detection Scanning ROI Simulator", 2020 IEEE Sensors, Rotterdam, Netherlands, 25-28 Oct. 2020. DOI: 10.1109/SENSORS47125.2020.9278765

- **A. C. Abad**, A. Ranasinghe, "Low-cost GelSight with UV Markings: Feature Extraction of Objects Using AlexNet and Optical Flow without 3D Image Reconstruction", International Conference on Robotics and Automation (ICRA2020), May 31 - June 4, 2020, Palais des Congrès de Paris, France

Workshop:

- **A. C. Abad**, D. Reid, A. Ranasinghe, "Pilot Study: Low Cost GelSight Sensor," Workshop on ViTac: Integrating Vision and Touch for Multimodal and Cross-modal Perception, International Conference on Robotics and Automation (ICRA) 2019 ViTac Workshop. May 20-24, 2019 Montreal, Canada.

1.8 Thesis Structure

This thesis is structured as follows:

- **Chapter 1** introduces the focus of the thesis and explains the motivation for the work. This chapter discusses the aims and objectives of developing a system that combines vision and touch to enhance the immersive experience. The input device is a visuotactile sensor, and the corresponding output device is an untethered haptic hand wearable.

- **Chapter 2** presents previous work, gaps, and challenges on visuotactile sensors with emphasis on the GelSight sensor. This chapter covers related literature on the design and development of tactile displays and haptic wearables.

- **Chapter 3** presents the design and development of a low-cost GelSight-like visuotactile sensor called HaptiTemp. This sensor can sense haptic primary colours *(force, vibration, and temperature)* and can classify tactile images using a machine vision camera.
- **Chapter 4** presents the design and development of an untethered multimodal haptic hand wearable that can actuate haptic primary colours *(force, vibration, and temperature)* and has fine-grained cutaneous feedback.
- **Chapter 5** presents a unified visual-haptic system. The sensor can transmit tactile information, temperature data, and tactile images wirelessly. An untethered multimodal haptic hand wearable with haptic primary colours *(force, vibration, and temperature)* and fine-grained cutaneous feedback uses the information transmitted by the HaptiTemp sensor to enable the user to feel the object contacted by the HaptiTemp sensor.
- **Chapter 6** presents the conclusion, recommendation, and future work. This chapter concludes, summarises the findings in this thesis, and discusses future improvements and possible future research directions in line with visuotactile sensing and actuating.

1.9 Chapter Summary

This chapter discussed and explained the thesis's background related to combining vision and tactile (visuotactile) in sensing and actuating haptic primary colours known as *force, vibration, and temperature*. The motivation of this thesis is to extend the human touch by creating a sensor capable of sensing haptic primary colours, and an untethered multimodal haptic hand wearable with haptic primary colours and fine-grained cutaneous feedback. The objective is to develop a visuotactile sensor as an input device, and an untethered multimodal haptic hand wearable as an output device. An integrated visuotactile system combines the visuotactile sensor with the untethered multimodal haptic hand. This chapter enumerated the contributions of this thesis as well as the contributed published papers.

2
Literature Review

2.1 Abstract

This chapter presents the related work about haptic sensors and haptic displays that focus on visuotactile sensing and actuating. Firstly, the chapter presents visuotactile sensors with emphasis on GelSight sensor technology. Secondly, the chapter discusses the different tactile matrix actuators with various technologies and modalities related to actuation in giving haptic feedback to the user. Finally, this chapter presents the diverse haptic hand wearables for teleoperation and Virtual Reality (VR) environments.

2.2 Introduction

Whenever we touch something, we usually sense multiple tactile parameters at once. For example, we feel the texture of a metallic object as we feel its temperature and might even recognise the tactile patterns, like in the case of a coin. The human skin has a remarkable capability to sense different tactile parameters, such as force, temperature, texture, simultaneously. It would be great if we could create one sensor the mimics the skin in sensing multiple tactile parameters at the same time. This device could be useful in robotics exploration and teleoperation. Among the different touch or haptic sensors, those with deformable transducers or flexible

materials have skin-like structure. Typically, sensors with gel-like sensing material have a camera that captures gel deformations. These sensors belong to a class of sensors called visuotactile where vision and touch information are combine. Moreover, if we could create a wearable to actuate the tactile parameters from a multimodal or visuotactile sensor, we could have an approximate tactile sensation of the things beyond our reach. This chapters covers the different literature related to visuotactile sensors and haptic hand wearables.

2.2.1 The Human Skin

A good haptic sensor must be close to the ability of the human skin to gather tactile or haptic parameters of an object being touched. In order to mimic the human skin, there is a need to understand how the skin detects the stimuli related to touch sensation and perception. The haptic system uses "cutaneous" inputs derived from mechanoreceptors and thermoreceptors embedded in the skin together with "kinesthetic" inputs from mechanoreceptors embedded in muscles, tendons, and joints [12]. The four types of mechanoreceptors in the human skin are shown in Figure 2.1 based on the illustration of the cross-section illustrated by Kajimoto et al. [22]. They are the Merkel cell (Slow Adapting type 1 or SA I), Meissner corpuscle (Rapid Adapting or RA), Ruffini ending (Slow Adapting type 2 or SA II), and Pacinian corpuscle (PC). According to Lederman and Klatzky [12], the mechanoreceptors have different response characteristics relative to the size of their receptive field (small vs. large) and their relative adaptation rate (i.e., response to onset/offset of skin deformation vs. continued response during sustained skin deformation). Meissner and Pacinian are categorised as Fast Adapting 1 and 2 (FA 1 and FA 2), respectively, as shown in Table 2.1. Lederman and Klatzky [12] also described the four mechanoreceptors relative to feature sensitive and associated functions. Merkel mechanoreceptor (SA I) is sensitive to sustained pressure and sensitive to very low-frequency detection (< 5 Hz) for coarse texture perception and pattern form detection. Meissner mechanoreceptor (FA I) is sensitive to temporal changes in skin deformation (5 to 40 Hz) for low-frequency vibration detection.

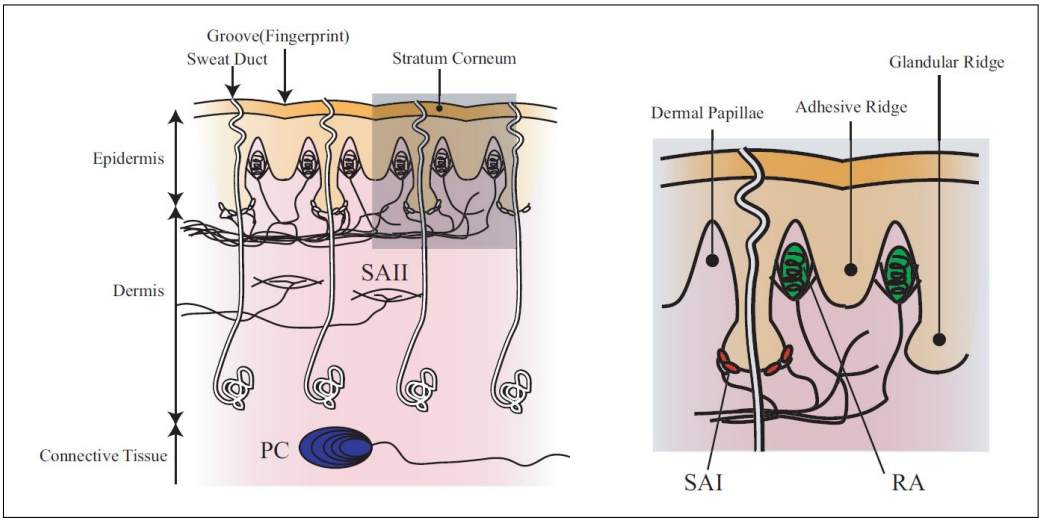

Figure 2.1: The cross section of the human skin [22]

.

Table 2.1: Response Characteristics of the Four Mechanoreceptors Populations [12].

Adaptation Rate	**Small receptive field**	**Large receptive field**
Slow	Slow-adapting type I (SA I) (Merkel)	Slow-adapting type II (SA II) (Ruffini)
Fast	Fast-adapting type I (FA I) (Meissner)	Fast-adapting type II (FA II) (Pacinian)

Pacinian mechanoreceptor (FA II) is sensitive to high-frequency vibrations (40 to 400 Hz) for fine texture perception. Ruffini mechanoreceptor (SA II) is sensitive to sustained downward pressure and lateral skin stretch relative to the direction of object motion and force due to skin stretch.

Moreover, aside from the different mechanoreceptors, there are thermoreceptors such as the different free nerve endings in our skin that are capable of detecting warmth, cold, and pain [9].

2.2.2 Visuotactile Sensation and Perception

Haptics can supplement vision if eyesight is not damaged. Visuotactile refers to the combination of vision and haptics. Curiosity in the study of the combination of vision and tactile, known as visuotactile, started in the 18th century [7], motivated by

Molyneux's question [23] stated briefly as: if a blind person was made to see, would he be able to recognise a sphere and a cube previously only known to him by touch?

The question posed by Molyneux concerns visuotactile sensation and perception. Morgan described how it was initially handled as a philosophical problem [7], but it was later addressed by psychologists studying visuotactile perception and coordination in the 1970s, according to Zhang [24]. The study of visuotactile perception has expanded beyond philosophers and psychologists to include roboticists, technologists, and engineers working in the domains of haptics, tactile robotics, machine vision, and artificial intelligence [1, 5, 7].

2.2.3 The Haptic Primary colours Sensors and Actuators

The HPC theory discussed in Chapter 1 put forward a haptic analogy of the primary colours of light. There are devices developed to realise the HPC theory and put it into applications. Kato et al. developed a "Soft Finger-tip Sensing Probe Based on Haptic Primary Colors" [25] by combining discrete components such as a force sensor, accelerometer, and the thermistor in a single module as shown in Figure 2.2. There is also a commercially available finger-shaped tactile sensor known as BioTac [26] sensor, which is capable of sensing the haptic primary colours as shown in Figure 2.3. So far, all the haptic primary colours sensors discussed have different discreet sensing elements combined into one module, and cannot do tactile image recognition. The aim of this thesis is to develop a fully unified and monolithic HPC sensor with tactile image recognition capability.

On the other hand, there are HPC displays such as "Electro-Tactile Display with Tactile Primary Color Approach" by Kajimoto et al. [22], and HPC Stacked Autoencoder by Kato et al. [27]. Haptic wearables with HPC feedback are also being developed, such as the "Haptic Display Glove Capable of Force/Vibration/Temperature" by Kato et al. [28].

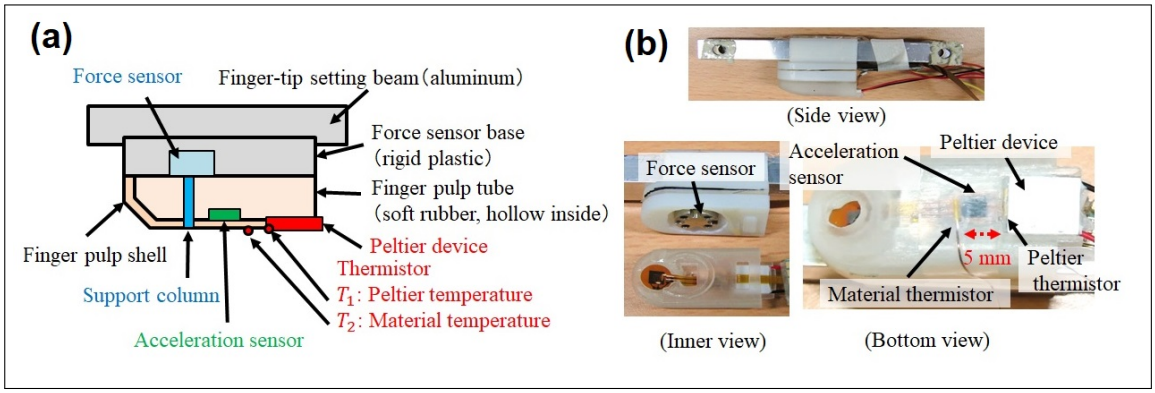

Figure 2.2: (a) Schematic of HPC Soft Finger-tip Sensing Probe, and (b) actual sensor module[25]

.

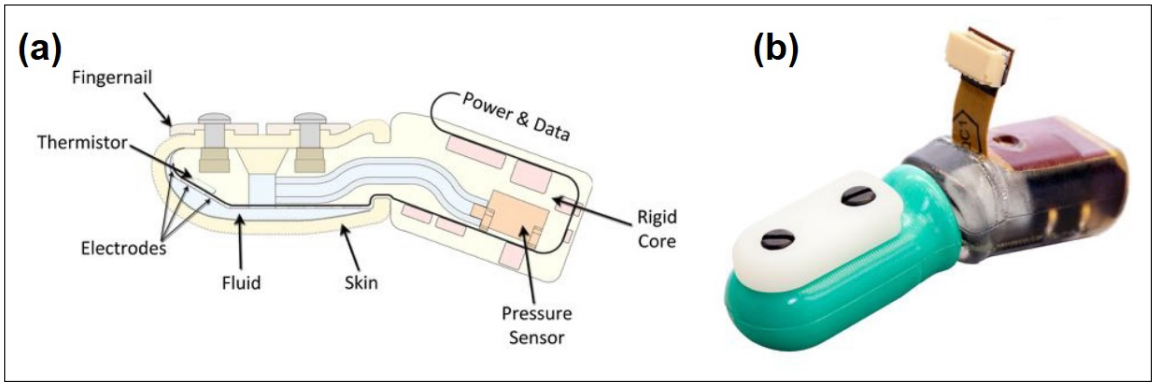

Figure 2.3: (a) BioTac sensor schematic, and (b) actual BioTac sensor module [26]

.

2.3 Visuotactile sensors

If an HPC sensor parallels the eye in sensing primary colours of light, a visuotactile sensor combines vision and haptics information. A visuotactile sensor uses physical contact to modulate visible light, creating a force or pressure map on the flexible material or deformable membrane. This map is the tactile image that may be studied in real-time or saved for later processing. The tactile image could include tactile markers to trace deformations on the flexible material or can be a retrographic image [29] for 3D image reconstruction, object recognition, and metrology. An ideal visuotactile sensor is like a flexible mirror that can capture a high-resolution tactile image embedded with tactile information about the contacted object. The embedded tactile information could be in form of force deduced from the markers,

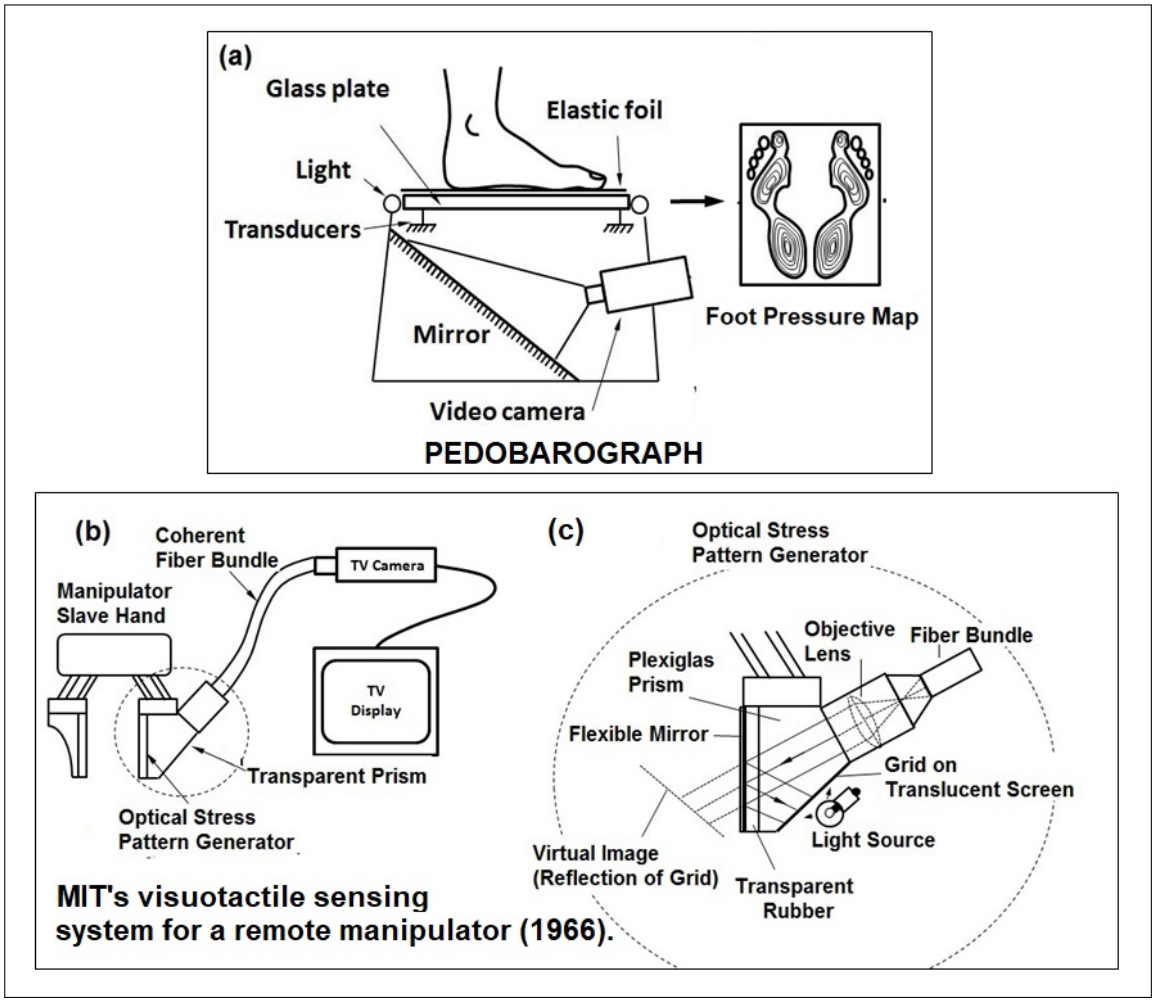

Figure 2.4: Visuotactile sensors in the 1960's: a) the pedobarograph [30, 31, 32] for foot-pressure pattern, and b) the earliest visuotactile sensor used in telerobotics [33].

vibrations, and temperature. This thesis produced the HaptiTemp sensor, which is closest to the ideal visuotactile sensor. This can sense haptic primary colours (force, vibration, and temperature) and classify tactile images. It has a fast temperature response that can trigger a robotic arm to mimic the human reflex response.

The earliest visuotactile sensors were developed during the 1960's. The first visuotactile sensor is the pedobarograph developed by Chodera in the 1960's [30, 31]. It was developed not for robotics but for human gait research. It can capture pressure distribution beneath the feet. The pedobarograph, as shown in Figure 2.4 [32] has an elastic material (plastic foam or foil) on top of a clear plate. Through Total Internal Reflection (TIR), light is diffused from the side of the transparent plate. A

foot pattern based on foot pressure is generated as the foot presses the flexible foil.

Moreover, during the same period as the development of the pedobarograph for gait analysis, MIT lab began developing visuotactile sensors, like tiny pedobarographs, that could be attached to a robotic arm [33]. Strickler and Sheridan from MIT [33] presented the first visuotactile sensing system in 1966 for a remote manipulator. They investigated different ways of producing high contrast optical stress patterns using fiber optics and television systems. The schematic of the design is shown in Figure 2.4b and Figure 2.4c. The MIT's visuotactile sensor's application to robotics inspired other researchers to develop more visuotactile sensors.

2.3.1 Visuotactile Sensors with no Tactile Markers

The pedobarograph and MIT's visuotactile sensor for telerobotics during the 1960's have planar structure and do not have tactile markers for tracking the deformation of their flexible material. Aside from planar structure, there are visuotactile sensors with hemispherical shape similar to a finger shown in Figure 2.5. These hemispherical sensors do not have tactile markers. Begej's fingertip-shaped sensor [34] in 1988, as shown in Figure 2.5a, have multiple bundles of optical fibers inside the sensor to detect change in TIR and locate the point of contact during sensor's operation. Maekawa et al. [35] developed a similar sensor structure like with Begej's sensor and produced three different prototypes with different diameters as shown in Figure 2.5b. Both Begej's and Maekawa's prototypes can locate the contact point during sensor operation but cannot produce a clear image of the contacted image. A more sophisticated finger-shaped hemispherical visuotactile sensor, known as GelTip [36], was developed by Dan and Shan in 2020 that can locate contact point and can produce a clear image of the texture of the contacted object as shown in Figure 2.5c. The GelTip has no markers for tracking gel deformations because the main function of the sensor is to localise point contact and to capture high-resolution tactile image.

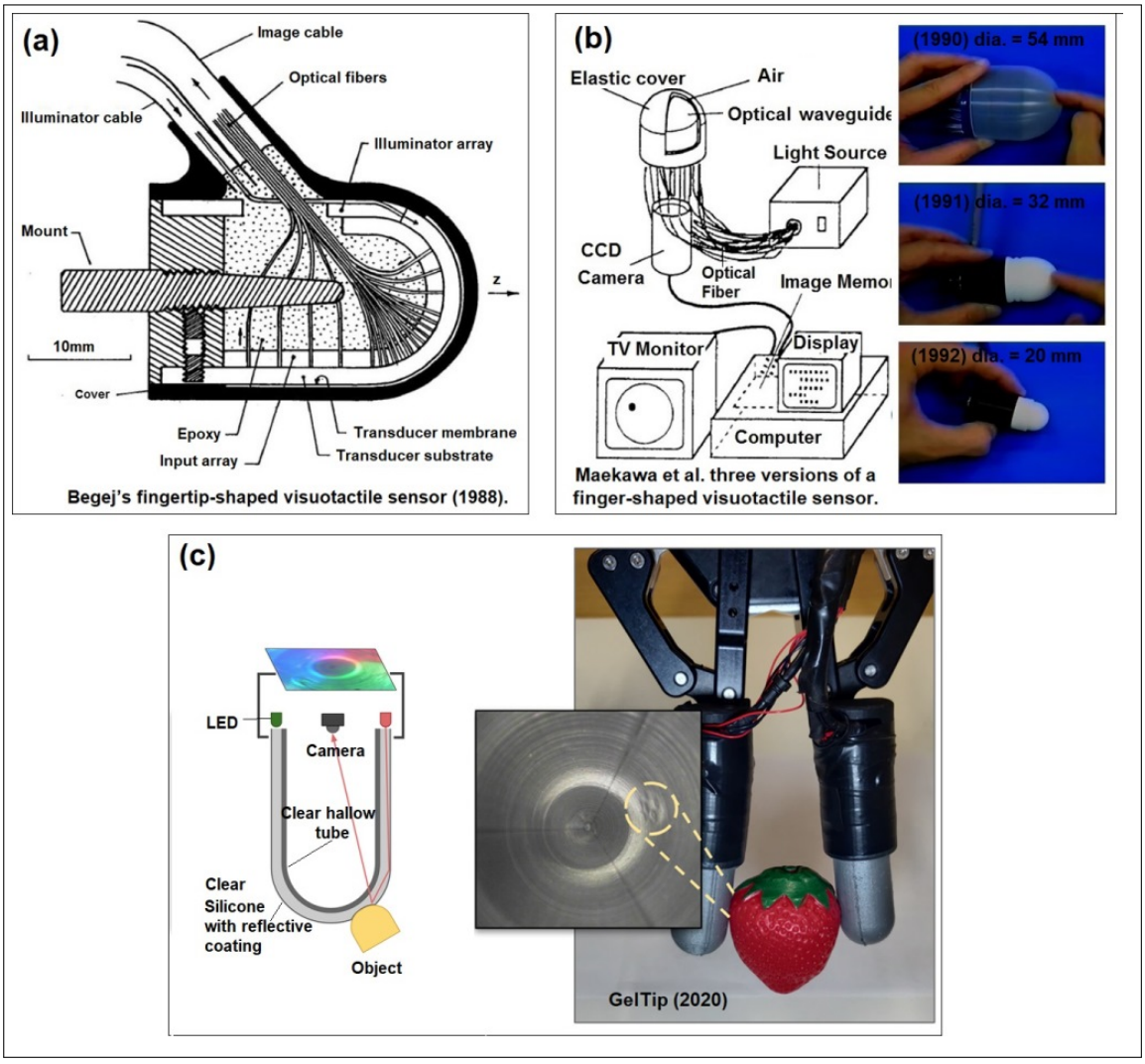

Figure 2.5: Visuotactile sensors with no markers.a)Begej's fingertip-shaped sensor [34], b)Maekawa et al. hemispherical visuotactile sensors [35], and GelTip [36].

2.3.2 Visuotactile Sensors with Microtextures as Tactile Markers

There are visuotactile sensors that has microtextures in the flexible material or on the transparent support plate as shown in Figure 2.6. The mictrotextures can be in form of pyramidal or conical shapes like like an inverted egg tray in the silicone rubber developed by Tanie et al. [37] as shown in Figure 2.6(a), that is also present in the transducer membrane in Begej's planar sensor [34] as shown in Figure 2.6(b), and in the cone feelers and pyramidal projections in Ohka et al. three-axis visuotactile sensor [38, 39] as shown in Figure 2.6(c), respectively. Ohka

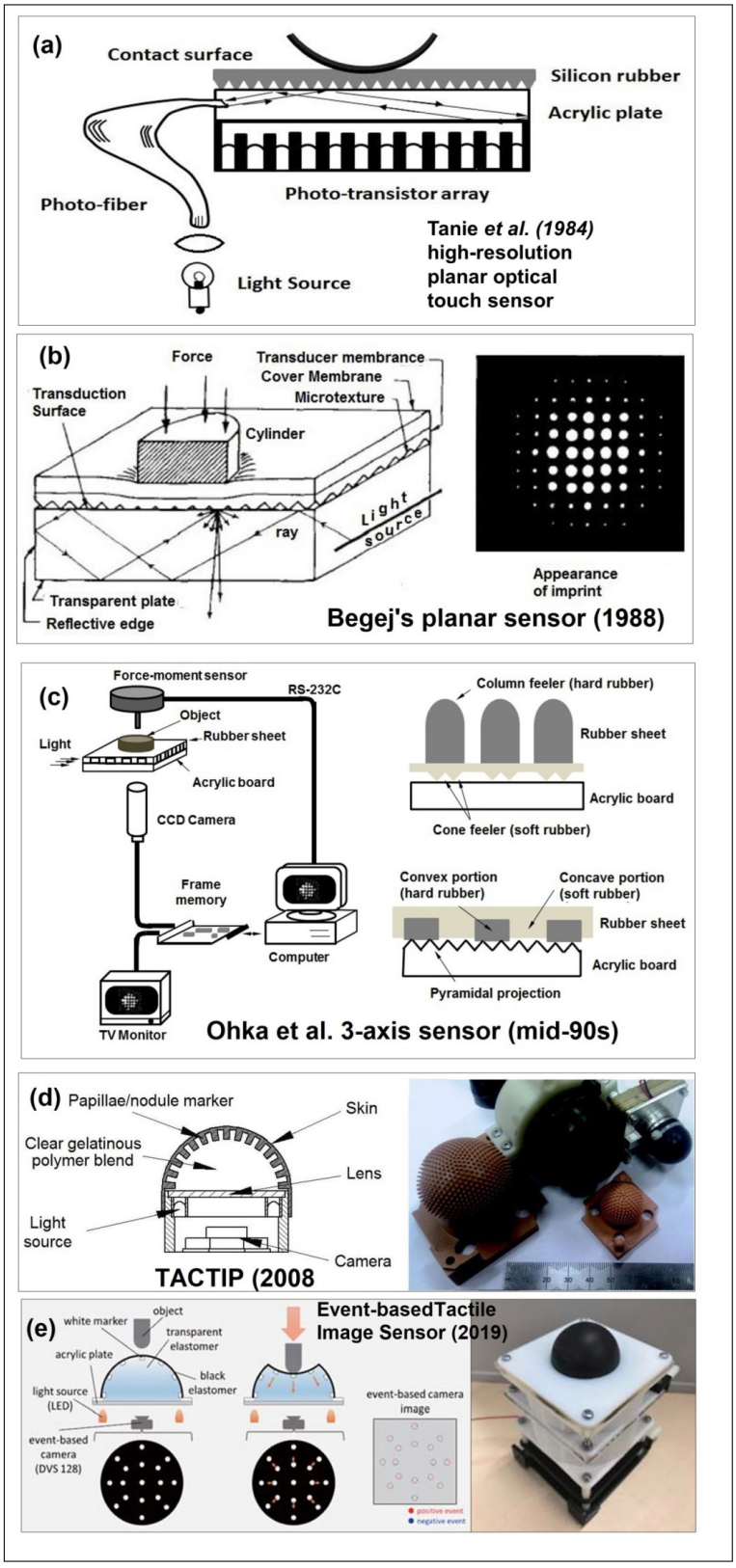

Figure 2.6: Visuotactile sensors with microtextures or microprojections for tactile analysis. a) Tanie et al. sensor with microtextures in silicon rubber [37], b) Begej's planar sensor [34], c) Ohka et al. sensor with column feelers and pyramidal projections [37], d) TACTIP [40, 41], and event-based tactile image sensor [42].

et al. reported that pyramidal projections can also be made not only on the flexible material, but also on the transparent acrylic board as shown in Figure 2.6(c). There are also microtextures in the form of column feeler [37] as shown in Figure 2.6(c), papillae projections as used in TACTIP sensor [40, 41] as shown in Figure 2.6(d), and white nodules in the event-based tactile sensor [42] as shown in Figure 2.6(e). The microtextures or microprojections changes shapes as shown in Figure 2.6(b), when contacted by an object on which tactile forces can be inferred. The visuotactile with microtextures tactile markers are only used for tactile forces analysis and cannot produce high-resolution tactile images like the GelTip in Figure 2.5c.

2.3.3 Visuotactile Sensors with Tactile Markers Embedded in the Flexible Material

There are various visuotactile sensors with tactile markers embedded in the flexible material as shown in Figure 2.7. The finger-shaped GelForce sensor [43, 44, 45] has blue and red beads, as shown in Figure 2.7a, used to detect 3D vector distribution. Another sensor with embedded markers was developed by Lin, and Wiertlewski [46] with dye markers integrated into the flexible material in 2019. Semi-transparent two-colour dye markers, rather than spherical makers, are arranged in two-layer arrays that overlap, as seen in Figure 2.7b. In contrast with the red and blue embedded markers in GelForce and the dye markers used by Lin, and Wiertlewski that are arranged in rows and columns, Sferrazza et al. [47] introduced fluorescent green spherical markers randomly placed in the gel material as shown in Figure 2.7c. Using a computer vision algorithm, the movements of the luminous green markers are tracked to deduce the force and pressure applied to the sensor. Visuotactile sensors with embedded markers in the flexible material are for tactile sensing only. They cannot produce high-resolution tactile images like the visuotactile sensors with microtextures tactile patterns.

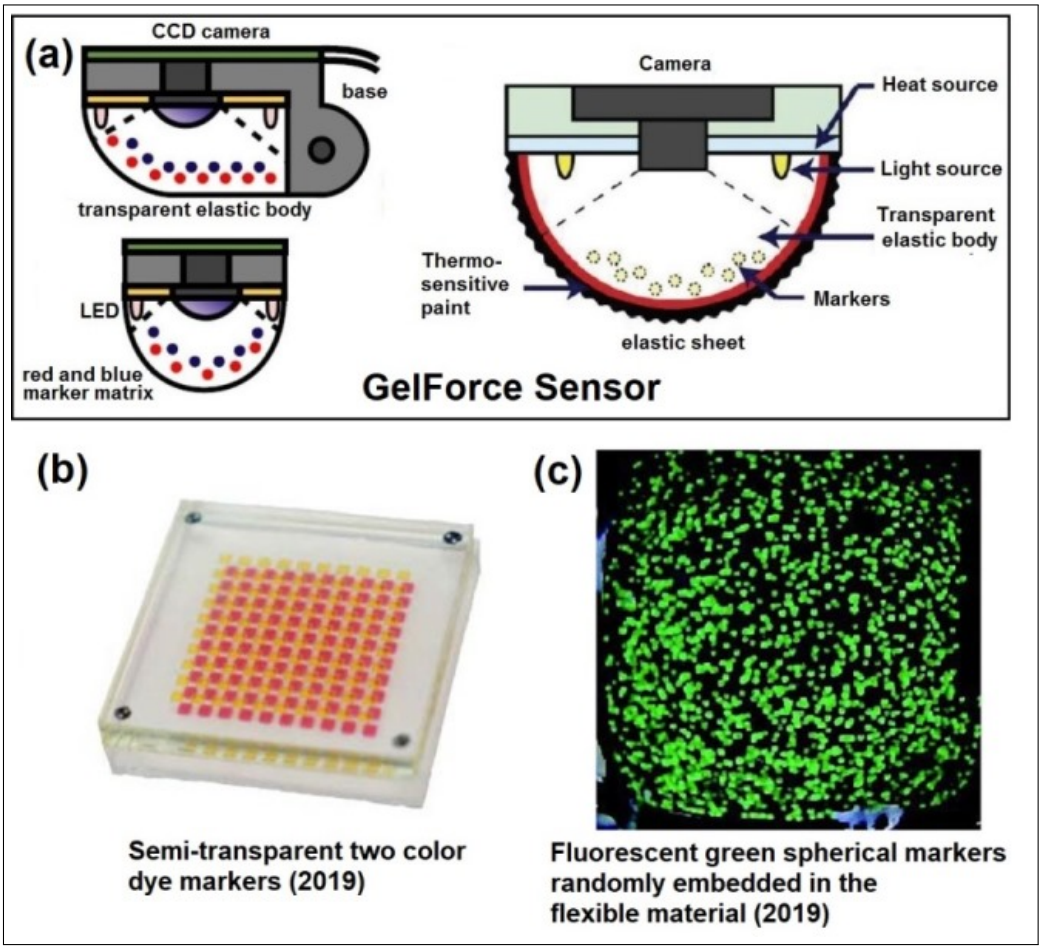

Figure 2.7: Visuotactile sensors with markers embedded in the flexible material. a) Thermosensitive finger-shaped GelForce [43, 44, 45], Lin, and Wiertlewski [46] dye markers, and Sferrazza et al. fluorescent green spherical markers [47].

2.3.4 Visuotactile Sensors with Skin-printed Tactile Markers

There are gel-type visuotactile sensors that has tactile makers printed on their skin or gel covering. Harvard Robotics Lab created in year 2000 a human-fingertip-like visuotactile sensor with a flexible membrane and skin markers [48] as show in Figure 2.8a. It has a metal housing that houses the camera, a clear window, and a sensing area of a roughly elliptical latex membrane filled with transparent gel. Grid dots are drawn at particular points on the membrane's inner surface. A metal fingernail supports the membrane. Tactile forces can be inferred from the movements of the skin markers but it cannot produce high-resolution tactile images. Unlike the opaque skin of other visuotactile sensors, the FingerVision [49, 50] has a transparent

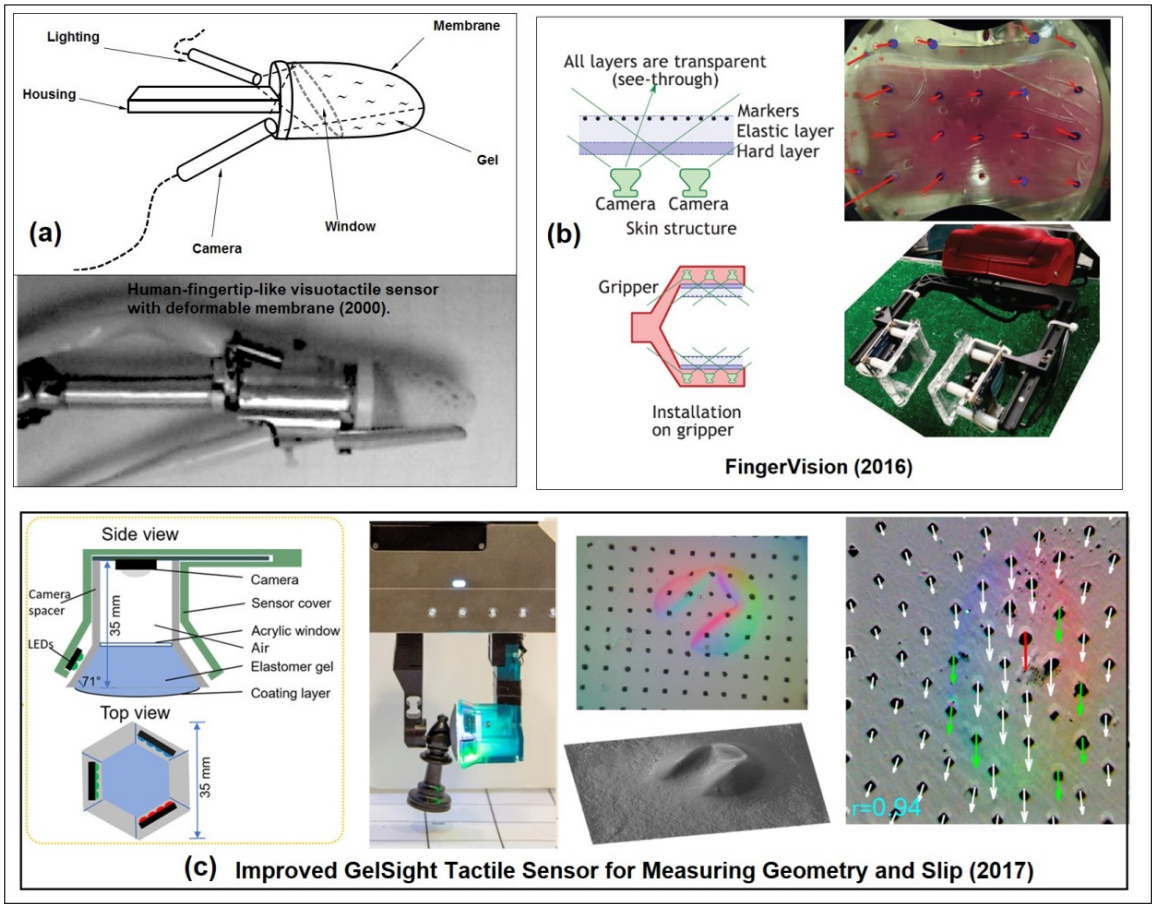

Figure 2.8: Visuotactile sensors with printed markers on the reflective coating. a) human-fingertip-like sensor [48], b) FingerVision [49, 50], and improved GelSight sensor for measuring geometry and slip [51].

coating printed with markers to track gel deformations as shown in Figure 2.8b. Because of the transparent sensor, it was claimed in [49, 50] that the FingerVision sensor has extensive information but this sensor was not used for tactile image recognition. Between the visuotactile sensor that has opaque skin and transparent coating, the GelSight sensor [51] presented in Figure 2.8c has a reflective coating with printed tactile markers to track gel deformations when contacted by an object. Moreover, GelSight sensor can be used to capture high-resolution tactile images that can be used for measuring microgeometry of the contacted object.

The visuotactile sensors discussed so far focused only on tactile sensing related force estimation and localisation of contact area. Though some of these visuotactile sensors produce tactile images, the clarity or resolution of these images is not that

Figure 2.9: The retrographic sensor [29]. (a) Oreo cookie pressed to the sensor, (b) retrographic image at other side of the sensor, and (c) reconstructed 3D image.

high compared to the tactile images captured by the GelSight sensor. The following sections are the details and research gaps related to the GelSight sensor.

2.4 The GelSight Sensor

Johnson and Adelson of MIT introduced the retrographic sensor [29] in 2009, a novel small high-resolution pedobarograph-like sensor that translates surface contour and pressure into a picture. It is a visuotactile 2.5D scanner that converts surface texture and shape into images. The retrographic sensor is a transparent elastomer with a reflective coating that produces an image of the contacted object on the other side of the flexible material as shown in Figure 2.9.

The retrographic sensor can be put on a clear supporting plate with LED lights and a camera to form the GelSight sensor [52]. The term "GelSight" was first used in 2013 to describe the whole setup consisting of a retrographic sensor mounted on a clear supporting plate with LED lights and a camera [52] as shown in Figure 2.10. The GelSight sensor combines visual and tactile sensing to capture tiny surface geometry as small as 2 microns [53] , with sensitivity and resolution far exceeding human fingertips [54]. It works like a human eye-skin extension device for visual and tactile texture examination. Because it can produce an image with tactile information, it can be referred to as a visuotactile flexible mirror.

The GelSight sensor can be used to reconstruct a high-resolution 3D image of the microgeometry of the contacted object using a photometric stereo algorithm. The GelSight sensor has a unique niche in that it can capture its deformation in response to pressure changes [29]. Unlike the FingerVision sensor that has transparent

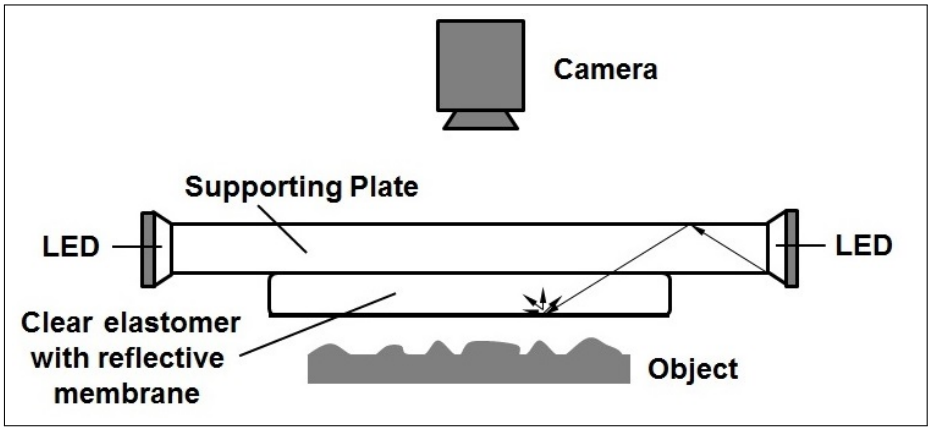

Figure 2.10: The structure of GelSight sensor [52].

flexible material, the GelSight sensor has opaque reflective coating and only the images of the contacted surfaces are captured. It can remove the object's colour, resulting in a monochrome image of tactile texture or contour pattern. When a textile with multiple colourful patterns is pressed against the GelSight sensor, only a monochrome image of the weave pattern appears.

It can remove the luster of a shiny object, such as a metallic coin, that would be difficult to remove with just image processing. Because of its Bidirectional Reflectance Distribution Function (BRDF) [29], the GelSight sensor can execute rapid colour and luster image filtering. It works like a refreshable mold, revealing the shape and texture of the object pressed against it.

Though the GelSight sensor's creators (Johnson and Adelson) initially focused on high-resolution 3D image reconstruction for microgeometry and metrology analysis, they also reported that the sensor could be used as a human skin model to study skin deformation when touched by objects such as cosmetic products, food, and clothing [29]. It can also be utilised as a tactile sensor in robots to create a soft fingertip with a sensitivity that exceeds human skin. In 2014, this forecast about the GelSight sensor being used in robotics came true [55].

The GelSight sensor evolution from 2009 to 2022 is shown in Figure 2.11. The GelSight sensor has progressed from the bulky cube structure with 30cm side length described in [29, 56], to a bench configuration [53], a portable version [53, 54], and a desktop configuration [52]. The GelSight sensor was downsized even further to

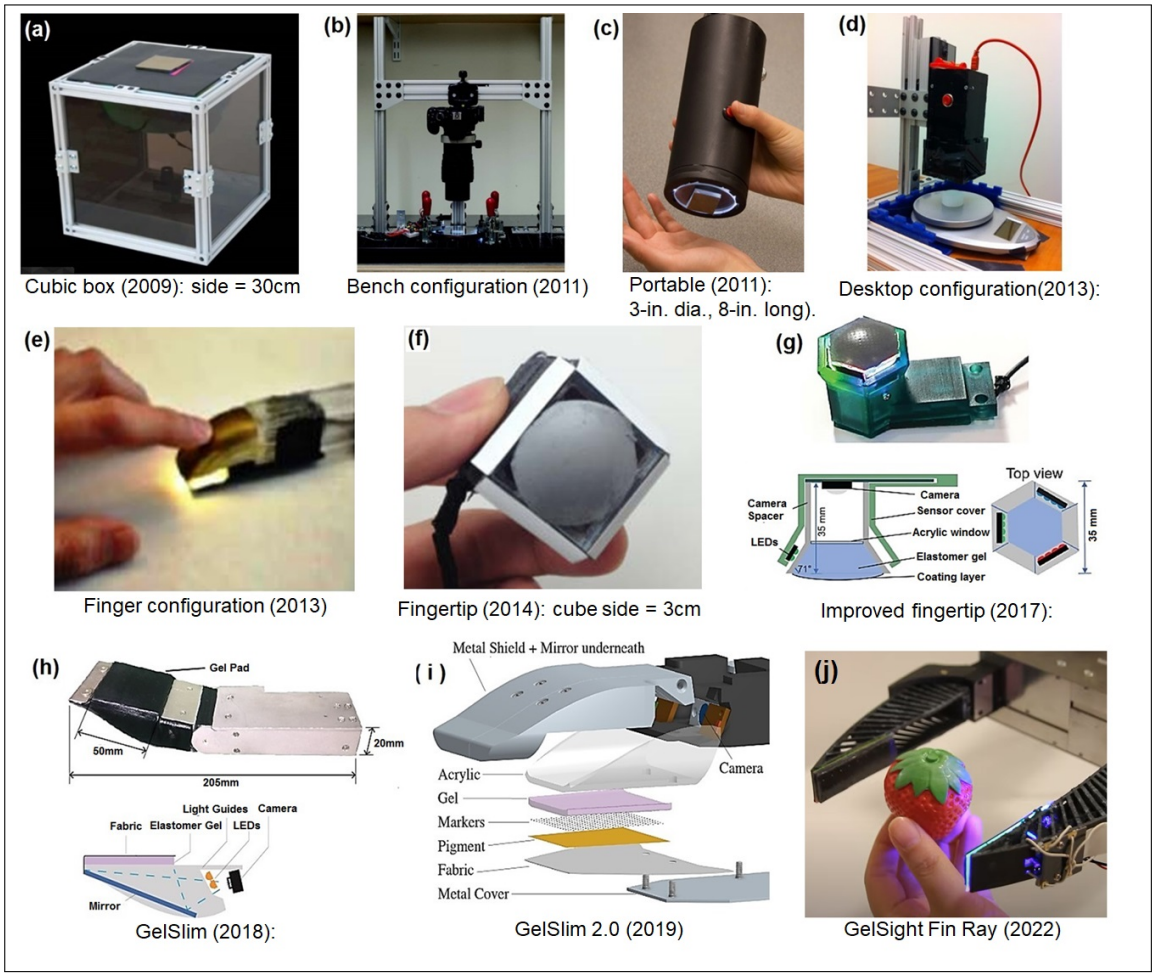

Figure 2.11: The GelSight sensor evolved from bulky cube structure of 2009 to GelSight Fin Ray of 2022. a) Cube configuration [29, 56], b) bench configuration [53], c) portable configuration [53], d) desktop configuration [52], e) finger configuration [54], f) fingertip [55], g) improved fingertip [51, 56], f) GelSlim [57], GelSlim 2.0 [58], and GelSight Fin Ray [59].

develop a fingertip GelSight sensor that could be used in a robotic arm. This fingertip GelSight sensor was first demonstrated in [55] and then upgraded in [51]. GelSight launched a new era in 2018 named GelSlim [57], which is a compact design with a skin fabric gel covering for durability, as illustrated in Figure 2.11h. In 2019, the GelSlim was upgraded to GelSlim 2.0 [58], which featured a new hardware design and greater illumination as shown in Figure 2.11i. The latest GelSight sensor configuration is the GelSight Fin Ray (2022) [59] that has a mechanically compliant external structure as shown in Figure 2.11j.

2.4.1 Retrographic Sensor

Johnson et al. [29, 53] coined the term "retrographic sensor" to describe the first component of the GelSight sensor described by Jia et al. in [52]. As illustrated in Figure 2.9a and Figure 2.9b, it is comprised of a clear elastomer with a reflective coating on one side. It is like a mechano-optical filter that only shows the contacted object's tactile image that can be used for 3D reconstruction, as shown in Figure 2.9c. The following is a more detailed overview of the clear elastomer and reflective coating:

2.4.1.1 Clear Elastomer

When creating a clear elastomer, it is important to consider the parameters such as optical transparency, resilience, hardness, stretchability, and fabrication complexity [56]. Current GelSight elastomers are manufactured in the lab with a thermoplastic elastomer (TPE), which requires an oven to melt in a mould, or silicones, which are made up of two separate liquid portions that, when mixed together, form a firm gel [60]. The curing time of around 6 to 7 hours [60], quality consistency [61], and the development of air bubbles within a gel that requires a vacuum pump for degassing [60, 61, 62] are the three main problems in creating a transparent flexible material. Apart from the difficulties in generating clear elastomers in the lab, the elastomer can be easily broken during robotic gripping and needs frequent maintenance, according to [63].

The HaptiTemp sensor developed in this thesis used a Commercial-Off-The-Shelf (COTS) clear silicone cosmetic sponge as the flexible material. By using COTS clear silicone gel, the time consuming and complicated process of creating a clear elastomeric slab can be skipped.

2.4.1.2 Markers on the Reflective Coating

Yuan introduced permanent tactile markers in the form of dots or triangles on the reflective coating of the GelSight sensor in 2014 [60]. The motion of the markers [56, 60] can be used to deduce normal force, shear force, and slip. Permanent markers for the GelSight sensor can be printed in a dense quasi-random triangular

pattern or a grid-like arrangement using a stencil pattern or transfer paper. In GelSlim 2.0 [58], grid dots were also added.

The permanent markers are not present in the GelSight sensor utilised in detecting, identifying, and measuring surface texture [29, 54] and microgeometry [53], lump detection [52], manipulation and localisation of small components [55], and tactile mapping and localisation [64]. The GelSight sensor with permanent markers has been utilised in research on force, shear, slip [56, 51, 65], and hardness estimation [66]. Higher accuracy displacement fields can be achieved by increasing marker density, according to Yuan et al. [65], but this will compromise the GelSight's capacity to measure a heightmap. Despite the permanent markers' ability to capture the magnitude and direction of force applied, Li et al. reported that the GelSight is limited in its ability to accurately measure normal force, shear force, and torque because it is difficult to extract force-related information from the GelSight images due to the presence of numerous markers merging with the tactile information in the image [67]. The F-TOUCH (Force and Tactile Optically Unified Coherent Haptics) sensor, a GelSight-like sensor, demonstrated a novel solution to extract accurately force-related information, such as force and torque, along six axes by incorporating a deformable spring-mechanism structure, to measure [67].

According to Dong et al. [51], a GelSight sensor with permanent markers can be utilised to detect geometry using a photometric stereo algorithm and measure slip by tracking permanent markers. However, permanent markers in the GelSight sensor's reflective coating may conceal some crucial image elements that could be used for 2D image processing for object classification, such as textile type recognition based on weave patterns.

The HaptiTemp sensor developed in this thesis uses switchable UV markers in the reflective coating. The UV markers can be made visible or invisible using UV LEDs, creating a unified visuotactile sensor for both tactile image recognition and force analysis.

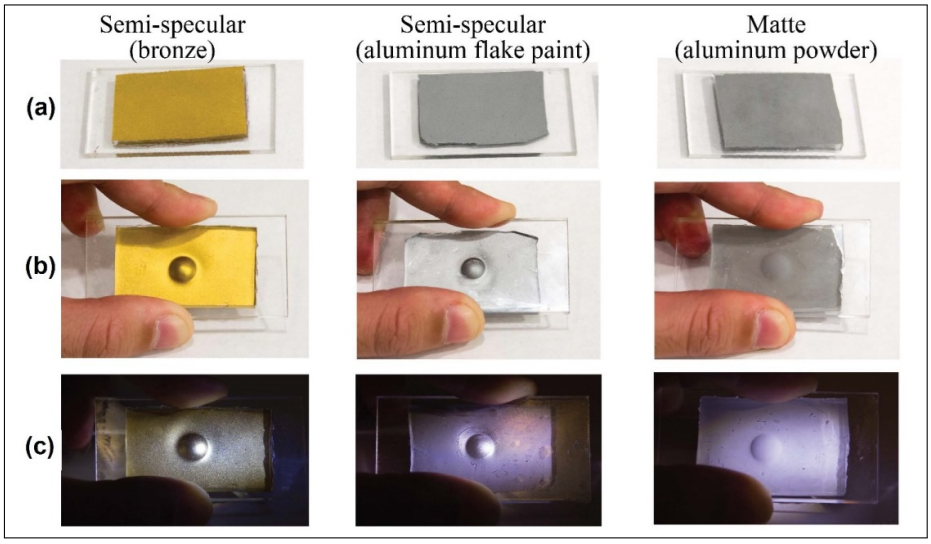

Figure 2.12: Semi-specular coating captures microgeometry on the surface normal, whereas matte coating is excellent for measuring generic forms, as documented in [56]. (a) Outside view, (b) inside view, and (c) inside view with light from the side.

2.4.1.3 Thermochromic Pigments

The GelSight sensor's reflective coating discussed in the previous section is not thermosensitive. By using thermosensitive pigments on the reflective coating, the HaptiTemp sensor developed in this thesis can sense temperature. This temperature sensing capability is not present in the GelSight sensor. There are different types of thermochromic materials such as the thermochromic liquid crystal sheet [68] as shown in Figure 2.13(a)i, thermochromic liquid crystal ink [69] as shown in Figure 2.13(a)ii, and thermochromic pigments as shown in Figure 2.14 and Figure 2.15.

The activated state of thermochromic liquid crystal sheet, colour-to-colour thermochromic pigments, colour-to-translucent thermochromic pigment, and multiple colour-to-translucent thermochromic pigments with different temperature thresholds as shown in Figure 2.13(b), Figure 2.14(b), and Figure 2.15(b) respectively.

Thermosensitive liquid crystal sheets were used by finger-shaped GelForce [45, 70]. Thermochromic liquid crystals are water-based thermosensitive materials that cannot be dissolved in solvents [69]. In contrast, thermochromic pigments can be dissolved in solvents, making it possible to mix in a silicone solution that can be airbrushed on a clear silicone gel. There are two types of commercially available

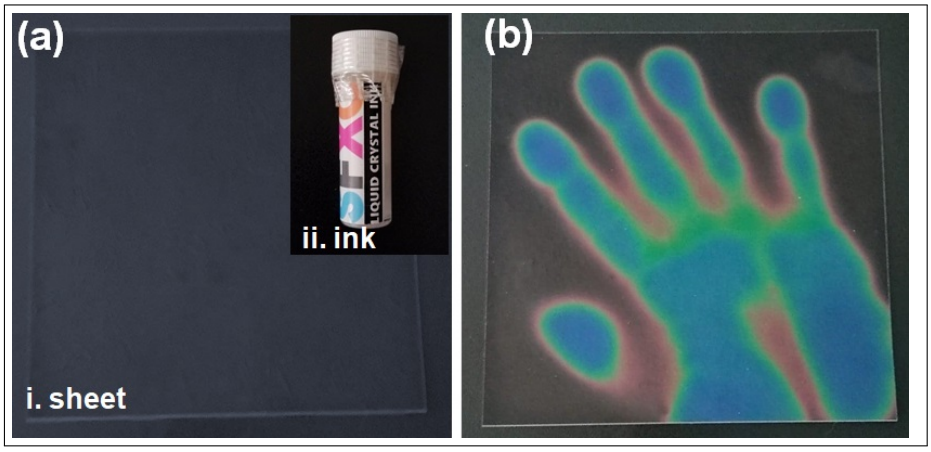

Figure 2.13: Thermochromic Liquid Crystal Display (LCD). a)i. Inactive thermosensitive liquid crystal sheet (25° to 30°C) [68], a)ii. Sprayable liquid crystal ink, b) liquid crystal thermocolour sheet with threshold 25° to 30°C [68].

thermochromic pigments: 1) pigments that change from one colour to another colour [71] as shown in Figure 2.14(a) with an activated state as shown in Figure 2.14(b), and 2) pigments that change from one colour to translucent of semi-transparent [72] as shown in Figure 2.15(a) and its activated state as shown in Figure 2.15(b). Type 2 thermochromic pigments can be of different colours, as shown in Figure 2.15(c).

2.4.2 Transparent Plate Support

In a GelSight sensor, a clear transparent glass plate or acrylic plate was utilised to support the flexible material and as a light waveguide to disperse light through TIR. Early GelSight sensors [29, 53, 54, 52] used glass plates, whereas newer sensor types (such as fingertip GelSight and GelSlim) [55, 57, 58] used acrylic plates. Acrylic plates are more durable and lightweight compared to glass.

2.4.3 Lighting

Uniform (controlled) lighting is required to illuminate the flexible material. GelSight sensors use monochromatic or multicoloured lighting. The GelSight sensor employs light-emitting diodes (LED). All GelSight sensor architectures contain multicoloured lighting, with the exception of GelSlim [57], which uses two neutral white, high-powered, surface-mount LEDs (OSLON SSL 80) on either side of the finger.

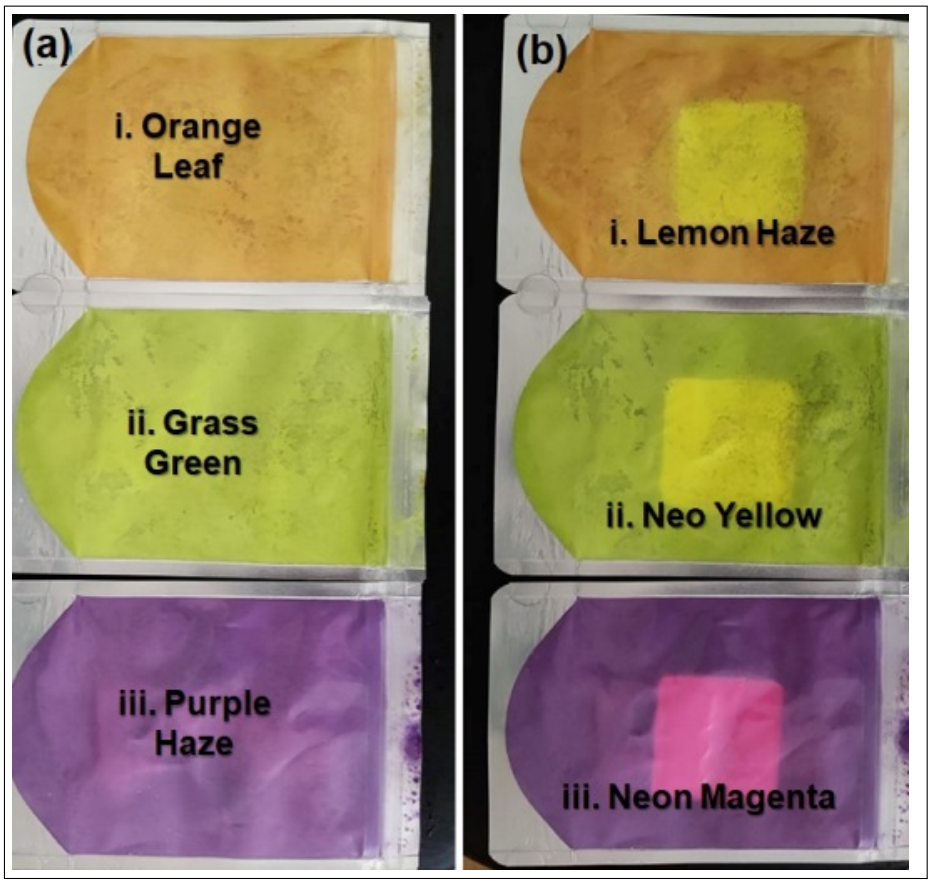

Figure 2.14: Colour-to-Colour changing thermochromic pigment. (a) inactive colour-changing thermochromic pigment (27°C) [71]. (b) activated colour to colour thermochromic pigments with 27°C threshold.

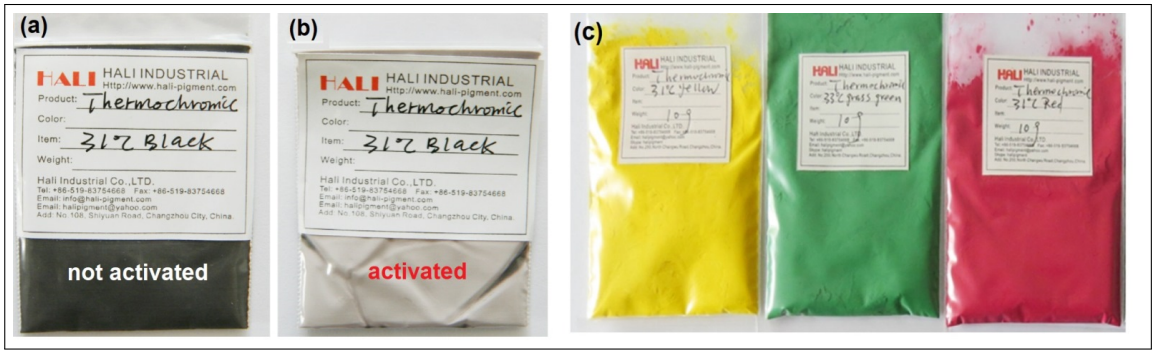

Figure 2.15: colour-to-translucent changing thermochromic pigment. (a) inactive black thermochromic pigment turns (b) white to translucent when activated. (c) thermochromic pigment comes in different colours and temperature thresholds [72].

For 3D image reconstruction, multicoloured lighting was used. For the photometric stereo method, multicolour LEDs at various locations are required. Different LEDs with different colours mounted at different points around the slab are necessary to detect the surface normal, according to Yuan [60]. Moreover, Yuan discussed two ways of using a photometric stereo algorithm for 3D image reconstruction using differentiated illumination: 1) turning on LEDs at different locations consecutively and taking multiple pictures of the same scene, or 2) turning on multicolour LEDs simultaneously and taking a single picture. The reflection of the different colour LEDs can be determined by taking different channels of the colour image.

The HaptiTemp sensor developed in this thesis introduces the use of UV light to switch on or off the UV markings. UV LEDs are needed to show or to hide the presence of UV markings in the reflective coating by switching the UV LEDs.

2.4.4 Digital Camera

The retrographic image on the reflective skin of the GelSight sensor can be recorded using a digital camera. Video recording can also be done, such as recording a pulse-rate [73]. The 2009 GelSight sensor [29] used a Canon DSLR (EOS-1D Mark III) and a 100mm macro lens at a distance of 40cm from the sensing element. The portable configuration used a 0.8 MP Point Grey Flea2 camera [53], while the bench configuration employed an 18 MP Canon EOS Rebel T2i camera with macro lens MP-E 65mm placed vertically [53]. The fingertip size configuration [55] has employed the Logitech C310, which has a 5 MP resolution, making a miniature GelSight sensor. Moreover, in GelSlim configuration [57], a small digital camera known as the Raspberry Pi Spy Camera was utilised.

All the digital cameras used by the different GelSight sensor configurations are passive. All image processing is done on a desktop or laptop computer. The thesis introduces a machine vision camera to the HaptiTemp sensor making it a stand-alone sensor capable of sensing and doing tactile image classification within the sensor module.

2.4.5 GelSight Sensor Software

The image captured by the GelSight sensor can be called retrographic or tactile image. The image of the deformation of the clear elastomer with reflective coating taken by the camera on the reverse side of the slab is known as the retrographic image. This is a two-dimensional tactile image of the object's pressure points or contact area with the GelSight sensor. Retrographic images are used for visual texture analysis, microgeometry, form measurement, 3D image reconstruction, object detection, and classification in general. Moreover, a retrographic image can have dot markers to deduce normal force, shear force, and slip [56, 60].

There are different GelSight sensor image processing techniques reported [29, 53, 54, 52]. In 2009, the retrographic images were subjected to a 3D image reconstruction process known as the photometric stereo algorithm [29]. The 3D reconstruction algorithm can accurately and efficiently capture shallow microgeometry independent of how the material scatters light [53]. Surface texture and shape measurements and microgeometry capture were accomplished using the photometric stereo technique. In addition to the photometric stereo technique, Local Binary Patterns (LBP) supplemented with multi-scale pyramid and Hellinger distance metric can be used to detect and recognise surface textures, as stated in [54]. In addition, as reported in [52], a typical Support Vector Machine (SVM) classifier with a supervised learning technique was utilised for lump detection [52]. The fingertip GelSight sensor in [55] used the Binary Robust Invariant Scalable Keypoints (BRISK) [74] algorithm, which locates robust keypoints with binary descriptors and the feature-based RANDOM SAmple Consensus (RANSAC) [75] algorithm operating on a height-map generated by the photometric stereo algorithm to create tactile maps.

Optical flow algorithm [76] based on Lucas-Kanade (LK) [77, 78] are used for GelSight sensor with dot markers to analyse gel deformations. Image segmentation and tracking of centroids of the dot markers were also applied. Partial slip during shear loading can be deduced from the displacement field of dot markers using the tracking-surface-marker method presented in [65].

Convolutional Neural Network (CNN) and Recurrent Neural Network (RNN) deep learning algorithms were introduced to the GelSight sensor in 2017 [79]. According to Yuan et al. [80], the use of deep learning has substantially advanced the success of computer vision. CNN was used in numerous GelSight investigations relating to object detection, and classification, as well as cross-modal analysis [64, 81, 82].

However, all the machine vision algorithms discussed are implemented using a desktop or laptop computer. The HaptiTemp sensor developed in this thesis uses machine vision algorithms to classify tactile images in a stand-alone configuration. The HaptiTemp can do sensing and tactile image classification simultaneously.

2.5 Tactile Matrix Actuators

Over the last decades, research on haptics and development of tactile actuators has increased and has grown into an interdisciplinary research covering vision substitution system for the blind and visually impaired[83, 84], psychophysics[85], perception[12], virtual reality (VR), biomedical engineering, mechanism design and control, material recognition[86], telecommunications[87], telerobotics[88, 89], and Human-Computer Interaction (HCI) [90].

Tactile displays or matrix of tactile actuators for vision substitution have a long history that started in the 1960s to early 1970s [91, 92, 93].They have a matrix of pins (taxel or tactile pixel) [97] arranged by lines and columns that can be lifted or lowered. A tactile matrix actuator is a human-computer interface that can reproduce as closely as possible the tactile parameters of an object, such as shape, surface texture, roughness, and temperature.

One of the most popular tactile matrix actuators is the Optical Tactile Converter (OpTaCon) as a reading machine for blind people in which a facsimile of ordinary printed material is presented as tactile patterns from a dense vibrating array of piezoelectric pins [92]. The first OpTaCon was made by Linvill and Bliss in 1966 [92] that has 12 x 8 or 96 piezoelectric bimorph tactile stimulators spaced 1/8 inch interval as shown in Figure 2.16(a). The 12 x 8 tactile matrix corresponds to the photoconductor array as shown in Figure 2.16(b).

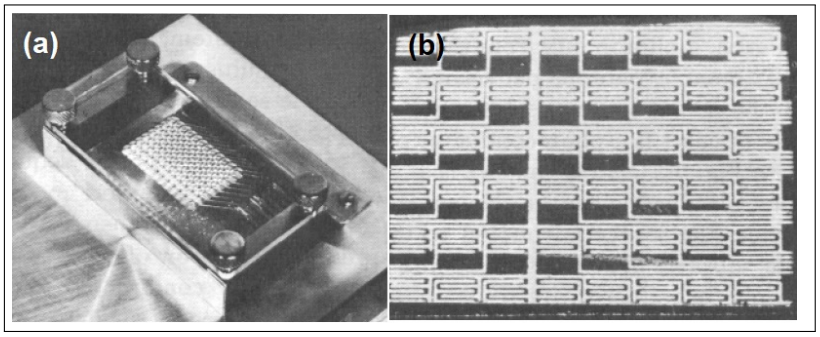

Figure 2.16: 12 x 8 OpTaCon adapted from [92].

In 1969, Bliss introduced a more dense OpTaCon that has 24 x 6 or 144 piezoelectric bimorph tactile stimulators [93] as shown in Figure 2.17 that fit on a single fingertip. This 144 tactile pin OpTaCon was used for reading aid for the blind and environment sensing [83] as shown in Figure 2.18(a) and Figure 2.18(b), respectively. The environment sensing OpTaCon uses a 12 x 12 phototransistor corresponding to the 144 tactile pins in a 1.25-inch square in the device's handle.

The untethered fine-grained haptic wearable developed in this thesis got the inspiration with the Bliss' dense OpTaCon used for environment sensing as shown in 2.18(b). Instead of grouping the tactile pins for hand exploration, the tactile pins were distributed to the fingertips in a 4x4 tactile matrix display. In contrast with the OpTaCon, the fine-grained haptic wearable in this thesis is not for vision substitution but for tactile augmentation to a visual system and VR/XR environment to enhance the immersive experience.

Tactile matrix actuators come in different sizes and pin numbers ranging from 2x2, such as the TACTAcT4 [94, 95] as shown in Figure 2.19 to 64x72 tactile matrix display from Dot Company [96] as shown in Figure 2.20.

Tactile matrix actuators can be interfaced with computers, mobile phones, and other communication devices. It can also be used in online browsing and e-shopping, telecommunications, telerobotics, and virtual reality (VR) applications [97]. Generally, sizeable tactile matrix actuator pins are not grouped by 6 or 8 pins like the Braille cell. All pins have the same displacements as other pins [97, 98]. In a Braille-like tactile matrix actuator, the user needs to move the hand or finger to

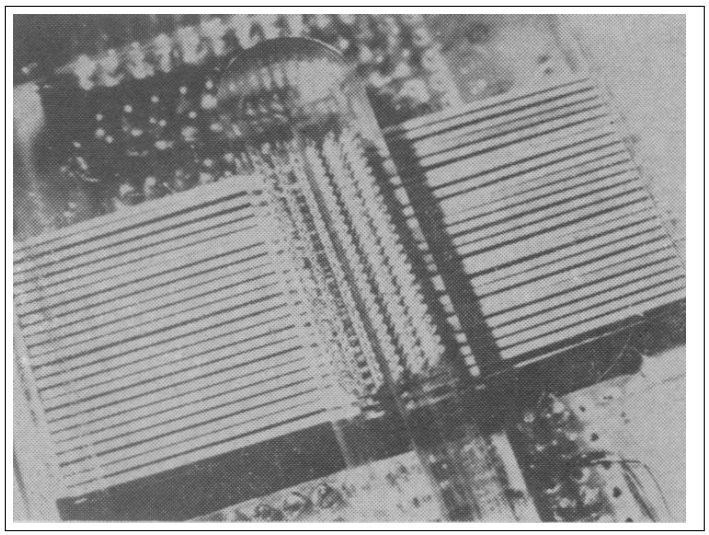

Figure 2.17: 24 x 6 OpTaCon adapted from [93].

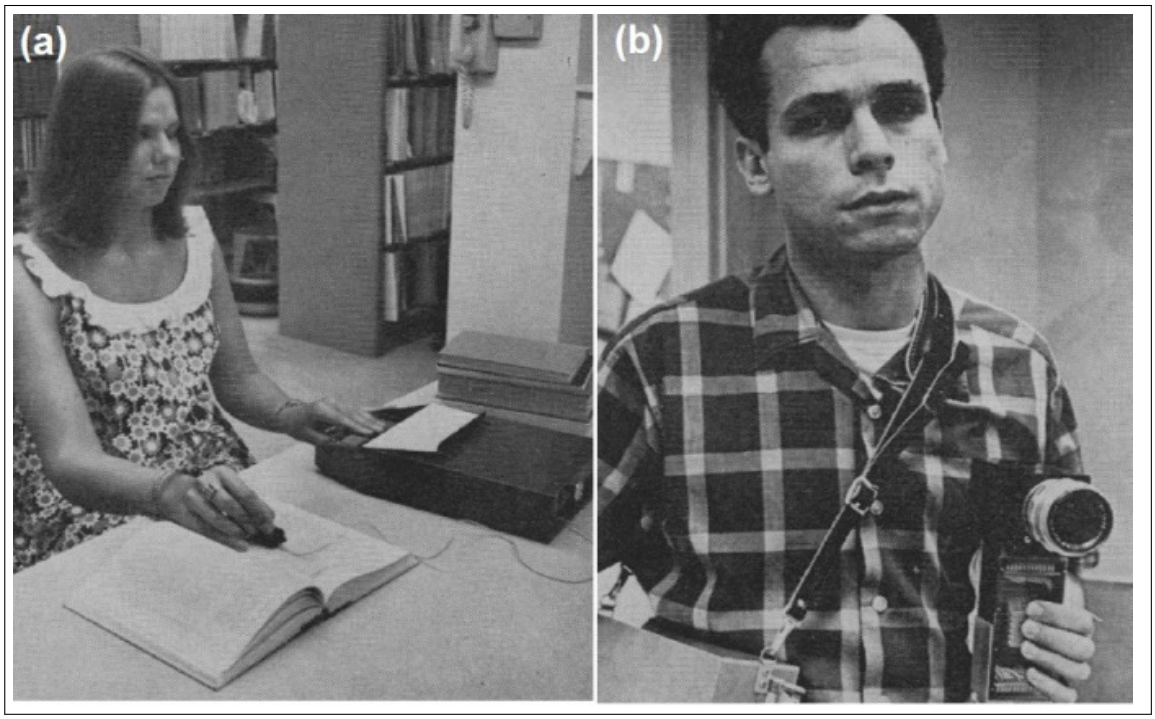

Figure 2.18: 24 x 6 OpTaCon for (a) reading aid for the blind and (b) environment sensing adapted from [83].

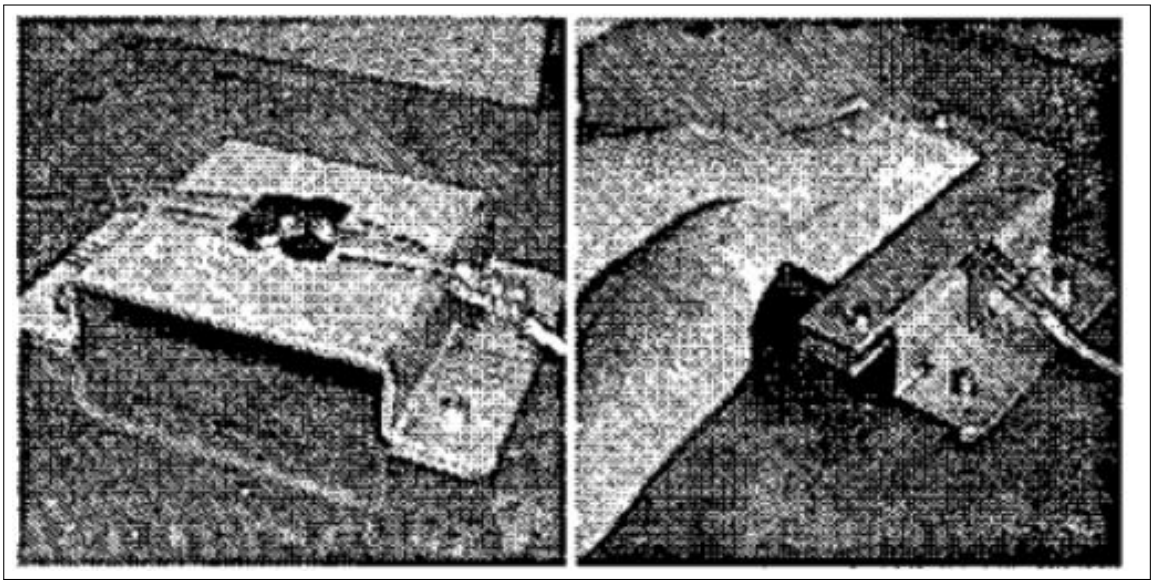

Figure 2.19: TACTAcT4 is 2x2 Fingertip tactile matrix made from solednoid adapted from [94, 95]. These are the only available pictures.

Figure 2.20: 64x72 tactile matrix display from Dot Company [96]

explore the activated pins. In contrast, the finger does not need to move in a fingertip tactile matrix actuator because the fingertip covers the whole tactile matrix actuator. Aside from a matrix of pins that can go up and down, tactile matrix actuators can also be made of pins or nodes that vibrate at different frequencies [99, 100].

One of the main goals in haptics research is to develop an effective and efficient tactile "display" for a human–machine interface that can reproduce as closely as possible the natural feel of an object. Tactile matrix actuators are not only for vision substitution systems [83, 84], but they can also be used in human–computer interaction (HCI) [90, 101, 102], telecommunications [87, 88], telerobotics [89], biomedical engineering [17], material recognition [86], and to enhance the immersive experience in online shopping [18] and VR environments [97, 98].

Tactile matrix actuators can be made from different forms of tactile actuators (tactors) such as solenoids [84, 97, 98], voice coil motors [103], piezoelectric [83, 104, 105], shape memory polymer (SMP) [106], smart memory alloy (SMA) [107, 108], stepper motor [109], and pneumatic [110, 111].

2.5.1 Fingertip Tactile Matrix Actuators

Fingertip tactile matrix actuators have been around since the 1960s and are designed to help the visually impaired. The OpTaCon [83] is one of the most popular fingertip tactile matrix actuators, as discussed in the previous section, but it is not untethered, handheld, wearable, or strapped on a finger. One example of a modern handheld fingertip tactile matrix actuator is the Braibook device, the first braille e-reader [112] as shown in Figure 2.21. But compared to OpTaCon, which has 144 tactile pins, Braibook has only eight tactile pins.

Fingertip tactile matrix actuators have been incorporated into computer mice to enable the visually impaired to use the computer and feel the images on the screen. The first commercially available pin-array augmented mouse was released by Virtouch Ltd (www.virtouch2.com) [113]. Unfortunately, this company is now closed. Two tactile computer mice were produced by Virtouch: (a) VTMouse, a virtual tactile matrix actuator with three 4x8 pin arrays as shown in Figure

Figure 2.21: 4x2 Braibook device. [112]

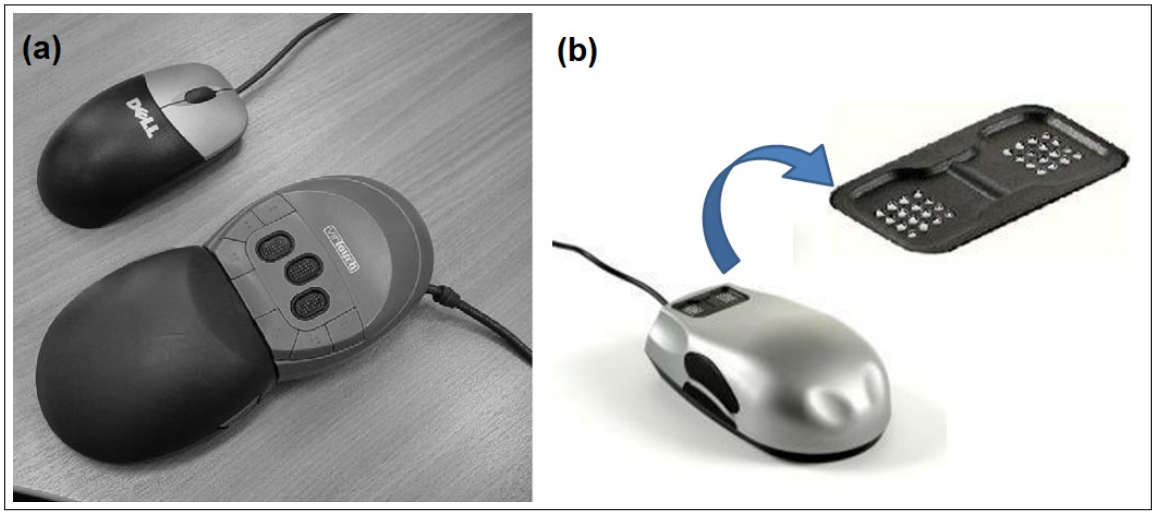

Figure 2.22: VirTouch tactile mice: (a) VTMouse a virtual tactile matrix actuators with three 4x8 pin arrays compared to standard mouse, and (b) VTPlayer tactile augmented mouse with two arrays of 4x4 pins adapted from [113].

2.22(a), and (b) VTPlayer tactile augmented mouse with two arrays of 4x4 pins as shown in Figure 2.22(b).

There are other tactile augmented computer mice such as the ones made by Watanabe et al. [114] as shown in Figure 2.23 and the low-cost tactile mouse made by Owen et al. [115] as shown in Figure 2.24. The tactile matrix in the computer

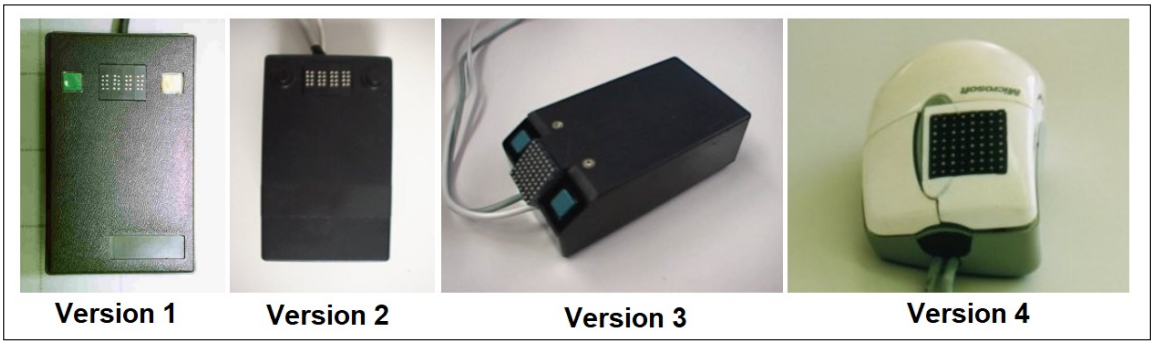

Figure 2.23: Four versions of tactile mice made by Watanabe et al. adapted from [114].

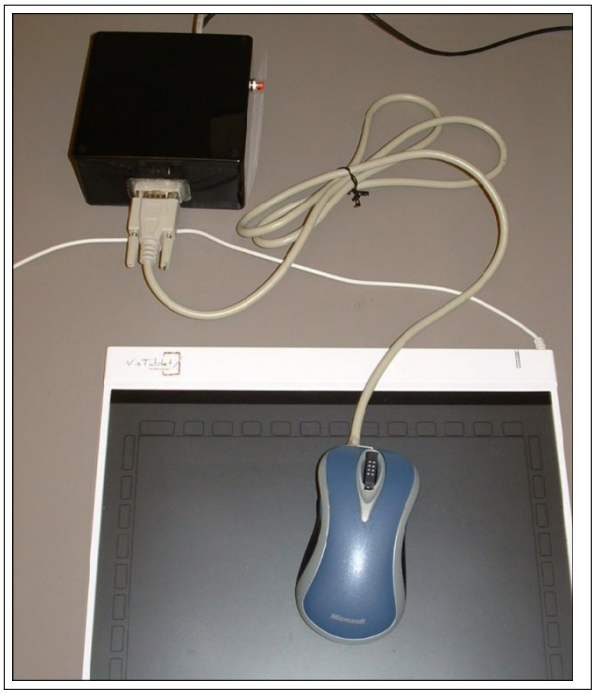

Figure 2.24: Low-cost tactile mouse made by Owen et al. adapted from [115].

mice discussed is made from piezoelectric tactile pins, which are commonly used in Braille cells. Tactile mice are used for 2D image scanning and are tethered or wired to a computer. It would be a significant improvement if these tactile matrices could be strapped on a finger and be activated wirelessly or untethered so that they can be used to feel not only 2D images but also 3D virtual objects in a VR environment.

The untethered fine-grained haptic wearable developed in this thesis has 4x4 tactile matrix actuator on each fingertips and can be used while holding any computer mouse. In effect, any computer mouse can function like a tactile mouse similar to those previously discussed.

Figure 2.25: 3x3 fingertip pneumatic balloon actuator array made by King et al. adapted from [116].

Fingertip tactile matrix actuators are not only for helping the visually impaired but can also be used as tactile augmentation for vision systems for telerobotics, telesurgery, and VR environment. As illustrated in 2.25, King et al. demonstrated a tactile matrix display in the form of a 3x2 pneumatic balloon actuator array that may be employed as cutaneous haptic feedback for surgical robotic equipment [116]. This balloon actuator display is suitable for mounting on the master controls of the da Vinci Surgical System [117]. Although the fingerpad is small, flexible, and light, the complete setup incorporates electro-pneumatic pressure regulators and an air supply, which is big, heavy, and difficult to transport. The novel untethered fine-grained haptic glove developed in this thesis is portable, light-weight, and no wires or air tubing compared to pneumatic based haptic devices.

Other cutaneous haptic feedbacks used in surgical robotic tools include the vibrotactile by McMahan et al. (2011), which can be added to Intuitive Surgical's existing da Vinci Surgical System to offer vibrotactile feedback of tool contact accelerations [118], the skin stretch or tangential motion cutaneous haptic feedback for grip control in laparoscopy demonstrated by van der Putten et al. citevan,

and the fingertip skin deformation cutaneous haptic feedback presented by Meli et al. [119] in 2014 for robot-assisted surgery.

Pacchierotti et al. developed cutaneous feedback of fingertip for palpation in robotic surgery in 2016 that incorporated fingertip skin deformation and vibrotactile feedback while ensuring the teleoperator's stability [120]. Pacchierotti et al. showed that cutaneous haptic feedback could be used to improve the performance of robotic teleoperation systems while ensuring their safety, even in the face of destabilising factors such as communication delays and harsh contacts, as illustrated in Figure 2.26.

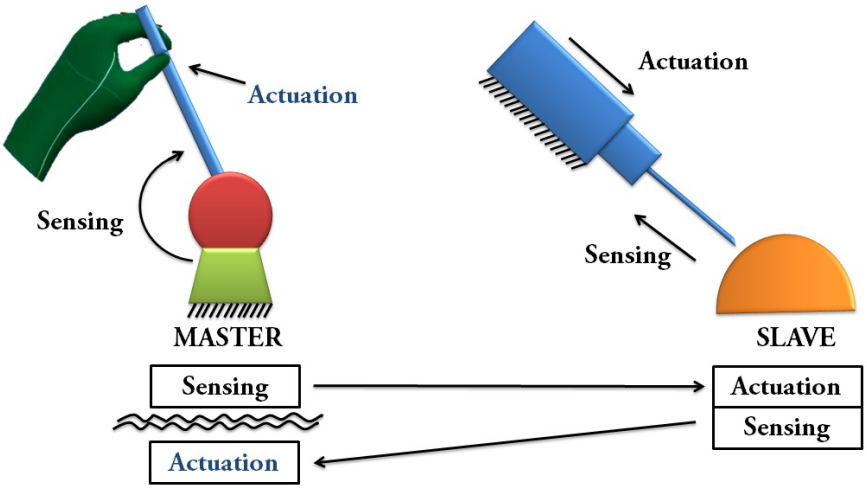

Figure 2.26: Teleoperation system with ungrounded cutaneous feedback based on the diagram by Paccheirotti et al. [16].

In the da Vinci robot, force feedback is given to the joystick or master controller whenever the surgical instrument or slave device is in contact with the medical phantom or actual body organ. However, fine-grained wearable haptic cutaneous feedback from the medical phantom in the form of vibration or texture can help the surgeon control the device in a more stable manner as compared to force feedback only [120]. Force feedback is limited to conveying information about the medical phantom in the da Vinci setup.

The sense of touch is essential for surgeons to perform tissue palpation. Li et al. [122] reported several tactile sensing that can be used to translate this touch information during surgery. They also proposed methods for providing partial

Figure 2.27: Microfluidic skin from Haptx. Fingertip size illustration with tactile actuators can displace skin up to 2mm. Picture from Haptx [121].

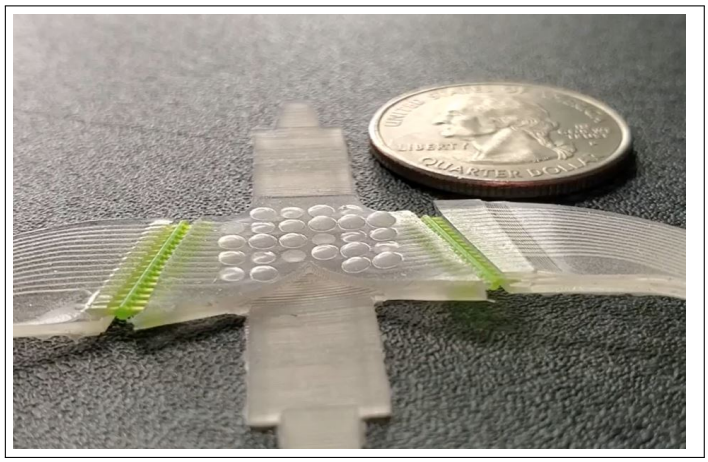

Figure 2.28: Miniaturised pneumatic actuators from Meta Reality Labs Research which use air pressure to create force. Picture from Meta Reality Labs Research [125].

haptic feedback and mimicking the physical interaction between surgical tools and human tissue during surgery to overcome the loss of touch during robotically assisted surgical procedures. The benefits of haptic feedback during surgery have been discussed and demonstrated by Li et al. [122] and Konstantinova et al. [123].

2.6 Haptic Wearables

Haptic wearables are devices worn on the fingers, hands, or other parts of the body that have cutaneous (related to skin) and/or kinesthetic (related to limb position and movement) feedback to enhance the user's immersive experience in the fields of telerobotics and VR environments. Haptic wearables are often used in conjunction with an image or visual monitor in the form of a television screen,

Figure 2.29: Commercial haptic gloves reported by Caeiro-Rodríguez et al. [126].

computer monitor, or VR/XR headset, to form a visual-haptic system for enhanced immersive experience. Haptic wearables, also called exoskeletons, can also be used in rehabilitation, such as the "Attention-Controlled Hand Exoskeleton" of Li et al. [124] used for the rehabilitation of finger extension and flexion. A haptic wearable can be a counterpart of a visuotactile sensor to actuate the tactile parameters detected by the sensor to give the user a sense of touch and feel the tactile parameters such as edges, shapes, and temperature of the image projected on the visual screen.

The wearability and portability of haptic wearable devices [17, 18, 37] that give cutaneous feedback are being explored in spatial computing research, which can directly affect the immersive experience. The realisation of a compact fingertip tactile display aiming at integration with a kinesthetic or force feedback system is a real challenge [18].

There is still a lot of work to be done to reduce the size of tactile displays without sacrificing transducer strength, spatial resolution, or bandwidth. The review paper from Pacchierotte et al. [17] on wearable haptic systems for the fingertip and hand in 2017 presents a taxonomy of wearable fingertip systems comparing their actuation technology, weight, and dimensions at the fingertip. The performance and effectiveness of teleoperation and immersive systems can be enhanced by cutaneous feedback that provides an effective way to simplify the design of a haptic wearable [17]. Moreover, Caeiro-Rodríguez et al. reported in 2021 a comprehensive and systematic review of commercial smart gloves and their applications [126]. The different commercial haptic gloves are shown in Figure 2.29. These haptic gloves are untethered and have vibrotactile, but they have no tactile display or tactile matrix actuators.

Two of the most advanced haptic hand wearable that includes tactile display or matrix of actuators are the haptic hand wearable from Meta Reality Labs Research [127] as shown in Figure 2.30 and Haptx hand wearable [121] as shown in Figure 2.31. Both haptic hand wearables have pneumatic-based tactile actuators and have wires or tubes connected to the air supply and control board. The Haptx hand wearable can be used to sense by the user the tactile feedback of telerobotic

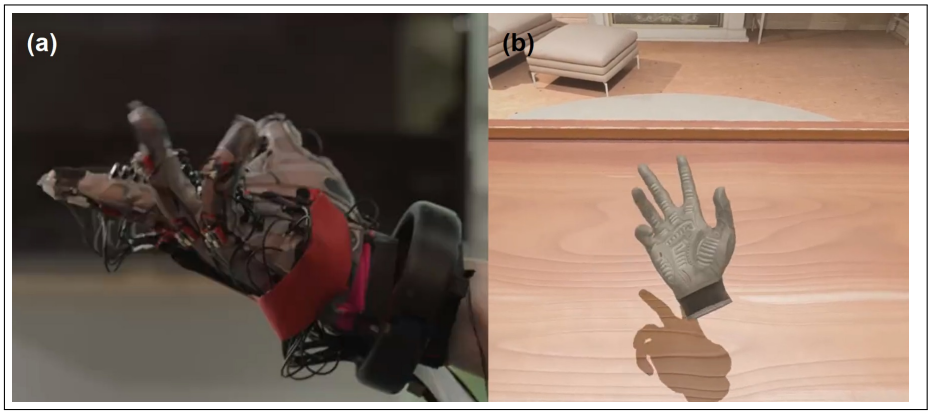

Figure 2.30: Reality Labs' haptic gloves to bring the sense of touch to the metaverse. (a) actual haptic hand wearable, and (b) the VR hand avatar corresponding to the actual hand wearable. Picture from Meta Reality Labs Research [127].

Figure 2.31: HaptX Gloves DK2 have 133 points of tactile feedback per hand. Picture from Haptx [121].

hands with Syntouch Biotac [26] sensor as demonstrated by Jeff Bezos at Amazon re:MARS conference in Las Vegas on June 5, 2019, with a snapshot as shown in Figure 2.32. The Tactile Telerobot is a joint collaboration between Shadow Robot Company, HaptX, and SynTouch [128].

The haptic wearables from Meta Reality Labs Research and Haptx are tethered as shown in Figure 2.30, Figure 2.27, and Figure 2.32 because the actuators are based on pneumatic technology. It would be a great contribution to telerobotics, telemedicine, and VR applications if there is an untethered multi-modal portable haptic hand

Figure 2.32: Jeff Bezos operates a Tactile Telerobot using Haptx hand wearable. Snapshot from Haptx [128].

wearable with high-resolution cutaneous feedback, force feedback, temperature feedback, and varying tactile pin height activation capability all in one device.

Although the finger-pad of pneumatic-based haptic systems is compact, flexible, and lightweight, like the ones from Haptx and Meta Lab, the overall setup is bulky, heavy, and not easily portable because it includes electro-pneumatic pressure regulators and air supply. The untethered multimodal fine-grained haptic wearable developed in this thesis is portable, compact, and lightweight.

2.7 Chapter Summary

This chapter summarised the different literature about haptics, emphasising visuotactile sensors that combine vision and touch modalities. The evolution of visuotactile sensors from the large pedobarograph to the compact and miniature GelSight sensor configuration has been discussed. Among the visuotactile sensors discussed, more emphasis has been given to the GelSight sensor due to its high spatial resolution in vision and high sensitivity in tactile sensing. Research gaps and challenges in creating a GelSight sensor have been highlighted. The use of switchable markers could unify tactile image recognition and force analysis because markers are not needed in tactile image recognition but are needed in tactile image

analysis to track gel deformations. Moreover, the current GelSight sensor can sense force and vibration but not temperature. A GelSight-like sensor might be able to sense haptic primary colours known as force, vibration, and temperature if the reflective layer can be made thermosensitive.

Furthermore, this chapter discussed the different tactile matrix actuators and haptic hand wearables used in telerobotics and VR applications. It covers vision substitution tactile matrix displays from the 1960s, such as the OpTaCon device, to the advanced and sophisticated haptic VR hand wearables from Meta and Haptx. One of the significant challenges in developing tactile matrix displays and haptic wearables is the form factor for miniaturisation and portability. The pneumatic technology used in Haptx and Meta glove are bulky and have long wires connecting the glove to the control unit. It would be a significant contribution if an untethered, fine-grained haptic hand resolution with force, vibration, and temperature feedback could be developed which is one of the objectives of this thesis.

3

HaptiTemp: A Low-cost GelSight-like Visuotactile Haptic Primary Colours *(force, vibration, and temperature)* Sensor

3.1 Abstract

This chapter presents the HaptiTemp sensor, a unified low-cost GelSight-like visuotactile sensor capable of sensing haptic primary colours *(force, vibration, and temperature)*. The HaptiTemp sensor has switchable UV markers that can be made visible using UV LEDs and tracked using an optical flow algorithm for tactile force analysis. The novel switchable UV markers in the HaptiTemp sensor can mitigate the trade off between marker density and showing clear tactile images. The HaptiTemp sensor can measure vibrations by counting the number of blobs or pulses detected per unit time using a blob detection algorithm. This is the first time in a GelSight-like sensor that vibration measurement has been demonstrated. Another novel feature feature of the HaptiTemp sensor is its ability to sense temperature. The HaptiTemp sensor has a novel thermosensitive reflective layer with a rapid temperature sensing capability of 643 *ms* comparable to humans' withdrawal reflex response. It can detect temperature changes at 19 °C/second

(from 31°C to 50°C in real-time). Moreover, the HaptiTemp sensor can capture high-resolution tactile images similar to the GelSight sensor. But unlike Gelsight, HaptiTemp uses a machine vision camera for stand-alone haptic primary colours *(force, vibration, and temperature)* detection and tactile image classification in wireless mode without needing an external computer. The HaptiTemp sensor can do simultaneous temperature sensing and image classification using the OpenMV Cam H7 Plus camera. This novel capability was not reported before by any tactile sensor. The HaptiTemp is the closest thing to the human skin in tactile sensing, tactile pattern recognition, and rapid temperature response.

3.2 Introduction

The gathering of visual and tactile information using a single sensor is known as visuotactile sensing. The tactile image produced by this visuotactile sensor can be utilised for texture recognition, and tactile force analysis. A passive camera, such as a webcam, or a machine vision camera with embedded computational intelligence and wireless connectivity for teleoperation can be utilised in visuotactile sensing. The conceptual framework for a visuotactile sensor that uses a machine vision camera and wireless communication is shown in Figure 3.1.

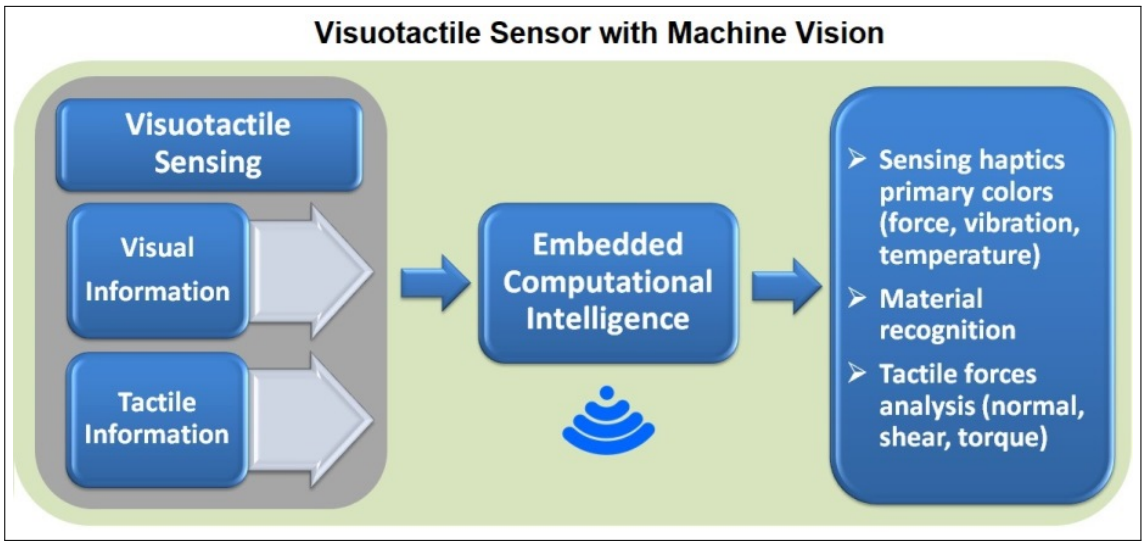

Figure 3.1: The conceptual framework for a visuotactile sensor with machine vision camera.

A visuotactile sensor works like a refreshable mould or flexible mirror, transforming physical contact on a flexible material with a reflective layer into a tactile image that a camera may see or capture. Tactile images captured by a visuotactile sensor can be evaluated in real-time to analyse tactile forces such as slip, shear, and torque or can be stored for future image processing. High-resolution tactile images, like those from the GelSight sensor [29], can be used for texture recognition or classification. A comprehensive literature review on visuotactile sensors is reported in [129].

The visuotactile sensor developed in this thesis is known as the HaptiTemp sensor. The term "HaptiTemp" combines "Haptics" and "Temperature" to emphasise that this visuotactile sensor has a novel combined tactile and temperature sensing capability like the human skin.

Because of its excellent spatial resolution in vision [61] and high sensitivity in tactile [62], the GelSight sensor [29] has become the reference of HaptiTemp sensor developed in this thesis. The GelSight sensor has demonstrated its worth in a variety of haptics, computer vision, and robotics applications. However, there are several limitations and areas of improvements with the present GelSight sensor that were addressed by the HaptiTemp sensor.

The HaptiTemp sensor has the following novelty or advantages relative to the GelSight sensor:

1) The HaptiTemp Sensor has novel switchable UV markers:

Permanent markers have divided the GelSight sensor into two distinct sensors: one without markers and one with markers. Permanent markers can be viewed from the perspective of image processing as either image features that can aid in the analysis of force, shear, and slip or as a feature that is not necessary in image recognition or classification. Permanent markers may be viewed as noise that degrades some crucial 2D image properties, particularly if they are larger than the image features.

Additionally, according to Yuan et al., increasing markers' density can impact the GelSight sensor's capacity to measure height maps [65]. The images provided in

[82, 131, 132], where the GelSight sensor with permanent dot markers was employed in fabric or textile characterisation, demonstrate the problem that markers can be a noise and may mask patterns in 2D images. The use of two kinds of GelSight sensors, with and without markers, is presented in [133]. The HaptiTemp sensor developed in this thesis can mitigate the trade-off between marker density and the GelSight function of providing a clear tactile image for image classification by using switchable UV markers that can be made visible using UV LEDs.

2) The HaptiTemp sensor is a low-cost GelSight-like sensor that uses COTS cosmetic silicone sponge:

Current GelSight sensor's elastomers are manufactured in the lab with thermoplastic elastomer (TPE), which requires an oven to melt in a mould, or silicones, which are made up of two separate liquid portions that when mixed together form a firm gel [60]. The long curing period of around six to seven hours [60], quality consistency [61], and the development of air bubbles within a gel that requires vacuum pump degassing [50, 60, 61] are three main problems in generating a transparent elastomer. Apart from these issues, the GelSight sensor elastomer can be easily broken when performing contact-intensive manipulation tasks like gripping [63]. The HaptiTemp sensor has skipped the complex process of creating a clear elastomer and long curing time using commercially available silicone cosmetic sponge.

3) The HaptiTemp sensor can measure vibrations:

The HaptiTemp sensor can measure vibrations by counting the number of blobs or pulses detected per unit time using blob detection algorithm. This is the first time in a GelSight-like sensor that vibration measurement has been demonstrated.

4) The HaptiTemp has thermosensitive reflective layer:

The HaptiTemp sensor can detect temperature. The first of its kind in any GelSight-like sensor that can capture high-resolution tactile images. It has a similar structure to the GelSight, but the reflective coating has been enhanced by using thermosensitive colour pigments, making it capable of detecting the temperature of the contacted object. By having a thermosensitive reflective layer, the HaptiTemp sensor becomes a fully Haptic Primary colour visuotactile sensor capable of detecting

force, vibration, and temperature. Moreover, the HaptiTemp sensor has a very fast temperature response of 643 *ms* similar to the human withdrawal reflex. The rapid temperature response of the HaptiTemp sensor is comparable to the less than one second time withdrawal reflex response of the human autonomic system to extreme heat [130]. The HaptiTemp sensor can detect temperatures from 31°C to 50°C which is much wider than the GelForce sensor's temperature range of 32°C to 35°C.

5) The HaptiTemp sensor can do tactile sensing, temperature sensing, and image classification in a stand-alone configuration:

The HaptiTemp sensor uses a machine vision camera, the OpenMV Cam H7 Plus Camera, that has embedded machine learning hardware and image processing capability in a stand-alone module with WiFi connectivity. Using a machine vision camera, the HaptiTemp sensor has become a compact, portable, and stand-alone module that can do tactile sensing and image classification in wireless mode without needing an external computer during operation. This is the first time any GelSight-like sensor has used a machine vision camera to make it a stand-alone sensor module that can do tactile sensing and image recognition. The HaptiTemp sensor can do simultaneous temperature sensing and image classification, a novel capability not yet reported or demonstrated by any tactile sensor.

3.3 HaptiTemp's Hardware

The HaptiTemp sensor is based on GelSight sensor technology, which has four essential components based on the listing made by Jia et al. [30]: 1) clear elastomer with a reflective coating on one side, also known as the retrographic sensor [29], 2) transparent plate support for the elastomer, 3) controlled and uniform lighting usually from Light Emitting Diodes (LED), and 4) camera to capture the retrographic image [29, 61] or the tactile image of the contacted object.

The schematic of the HaptiTemp sensor is shown in Figure 3.2(a). It is similar to the schematic of the GelSight sensor, but the gel material has a thermosensitive reflective coating on top of the UV markers. The HaptiTemp sensor has two prototypes. The first prototype, as shown in Figure 3.2(b), uses a machine vision

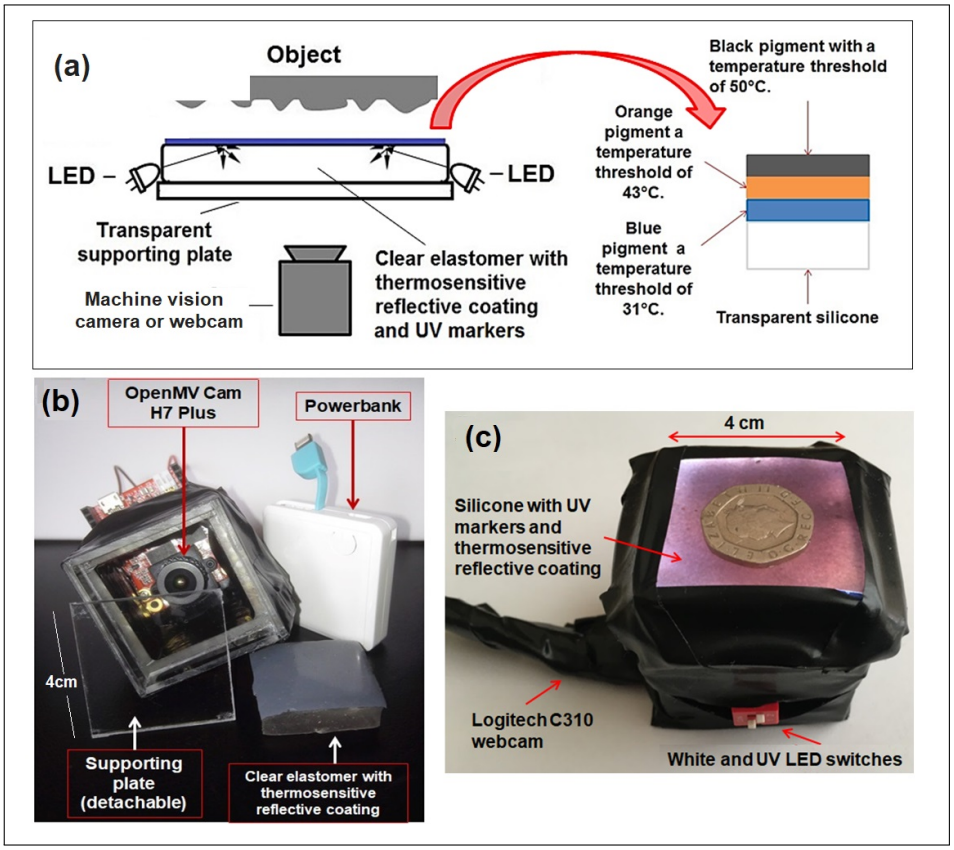

Figure 3.2: The HaptiTemp sensor with a cubic structure with a side-length of 4 cm. (a) The schematic of the HaptiTemp sensor. (b) The HaptiTemp sensor with machine vision camera (OpenMV Cam H7 Plus), and (c) the HaptiTemp sensor with ordinary webcam (Logitech C310).

.

camera (OpenMV Cam H7 Plus) for onboard tactile sensing and tactile image classification. In contrast, the second prototype, as shown in Figure 3.2(c), uses an ordinary webcam.

3.3.1 Clear Elastomer with Thermosensitive Reflective Coating

In 2009, Johnson and Adelson from MIT introduced a novel high-resolution visuotactile sensor made from a transparent elastomer with a reflective coating on one side that converted surface shape and pressure into an image. They called the device a “retrographic sensor" because it produces the image of the contacted object on the opposite side of the flexible material [29]. They introduced it not as a tactile sensor but as a 2.5D scanner for metrology, but gave insights that it may be used

for tactile sensing. The retrographic sensor, which later became the GelSight sensor, is like a human eye-skin extension because it can produce a high-resolution tactile image or an image of the contact area between the sensor and the object of interest.

3.3.1.1 Clear Elastomer

Fabrication of a clear elastomer is one of the challenges in constructing a GelSight-like sensor. Yuan [60] discussed how to create a clear elastomer using commercially available polymers: Solaris® from Smooth-on Company, and XP-565 from Silicones Inc. Both of these polymers come in two liquid parts (A and B) that are mixed together to form a clear silicone gel. Solaris® has a mixing ratio of 1:1, while XP-565 has a typical mixing ratio of around 1:10 by weight [60]. After mixing the two parts, the liquid mixture is put into a vacuum pump for degassing. The mixture is poured into a mould, either a flat tray or a concave mould and let solidify for about six or seven hours. The hardness of the elastomer can be adjusted by changing the ratio of parts A and B [56, 60].

The HaptiTemp sensor used a clear Commercial Off-The-Shelf (COTS) silicone cosmetic sponge to skip the lengthy curing time (6-7 hours) [60], as well as the degassing process to remove the silicone gel bubbles [60, 61, 62]. An elastomeric slab made from COTS silicone sponge is shown in Figure 3.3. COTS silicones have different Shore A values such 7 and 2.5 as shown in Figure 3.4(a) and Figure 3.4(b) respectively. The silicone sponge may also have a cushion or foam, as shown in Figure 3.3(a), that can be easily removed by cutting the edges, as shown in Figure 3.3(b). There is also a COTS silicone sponge with only clear plastic, as shown in Figure 3.3(c). COTS silicone come in different variety of sizes, colours, and shapes.

Although the 8 *mm* thickness of COTS clear silicone is thicker than the 1 *mm* to 2 *mm* thickness utilised in current GelSight sensor devices [60], it may have a significant benefit in sensing normal force since it allows for more downward pressure. In comparison to the original GelSight elastomer as shown in Figure 2.9a and in this video [73], the COTS elastomer is thinner.

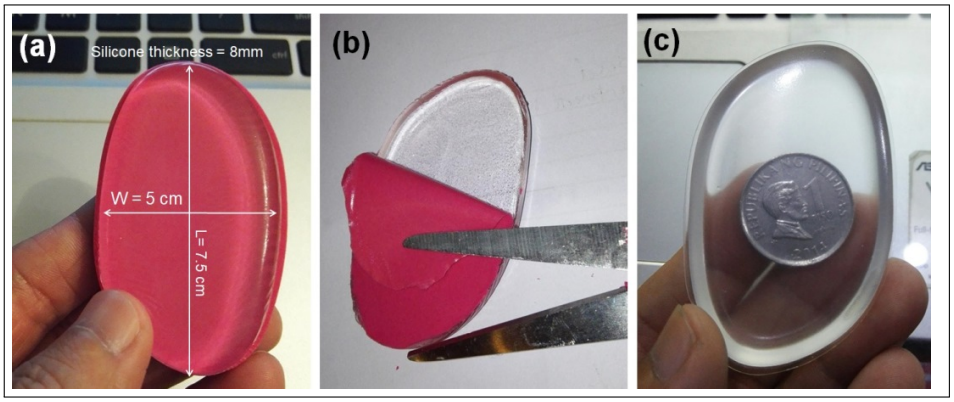

Figure 3.3: COTS clear silicone sponge. (a) Clear silicone with cushion. (b) remove the cushion by cutting the edges, and (c) clear silicone after cushion removal

.

(a) Shore A reading for transparent silicone sponge.

(b) Shore A reading for silicone with pink cushion.

Figure 3.4: Hardness of COTS silicone sponges (Shore A measurements) which are close or within the Shore A values (Shore A 5-20) used in GelSight sensors as reported in [56].

3.3.1.2 Thermosensitive Reflective Coating

The silicone, as shown in Figure 3.3(c), can be painted on either side as shown in Figure 3.5a. Silver metallic spray paint can be used as a reflective coating without removing the thin plastic covering of the silicone sponge. However, higher resolution tactile images can be captured by removing the thin plastic covering of the silicone sponge of Figure 3.3(c). Commercially available spray paint in cans does not stick properly on silicone. The reflective coating that can be used in silicone has been discussed in [60, 56] which is a silicone-based paint with colour pigment. There is a need to create a silicone mixture with colour pigment to be sprayed on a clear silicone gel. The thin layer of coloured silicone will bind with

the clear silicone to form one silicone slab. Psycho Paint® [134] silicone mixture from Smooth-On Inc. and white and black pigments of Silc Pig™ [135] were mixed to create a grey colour similar to aluminium. Psycho Paint® with pigment were diluted using Novocs™ Matte [136] and used an airbrush to spray the mixture on the silicone sponge as shown in Figure 3.3(b).

(a) After coating: the silicone sponge in Fig. 1(a).

(b) After coating: the silicone sponge in Fig. 1(b).

Figure 3.5: After coating.

The thermosensitive reflective coating of the HaptiTemp sensor is made using thermochromic pigments instead of the ordinary pigments reported by Yuan et al. [56]. The HaptiTemp sensor is the first GelSight-like sensor that uses thermosensitive pigments in the reflective coating. A hot or cold (binary temperature) sensor can be developed using a single layer of thermochromic pigment that changes from its base colour, as shown in Figure 3.6(a), to translucent when it reaches the thermal threshold, as shown in Figure 3.6(b). In this example, a black pigment with a 31°C temperature threshold turns white to translucent whenever the sensor is in contact with the human body. Because of the translucent property of the second type of thermochromic pigments when its the temperature threshold is reached, different pigment layers of different colours with increasing thermal thresholds can be put on top of the other to sense different temperature ranges as shown in Figure 3.7(a) and Figure 3.7(b) respectively. The layering of different thermochromic pigments with different thresholds made it possible to expand the temperature sensing range of the HaptiTemp sensor.

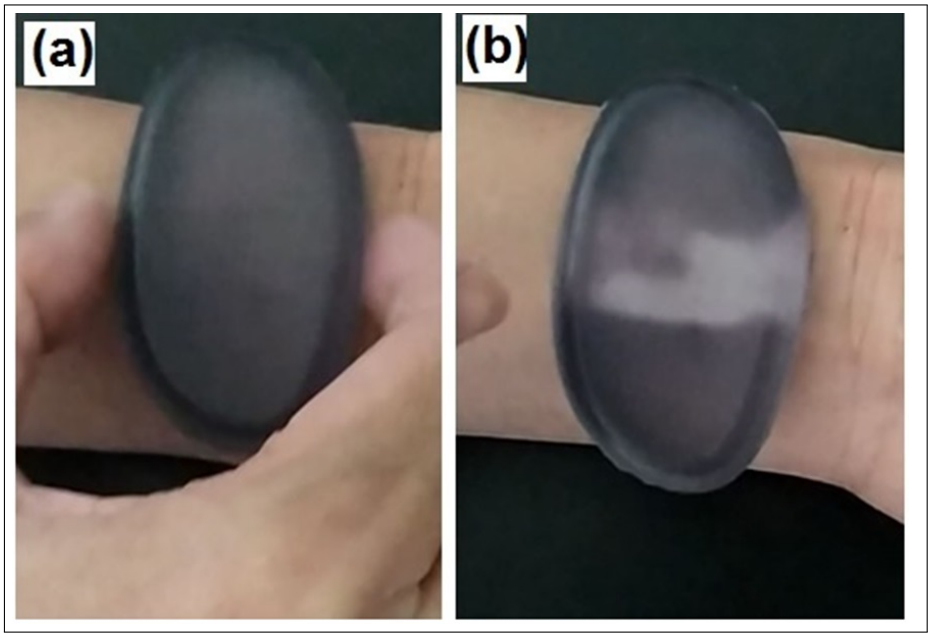

Figure 3.6: colour-to-transparent changing thermochromic pigment. (a) inactive black thermochromic pigment with 31°C threshold, (b) thermosensitive pigment was activated by body heat.

In contrast to the finger-shaped GelForce that used thermosensitive liquid crystal sheets [45, 70], the HaptiTemp sensor used different layers of thermochromic pigments with different colours and thresholds painted on the reflective coating. The HaptiTemp sensor has a wider temperature range of 31°C-50°C compared to the 32°C-35°C of GelForce. Moreover, the HaptiTemp sensor can capture high-resolution images which the GelForce cannot do.

Three thermochromic pigments, from Hali [72], that change colour to translucent when activated were arranged on top of each other with increasing thresholds, as shown in Figure 3.7(a). The blue pigment with threshold of 31°C is closest to the clear silicone slab, then the orange pigment with threshold of 43°C was painted on top of the blue pigment, followed the black pigment with a 50°C temperature threshold. The layering of pigments is shown in Figure 3.7(b). Each thermochromic pigment becomes translucent whenever its temperature threshold is reached, making it possible to make a gradient change in colour. From the camera's point of view, the blue layer becomes transparent to show the orange pigment when the temperature threshold of blue is reached. The same holds true when the temperature crosses the

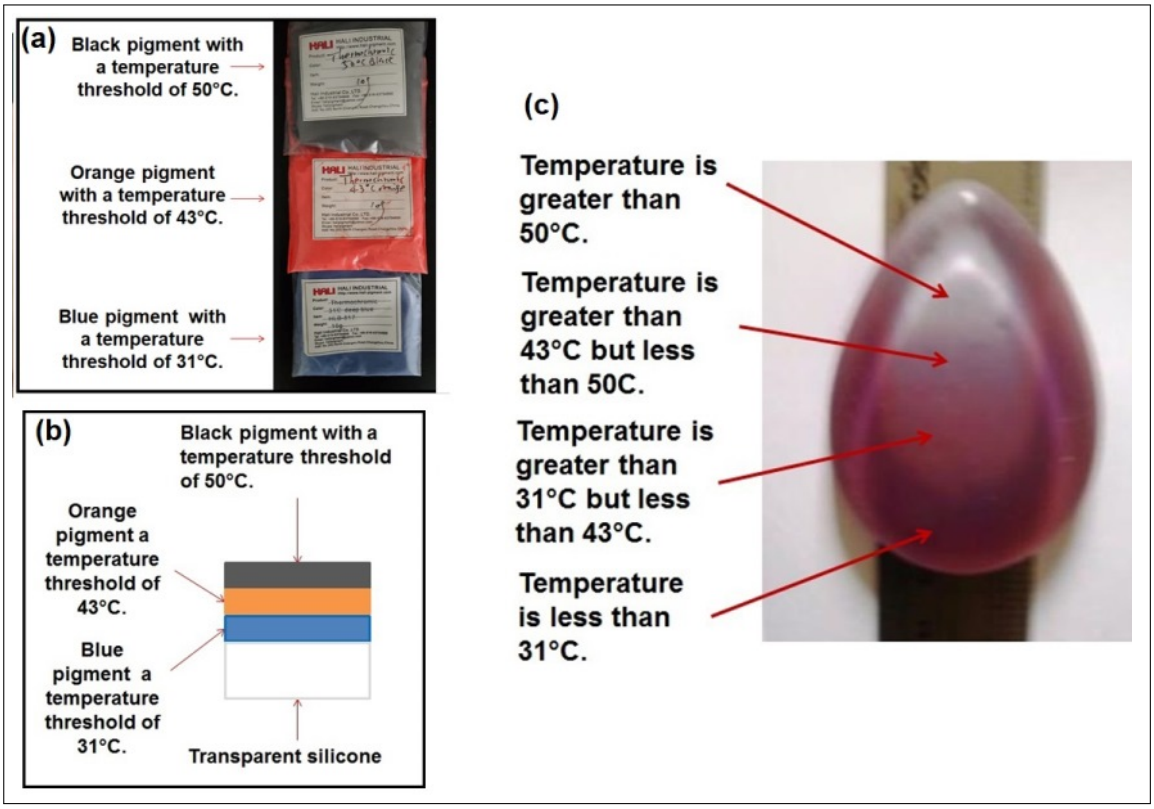

Figure 3.7: colour-to-transparent layered thermochromic pigments. (a) three thermochromic pigments [72] with different thresholds: blue (31°C), orange (43°C), black (50°C). (b) cross section of HaptiTemp sensor's gel material, and (c) HaptiTemp sensor's gel at different temperatures.

orange-to-black transition point. The layering order of increasing the temperature threshold from the clear gel is very important to sense a wide range of temperatures. The HaptiTemp sensor, which has layers of thermochromic pigments, displayed multiple colours when it was placed on top of a metal ruler that had been heated at one end, as seen in Figure 3.7(c), which depicts the temperature gradient of the metal ruler. Please note: that this is just a visual representation of temperature-sensitive colours. This feature has been carried out to design the cover temperature-sensitive visuotactile sensor with machine vision. The automation is presented with characteristic curves to demonstrate the temperature gradient.

3.3.1.3 Switchable UV Markers

The GelSight sensors that are created in the lab can either have permanent markers or not. GelSight sensors with markers are best for force, slip, shear, or torque

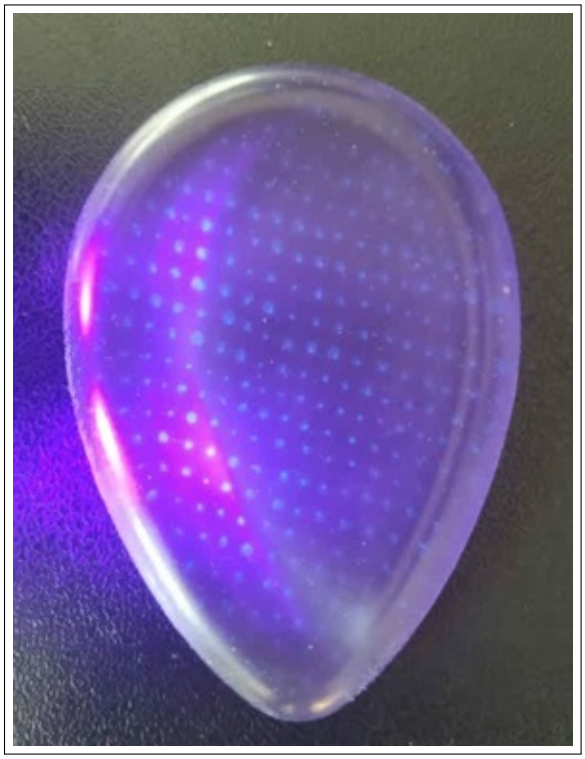

Figure 3.8: UV markers.

analysis. On the other hand, GelSight sensors with no markers are best for texture recognition and microgeometry analysis because the markers can obscure some important image features. Yuan first introduced permanent markers in 2014 [60], placing dots or triangles on the GelSight sensor's reflective layer. For estimation is done using an optical flow algorithm or flow vector arrows to track the movement of markers as the gel deforms when contacted by an object [56, 60]. GelSight sensor used in microgeometry [61], lump detection [30], texture analysis [29], and tactile mapping [64] do not have grid dots or permanent markers. On the other hand, GelSight sensor used in hardness estimation [66] and measurement of shear and slip [56, 65, 51, 81] has permanent markers.

However, the permanent markers in the reflective coating of the GelSight sensor might conceal some important image features that are helpful for object recognition [129]. Permanent markers might negatively affect some important 2D image features, especially if these markers are more significant than the image features [56]. This issue might be observed in the images presented in [82, 131, 132] where the GelSight

sensor with permanent markers was used in textile characterisation and classification. Moreover, the capability of the GelSight sensor to measure contact surfaces' height map is affected by the density of permanent markers [65].

By using the switchable UV markings, the trade off between marker density and the GelSight sensor's function of showing a clear tactile image for objection recognition can be mitigated or eliminated. In one grip or in one press, the tactile image of the object be recognised or classified through 2D image feature extraction, and study shear and slip can be recorded.

Permanent markers might be treated as noise in 2D image processing. The HaptiTemp sensor has the UV markers printed into the gel, as shown in Figure 3.8. These UV markers can then be clearly tracked when activated by UV light. Slip, shear, and torsion can be visualised using an optical flow algorithm and vector arrows to track these markers. The development of a unified visuotactile sensor that can be utilised for tactile image classification and tactile force analysis using one elastomeric slab was made possible through switchable UV markers. The use of switchable UV markers lessens the drawbacks of permanent markers that could obscure some crucial image details that could be useful for image recognition and classification, especially if the markers are more significant or larger than the image features.

3.3.2 Transparent Plate Support

Transparent plate support for the clear gel can be a glass or clear acrylic plate. Aside from the original GelSight sensor made in 2009 [29] that uses a glass supporting plate, all other GelSight sensors use a clear acrylic supporting plate because an acrylic plate is more durable and lightweight compared to glass. A clear acrylic plate 4 cm x 4 cm x 2 mm is used for prototypes shown in Figure 3.2(b) and Figure 3.2(c).

The HaptiTemp sensor used clear acrylic plate support. Clear acrylic plates can be used as supporting plates for the gel as well as waveguides to produce uniform lighting similar to fingertip GelSight [32]. Although the silicone sponge can be cut to any size using a blade, different sensor structures can be made using

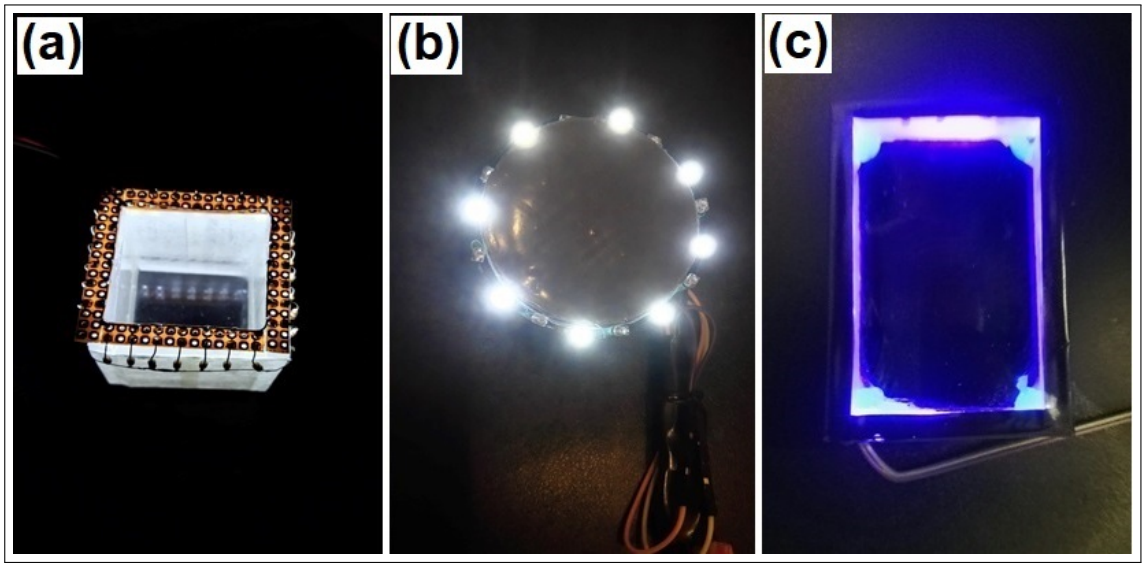

Figure 3.9: LED lighting with 1.8mm ultra-bright white and UV LEDs arranged alternately: (a) cube with white LEDs on, (b) circular configuration, (c) 1.8 mm UV LEDs illuminating a rectangular box.

acrylic plates such as cubes as shown in Figure 3.9a, cylindrical as shown in Figure 3.9b, and rectangular configurations Figure 3.9c.

3.3.3 LED Lighting

All other GelSight sensor structures feature multicoloured LED lighting for the photometric stereo technique, with the exception of GelSlim [57], which employs two high-powered, neutral white, surface-mount LEDs (OSLON SSL 80) on both sides of the finger. Since the HaptiTemp sensor focus only on tactile sensing and image classification, monochrome lighting is enough.

Because the HaptiTemp sensor has switchable UV markers, the use of UV LEDs as a new form of lighting is introduced in this thesis. Alternating 1.8 *mm* white and UV LEDs are mounted on HaptiTemp sensor. White LEDs are on, as shown in Figure 3.9a and Figure 3.9b, while UV LEDs are on, as shown in Figure 3.9c. The white and UV LEDs can be switched on or off manually using a small mechanical switch or electronically using the built-in General-Purpose Input/Output (GPIO) pins of the machine vision camera.

3.3.4 Machine Vision Camera

Current GelSight sensors use an ordinary passive camera such as a webcam and raspberry pi camera. All the image processing, with or without the help of artificial intelligence, was done using a desktop or laptop computer. Thus, a more compact and unified stand-alone solution is presented in this thesis using a machine vision OpenMV Cam H7 Plus camera for onboard tactile image recognition. It has a built-in STM32H743II ARM Cortex M7 processor capable of Edge Impulse integration for easy training of TensorFlow Lite Models [137].

A machine vision camera, as opposed to a passive camera, features embedded machine learning hardware, GPIO ports, and an image processor that may have a machine vision library that can perform image processing in real time. Image classification can be done within the camera module without needing an external computer.

The webcam can be swapped out with a machine vision camera to create a standalone GelSight-like sensor that can classify images and analyse haptic forces. There are a machine vision camera modules on the market, such as M5StickV [138], Sipeed MAix Go [139], Jevois [140], Kittenbot Koi AI [141], Google AIY vision kit [142], Huskylens [143], OpenCV AI Kit (OAK) [144], and OpenMV Cam H7 Plus [137]. The OpenMV Cam H7 Plus was used in the HaptiTemp sensor, as shown in Figure 3.2(b), because it can do image classification and image processing at the same time.

The first GelSight-like sensor that makes use of a machine vision camera is the HaptiTemp sensor. The HaptiTemp sensor, as shown in Figure 3.2(b), differs from earlier prototypes of the GelSight sensor. By turning the lens cover, the OpenMV Cam H7 Plus lens focus can be manually changed. In order to expose the machine vision camera, the HaptiTemp sensor features a removable supporting plate for the silicone. As a result, when the thermosensitive silicone is removed, the OpenMV Cam H7 Plus machine vision camera can be utilised for common applications such as image acquisition, image feature analysis, and pattern recognition. The machine vision camera can be utilised for the common purposes of image capture when

the silicone material has been removed. The HaptiTemp sensor's modular design increases the novelty and adaptability of employing a machine vision camera.

3.4 HaptiTemp's Software

3.4.1 Software: Firmware and Application Layer

The image processing was done with the aid of Python and OpenCV software. The tracking of UV markers using optical flow algorithm [76] and flow vector arrows was done to see the forces acting on the gel as it deformed when an object came into contact with the sensor. Additionally, by counting how many blobs are recognised each second using the blob detection algorithm [145], vibrations can be calculated. Using the Arduino microcontroller and PID controller library, ThermoElectric Generator (TEG) with a thermistor as temperature feedback were used to set different temperatures. The HaptiTemp sensor's capability to sense temperature was tested using the TEG. Hue values at 30°C, 35°C, 40°C, 45°C, and 50°C were recorded in the text file data log using the built-in OpenCV function to record HSV values in a specified Region Of Interest (ROI).

3.4.2 OpenMV

The OpenMV integrated development environment (IDE) that uses MicroPython programming language is the premier IDE for use with OpenMV Cam. It features a powerful text editor, debug terminal, and frame buffer viewer with a histogram display, and built-in machine vision code examples [146]. Using OpenMV IDE, datasets were built and uploaded to Edge Impulse [147] in the cloud. Transfer learning with MobileNetV2 was used to generate a TensorFlow Lite Convolutional Neural Network (CNN) that runs on board with the OpenMV Cam H7 Plus. A step-by-step tutorial on how to do image classification using OpenMV IDE and Edge Impulse can be found in these links: [148], and [149].

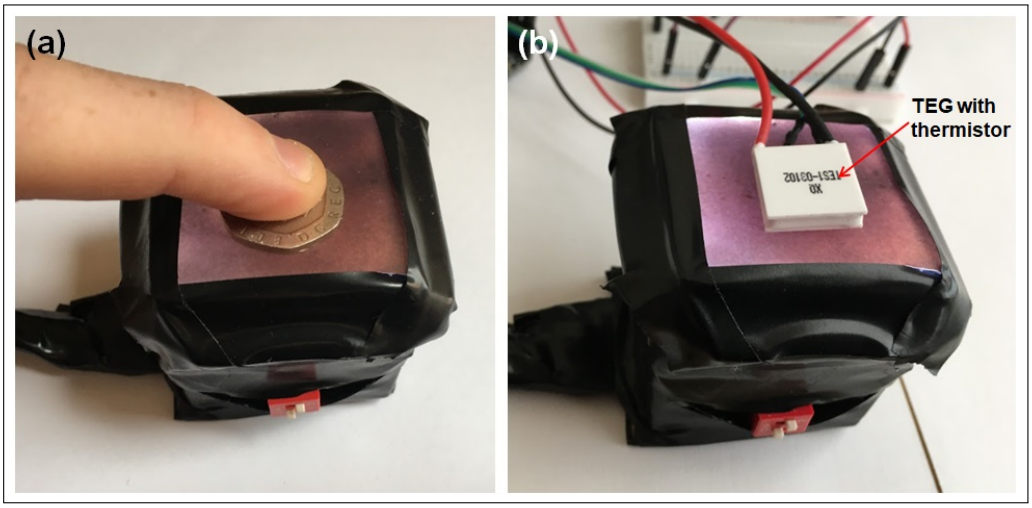

Figure 3.10: Test setups: (a) force and vibration tests, and (b) temperature test.

3.5 Sensor Testing and Validation

The HaptiTemp sensor is a GelSight-like visuotactile sensor that can sense not only force but also vibration and temperature, thus making it a haptic primary colours sensor. For the force and vibration tests, an object is pushed on the sensor, as shown Figure 3.10(a). With the use of TEG with PID controller, the HaptiTemp sensor was tested at different temperatures as shown in Figure 3.10(b). A thermistor was used as temperature feedback. The HaptiTemp sensor can also classify tactile images using a machine vision camera. The force sensing methodologies are primarily based on the methods reported in different GelSight sensor papers [34, 150]. When an object is pushed on the sensor, an image or a blob is created and can be analysed using image processing technique known as "blob detection algorithm". Though vibration or pulse rate sensing was demonstrated using a GelSight sensor in a YouTube video [73], no paper was published about this. For the first time in GelSight-like sensors, this thesis presents a method of measuring vibrations by counting the number of blobs or pulses per unit time using blob detection algorithm. Moreover, since the temperature sensing capability of the HaptiTemp sensor is a novel contribution, different testing methodologies are presented in this chapter.

Furthermore, the tactile image recognition methodology is based on the existing usage of available machine vision algorithms such as AlexNet and MobileNet. More

details about the different approaches and methodologies are presented in the following sections:

3.5.1 Force Sensing

Flow vector arrows indicating the direction and amount of force applied by the object contacting the gel can be visually presented by switching the UV markers using UV LEDs and tracking them with an optical flow algorithm. A dynamic bounding box that follows the contour of the blob [145] and a reference bounding box that does not rotate can be used to further visualise force and direction. The dynamic bounding box calculates the contacted object's approximate length and width. As the normal force increases, the bounding boxes' surface area grows. To determine the direction of motion within the frame, the movement of the blob's center can tracked and compute the tilt or shear angle relative to the reference bounding box. This approach is comparable to the pose estimation method put forth by She et al. [150].

3.5.2 Vibration Sensing

Vibrations in Hertz or beats per minute can be calculated by counting the number of blobs detected per unit of time using a blob detection algorithm [145]. The maximum possible vibration that the HaptiTemp sensor can detect is half the frame rate of the camera used by the sensor. The vibration sensing capability of the HaptiTemp sensor was tested using a small solenoid activated at a 5 Hz tapping frequency attached to it.

3.5.3 Temperature Sensing

The HaptiTemp sensor was evaluated using TEG TES1-03102 15 mm x 15 mm Peltier ThermoElectric Generator (TEG). The temperature was deduced from the Lightness value from the LAB colour space and the Hue value from the HSV colour space.

3.5.3.1 Temperature Test using LAB colour Space

The OpenMV Cam H7 Plus machine vision camera, which features LAB colour space library functions, was employed for this test. A 2.4V DC power supply using two rechargeable dry cells was used to heat the TEG slowly. Using two identical TEGs, one has a thermistor and the other connected to the HaptiTemp sensor, the temperature reading and the LAB mode values were recorded, respectively, as the TEG's temperature rose. The temperature sweep time took 23 s from 23°C to 55°C. The HaptiTemp sensor uses LED lighting for uniform and controlled lighting.

3.5.3.2 Temperature Response time

Using the same setup with machine vision camera, temperature response time was recorded with respect to the machine cycle time of the microcontroller. By supplying a 3.6V DC supply to the TEG, it heats up faster compared to a 2.4V DC supply covering the same span of L mode values. The thermistor has a slower response compared to the HaptiTemp sensor. The epoxy encapsulated NTC thermistor used in the testing has a response time of 19.54 s for temperature changes 25°C to 41°C based on this report [151]. The response time of the HaptiTemp sensor was measured by flipping the TEG's hot and cold plates and recording the time at which the sensor's reflective layer changes from blue to transparent.

3.5.3.3 Temperature Test using HSV colour Space

In this test, the HSV values within a specified ROI were captured using a webcam and a computer with the OpenCV library. A TEG stabilised by a PID controller with thermistor temperature feedback was used as a stimulus in testing the HaptiTemp sensor. Average hue values were captured and recorded inside a 40 x 40 pixel ROI at temperatures of 25°C, 30°C, 35°C, 40°C, 45°C, and 50°C. Ten trials were recorded for each temperature. The temperature test of HaptiTemp has a more comprehensive range compared to the 32°C-35°C range of finger-shaped GelForce [45, 70].

3.5.4 Tactile Image Recognition

The HaptiTemp sensor has the flexibility to use ordinary webcam like a typical GelSight sensors, or a machine vision camera for stand-alone tactile sensing and image classification. This section discusses the use of machine vision algorithms such as AlexNet and MobileNet in tactile image processing using transfer learning.

3.5.4.1 Tactile Image Recognition using a Personal Computer (centralised computing)

When the HaptiTemp sensor uses a webcam, the setup mimics the central nervous system where all the captured tactile images are processed and classified using a desktop or laptop computer. In this thesis, object recognition was demonstrated using the low-cost GelSight-like sensor with UV markings to recognise five different coins One Peso old (1PHO), One Peso new (1PHN), One Pound UK (1UK), Five Peso (5PH), and Ten Peso (10PH) using Convolutional Neural Network (CNN) named AlexNet [152]. Five hundred images for each coin were captured to train the CNN. AlexNet is a CNN trained on more than a million images from the ImageNet database [38]. It is eight layers deep and could be used to classify images into over a thousand different object categories. It has learned diverse feature representations for a wide range of images. This thesis used tactile images with 227 by 227 pixels to train the AlexNet through transfer learning using a personal computer and MATLAB R2019a.

Figure 3.11: Different coins for recognition test: (a) One Peso old (1PHO), (b) One Peso new (1PHN), (c) One Pound UK (1UK), (d) Five Peso (5PH), and (e) Ten Peso (10PH)

3.5.4.2 Tactile Image Recognition using Machine Vision Camera

When the HaptiTemp sensor uses the OpenMV Cam H7 Plus machine vision camera, the setup mimics the peripheral nervous system, where tactile images are processed not on a personal computer but on a stand-alone machine vision camera capable of edge computing for distributed processing. Different tactile images were collected using Edge Impulse [149] and a machine vision camera, the OpenMV Cam H7 Plus, to form a dataset. Then, a transfer learning to train a MobileNet neural network was executed and deployed the system to the machine vision camera for stand-alone tactile image classification. According to [149], 30 images are sufficient, yet 40 image samples from each of the five different objects were collected: the one-pound UK coin, the hex end of a precision screwdriver, and I, O, and X letters from a cookie stamp. Forty (40) images of the blank screen when there is no object being touched by the sensor were also collected and included in the dataset. A total of 240 images were captured and uploaded to the Edge Impulse cloud, which automatically divided them into 182 training samples and 58 testing samples. The number of image samples needed for transfer learning using MobileNet neural network is much smaller compared to the AlexNet used as discussed in the previous section. The MobileNet neural network architecture is designed for stand-alone image classification for edge computing.

3.5.5 Simultaneous Temperature Sensing and Image Classification

The HaptiTemp sensor can do temperature sensing and image classification simultaneously by combining the algorithms of temperature sensing and tactile image classification. The two algorithms work simultaneously inside the machine vision camera, the OpenMV Cam H7 Plus. This novel capability of the HaptiTemp sensor to sense tactile parameters and do tactile image classification simultaneously within the sensor module without needing an external computer has not been demonstrated or reported before by any tactile sensor. The simultaneous sensing and image classification can be done if the machine vision camera has image

processing library and machine learning hardware on the same module. Unlike other machine vision cameras that can only do image classification through transfer learning, the OpenMV Cam H7 Plus Camera has an image processing library that can run simultaneously with image classification. The results of temperature sensing and tactile image classification can be combined into a single frame.

A UK one-pound coin and the end of a hex screwdriver were used to demonstrate the combined temperature and tactile image classification test. These two metals were pressed to the sensor when they were cold, and the results were recorded. Then, the objects were heated and pressed again to the sensor. The temperature of the object, as well as the tactile image classification, were recorded.

3.5.6 Wireless Connectivity

Using a WiFi module WiFi module [153], the HaptiTemp sensor with OpenMV Cam H7 Plus machine vision camera can be wirelessly connected for teleoperation applications. Thus, making HaptiTemp an untethered, portable, and stand-alone sensor. The WiFi module uses an ATWINC1500 network controller. Images can be transmitted via WiFi in two possible modes: 1) station mode, which is the default mode wherein the module connects to an access point as a client, and b) the Access Point (AP) mode, wherein the module acts as a hotspot and can accept connection from a client [154].

3.6 Results

3.6.1 Force Sensing

The HaptiTemp sensor has a novel tactile switchable UV markers on the reflective coating for tactile sensing and analysis. When the UV markers are invisible, the result is like the typical image produced by the GelSight sensor, as shown in Figure 3.12(a) and Figure 3.12(c). UV markers are tracked with algorithms such as optical flow when studying shear and slip. Forces in the form of slip and shear from the contacted object can be deduced from the gel deformations with UV markers using an optical flow algorithm. The novel UV markers have been taken into account to

make an optical flow vector. The results showed that the optical flow vector could be used to deduce slip/shear, magnitude, and direction of the applied force to the coin pressed towards the elastomer as shown in Figure 3.12(e) and Figure 3.12(f). The length of the arrow pointing in the direction of the applied force increases as more force is exerted on the coin. Moreover, a torque or rotational force can also be visualised using the flow vector arrows. The displacement field from the fingertip twisting the elastomer in an anticlockwise and clockwise direction are shown in Figure 3.12(g) and Figure 3.12(h), respectively. Yuan et al. reported a detailed analysis of how to analyse shear and slip based on GelSight sensor markers' displacement field [34].

Moreover, a dynamic bounding box that rotates relative to a reference bounding box that does not rotate can also be used to visualise force and tilt or rotation. The dynamic bounding box measures the approximate length and width of the contacted object as shown in Figure 3.12(i). The area of the bounding boxes becomes bigger as the normal force increases. The tilt angle or shear angle can be computed relative to the reference bounding box, and the movement of the centre of the blob can be tracked to know the direction of motion within the frame.

3.6.2 Vibration Sensing

Vibrations results by counting the number of blobs detected or pulses per unit of time are shown in Figure 3.13. The tip of a small solenoid vibrating at 5 Hz using Pulse Width Modulation (PWM) is put on top of the HaptiTemp sensor. Images of the pulses are recorded. The machine cycle time of the first pulse detected is the reference time for the next pulses, as shown in Figure 3.13(b). Between Figure 3.13(b) and Figure 3.13(c), the elapsed time for one pulse or blob detected is 200 ms equivalent to 5 Hz. Moreover, like the GelSight sensor, the HaptiTemp sensor is sensitive enough to sense human pulse.

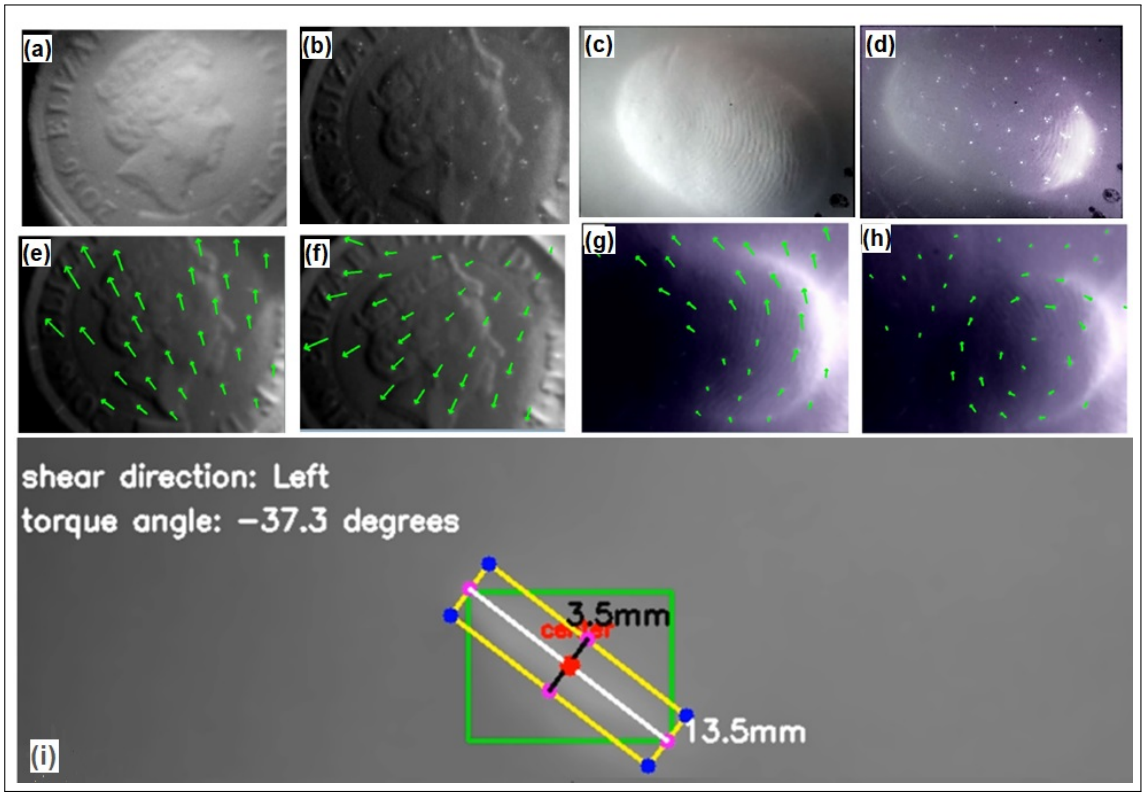

Figure 3.12: Force test. (a) One UK pound coin with UV off, (a) One UK pound coin with UV on, (c) fingertip with UV off, (d) fingertip with UV on, e) upward flow vectors, f) downward flow vectors, (g) counterclockwise flow vectors, (h) clockwise flow vectors, and (i) yellow dynamic bounding box that rotates relative to green reference bounding box used to visualise force and rotation.

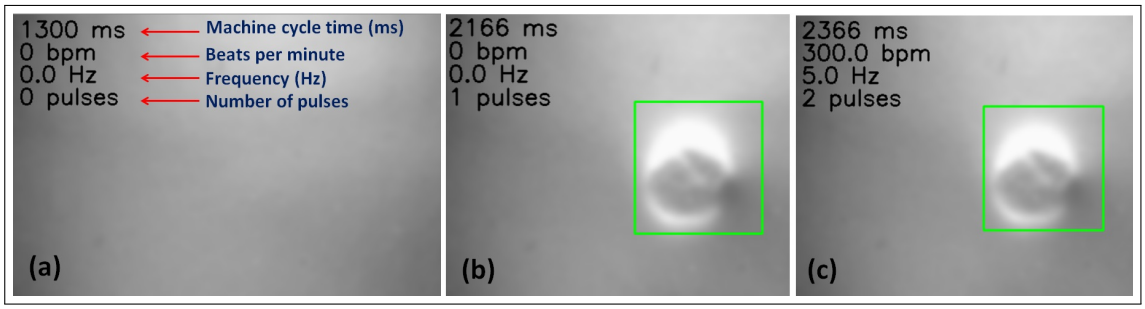

Figure 3.13: Vibration test. (a) No object on the sensor, (b) the first blob detected is counted as one pulse, and the machine cycle time is recorded as the reference time. (c) The second pulse is detected, and the machine cycle time is compared to the first reference time to get the frequency.

3.6.3 Temperature Sensing

3.6.3.1 Temperature Test using LAB Colour Space

The HaptiTemp sensor has a thermosensitive reflective coating made up of different layers of thermosensitive pigments with different temperature thresholds. When the sensor is placed on top of a metal ruler heated at one end, different pigments are activated, as shown in Figure 3.7(c). The actual test video can be found here [155].

The temperature test results captured by the HaptiTemp sensor are shown in Figure 3.14. As the temperature increases, the colour of the reflective coating changes. The machine vision camera in this study processes data in LAB colour space where 'L' is the lightness value ranging from 0 (black) to 100 (white), 'A' is the green-red axis ranging from -128 to +128, and 'B' is the blue-yellow axis ranging from -128 to +128 [156, 157]. A Region Of Interest (ROI) is demarcated by a white line as shown in Figure 3.14 and Figure 3.17 and recorded the L, A, and B mode values or the dominant colour values in the LAB colour space within the ROI. The size and position of the ROI can be changed to select the part of the tactile image where the temperature is to be measured. It can also be set as a dynamic bounding box that captures the blob temperature of the contacted object. During the testing, the ROI was fixed in the middle of the frame as shown in Figure 3.14. When an object touches the HaptiTemp sensor, the approximate temperature of the contacted object can be known based on the colour changes and the known temperature thresholds of the thermochromic pigments used in the reflective layer. The L, A, and B mode values and the thermistor temperature reading were recorded and plotted as shown in Figure 3.15. The HaptiTemp sensor covers a wider temperature range of around 31°C - 50°C which is much wider than 32°C - 35°C temperature range of thermosensitive GelForce [70, 45].

Based from the HaptiTemp sensor's response graph, as shown in Figure 3.15, 'L' or the Lightness value in LAB mode, varies directly with the temperature. Thus, the temperature of the object touching the sensor can be estimated within the temperature range of 31°C-50°C where 'L' has a linear relationship with temperature and also corresponds to the minimum and maximum temperature thresholds of the

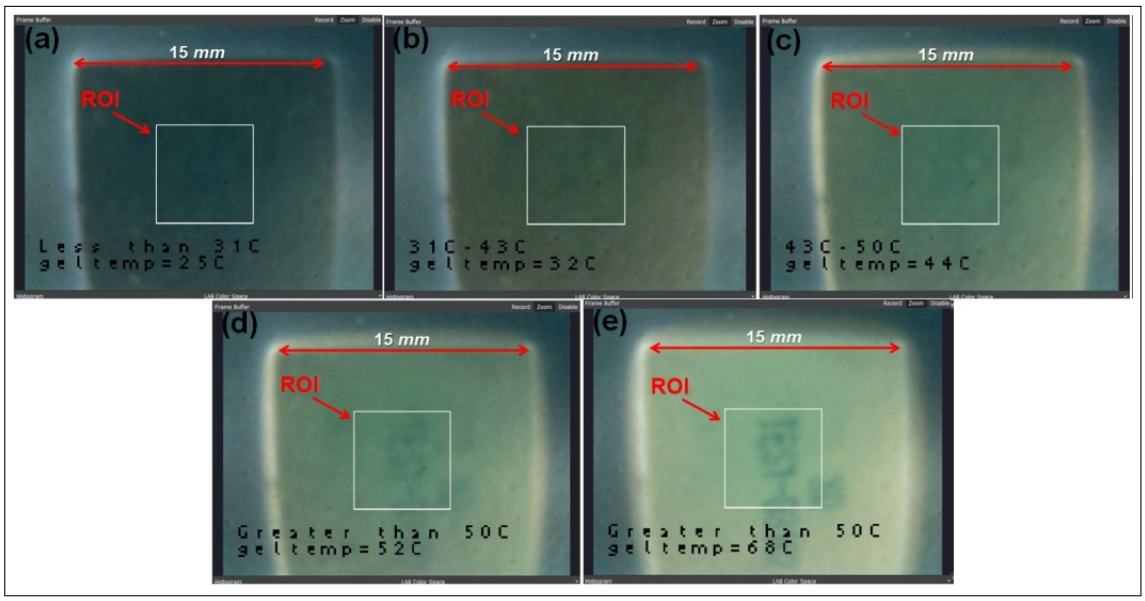

Figure 3.14: Temperature test results: (a) dark blue (less than 31°C), (b) orange (31°C-43°C; (c) orange becomes transparent to black pigment at 43°C; (d) topmost pigment becomes transparent at temperature greater than 50°C; (e) the reflective coating becomes transparent enough to show the markings on TEG at temperature greater than 50°C. The actual test video can be found here [155].

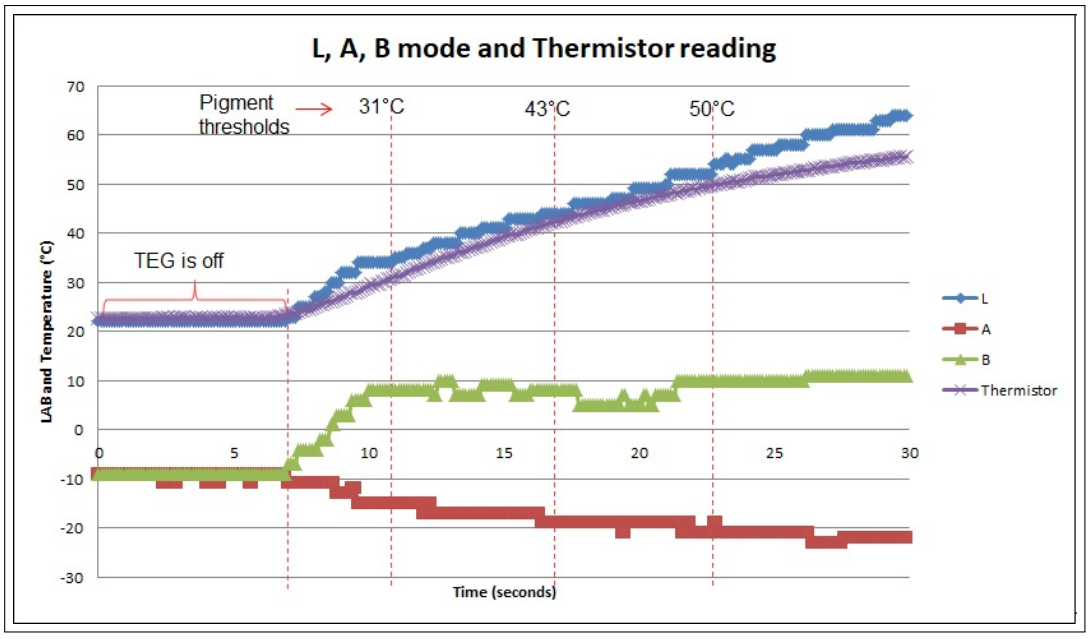

Figure 3.15: LAB mode values and thermistor reading in the temperature sweep with 23 seconds elapse time covering all the pigment thresholds.

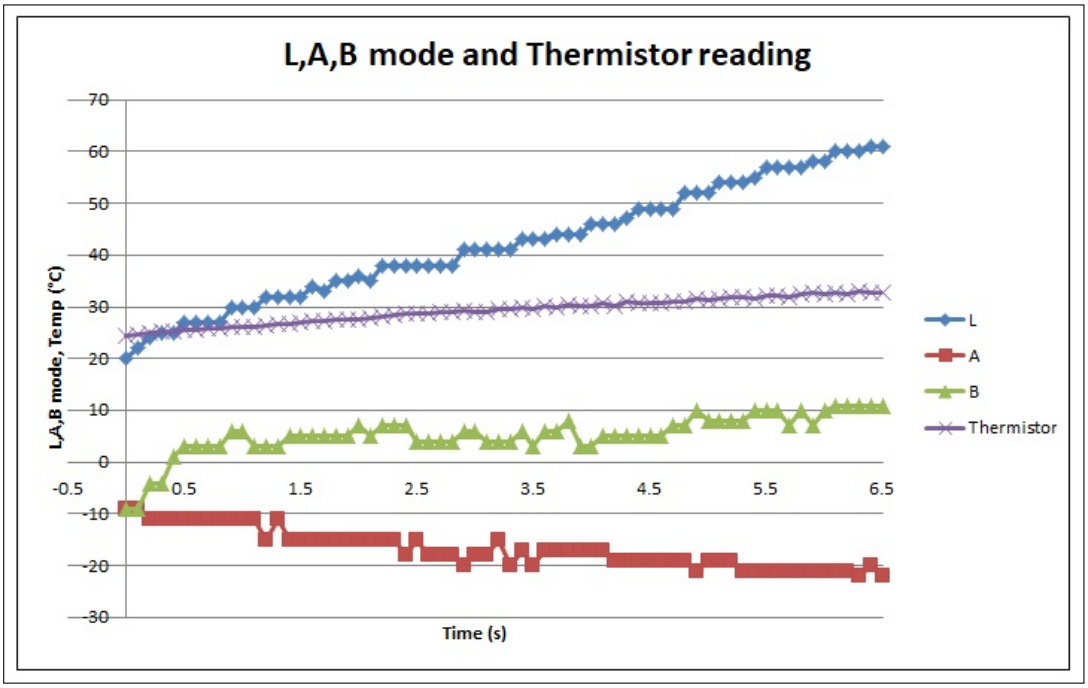

Figure 3.16: HaptiTemp vs thermistor response. LAB mode values vs thermistor reading during the 6.5 seconds temperature sweep test. TEG supply is 3.6V DC supply.

thermosensitive pigments of the sensor. Instead of relating temperature as a function of hue like in the case of finger-shaped GelForce, HatiTemp sensor's temperature measurement to the lightness value ('L') captured by the machine vision camera. Thus, the temperature measurement equation of HaptiTemp sensor can be written as temperature *(T)* as a function of lightness *(L)*, as shown in Eq. (1).

$$T = f(L) \tag{3.1}$$

3.6.3.2 Temperature Response time

The HaptiTemp sensor's response time to temperature changes has been tested using a TEG. By supplying a 3.6V DC supply to the TEG, it heats up faster compared to a 2.4V DC supply covering the same span of L mode values in just 6.5 *s* instead of 23 *s* as shown in Figure 3.16. The TEG's temperature response time varies with the supply voltage. The higher the supply voltage, the faster the TEG's temperature changes. The thermistor has a slower response compared to HaptiTemp sensor. The epoxy encapsulated NTC thermistor used in the testing has a response time

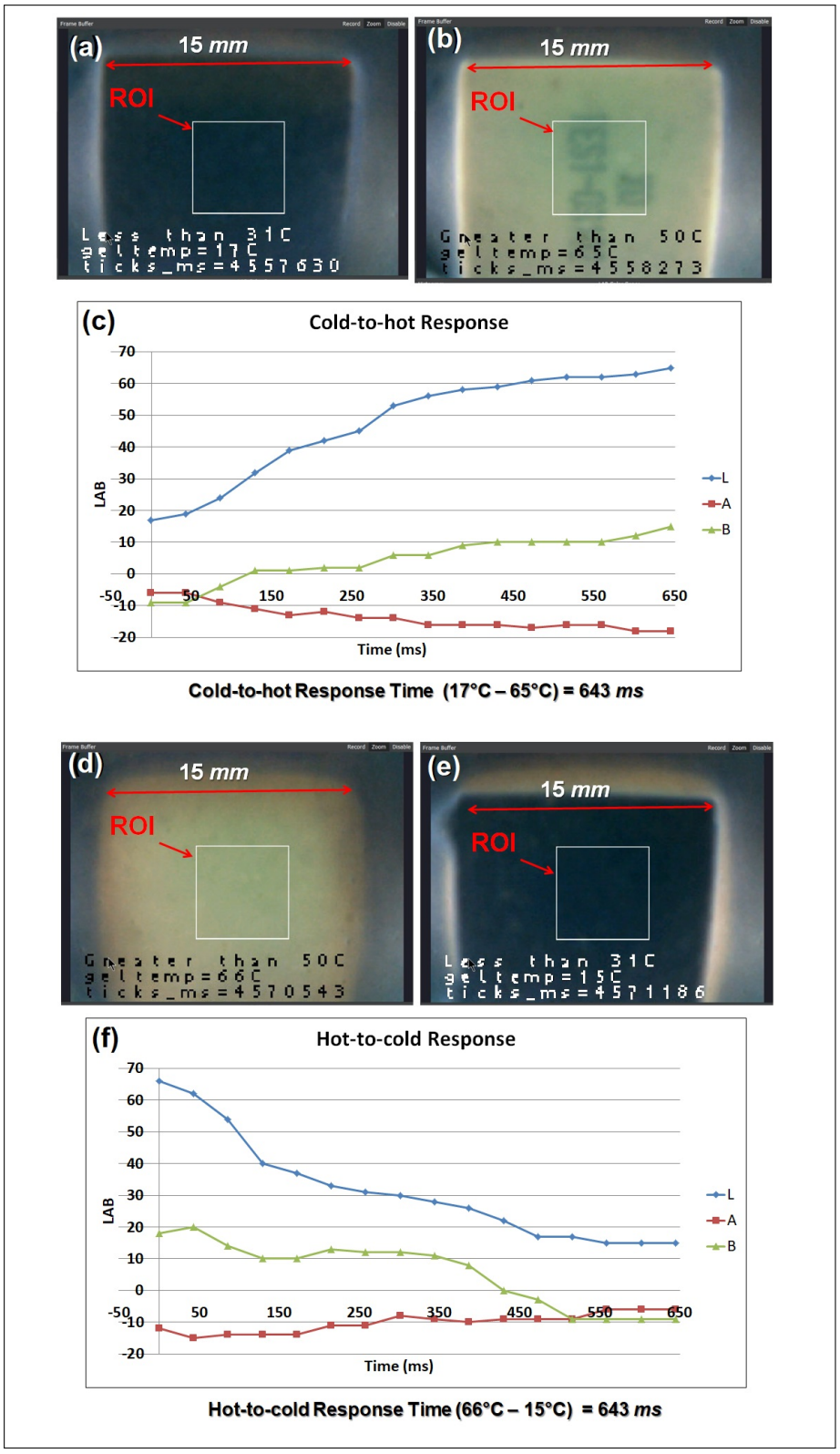

Figure 3.17: Response time. (a) below the 31°C threshold, (b) the reflective layer changes to semi-transparent indicating temperature above 50°C. c) cold-to-hot response. Moreover, hot to cold response time pictures can be seen from Fig. 3.17(d) and Fig. 3.17(e), respectively. f) hot-to-cold data. The actual test video can be found here [155].

of 19.54 *s* for temperature change 25°C to 41°C based on this report [151]. The "ticks_ms" in Figure 3.17 is the machine time in milliseconds showing the elapsed time between two events. A response time of 643 *ms* for cold-to-hot and hot-to-cold was recorded. The response time results of HaptiTemp sensor are shown in Figure 3.17. The minimum thermochromic pigment threshold of 31°C and the maximum thermochromic pigment threshold of 50°C are covered by the response time test. The ROI's dark blue hue, as shown in Figure 3.17(a) and Figure 3.17(e), shows that the blue thermochromic pigment is not activated and that TEG's temperature is below the blue thermochromic pigment's threshold of 31°C. Moreover, Figure 3.17(b) and Figure 3.17(d) show that the thermochromic pigment with a 50°C threshold has been activated making the reflective layer of HaptiTemp sensor translucent.

Knowing that the temperature and lightness value has a linear relationship within the temperature range of 31°C-50°C, the calibration equation can be written as

$$T = L \pm C \tag{3.2}$$

where *(T)* is temperature, *(L)* is the lightness value, and *(C)* is the offset value.

The HaptiTemp sensor can trigger a fast response when applied to a robotic arm similar to a human reflex response of when a person accidentally touches a hot object. The human reflex response can be demonstrated by setting up a temperature threshold on the HaptiTemp sensor to signal the robotic arm to retract. Two setups are presented in Figure 3.19 and Figure 3.20. The first setup, as shown in Figure 3.19, mimics the central nervous system where all the processing of information captured by the HaptiTemp sensor that uses a webcam is done on a laptop computer. The Dobot robotic arm retracts when touching a hot object, as shown in Figure 3.19 as soon as the hot object triggers the sensor. In contrast, the second setup has the HaptiTemp sensor that uses a machine vision camera, OpenMV Cam H7 Plus Camera, as shown in Figure 3.20, connected to one degree of freedom robotic arm (one servo) can reproduce a similar reflex response without the need for an external computer. This second setup mimics the human peripheral nervous system that acts on human reflex responses without passing the information to the central

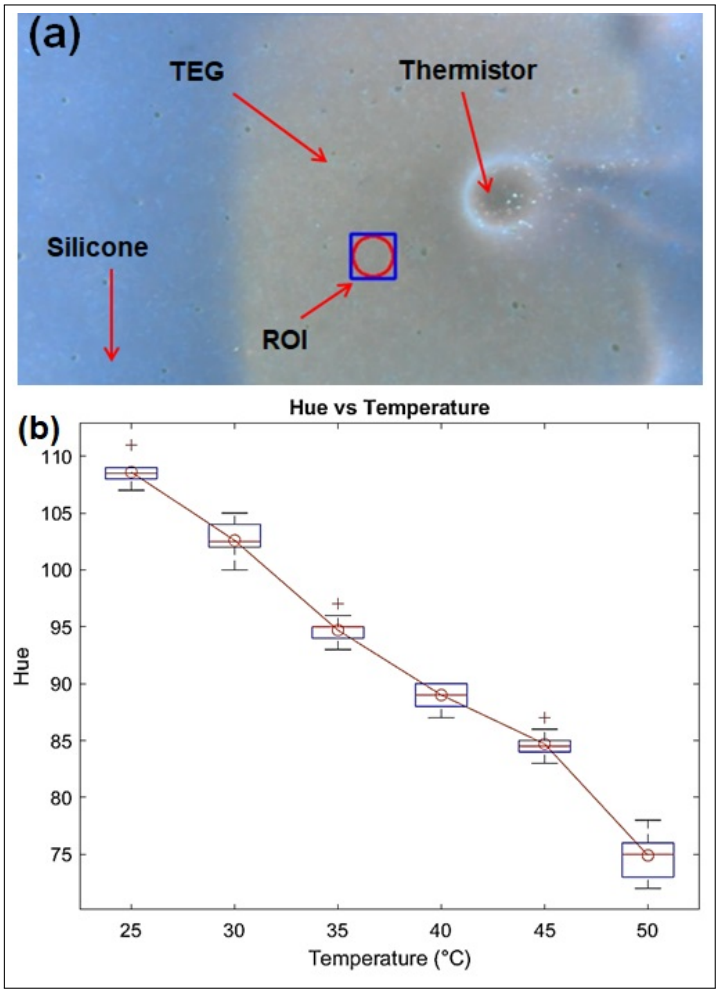

Figure 3.18: Temperature test.

nervous system to execute the retraction or withdrawal movement when a hot object is touched. The OpenMV Cam H7 Plus Camera has a built-in microcontroller that can control a servo motor [158] and a DC motor [159].

If the robotic hand with the HaptiTemp sensor touches a cold TEG, the robotic arm continue to touch the object as shown in Figure 3.19(a) and Figure 3.20(a). But if the TEG is hot enough to break the temperature threshold of the HaptiTemp sensor, a signal to retract the robotic arm is executed as shown in Figure 3.19(b) and Figure 3.20(b).

3.6.3.3 Temperature Test using HSV Colour Space

Using the OpenCV library that has a built-in function for HSV values recording and using TEG stabilised by a PID controller at temperatures 25°C, 30°C, 35°C,

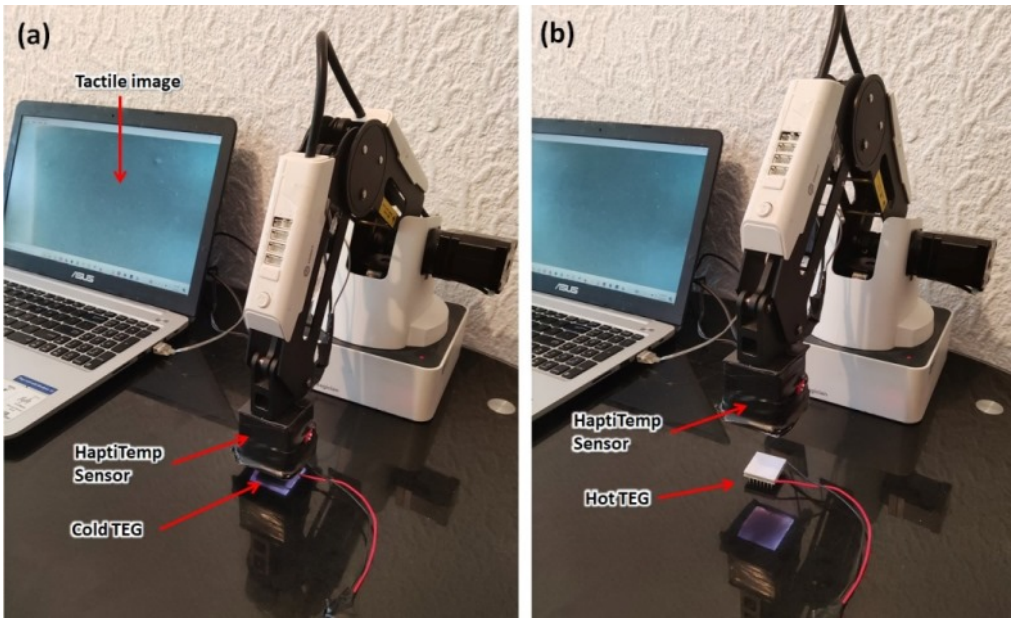

Figure 3.19: Dobot robotic arm with HaptiTemp sensor. (a) Robotic arm touching a cold TEG. (b) Touching a hot TEG triggers the arm to retract or go up.

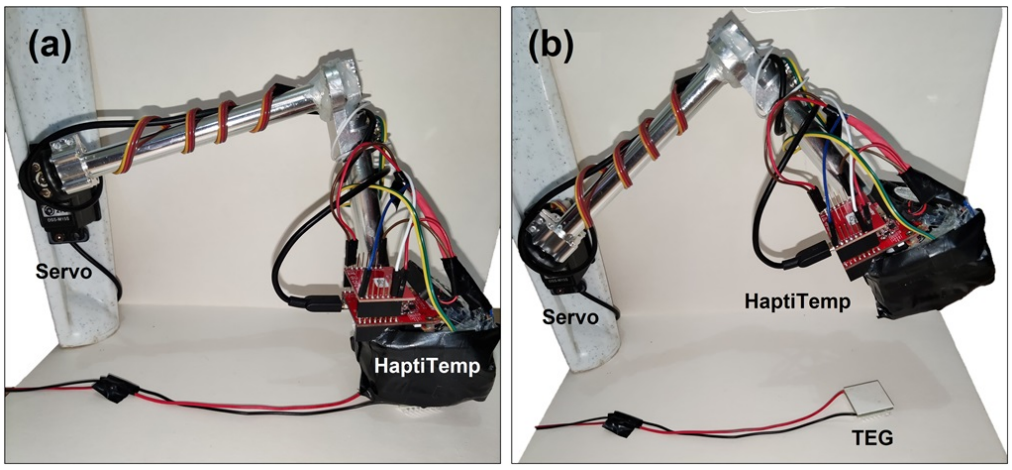

Figure 3.20: One degree of freedom (1-dof) robotic arm with HaptiTemp sensor. (a) 1-dof robotic arm touching a cold TEG. (b) 1-dof touching a hot TEG triggers the arm to retract or go up.

Table 3.1: Hue vs temperature.

	25°C	30°C	35°C	40°C	45°C	50°C
Hue(mean)	108.68	102.60	94.70	89.00	84.70	74.90
STDEV	1.07	1.51	1.25	1.05	1.16	1.91

40°C, 45°C, and 50°C, ten trials were run to record the HUE within 40-pixel x 40-pixel ROI. The tabulated readings are shown in Table 3.1. Similar to [45, 70], hue value varies inversely proportional with temperature in the range of 25°C to 50°C, as shown in Figure 3.18(b) and we can relate temperature as a function of hue, as shown in Eq. (1).

$$T = f(H) \tag{3.3}$$

We can write the calibration equation as:

$$T = mH + C \tag{3.4}$$

where *(T)* is temperature, *(m)* is the slope, *(H)* is the Hue value, and *(C)* is the offset value.

3.6.4 Tactile Image Recognition

This section discusses the results in using machine vision algorithms such as AlexNet and Mobile in tactile image classifications.

3.6.4.1 Tactile Image Recognition using a Personal Computer (Desktop or Laptop)

Even by simple visual inspection, a coin's embossed image, a fingerprint, and a bank note marking can all be seen imprinted onto the silicone sponge's reflective coating with adequate background light and a clear glass support for the silicone sponge, as shown in 3.21a, Figure 3.21b, and Figure 3.21c, respectively. Aside from embossed image, a sunken or depressed image of a USB marking can also be observed, as shown in Figure 3.21d.

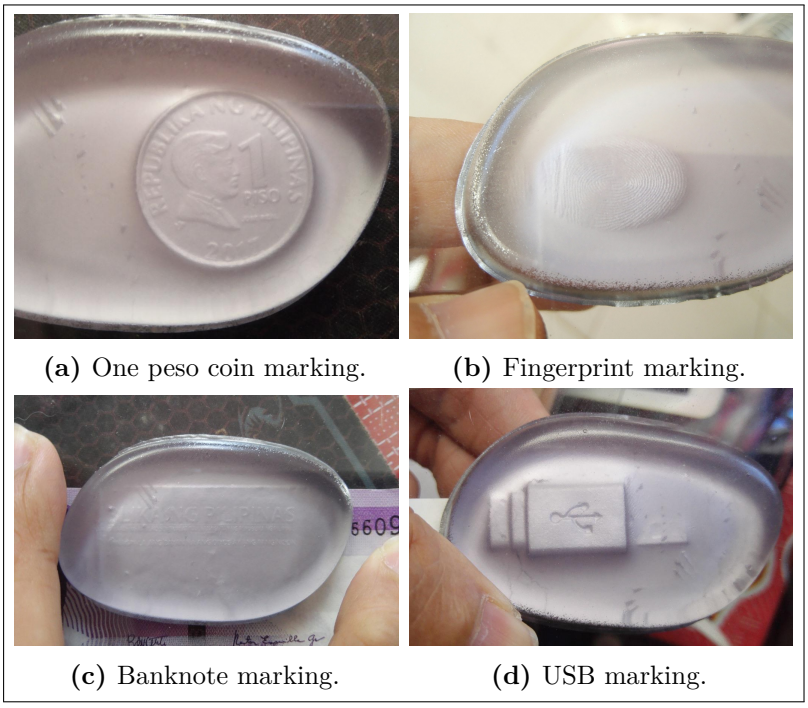

(a) One peso coin marking. **(b)** Fingerprint marking.

(c) Banknote marking. **(d)** USB marking.

Figure 3.21: Results from visual inspection.

Clear tactile images can be captured by the camera such as the coin markings shown in Figure 3.22a and Figure 3.22d, the bank note marking shown in Figure 3.22b and the fingerprint marking shown in Figure 3.22c.

Figure 3.23 shows the results of coin recognition using AlexNet. The percent (%) probability for classification is shown below every coin image. The 2D features were extracted and were used to recognise five coins with (93.4%) mean accuracy. However, when two faces are presented on the coin, accuracy of recognition went down to 90% as shown in confusion matrix in Figure 3.24. AlexNet in CNN has been treated as an algorithm to extract features. Unlike in previous studies [51, 56, 64], object recognition in HaptiTemp sensor can be done without 3D image reconstruction. The simple mechanical filter of the HaptiTemp sensor can only show the tactile image of the contacted object and can can be recognised or classified using machine learning algorithms such as AlexNet. Moreover, partial image of One Pound (UK) can still be correctly classified with 85.1718% probability as shown in Figure 3.25.

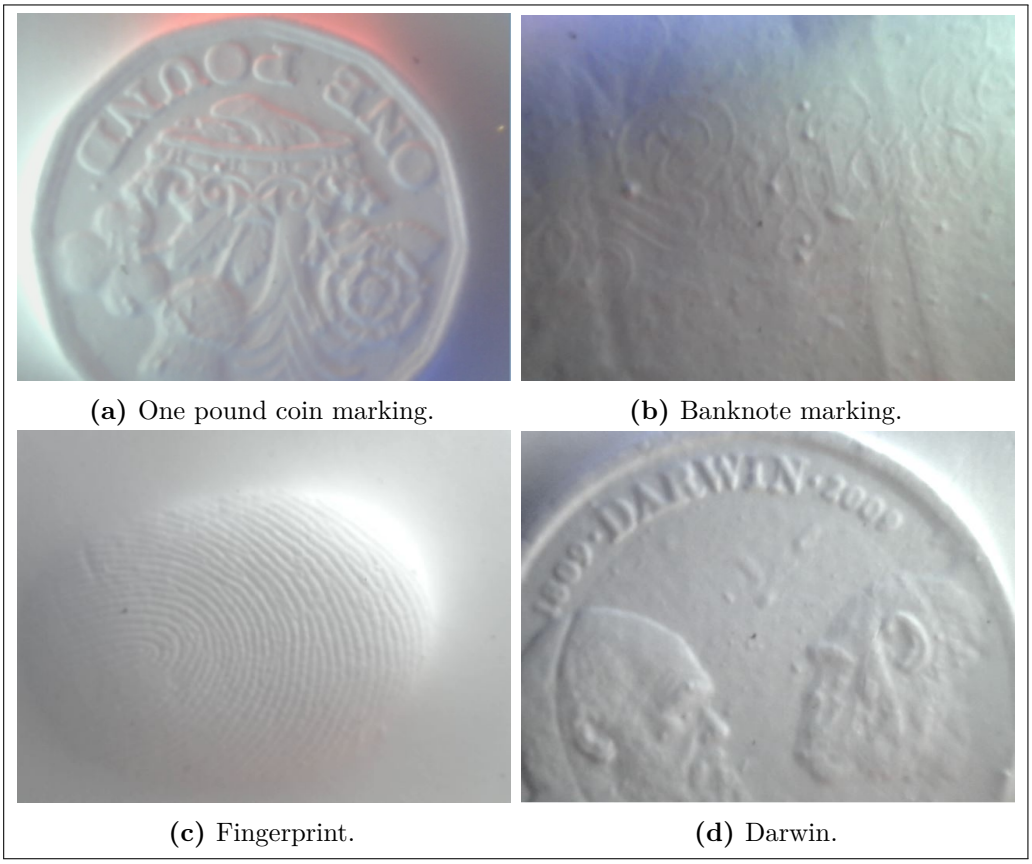

(a) One pound coin marking. **(b)** Banknote marking.

(c) Fingerprint. **(d)** Darwin.

Figure 3.22: Captured tactile images.

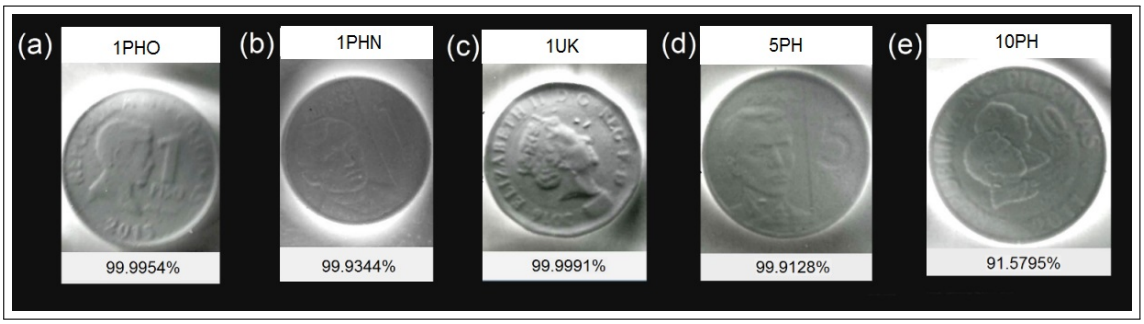

Figure 3.23: Coin recognition results using AlexNet: (a) One Peso old (1PHO), (b) One Peso new (1PHN), (c) One Pound UK (1UK), (d) Five Peso (5PH), and (e) Ten Peso (10PH).

3.6.4.2 Tactile Image Recognition using Machine Vision Camera

The neural network MobileNetV2 from Edge Impulse was trained using transfer learning and achieved a 97.3% accuracy during testing. The Edge Impulse makes a complete package of the trained model ready to be deployed on a machine vision camera. The tactile image classification results using the OpenMV Cam H7 Plus

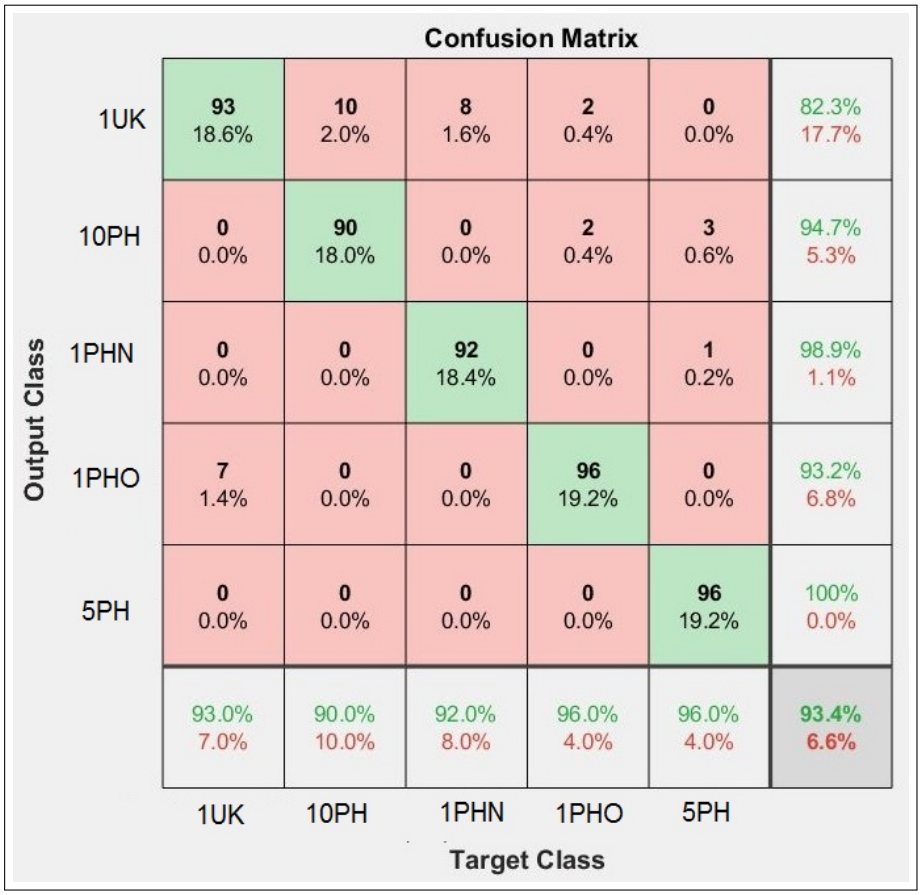

Figure 3.24: Confusion matrix for coin recognition using AlexNet.

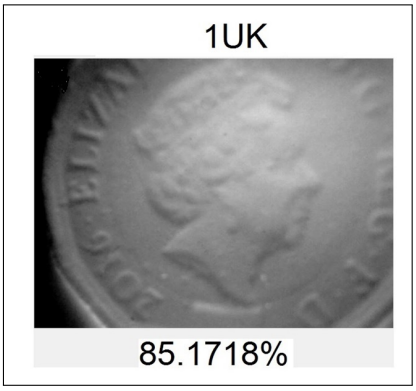

Figure 3.25: Partial coin recognition result.

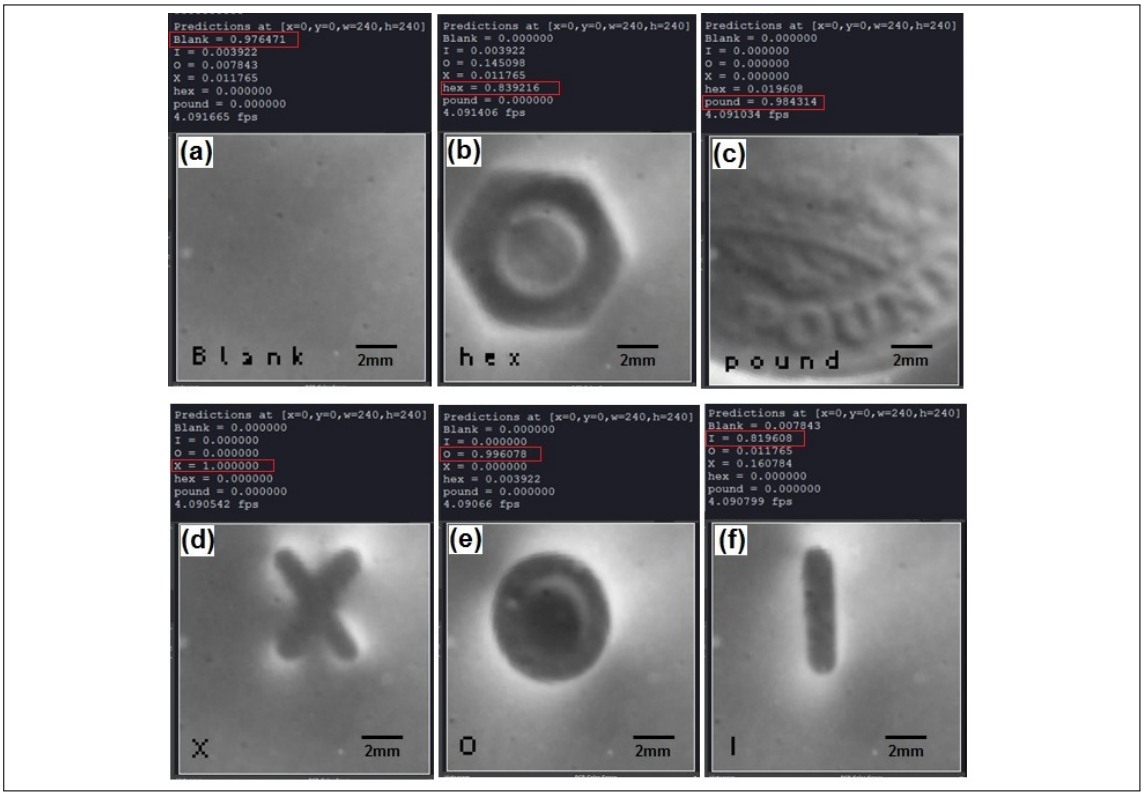

Figure 3.26: Tactile image classification using the OpenMV Cam H7 Plus camera: a) blank result, b) hex end of a screwdriver, c) UK one pound coin, and the cookie stamp letters X, O, I are shown in d), e), and f) respectively.

machine vision camera are shown in Figure 3.26. There was an error in classifying a 'hex' as an 'o'. The prediction results are at the top of each image and the confusion matrix is shown in Figure 3.27. Besides the confusion matrix is the on-device performance measured on the OpenMV Cam H7 Plus machine vision camera.

3.6.5 Simultaneous Temperature Sensing and Image Classification

The simultaneous temperature sensing and image classification test results are shown in Figure 3.28. The image recognition algorithm displays a 'Blank' result with the gel temperature in the display image frame when no object is pushed against the HaptiTemp sensor, as shown in Figure 3.28a. The cold end of a hex screwdriver and the cold UK one-pound coin were pressed to the sensor and recorded the results as shown in Figure 3.28b, and Figure 3.28d, respectively. The image results when the end of a hex screwdriver and the UK one pound coin were heated

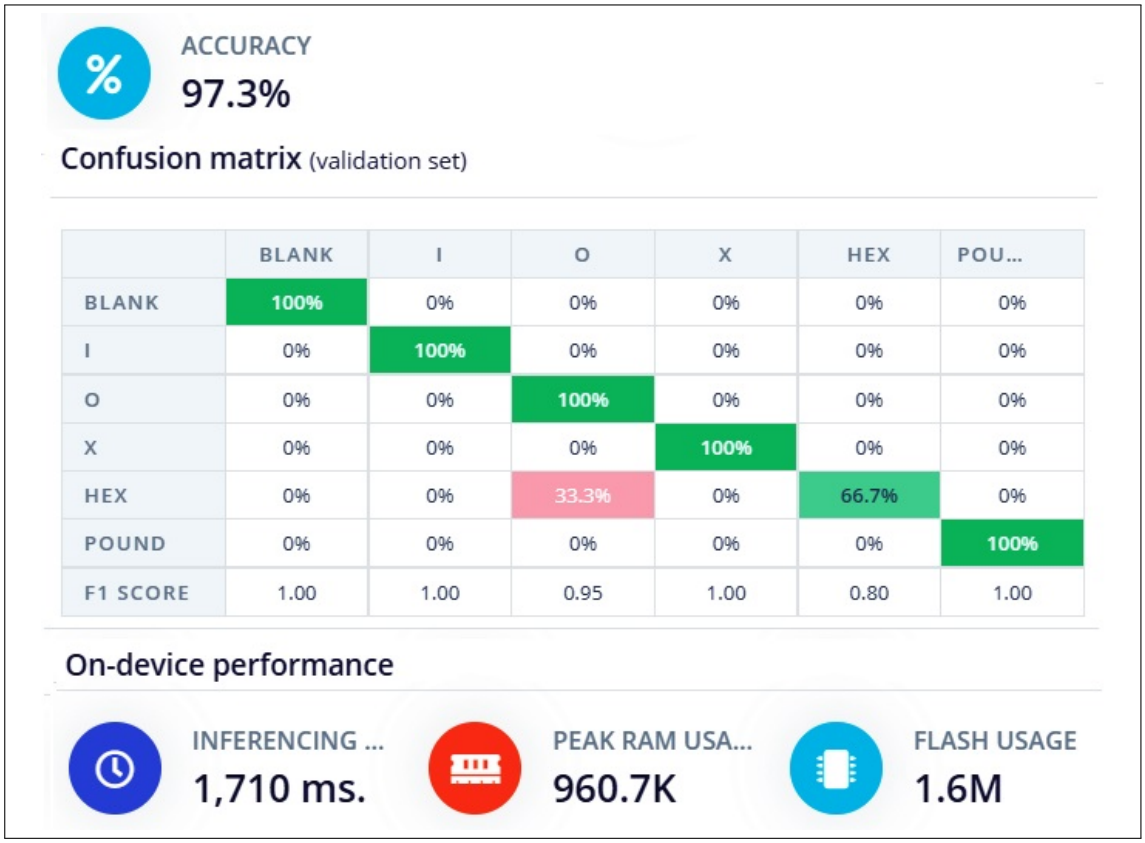

Figure 3.27: Confusion Matrix and On Device Performance produced by Edge Impulse.

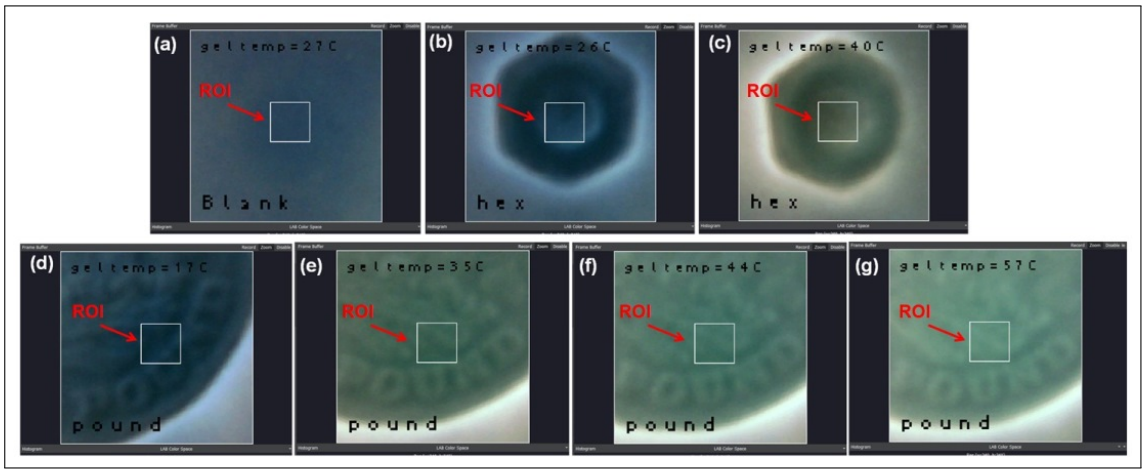

Figure 3.28: Simultaneous temperature sensing and image recognition test results.

using the TEG, and pressed each one to the sensor are shown in Figure 3.28c and Figure 3.28e, respectively. In a gradient temperature test for the coin, all the temperature thresholds (31°C, 43°C, and 50°C) of layered thermochromic pigments are shown in Figure 3.28d to Figure 3.28(g).

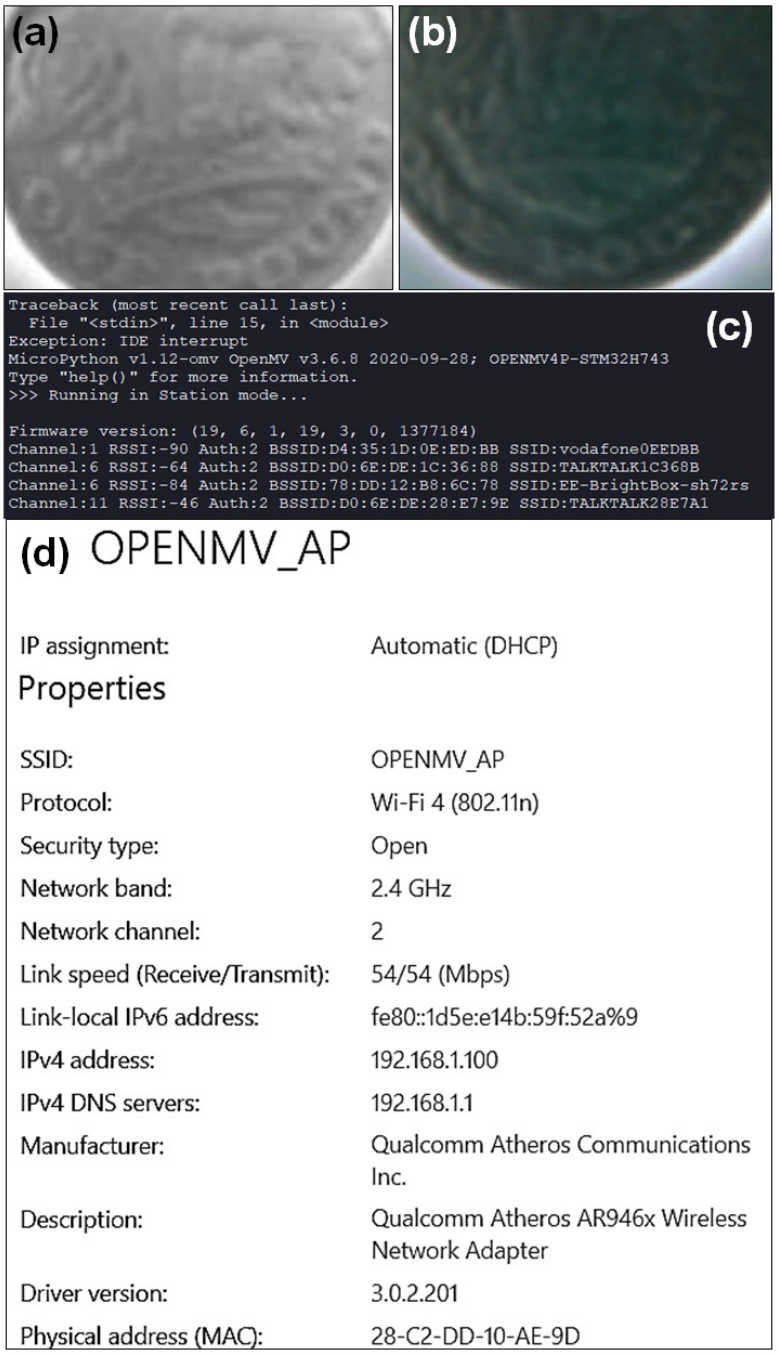

Figure 3.29: Station mode, and AP mode WiFi connections. (a) greyscale image, (b) RGB image, (c) available WiFi during station mode scanning test, and (d) the IP address and the OPENMV_AP connection properties.

3.6.6 Wireless Connectivity

Greyscale tactile images, as shown in Figure 3.29(a) and RGB images, as shown in Figure 3.29(b), can be transmitted via WiFi module of the HaptiTemp sensor. The available WiFi hotspots during the station mode scanning test of the machine vision camera are shown in Figure 3.29(c), and the IP address and the OPENMV_AP AP mode connection properties are shown in Figure 3.29(d).

3.7 Chapter Summary

In this chapter, a novel thermosensitive visuotactile sensor, called HaptiTemp sensor, was presented. This sensor is a compact and unified GelSight-like sensor made from a commercially available cosmetic sponge capable of detecting Haptic Primary Colours (force, vibration, and temperature). The gel material used in the sensor is a commercially available silicone cosmetic sponge. By using a commercially available clear cosmetic sponge, the long hours of curing time and degassing process in creating a clear silicone slab and the long hours of curing time has been skipped. The HaptiTemp sensor achieved a two-step unification relative to the GelSight sensor technology. First, Ultra Violet (UV) switchable markers were introduced on the reflective coating, making it possible to do tactile image recognition and force analysis using one sensor. The switchable UV markings and flow vector arrows produced by optical flow algorithm were used to show tactile forces. Second, a novel reflective layer made from different layers of thermochromic pigments with different colours and temperature thresholds is painted on top of UV markers, making it possible to sense not only force and vibration but also temperature with a rapid temperature response comparable to the withdrawal reflex response of humans.

None of the visuotactile sensors have multiple layers of thermosensitive pigments in the reflective coating to study changes in temperature that occur at a rate of 19°C/second (from 31°C to 50°C in real-time), nor do they have embedded machine vision technology for stand-alone tactile sensing and image classification in wireless mode. The HSV values were recorded and found out the hue value changes directly

proportional with the temperature at a similar rate. By subtracting an offset value from the recorded hue, the HaptiTemp sensor can be calibrated close to the thermistor reading. Moreover, aside from HSV colour space, the LAB colour space was also used to deduced the temperature. The "L" or "Lightness" value was recorded to measure temperature. The HaptiTemp sensor responds directly proportional with the L values as the temperature changes. Aside from force estimation and temperature detection, experiments were done to demonstrate how to measure vibrations by blob detection per unit of time.

Furthermore, with the use of machine vision camera, OpenMV Cam H7 Plus Cam, it was demonstrated that the HaptiTemp sensor can be trained to classify different tactile images in a stand-alone configuration without the need of a computer. A high success rate of 97.3% classification accuracy on five different objects using their tactile images was achieved in spite of a small dataset. Aside from image classification, the OpenMV Cam H7 Plus machine vision camera was used to record the LAB mode values. Test results show that the 'L' mode value in the LAB colour space recorded by the machine vision camera shows a linear relationship with temperature. Moreover, a response time of 643 *ms* for the cold-to-hot and hot-to-cold response that covers 31°C to 50°C was recorded.

Therefore, the HaptiTemp sensor is a compact and unified visuotactile haptic primary colours sensor with tactile image classification capability. HaptiTemp is the closest thing to the human skin in tactile sensing, tactile pattern recognition, and rapid temperature response.

4

A Multimodal Untethered Hand Wearable with Haptic Primary Colours *(force, vibration, and temperature)* and Fine-grained Cutaneous Feedback

4.1 Abstract

This chapter presents the development of a unified multimodal untethered haptic hand wearable with haptic primary colours and fine-grained cutaneous feedback. Three prototypes were presented and discussed. Prototype 1 is a multimodal haptic hand wearable with haptic primary colours *(force, vibration, and temperature)* feedback. Prototype 1 has mini-vibration motors on each fingertip, an annular TEG on the index finger for temperature feedback, and force feedback that restricts finger movements using a retractable ID badge holder. Prototype 2 has a 4x4 tactile matrix actuator, made from Metec P20 Braille cells, on each fingertip, forming the fine-grained (multi-point or multi-contact cutaneous feedback. In order to scan the surface or feel the edges of an image, a fine-grained haptic device is needed to actuate the texture and edges of the image. Each tactile pin on the 4x4 fingertip tactile matrix actuator can be controlled individually. This haptic hand wearable is unique in that it features the most tactile feedback actuators in an untethered, portable,

open-palm haptic glove design that can be adjusted to accommodate any size of hand. Moreover, three experiments involving human participants were conducted using the fine-grained haptic hand wearable: firstly, a spatial test was conducted to understand a human's ability to recognise the tactile patterns activated at different locations on the fingertip; secondly, a temporal test was conducted to understand a human's ability to recognise different vibrating patterns moving in different directions on the fingertip; and thirdly, a 2D image recognition test was conducted to understand a human's ability to recognise the lines, simple shapes, and edges. The two prototypes can work as individual wearable or can be combined to form Prototype 3, a unified untethered multimodal haptic hand wearable with haptic primary colours *(force, vibration, and temperature)* and fine-grained cutaneous feedback. The unified version can complement the HaptiTemp sensor to give the user force, vibration, and temperature feedback, as well as fine-grained cutaneous feedback, when exploring the surfaces or edges of a tactile image.

4.2 Introduction

We frequently touch the things we see within our grasp to feel them and convince ourselves that they are real because looks can be deceiving. Can the sense of touch be extended by developing a device to feel the things we see at a distance that we cannot reach, just as a camera, telescope, and microscope can expand human eyesight to see further, broader, and deeper than human eyes can typically see? Can we touch the moon? Can we extract tactile information from images? If we can only transmit the tactile signal captured by a haptic sensor and actuate or recreate the sensation, we can somehow feel what the sensor is touching.

Some work has already taken place to develop haptic devices for the hand to enhance the immersive experience and facilitate interaction with objects in a remote environment or virtual reality [17, 18]. One of the major determining factors in the success of spatial computing involves natural interaction with the real, augmented, or virtual environment. Naturalistic interaction aids communications, cooperation, and integration between humans and robots [17]. Conversely, if the interaction is

unnatural, communication between these agents is severely hindered. The comfort and wearability of haptic devices are also significant considerations that come as a combination of form factor, weight, shape, ergonomics, and functionality [17, 18]. Haptic feedback for wearable can be in the form of cutaneous stimuli, kinesthetic stimuli, or the combination of both types of stimuli [12, 17, 18].

Different haptic feedback have been developed such as mechanical, electrical-based and multimodal tactile module combining vibration and temperature *(vibro-thermal)* feedback was proposed by Nakatani et al. [185]. This vibro-thermal tactile device was further improved by Kato et al. and combined with a force display to simulate degrees of softness [27].

Recent research on haptic feedback tends to focus on the portability and miniaturisation of actuators with virtual reality (VR) applications to provide a more immersive experience [17, 18, 25]. According to [184], aside from vision and audio, the development of a portable tactile display is needed for all VR technology to present not only one sense but an integrated sense to enhance the immersive experience. If the HaptiTemp sensor is a unified sensor that can detect force, vibration, and temperature, and do image classification, a multimodal unified untethered haptic hand wearable with haptic primary colours *(force, vibration, and temperature)* feedback was developed in this thesis to complement the HaptiTemp sensor.

The realisation of a compact untethered haptic hand wearable with fine-grained fingertip cutaneous feedback, and vibro-thermal feedback aiming at integration with kinesthetic force feedback systems such as restricting finger movements during grasping or touching a 3D VR object is a real challenge. Tactile matrix actuators are devices that have at least four tactile actuators (tactors) grouped together to give tactile feedback to the user. Tactile matrix actuators are considered cutaneous feedback and are frequently used in vision substitution devices. They can, however, be utilised as a tactile complement to a visual system. Cutaneous feedback can be in the form of vibration produced by mini-vibration motors [100, 160, 161, 162], skin stretch or tangential motion to the skin [163], and tactile matrix actuator that produces tapping motion, creating vertical movements towards the skin, forming a

matrix of tactile pixels (taxel) [97] that triggers tactile mechanoreceptors: Meissner's corpuscles and Merkel's cells that are sensitive to edge pressure and flutter tap as reported by Visell [30].

This chapter presents hand wearables that can complement the HaptiTemp sensor. Prototype 1 is a multimodal haptic hand wearable that has minivibration motors on each fingertip, has force feedback that can restrict finger movement using a retractable ID badge holder with a small solenoid stopper, and a temperature feedback from ThermoElectric Generator (TEG) connected to the index fingertip, forming thermo-vibro feedback. Prototype 2 has fine-grained cutaneous feedback with 4x4 tactile matrix actuators on each fingertip; thus, 80 tactile pins total. Each tactile pin can be controlled individually using Arduino Nano 33 IoT microcontroller. The 4x4 tactile actuator matrix is made from commercially available Metec P20 Braille cells. In contrast to the pneumatic-based haptic gloves, this haptic wearable has the novelty of being untethered, portable, modular, and can be wirelessly connected to a computer or VR headset using Classic Bluetooth or WiFi. All the components of this haptic wearable are commercially available and the application was developed using open-source software. A tactile matrix simulator that can be controlled by a computer mouse has been developed for scanning 2D images using the fine-grained wearable. By using a mouse, the fine-grained haptic wearable has the novelty of easily converting any computer mouse into a tactile mouse without changing the mouse hardware. This haptic device has a maximum power consumption of 830 mW and a total weight of 204 g. The prototype can be used to scan a binary image or detect the edges of an image by using the Canny edge detection algorithm. Moreover, it can be fed with predetermined patterns such as Braille or tapping patterns. The untethered fine-grained haptic hand wearable was tested with human participants and can be integrated with hand tracking devices such as Leap Motion Controller to scan and feel the contours of tactile images or 2D VR objects.

Prototype 1 and Prototype 2 can work as stand-alone wearables or can be combine to form Prototype 3, a unified haptic hand wearable that has the same thermo-vibro

feedback as in the index finger of Prototype 1, but the thermo-vibro feedback is now mounted in the palm area to give way to the 4x4 tactile matrix actuator on the index fingertip. Furthermore, instead of just a stop-and-go mode for the retractable ID badge holder used in the Prototype 1, the unified wearable has a gradient resistance restricting finger movements using a mini-servo instead of a small solenoid.

More details about the wearable prototypes are discussed in the following sections of this chapter.

4.3 Prototype 1: Untethered Multimodal Haptic Hand Wearable

The untethered multimodal haptic hand wearable, as shown in Figure 4.1a, with haptic primary colours *(force, vibration, and temperature)* feedback, is made from commercial off-the-shelf components. Each fingertip has minivibration motor. The index fingertip has an annular TEG or Peltier device making it thermo-vibro haptic feedback as shown in Figure 4.1(b). Although the prototype has temperature, vibration, and force feedback like the haptic display wearable developed by Kato et al. [28], the focus of Prototype 1 is to apply a stopping force to restrict finger movement during touching or grasping of VR objects. Instead of using a bulky DC geared motor to control the thread for force feedback, a retractable ID badge holder was used inspired by Lucas [186] and put a small solenoid to stop the reeling as shown in Figure 4.1(c). Unlike the haptic hand wearable that used retractable ID badge holders with 3D printed parts presented by Lucas[186], the prototype in this thesis has no 3D printed parts and no potentiometer for sensing finger movement.

A Leap Motion Controller [178] was used for hand and fingertip tracking in the setup, as shown in Figure 4.2. This is an input optical hand tracking device that captures hand and finger movements. It can track them even when other parts of the hand obscure them. Moreover, a VR environment was developed in this thesis using Unity 2019. Each fingertip in the VR has a contact collider that detects a collision with a virtual object. If there is a collision between the VR hand fingertip with a 3D body, it signals to the haptic wearable's corresponding actuator. Both

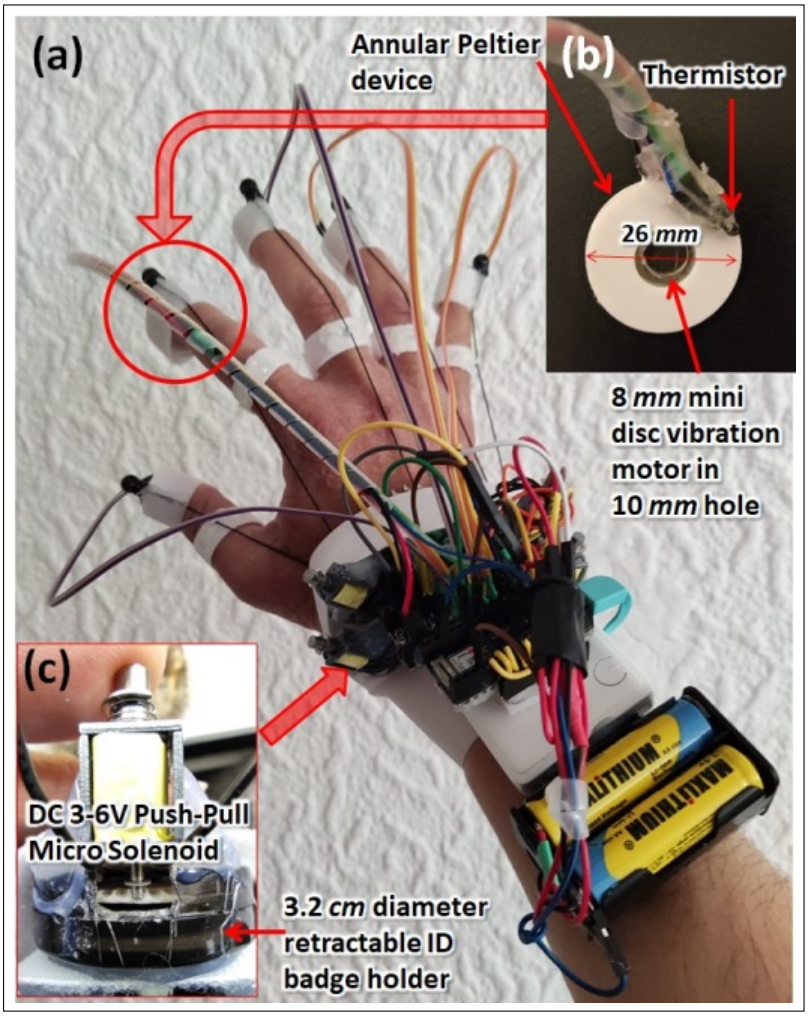

Figure 4.1: (a) Untethered haptic hand wearable with haptic primary colours *(force, vibration, and temperature)* feedback. (a) The haptic hand wearable has cutaneous and kinesthetic haptic feedback. Each fingertip has mini disc vibration motor. Aside from mini-vibration motor, (b) thermo-vibro feedback on the index fingertip, and (c) force feedback formed by combining a retractable ID badge holder and small solenoid stopper.

the vibration motor and solenoid are simultaneously activated whenever there is a collision. The solenoid stops the reeling of the retractable badge and restricts finger movement. The VR environment has a blue cylinder, a red cube, and a green sphere with collision detection. In this study, the Peltier device gets hot when the VR index fingertip touches the red cube and gets cold when it touches the blue cylinder, as shown in Figure 4.2. Actuation signals from the laptop are sent to the hand wearable via Bluetooth connection. Prototype 1 has an open palm design so that the Leap Motion Controller can track the hand and fingers. When any fingers

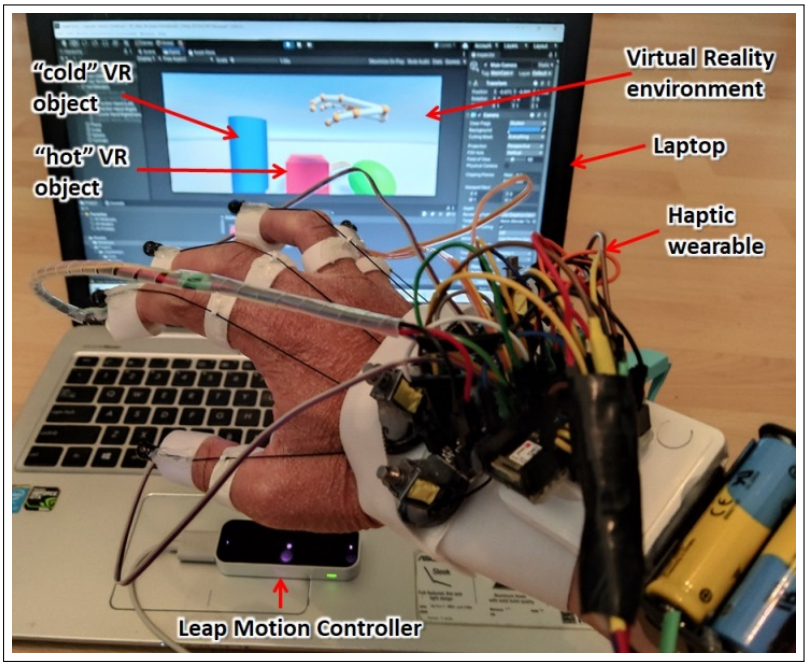

Figure 4.2: Untethered haptic wearable experimental setup. The blue cylinder in VR environment represent a "cold" VR object while the red cube represent a "hot" VR object.

collide with any 3D VR object, an activating signal is sent to the corresponding vibration motor and solenoid stopper. However, unlike the other fingertips, the index fingertip checks if it has touched a red square or blue cylinder. When the VR index fingertip touches the red square, a "hot" signal is sent to the Peltier device controller to make it hot. In contrast, the blue cylinder will send a "cold" signal, making the Peltier device cold when touched. The annular Peltier device has been moved to the palm area in the unified multimodal hand wearable to give way to the 4x4 tactile matrix for the index fingertip.

4.3.1 Schematic Diagram

The schematic diagram of the prototype is shown in Figure 4.3. The schematic is divided into five sections, namely: (a) power supply, (b) microcontroller, (c) thermoelectric, (d) vibration motor, and (e) solenoid section. A 5V DC power supply was used for the microcontroller and a 3V DC supply for the disc vibration motors and solenoids.

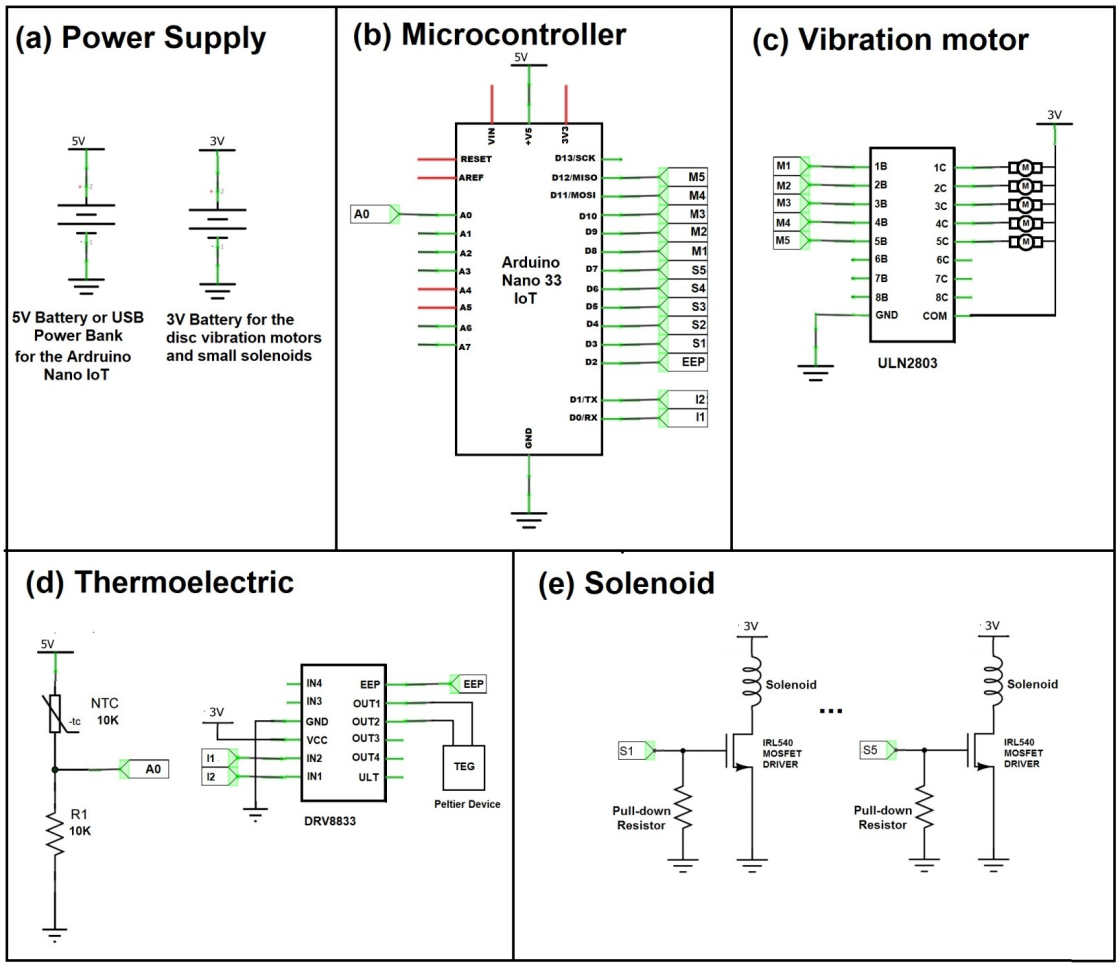

Figure 4.3: Schematic diagram of the Prototype 1 has 5 sections: (a) power supply, (b) microcontroller, (c) thermoelectric, (d) vibration motor, and (e) solenoid.

4.3.2 Hardware

An Arduino Nano IoT [173] is the microcontroller used to control the motor drivers (IRL540 and ULN2803) and h-bridge module (DRV8833). This microcontroller has WiFi and Bluetooth wireless connectivity. A simple vibro-thermal feedback module was developed, which is composed of an 8 *mm* disc vibration motor with 11000 *rpm* inserted on an annular Peltier device (TES1-04903 Thermoelectric Peltier) with a 10K NTC thermistor as its temperature sensor, as shown in Figure4.1(b). A 3.2 *cm* diameter retractable ID badge holder with a small solenoid stopper was used to stop and release the retractable thread. The plastic disc inside the badge holder can be exposed by cutting some portion of the casing. As shown in Figure 4.1(c), grooves on the edge of the badge's disc can be made using the tip of a hot

soldering iron. When the solenoid shaft is pulled down towards the groove, like a door lock mechanism, it will stop the turning of the disc, thus restricting the pulling of the string connected to the fingertip.

Moreover, aside from the vibration motor, the index fingertip has an annular Peltier element activated to get hot or cold depending on the trigger signal. For the sake of simple demonstration, logic "1" signal has been designated as "hot" signal and logic "0" for the "cold" signal. Actuation or activation signal for the annular Peltier device could be sent directly by the HaptiTemp sensor wirelessly or could be from a laptop computer. The logic signal is fed to the H-bridge module that controls the direction of current in the annular Peltier device.

4.3.3 Software

An Arduino IDE was used to develop the firmware that controls the vibration motors, solenoids, and the annular TEG. A VR environment was developed using Unity 2019.

4.4 Prototype 1: Testing and Validation

4.4.1 Force Feedback Test

Force feedback can be in the form of cutaneous feedback relative to the tactile pin heights or can also be a kinesthetic feedback from the restriction or resistance of finger movements using retractable ID badge holders. This kinesthetic force feedback is useful in touching 3D objects giving the user an illusion of touching a real object. This can be done by adding a collision detection on the fingertips or palm area of the VR hand avatar that will send activating signal to the corresponding tactile actuator of the haptic wearable. In order, to know the restricting force or pulling strength of a retractable ID badge holder, a force gauged was used. The pull force of ten pieces of 3.2 *cm* diameter retractable ID badge holders is recorded after pulling a 15 *cm* string and measuring vertically using a force gauge.

4.4.2 Vibration Feedback Test

Prototype 1 has mini-vibration motors on each fingertip to give vibration feedback. A Width Modulation (PWM) signal could be used to trigger the minivibration motors. An MPU-9250 accelerometer was used to capture the vibrations of the mini disc vibration motor.

4.4.3 Temperature Feedback Test

The performance of the annular TEG or Peltier device was evaluated by cooling it down for 3 seconds, turning it off until it stabilised, and warming it up for 3 seconds before turning it off again. Three cycles with a 2 *Hz* sampling time were recorded.

4.5 Prototype 1: Results and Discussion

4.5.1 Force Feedback Test

A force gauge was used to measure the pulling strength of the retractable ID badge holders. By pulling a 15 *cm* string and measuring vertically using a force gauge, the pull force of ten pieces of 3.2 *cm* diameter retractable ID badge holders ranges from 1.3N to 1.5N as shown in Figure 4.4(a) with a mean value of 1.4N and standard deviation of 0.067N. In Prototype 1, the small solenoid has a 1N push force perpendicular to the disc of the retractable ID badge holder, as shown in Figure 4.4(b). The groove on the circular disc of a retractable ID badge holder can withstand 15N tangential force.

4.5.2 Vibration Feedback Test

All mini disc vibration motors in Prototype 1 were activated, and the corresponding solenoid restricts finger movement whenever a fingertip in the VR hand touches a VR object. An MPU-9250 accelerometer was used to capture the vibrations of the motor, as shown in Figure 4.5.

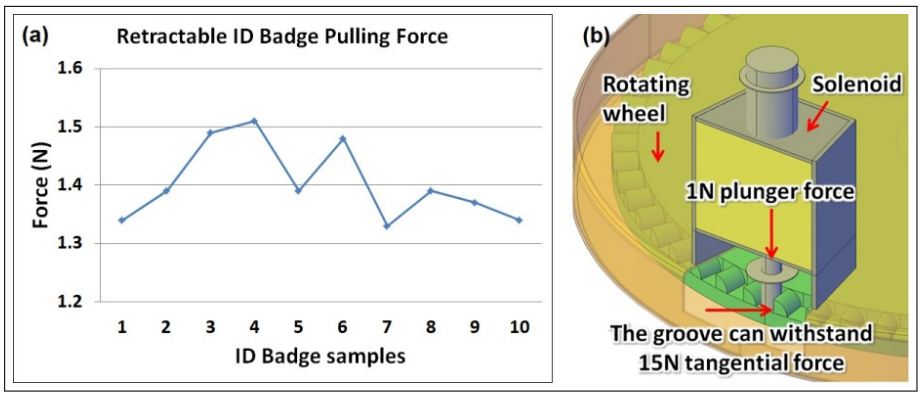

Figure 4.4: Force Test Results. (a) Retractable ID badge pulling force, (b) solenoid plunger force and groove stopping force.

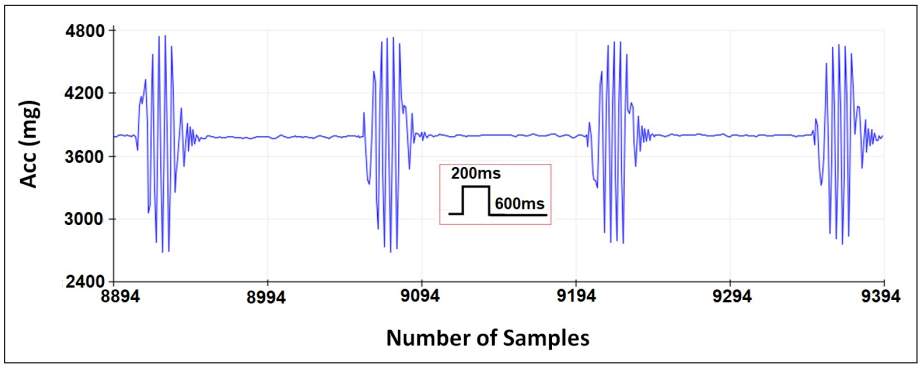

Figure 4.5: Vibration test results using MPU-9250 accelerometer.

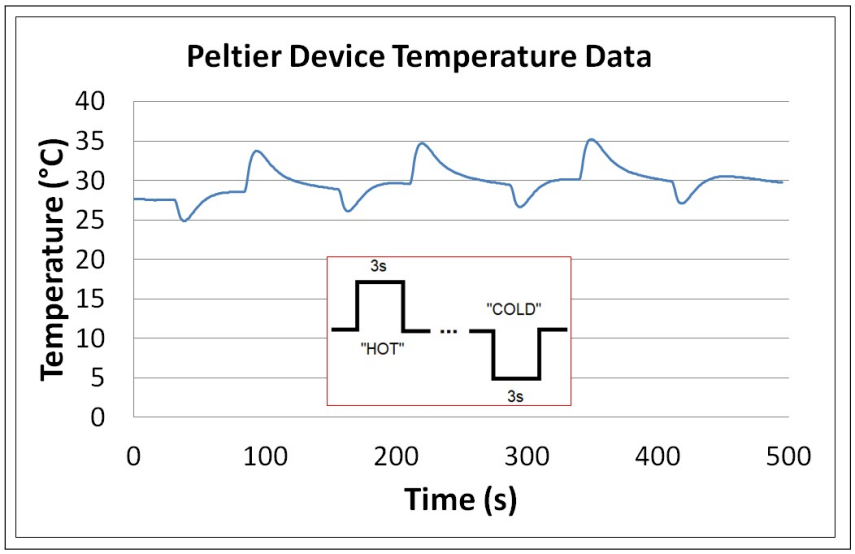

Figure 4.6: Temperature Test Results.

4.5.3 Temperature Feedback Test

The annular TEG, as shown in Figure 4.1b, was used to produce hot and cold sensations. Three cycles with 2 *Hz* sampling time were presented as shown in Figure 4.6. The ambient temperature is around 29°C. It was observed that once the Peltier device was heated up for 3 seconds, the cooling time from hot temperature to ambient temperature was twice as long as the warming up from cold to ambient temperature. The asymmetrical cooling and warming time has been reported in many papers [27, 185] and a four tile configuration has been proposed by [190] to improve the time to perceive temperature change by 36%.

4.6 Prototype 2: Untethered Haptic Hand Wearable with Fine-Grained Cutaneous Haptic Feedback

The majority of well-known haptic devices used in telerobotics and telemedicine, such Phantom and Omega, offer single point contact interaction [15]. They do not have tactile matrix actuators. Even if haptic devices have mini vibration motors as their haptic feedback, they may be regarded as cutaneous feedback but not as a tactile matrix actuator or tactile display if they are not grouped together.

The untethered fine-grained haptic hand wearable is shown in Figure 4.7. The device has a multi-point, fine-grained cutaneous feedback on the fingertips. This novel haptic hand wearable is untethered (WiFi and Bluetooth-enabled), lightweight (204 g), compact, modular, battery-powered with 830 mW maximum power consumption, and has a 4x4 tactile matrix actuator on each fingertip (80 tactile pins in total) that can be controlled individually using a small microcontroller. When every fingertip matrix is enabled and connected to Bluetooth, the prototype uses a maximum current of 166 mA at 5V supply. Around 3 mA of current are consumed by each fingertip module. The prototype can operate for six hours on a 1200 mAh rechargeable battery. Commercially available piezo-based Metec P20 Braille cells were used to develop the 4x4 fingertip tactile matrix actuators. The

little USB power bank is included in the system's overall weight of 204 g. Each fingertip module weighs only 19 g, with a 72 g controller board. The prototype's fingertip module weighs less than any of the fingertip tactile matrix actuators with pin array or pin matrix reported by Pacchierotte et al. [17].

4.6.1 Schematic Diagram

The schematic diagram of the fine-grained haptic hand wearable is shown in Figure 4.8. The power supply, microcontroller, and P20 Braille cells are the three building blocks that make up the entire system.

The battery or USB power supply and the 5V-200V DC-DC boost converter for the P20 Braille cells constitute the power block as shown in Figure 4.8a. The Arduino Nano 33 IoT [173] is the system's primary controller as shown in Figure 4.8b. It contains 8 analogue pins (A0—A7) and 14 digital pins (D0-D13). When necessary, the analogue pins can function as digital output pins. The Arduino Nano 33 IoT has seven analogue pins, and analogue pins A4 and A5 have built-in pull-up resistors for I2C connections which are floating or free pins as shown in Figure 4.8b. These free pins can be used in the future to drive various types of small vibration motors using I2C modules like the DRV2605L Haptic Motor Controller. In this study, one of the P20 Braille cells was connected to the analogue pin A0, which was designated as a digital output pin.

For analogue pins A1, A2, A3, A6, and A7, switchable pull-down resistors were employed, as indicated in Figure 4.8b. If reading analogue signals is required in future tests, pull-down resistors can be switched on or connected to ground to form voltage dividers ready to be connected to variable resistors, such as flex sensors. Pull-down resistors can be left floating, as in the case of this study, if they are to be utilised as digital output pins so that the signals will not be pulled to ground. The use of analogue pins is made more flexible by this switch. It is also important to note that Arduino Nano 33 IoT has a virtual serial port. The D0 and D1 digital pins are considered Serial1 but are declared digital output pins in this study.

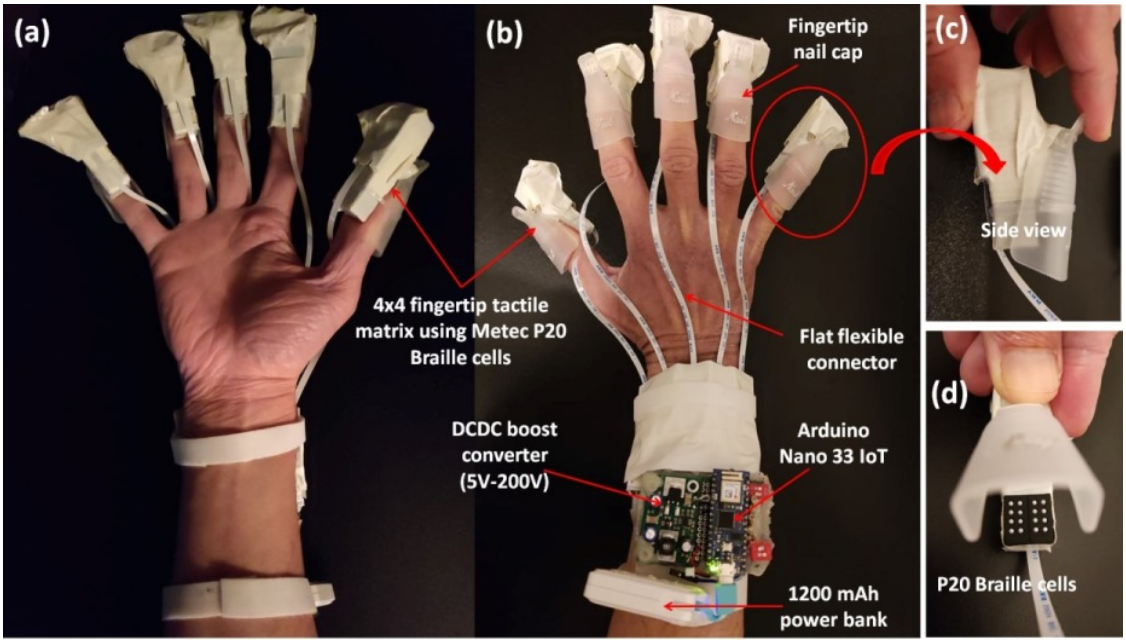

Figure 4.7: Untethered fine-grained haptic hand wearable with 80 tactile actuators (tactors). (**a**) Open-palm view, (**b**) open-backhand view, (**c**) side view of the fingertip tactile with clear rubber band, and (**d**) 4x4 fingertip tactile matrix made from two P20 Braille cells.

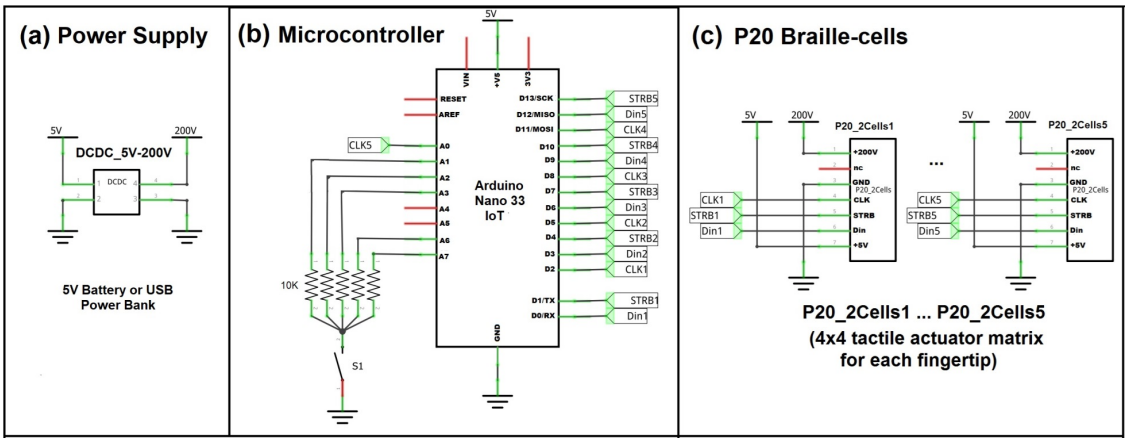

Figure 4.8: Schematic diagram of the untethered fine-grained haptic hand wearable: (**a**) power supply, (**b**) microcontroller, and (**c**) P20 Braille cells.

The schematic of P20 Braille cell with shift register is shown in Figure4.8c. There are three digital control pins, data-in (Din), strobe (STRB), and clock, as well as supply connections for 200 V, 5 V, and GND (CLK). The microcontroller is attached to the digital pins. To manage the five sets of 4x4 fingertip tactile matrix, fifteen digital output pins are required. Since there are only 14 digital pins, analogue pin A0 was declared as a digital out pin.

4.6.2 Hardware

The detailed parts of the fine-grained wearable are shown in Figure 4.7b. In contrast to the method of Malvezzi et al. [167] in customising a wearable for a target fingertip by taking into account its unique geometrical characteristics as well as some target performance metrics, the fine-grained haptic hand wearable in this thesis uses a plastic nail clip with a small clear rubber, as shown in Figure 4.7c, to fit the fingertip module securely to any size and shape of a fingertip. The exposed 4x4 matrix made from two P20 Braille cells is shown in Figure 4.7d.

The prototype's parts or modules are joined together or connected using sockets and removable wires. The wires connecting the fingertip modules to the control board are thin and lightweight Flat Flexible Cables (FFC). It is possible to use less number of fingertip modules by disconnecting the other fingertip modules, depending on the application. For instance, grasping requires five fingers, while pinching only requires the index finger and the thumb. The prototype's modular design add to the novelty and versatility of the device, which allows for simple mounting or part replacement. The interconnecting cables are adaptable enough to let the fingers flex and make a grabbing or grasping motion.

The palm and backhand views of the fine-grained haptic hand wearable prototype are shown in Figure 4.7a and Figure 4.7b, respectively. The DC–DC boost converter module and the microcontroller are shown in Figure 4.7b. The fingertip tactile matrices are mounted on each finger using a nail clip. The whole prototype is made from different commercially available breakout boards or modules integrated using sockets and plugs for easy mounting or replacing parts. This untethered

fine-grained haptic hand wearable has an open-backhand and open-palm thimble design similar to "weart" TouchDIVER [168] for easy hand tracking. But unlike the TouchDIVER, which has only three fingertip modules, this prototype has five fingertip modules. The prototype has an open-palm design similar to the Dexmo Haptic Force-feedback Gloves [169], and BeBop Forte Data Gloves [170]. The prototype's modular design could enhance and complement the force-feedback haptic and data gloves by providing fine-grained cutaneous feedback. The BeBop data glove offers six vibrotactile feedback, while the fine-grained prototype has 80 tactile feedback actuators. Moreover, the prototype can produce not only "up" or "down" tactile feedback from the P20 Braille cells but also different tapping or vibration patterns at different frequencies with varying duty cycles. Unlike the Dexmo and BeBop gloves, the prototype is made from low-cost Commercial Off-The-Shelf (COTS) components. Though the 80-tactile actuators are fewer than the HaptX Gloves DK2 haptic VR gloves with 133 tactile feedback points per hand [171], the prototype has the advantages of being untethered, compact, battery-powered, modular, and lightweight. This haptic hand wearable prototype has the novelty of having the highest number of tactile feedback actuators in an untethered, portable, open-palm haptic glove design that can fit any size of hand because of its flexibility and adjustability.

The prototype uses an Arduino Nano 33 IoT microcontroller, as shown in Figure 4.7b, which is mounted on a socket and can be easily removed or replaced when damaged. This small microcontroller has a built-in Bluetooth, BLE, and WiFi module for wireless communications. The u-blox NINA-W102 WiFi module on the Nano 33 IoT uses an ESP32 microcontroller [175]. It has an ATSAMD21G18 microcontroller chip and an ESP32 combined. The code or firmware runs on the ATSAMD21G18, which communicates with the ESP32 [176]. The ESP32 inside the Arduino Nano 33 IoT can be used for WiFi, BLE, and classic Bluetooth. Additional Bluetooth or WiFi modules are not necessary. Consequently, the control circuit is more compact.

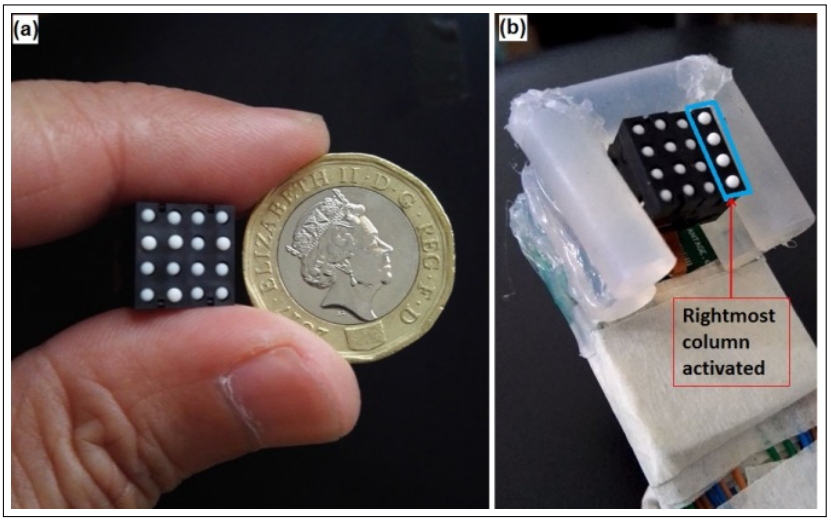

Figure 4.9: 4x4 Fingertip Tactile Matrix Actuator

A single fingertip tactile matrix, as shown in Figure 4.9 was initially developed. This device uses a commercially available solenoid-based Dot Braille cell [172] and has a bulky control box as shown in Figure 4.10. The solenoid-based Dot Braille cell has locking mechanisms to enable each tactile pin to stay up or down even when the device has no power, but the pushing force of the tactile pins is too weak to push the skin during the down to up pin transition. Because of this weak pushing force, a different commercially available Metec P20 Braille cell that uses piezo-based actuators was used for the fine-grained haptic hand wearable. The Metec P20 Braille cell [166] has a distinct and noticeable pushing force at the fingertip during the activation of the tactile pins. It has a compact and lightweight module containing a backpanel with shift register chips that can interface easily with a microcontroller. The hardware section provides more details on the specifications of the P20 Braille cell.

From the bulky structure shown in Figure 4.10, the fine-grained haptic wearable with 80 tactile actuators was made into a hand-mounted and portable design using P20 Braille cells with an Arduino Nano 33 IoT microcontroller. The 80 pins can be controlled individually in real-time using the small microcontroller. A simple application developed using Processing software was used to test the hardware capability of the prototype. Processing is open-source software with

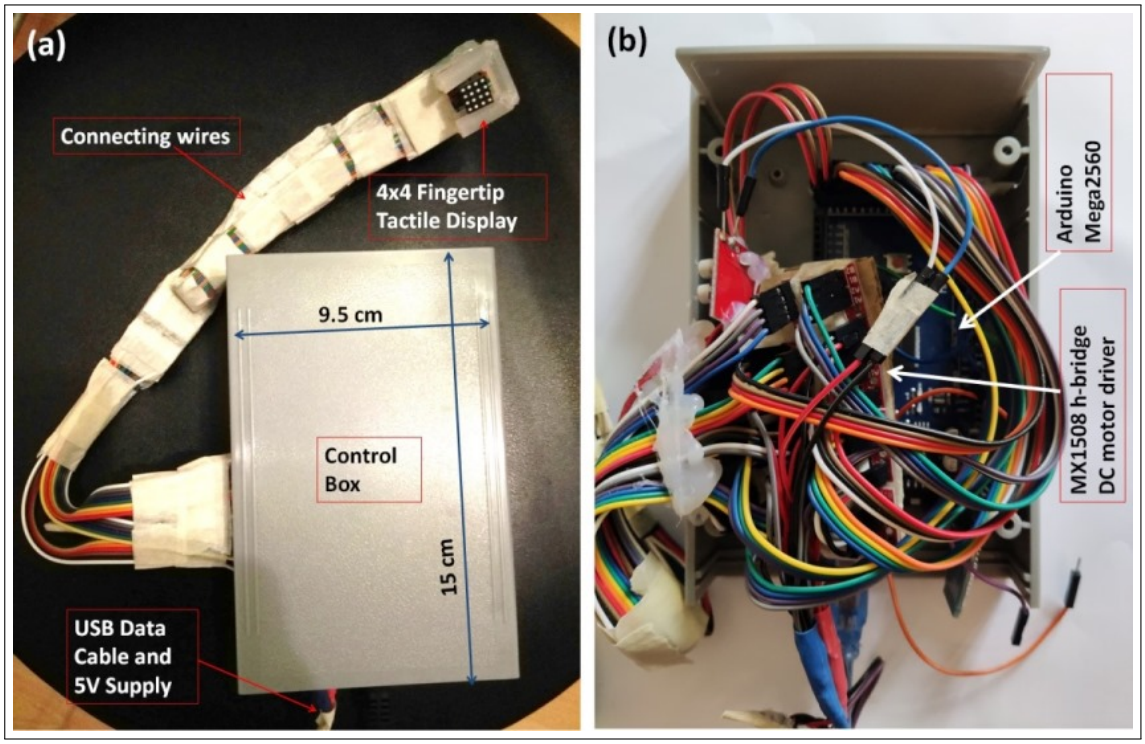

Figure 4.10: (a) 4x4 Fingertip Tactile Matrix Actuator using Dot Braille cell, (b) inside the control box is the Arduino Mega 2560 microcontroller and the MX1508 h-bridge DC motor drivers for the tactile pins.

an OpenCV library that is used in image processing and edge detection. A simulator was developed for five 4x4 tactile matrices corresponding to the tactile actuators for the fingertips.

The tactile matrices in this simulator need a hand-tracking device in order for them to move across the computer display. The simplest hand-tracking device is a computer mouse. The tactile matrices in the simulator can be anchored or pegged to a computer mouse pointer so that as the hand moves the mouse across the computer screen, the tactile matrices move accordingly. The only drawback in using a mouse pointer as an anchor is that all the tactile matrices in the simulator move in unison. In order to move the tactile matrices independently, a Leap Motion Controller could be used because it can track not only the hand but also the fingertips. The Leap Motion Controller has a hand avatar corresponding to the actual hand being tracked. Each tactile matrix in the simulator can be anchored individually to the fingertips of the hand avatar. Thus, making the five tactile

Table 4.1: Comparison of the "4x4 Fingertip Tactile Matrix" and "Untethered Fine-grained Haptic Hand Wearable".

	Initial 4x4 Fingertip Tactile Matrix [174]	**Untethered Fine-grained Haptic Hand Wearable**
Type of tactile actuator (tactor)	Dot Braille cell	P20 Braille cells
Technology used in the tactor	Electromagnet (solenoid)	Piezoelectric bimorph bender actuator
Number of tactors	16 electromagnet-based pins	80 piezo-based pins
Type of wearable	1 fingertip	5-finger exoskeleton haptic glove
Mode of data transfer	USB wire	USB wire or wireless (Bluetooth or WiFi)
Microcontroller	Arduino Mega 2560	Arduino Nano 33 IoT
Tactor driver	MX1508 (H-bridge motor driver)	HV509 Shift Register for P20 Braille cells
Supply Voltage	5 V DC	5 V DC (DC–DC boost to 200 V for P20 Braille cells)
Application software	Python	Processing, Unity
Tactile simulator controller	Mouse	Mouse, Leap Motion Controller, Oculus Quest2

matrices in the simulator move independently.

The tabulated comparison between the fingertip wearable that uses Dot Braille cells and the fine-grained haptic hand wearable that uses Metec P20 Braille cells is shown in Table 4.1.

The P20 Braille cell from Metec has eight dots driven by piezo-actuators (bending type) [166]. It has the smallest form factor among the Braille cells of Metec. They can be bought in a complete package together with an active backpanel with connecting cable and the DC–DC 5V-200V power supply. Because the piezo-based tactile actuators of P20 Braille cells operate at a 200 V supply, a small DC–DC

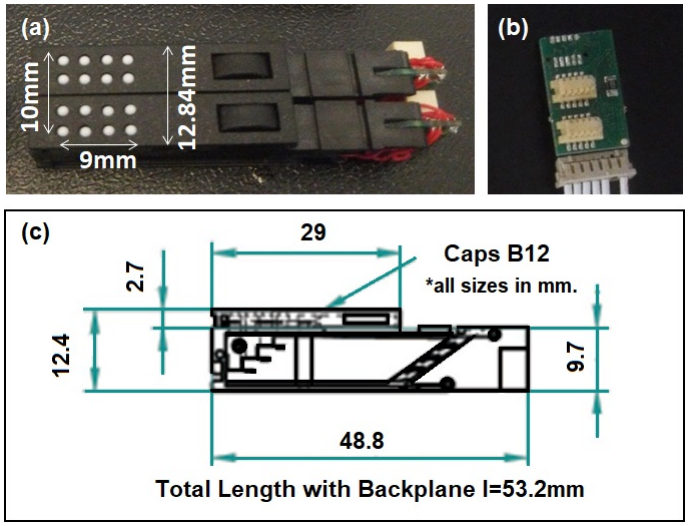

Figure 4.11: P20 Braille cell. (**a**) The 4x4 matrix from two pieces of P20 Braille cells, (**b**) two-position backpanel for two P20 Braille cells, and (**c**) P20 side-view dimensions [166].

boost converter is needed to raise the 5 V DC supply to 200 V [177] that can be purchased from Metec together with the P20 Braille cells. It has a printed circuit board (PCB) with dimensions of 26 mm x 38 mm.

By combining two P20 Braille cells, a 4x4 tactile matrix with 9 mm x 10 mm tactile surface can be formed as shown in Figure 4.11a. The cells can be stacked to create a larger Braille display. However, this study needs only to combine two P20 Braille cells for each fingertip using a two-position backpanel as shown in Figure 4.11b. The side-view dimensions of the P20 Braille cell [166] are shown in Figure 4.11c. The weight of a single cell is just 4.19 g.

The 16-bit HV509 high-voltage capable shift register chip is part of the active backpanel for the P20 Braille cells. Two P20 Braille cells can be controlled by a single chip. Though Metec provided a two-position backpanel for the 4x4 tactile matrix, the small surface-mount components in the circuitry made it challenging to expose the data out pin. It should have been easy to cascade or control the five 4x4 matrices using only three digital Arduino pins. Because of this, each of the 4x4 fingertip tactile matrices has been treated as an individual 16-bit register.

As a hand tracker, the Leap Motion Controller [178] is employed. This optical hand tracking system, which is compact, quick, and accurate, records the motion

of hands and fingers. It weighs 32 g and measures 80 mm x 30 mm x 11.30 mm in size. The controller's normal field of view is 140 x 120°, and it can track hands up to 60 cm (24 inches) away inside a 3D interaction zone. The software from Leap Motion can recognise 27 different hand components, including bones and joints. Even when they are hidden by other components, it can still track them. The Leap Motion Controller's fingertip and wrist coordinates serve as the 4x4 tactile simulator's reference points.

4.6.3 Software

The software for the fine-grained haptic wearable is divided into two categories: firmware and application. The firmware is the software used to program the microcontroller, while the application software is about the Graphical User Interface (GUI) for the tactile matrix simulator.

The flow chart for the software algorithm is shown in Figure 4.12. Each small section in every tactile matrix simulator is an ROI that computes the amount of black or white pixels. The simulator can be used to scan the surface or the edges of the binary image using the Canny edge detector algorithm. If the small section of the tactile matrix simulator is more than 50% black, it will be filled with the colour green, and the microcontroller sends an "on" or "up" signal to the assigned tactile pin. On the other hand, if the small section is less than 50% black, the microcontroller sends an "off" or "down" signal to pull down the assigned tactile pin.

The firmware handles data framing and manages the signals to activate the tactile actuators. The firmware is written in C/C++ and compiled using the Arduino IDE. It controls how the 8-bit shift registers linked to the tactile actuators function. There are two 8-bit shift registers for each 4x4 tactile matrix. Each cell is connected to an 8-bit shift register and can be controlled using one-byte data or a three-digit cell variable that can hold 000 to 255.

A fingertip tactile matrices matrix simulator was developed using Processing software to correspond with the actual tactile pins, as shown in Figure 4.13. Each of the 4x4 matrix in the simulator has 16 small sections corresponding to the 16

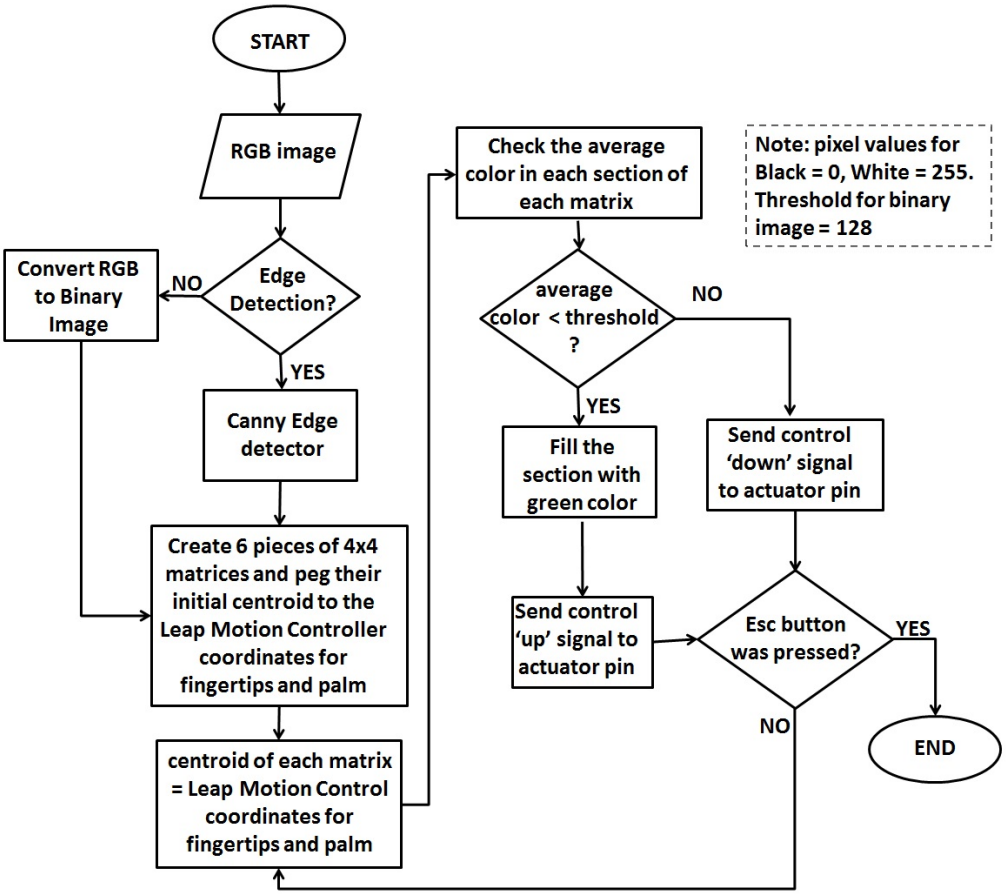

Figure 4.12: Tactile matrices simulator algorithm flow chart. There are five tactile matrices and each has 4x4 or 16 Region of Interest (ROI) corresponding to the 16 tactile pins on each fingertip of the hand wearable. Each ROI checks the average colour as it moves across a black-and-white background. If the ROI has more than 50% black pixel, this ROI turns green, and an “up" signal will be sent to the assigned tactile pin.

tactile pins of the fingertip module. Figure 4.13a and Figure 4.13b show the actual tactile pins activated for the index finger and thumb matrices corresponding to the green circles in the index and thumb matrices of the GUI shown in Figure 4.13c. Each matrix in the simulator can move across an image on the computer screen using a mouse. The tactile matrices can also be anchored on the fingertips and wrist coordinates extracted in real-time by the hand-tracking algorithm of the Leap Motion Controller.

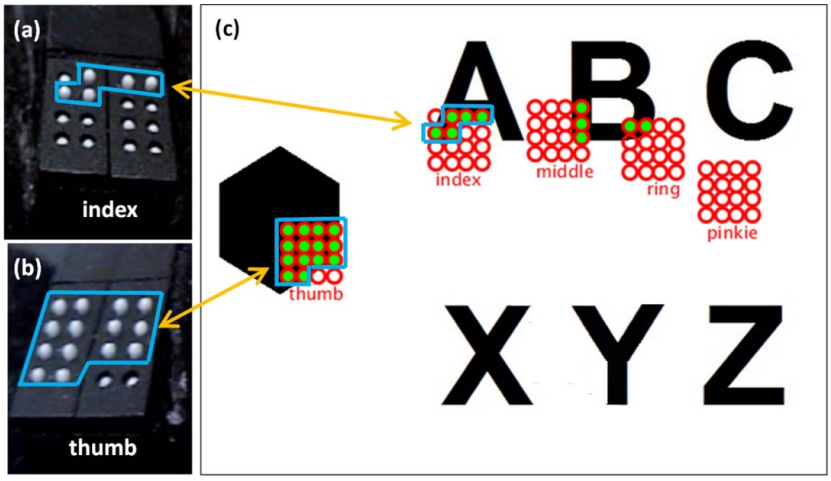

Figure 4.13: The fingertip tactile matrices and the graphical user interface (GUI) were developed using open-source software called Processing.
The activated pins of (**a**) index fingertip and (**b**) thumb tactile matrices correspond to each small section, and (**c**) corresponding activation of index shown in Figure 4.13a and thumb in Figure 4.13b are shown in shaded green in simulator matrices in the GUI.

4.7 Prototype 2: Testing and Validation

4.7.1 Ethical Clearance

In all experiments, human participants signed a written consent form approved by the ethics committee of Liverpool Hope University (LHU Approved Ethical Clearance: S–24-06-2019 SEL 087 and S–19-10-2021 SEL 5256).

4.7.2 Experimental Setup

The fine-grained haptic hand wearable connects wirelessly using both WiFi and conventional Bluetooth. Figure 4.14 shows the experimental setup. The hand will be hovering over a Leap Motion Controller, which will track the position of the fingertips and the pose of the hand. The coordinates of the fingertips are used to reference the simulator's five 4 by 4 tactile matrices. The tactile matrices in the simulator move across the computer screen as the hand or fingers move. To activate or deactivate the associated tactile actuator in the haptic hand wearable, the simulator tracks changes in each tactile matrix and sends a corresponding signal to the microcontroller. The fingertip tactile matrix simulator can also be driven

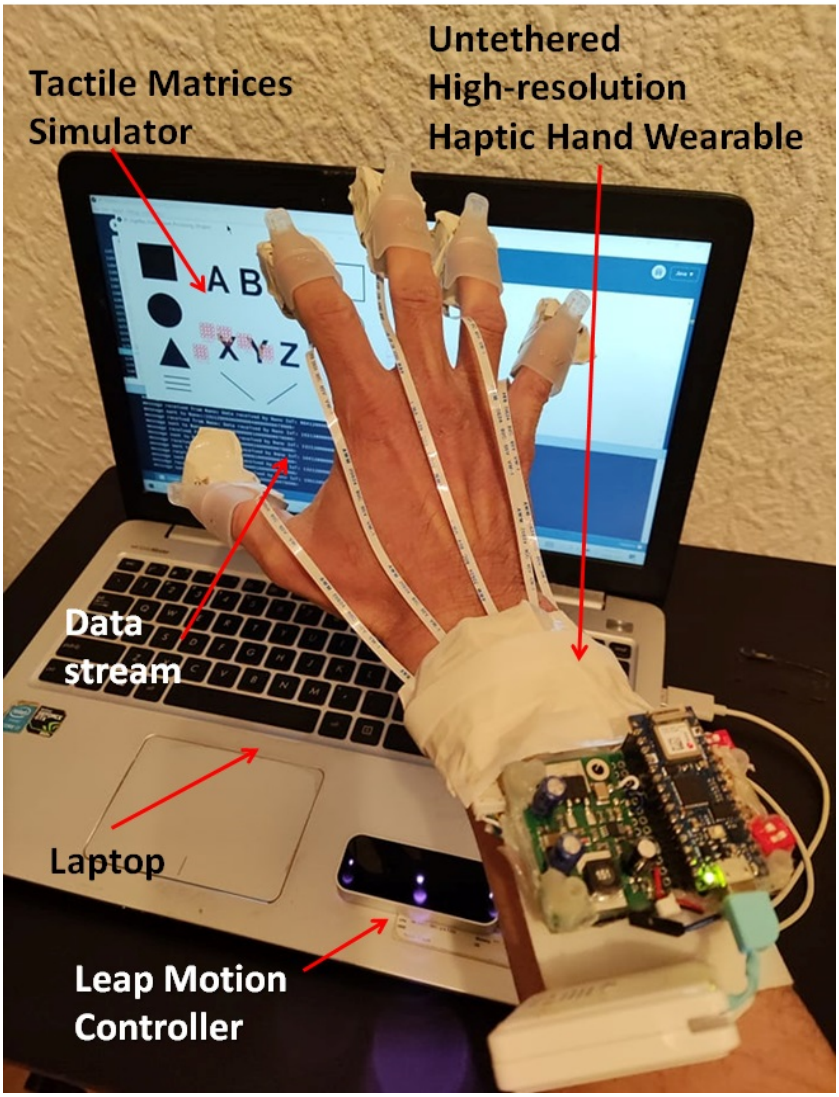

Figure 4.14: The integrated experimental setup for 2D scanning.

using a mouse instead of a Leap Motion Controller, as shown in Figure 4.15. The simulator and wearable haptic prototype 2 has the novelty of easily converting any computer mouse into a tactile mouse similar to the tactile mouse by Watanabe et al. [179], Hribar et al. [180], and Owen et al. [115]. The idea is when the surgeon hovers over the object on the screen and feels it by actuating fingertips, similar to how a surgeon would feel more subtle information via fingertips in open surgeries [117].

4.7.3 2D Surface Scanning and Edge Detection

The prototype can scan a surface, as shown in Figures 4.13 and 4.14, wherein all the tactors can be activated simultaneously when it covers a large area. The untethered

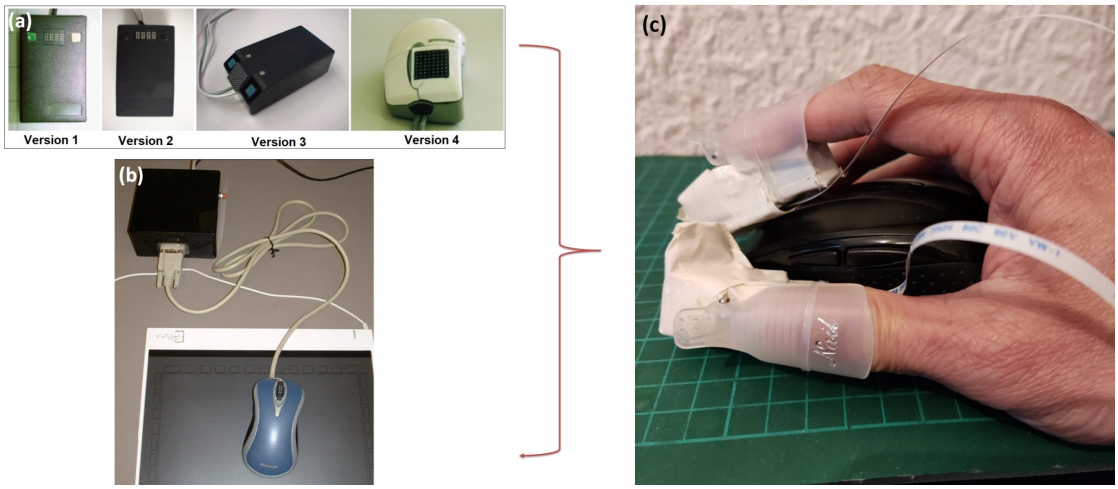

Figure 4.15: Tactile mice. When the user wears the fine-grained haptic wearable, any computer mouse can become a tactile mouse similar to the tactile mice presented in a) by Watanabe et al. [114] and Owen et al. [115].

fine-grained haptic hand wearable is an expanded version of the one fingertip tactile matrix actuator that used Dot Braille cells [174]. The hand wearable used P20 Metec Braille cells. Actual scanning test videos can be found in this link [181].

The prototype has edge detection capabilities in addition to surface scanning. Figure 4.16 shows the edge detection procedure utilising the Canny edge and Hough transform. The Canny edge detection algorithm is used to produce the output as white edges on a black backdrop, as shown in Figure 4.16b, from the given RGB image of a heart, as shown in Figure 4.16a. Because the prototype interprets a black colour pixel as a "up" signal for the actuator, it is necessary to flip this Canny edge result. The Canny edge result is now displayed as black lines with a white background as shown in Figure 4.16c by simply utilising the picture filter function "filter(INVERT)" without any spaces. The Hough transform for lines function in the OpenCV library can be used to create the image with thick lines as shown in Figure 4.16d. As shown in Figure 4.16e, the enhanced Canny edge image on a white background is subsequently fed as background in the tactile matrix simulator.

4.7.4 Tapping Vibration

One novel capability of the fine-grained haptic wearable is that it can produce a clear and distinct tapping or linear vibration on the fingertips. The tactile

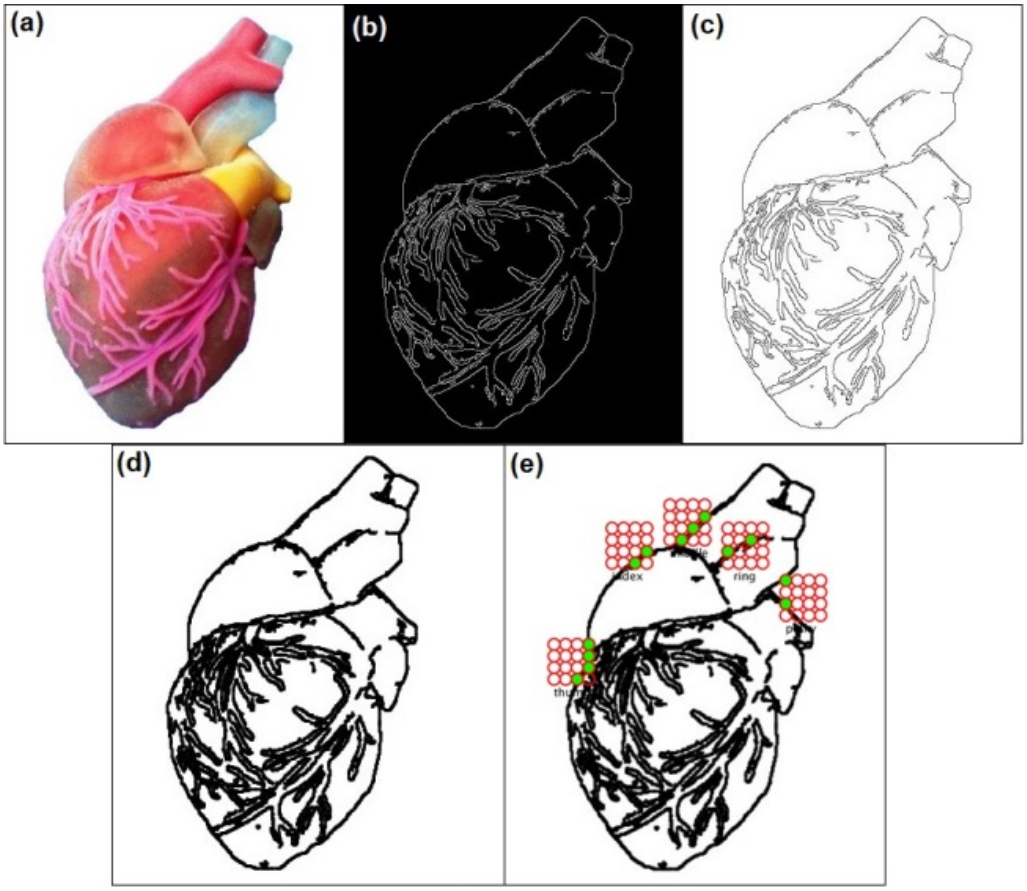

Figure 4.16: Edge detection result. (**a**) RGB image of a heart, (**b**) Canny edge result, (**c**) inverted Canny edge, (**d**) thickened Canny edge using Hough transform, and (**e**) edge detection with tactile matrices simulator. The processed RGB image using edge detection algorithm has become the background image of the tactile matrix simulator.

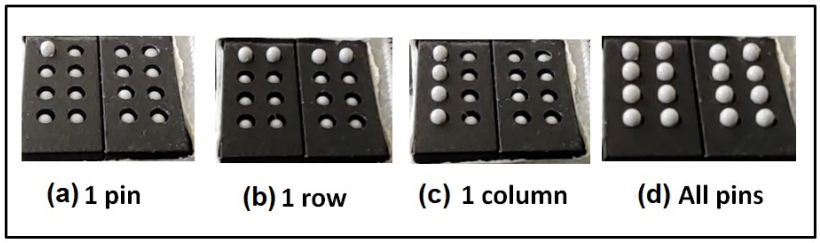

Figure 4.17: Tapping vibration can be achieved using (a) 1 pin, (b) 1 row, (c) 1 column, and (d) all pins.

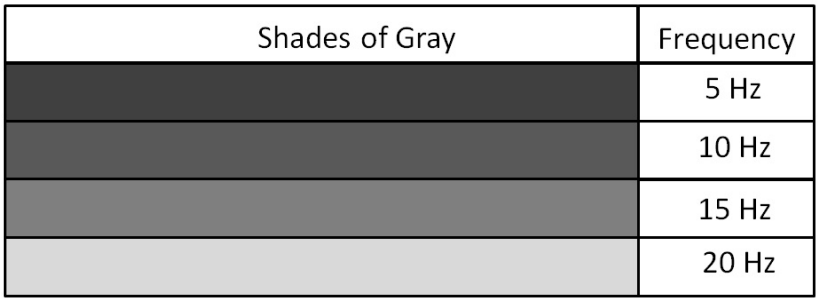

Figure 4.18: Different tapping frequencies can be assigned to various shades of grey.

pins of P20 Braille cells can be activated in a tapping manner and controlled using pulse signals at different frequencies and duration. In contrast with the mini-vibration motors that have buzzing vibrations and a fixed vibrating surface area, the fine-grained prototype can produce other vibrating surface areas such as point tapping by activating one pin, line tapping by activating a row, a column, and area tapping by activating all the pins in the 4x4 fingertip tactile matrix as shown in Figure 4.17(a)-(d), respectively.

Tactile pins can vibrate using 5 Hz, 10 Hz, 15 Hz, and 20 Hz frequencies as shown in Figure 4.18, which are within the range of frequencies that triggers the fingertip's tactile mechanoreceptors: Meissner's corpuscles and Merkel's cells that are sensitive to edge pressure and flutter tap as reported by Visell [30].

In one tapping test conducted, the topmost row vibrates at 5 Hz for 2 s, followed by succeeding rows going down with frequency increments of 5 Hz for each row. Rows or columns can execute the tapping pattern with increasing or decreasing tapping frequency. Aside from activating the pins by row or column, all the 16 tactile pins can vibrate simultaneously. By doing this, there would be a larger tapping area compared to a column or row vibration.

Moreover, instead of directly programming the pins to vibrate at a specific frequency, another parameter such as grey-scale values can be used to change the tapping frequency dynamically. Different tapping frequencies can be assigned to various shades of grey, as shown in Figure 4.18. As the ROI in the tactile simulator moves across a grey-scale image, the tactile actuator is activated with the corresponding tapping frequency. Unlike the Canny edge detection that uses binary

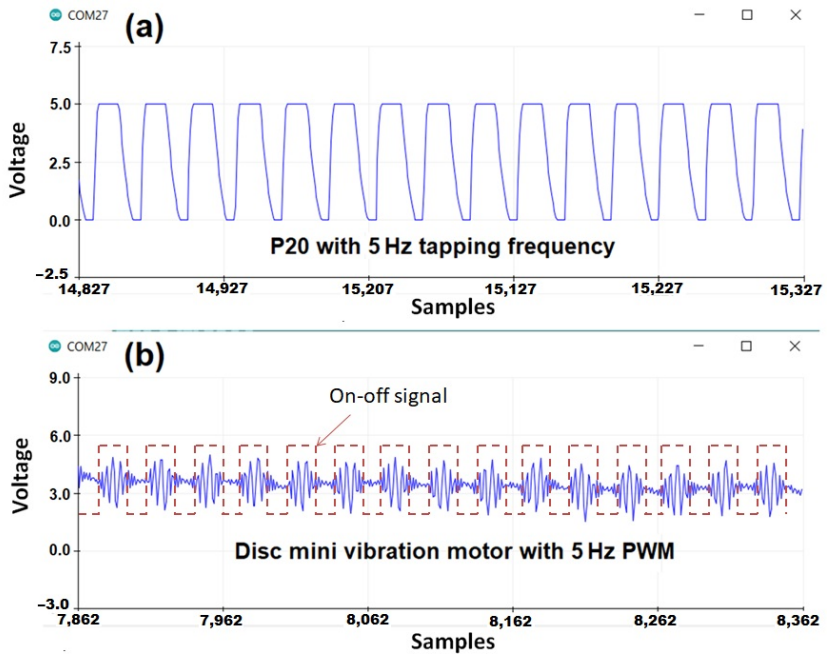

Figure 4.19: Tapping vs buzzing vibration. (**a**) Tapping: 5 Hz vibration has clear and distinct vibrations. (**b**) Buzzing: The low-frequency 5 Hz on–off signal for the vibration motor (in red dotted lines) has a high-frequency buzzing vibrations (in blue spikes).

scale or either on or off based on black and white pixels, the grey-scale image can be assigned with varying frequencies. This method can produce a gradient tapping intensities depending on the grey-scale image within the ROI. This grey-scale can be used to test 4 different intensities. In this case, these intensities are 5 Hz, 10 Hz, 15 Hz, and 20 Hz. Depending on the grey-scale values, humans perceive different intensities. The actual tapping test videos can be found in this link [181].

The actuators at the fingertips of the prototype can produce clear and distinct tapping vibrations compared to Eccentric Rotating Mass (ERM), and Linear Resonant Actuator (LRA) vibrotactiles with multiple frequencies combining low modulating frequency for the pattern and the inherent high-frequency due to their vibrating mass [182]. Each tactile pin in the 4x4 fingertip tactile matrix can vibrate up to 300 Hz, similar to the dynamic response of Metec P16 Braille cell reported by Owen et al. [115]. Comparison of tapping and buzzing vibrations are shown in Figure 4.19. ERM and LRA motors have intrinsic high-frequency vibrations based on their moving mass, but they can have another vibration based on how they are activated. This prototype can produce a point, line, and area tapping

vibrations that cannot be replicated using vibrotactile motors. When applied to haptics, the multiple vibrations on the ERM and LRA motors are more complex than the tapping vibrations that the prototype can produce. The prototype could be used as a test platform for future studies related to tapping vibrations perception on the fingertips based on a grey-scale image or contour map. Tapping frequency is another added feature to convey fine-grained information with more clarity to the surgeon/user, especially in laparoscopy.

4.7.5 Experiments Involving Human Participants using the Untethered Fine-grained Haptic Hand Wearable

Three tactile pattern recognition experiments involving nine human participants were conducted in this study, despite the prototype not being designed to replace vision but to augment it. Three experiments were carried out. Experiment 1 is a spatial test to determine how well a person can distinguish between tactile patterns that are activated at various positions on the fingertip. In Experiment 2, a temporal test is used to determine how well humans can distinguish between various vibrating patterns travelling in various directions on the fingertip. In Experiment 3, a 2D image identification test is used to examine how well humans can identify edges, lines, and basic geometric shapes.

4.7.6 Experiment Procedure

Nine right-handed individuals (seven males, two females with ages 23–60 years old) participated in the experiments after giving informed consent. The Dutch Handedness Questionnaire [183] was used to evaluate the handedness. The participants were instructed to feel or perceive the tactile patterns on their index finger and/or thumb using their most dominant hand. Patterns or activating signals were transmitted wirelessly from the laptop to the haptic wearable using Bluetooth communication, as shown in Figure 4.14. When the pins were actuated, participants were then asked what pattern they felt based on the printed patterns given to them, which are similar to the patterns in the graphical user interface (GUI) for each test. The responses of

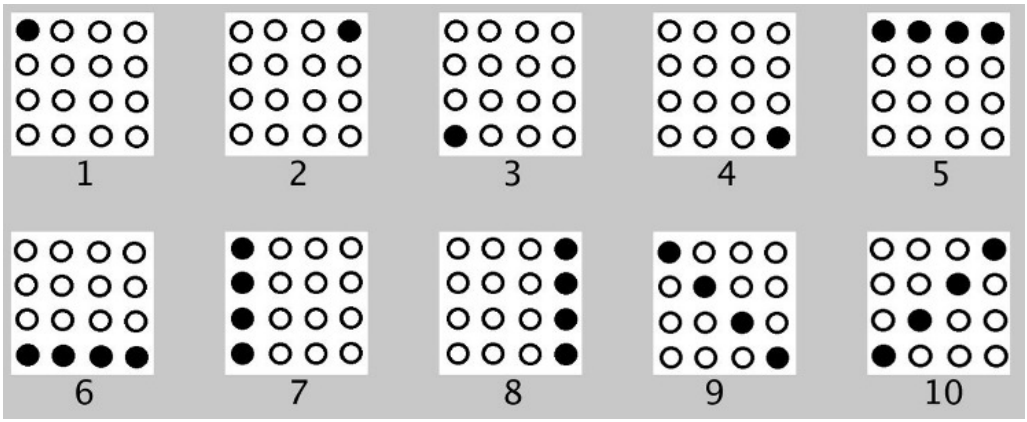

Figure 4.20: Patterns for spatial test.

the participants were recorded, and a log file was generated for each test. The log file contains played patterns and the participant's selection on the GUI after each trial.

4.7.7 Experiment 1: Spatial Test

Each participant was trained before the test using the index finger. Ten different patterns related to the perimeter, corners, or boundaries of the tactile matrix were activated in succession or the same sequence as shown in Figure 4.20. After the training, the ten patterns were played pseudo-randomly. The spatial test was further divided into two: (a) patterns were activated once, and (b) patterns were activated three times for each trial. There were three repetitions for each trial. Therefore, 30 trials were tested for single activation and 30 trials for 3x activation. The participants were then asked what patterns they perceived on their index fingers based on the patterns shown in Figure 4.20 for each trial.

4.7.8 Experiment 2: Temporal Test

Patterns of different frequencies move in different directions across the matrix in the temporal test, in contrast to the spatial test, where the activated pattern is in a fixed location inside the matrix for each trial. This temporal test is further divided into two parts: (a) using only the index finger and (b) using the index finger and/or thumb. Each human participant is trained before the test by running in sequence ten different patterns having different frequencies (10 Hz and 20 Hz)

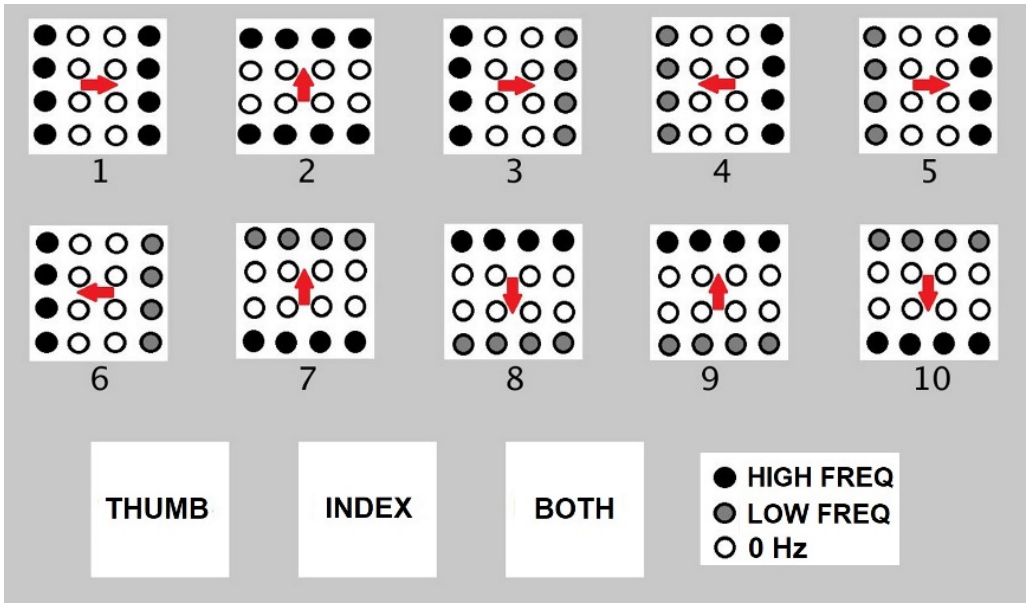

Figure 4.21: Patterns for temporal test.

and different directions of movement, as shown in Figure 4.21. Each pattern can be activated for the index finger only, for the thumb only, or for both the index finger and thumb simultaneously. During the testing, patterns were played pseudo-randomly, and there were three repetitions for each trial. The participants were then asked what patterns they perceived on their index fingers based on the patterns shown in Figure 4.21 for each trial.

4.7.9 Experiment 3: 2D Scanning Test

In the 2D scanning test, a setup similar to Figure 4.14 is used, but each participant used a computer mouse, as shown in Figure 4.15, to move the fingertip tactile matrices in the simulator, as shown in Figure 4.22. This experiment used two computer screens: one for the experimenter and one for the participant. During the training, the patterns using horizontal and vertical lines, and geometric figures, such as triangles, squares, and circles, in edge or plane figures, as shown in Figure 4.23 are displayed on the computer screen where each participant can see them. Each participant is then asked to feel the tactile pin actuation on their index finger and thumb as the mouse is moved across the edges or surface of the patterns in the computer display. During the testing, the patterns in Figure 4.23 are placed in

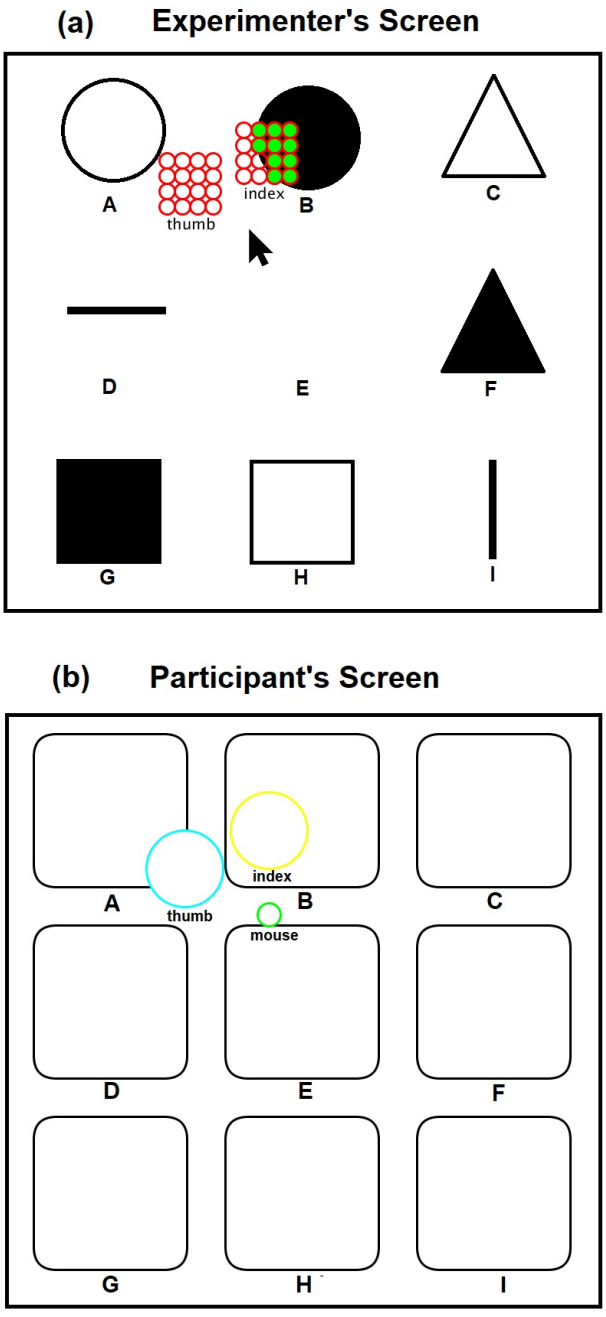

Figure 4.22: Patterns for 2D scanning test. (**a**) Experimenter's screen, (**b**) participant's screen. Participants were able to see empty boxes to explore and identify the objects A to I.

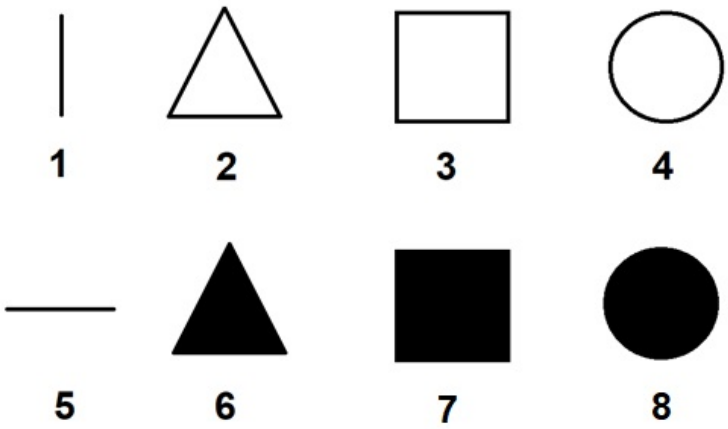

Figure 4.23: 2D training patterns.

a different order, as shown in Figure 4.22, which are visible to the experimenter but are concealed to the participants. The participants can only see the nine boxes in the participant's screen, as shown in Figure 4.22, with blue and yellow circles corresponding to the thumb and index tactile matrices, respectively. Moreover, the small green circle corresponds to the mouse pointer, which guides the participant during the scanning. Each participant is then asked to move their hand on top of the mouse to scan or explore each of the nine boxes and tell the experimenter what geometric figure or line they can perceive. The box can have a line or geometric shape, but it can also be empty or blank.

4.8 Prototype 2: Results and Discussion

4.8.1 Experiment 1: Spatial Test

On average, the participants were able to recognise the different patterns shown in Figure 4.20 with 95.93% accuracy. The average test time is 2 min and 2 s with an SD of 37 s. Participants were trained for 30 trials. There was an improvement in the accuracy from 77.78 to 100% with respect to the 30 trials, as shown in Figure 4.24. After 12 trials, participants' accuracy of recognition reached 100%.

The spatial test results for part 1 and part 2 graphed side by side are shown in Figure 4.25. The average test time to complete the first part of Experiment 1 is 2 min and 25 s with an SD of 35 s. The test time for the second part of

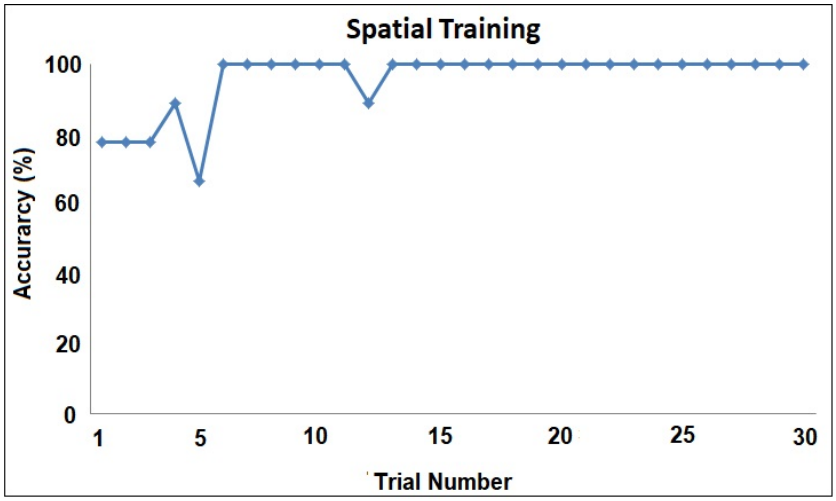

Figure 4.24: Spatial training results.

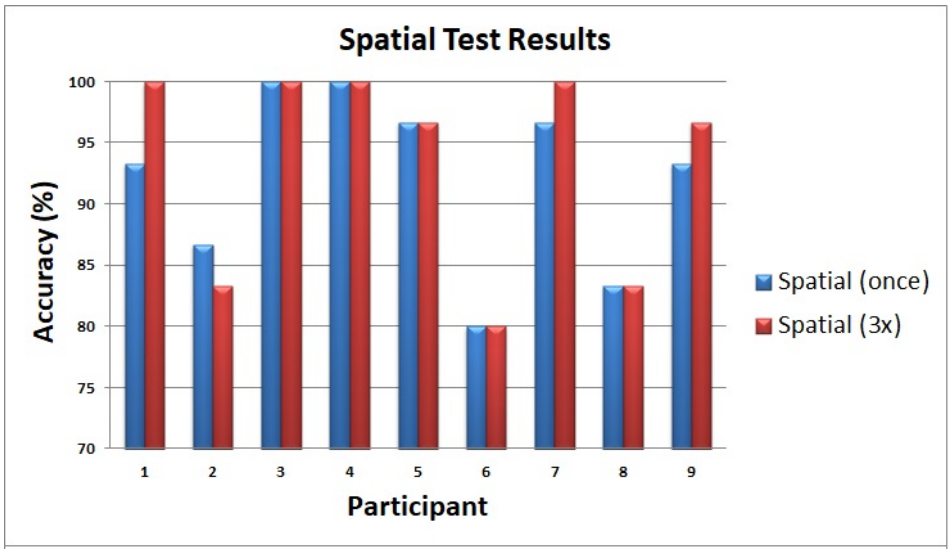

Figure 4.25: Spatial Test Results.

Experiment 1 is 2 min and 43 s with an SD of 10 seconds. The results show that the perception of patterns activated thrice has very minimal improvement compared to the situation when the patterns are activated once. On average, participants were able to recognise different patterns related to corners, diagonal, perimeter, or boundaries of the tactile matrix with 92.22% accuracy for patterns activated once and 93.33% accuracy for patterns activated three times. In general, it was noticed that, on average, tapping three times or a single time does not affect the responses. This would be useful in fast responses of humans in minimally invasive surgeries to react in real-time without time delay. Moreover, the results show that

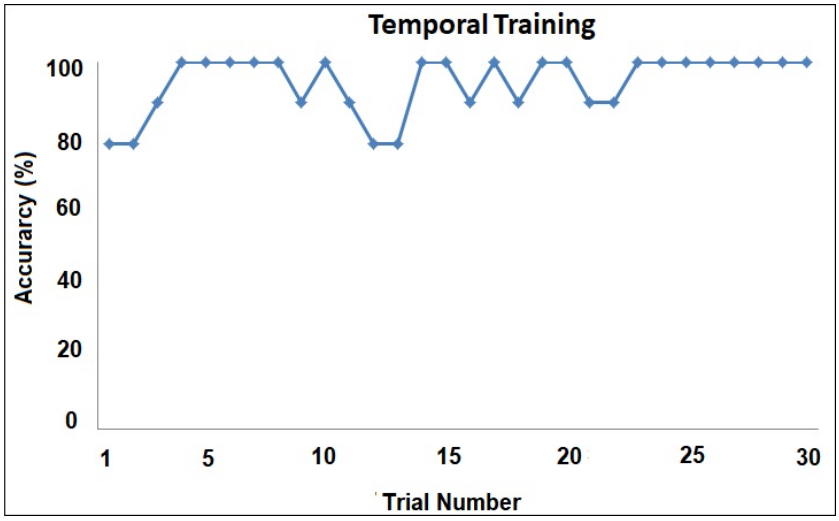

Figure 4.26: Temporal training results.

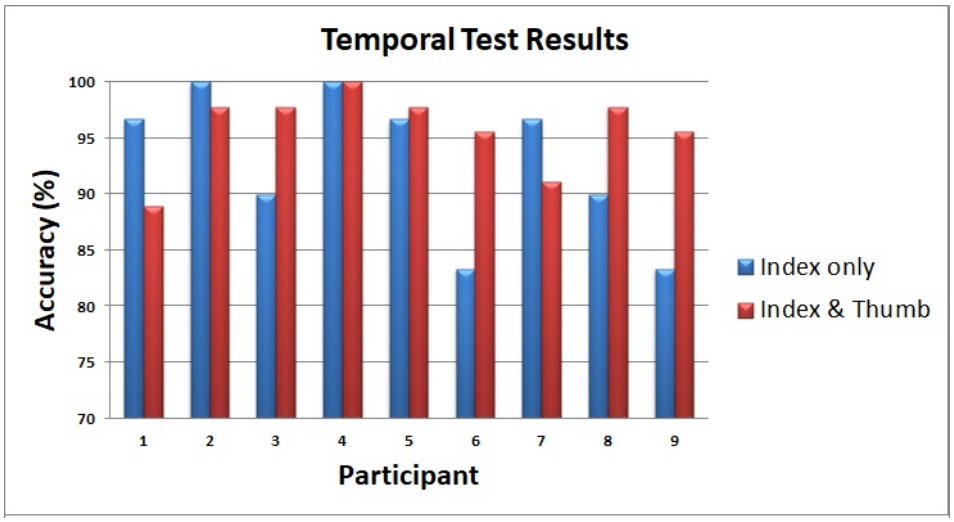

Figure 4.27: Temporal test results

.

single tapping is sufficient to feel the actuated patterns.

4.8.2 Experiment 2: Temporal Test

On average, the participants were able to recognise the different patterns shown in Figure 4.21 with 94.44% accuracy. The average test time is 9 min and 15 s with an SD of 1 min and 56 s. Participants were trained for 30 trials. There was an improvement in the accuracy from 77.78 to 100% with respect to the 30 trials, as shown in Figure 4.26. After 22 trials, participants' accuracy of recognition reached 100%.

The results of the temporal test for index finger only and the temporal test for

index finger and thumb are shown side by side in Figure 4.27. The average test time to complete the first part of Experiment 2 is 9 min and 18 s with an SD of 1 minute and 41 s. The test time for the second part of Experiment 2 is 15 min and 6 s with an SD of 1 minute and 3 s. In index-finger-only test, on the average, participants were able to recognise patterns vibrating at different frequencies moving in different directions with 92.96% accuracy. Moreover, the participants can clearly distinguish if the pattern is activated on the thumb only, index finger only, or on both index finger and thumb. On average, participants were able to recognise patterns with 95.80%. A single finger and double fingers exploration in temporal testing shows that a single finger is enough to recognise smooth surfaces/shapes. The combination of index and thumb helped to increase the accuracy from 92.96% to 95.80%.

4.8.3 Experiment 3: 2D Scanning Test

In the 2D scanning training, the participants are free to explore the different 2D geometric figures shown on the computer screen. On average, the exploration time for the whole training is 2 minutes and 1 second, with an SD of 22 seconds. Only the training time was recorded because the participants could directly see the 2D objects in the display during the training. The 2D patterns recognition accuracy is performed in the 2D scanning test.

Using the index finger and thumb, all the human participants in the 2D scanning test were able to distinguish an empty/blank box, a vertical line, and a horizontal line, as shown in the confusion matrix of Figure 4.28 with 100% accuracy. Moreover, participants were able to achieve a higher detection rate of 89% and 78% in detecting plane and edge square, respectively. The lowest accuracy is 56% for edge triangles, mostly confused with edge squares. A 56% average accuracy was obtained in recognising plane circles that confuses mostly with the plane square, not with vertical or horizontal lines or blank squares. Given the higher accuracy percentage values, humans need to be trained for the novel wearable to achieve techniques in recognition, as naive participants' recognition values are promising. Since surgeons are trained for surgeries, this system would be easily adapted to enhance techniques

Reference	Classified								
	blank		—	△	□	○	▲	■	●
blank	100%	0%	0%	0%	0%	0%	0%	0%	0%
|	0%	100%	0%	0%	0%	0%	0%	0%	0%
—	0%	0%	100%	0%	0%	0%	0%	0%	0%
△	0%	0%	0%	56%	33%	11%	0%	0%	0%
□	0%	0%	0%	11%	78%	11%	0%	0%	0%
○	0%	0%	0%	22%	11%	67%	0%	0%	0%
▲	0%	0%	0%	0%	0%	0%	67%	11%	22%
■	0%	0%	0%	0%	0%	0%	11%	89%	0%
●	0%	0%	0%	0%	0%	0%	11%	33%	56%

Figure 4.28: 2D scanning test confusion matrix.

in laparoscopic surgeries. Furthermore, these 2D scanning test results show that the prototype can be used as a vision substitution device as well. On average, the exploration time to complete the 2D scanning test is 4 min and 11 s with an SD of 32 s. The exploration time during testing is twice the training time.

4.9 Prototype 3: Unified Untethered Multimodal Fine-grained Haptic Hand Wearable

Prototypes 1 and 2 could be used as stand-alone modules or combined to form Prototype 3, a unified untethered haptic hand wearable with haptic primary colours (force, vibration, and temperature) and fine-grained cutaneous feedback, as shown in Fig. 4.29.

The annular thermo-vibro feedback from the index fingertip of Prototype 1 has been moved to the palm area in the unified wearable to give way to the 4x4 fingertip tactile matrix on the index finger. The force feedback of Prototype 1 was improved by creating a force feedback gradient using micro-servos instead of small solenoids.

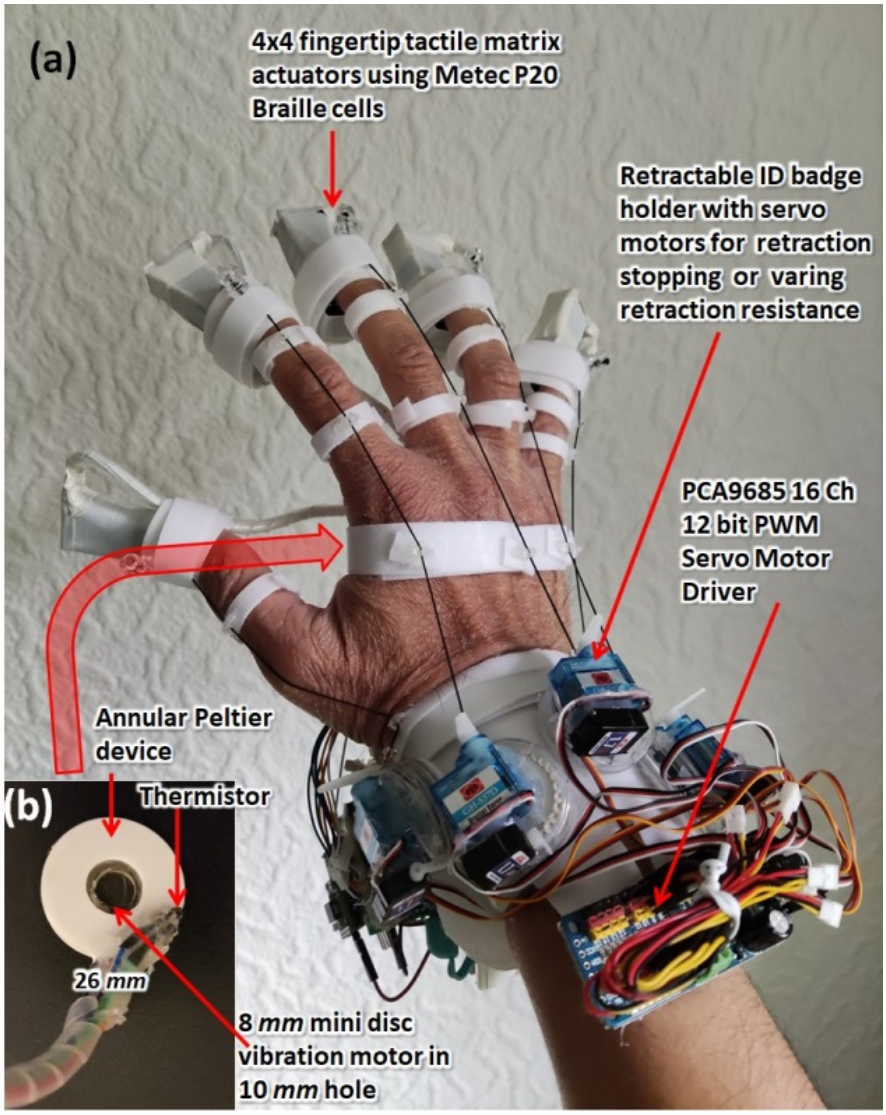

Figure 4.29: (a) Untethered fine-grained haptic wearable with haptic primary colours *(force, vibration, and temperature)* feedback. (b) an annular TEG with a mini-vibration motor placed at the palm of the haptic hand wearable.

For each retractable ID badge holder, there are two micro-servos, as shown in Figure 4.30(a). One micro-servo is for the stop-and-go mode like in Prototype 1 to simulate a hard VR object, and the other micro-servo is used to vary the retractable wire resistance by changing the angle, as shown in Figure 4.30(b), to simulate the varying softness or hardness of VR objects. Ten micro-servos can be controlled by the PCA9685 16 channel 12 bit PWM servo motor driver [187] connected to the Arduino Nano 33 IoT using I2C communication. Unlike the stop-and-go solenoid feedback of Prototype 1, mini-servos were used in the unified wearable. The mini-servos

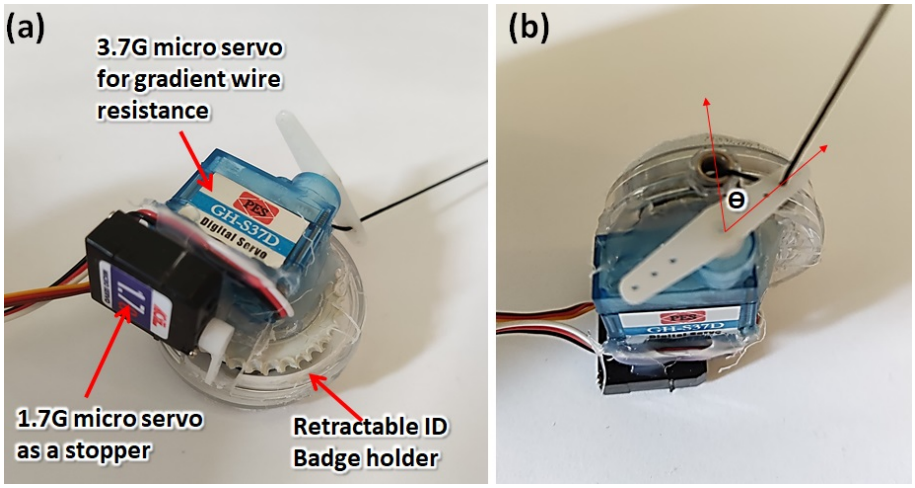

Figure 4.30: (a) Force feedback with stop-and-go and gradient retractable wire control. (b) The angle of retractable wire produces gradient resistance.

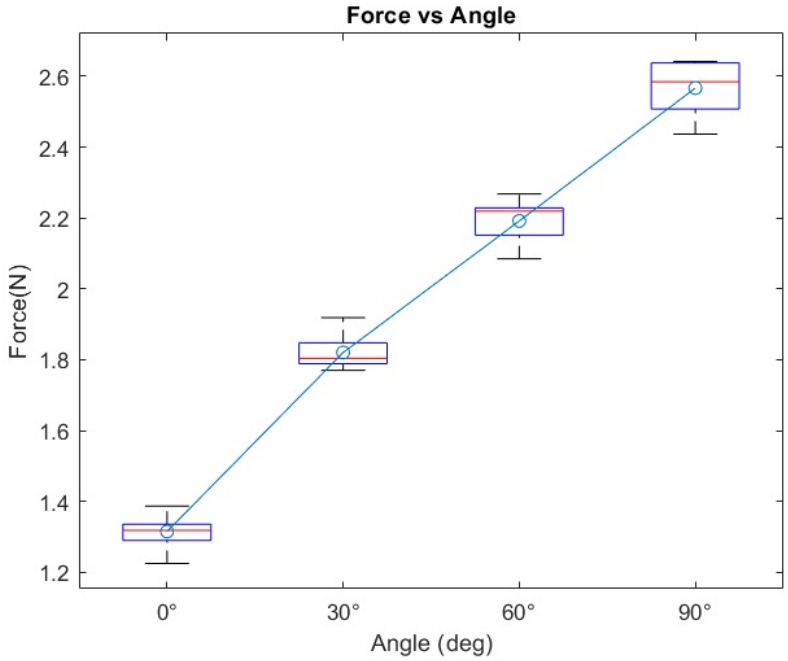

Figure 4.31: Resistance of the retractable wire at different angles.

consume little current compared to solenoids by a factor of seven.

A 1200 mAh USB power bank was used for the microcontroller, and four 1.5V dry cells were used for the mini-vibration motor and annular TEG. The 8mm disc vibration motor consumes 63 mA, while the Peltier device consumes a maximum of 1.5A at 3V. One of the drawbacks of Prototype 1 is the power consumption due to the solenoid stoppers that draw a large current of around 700 mA at 3V. The

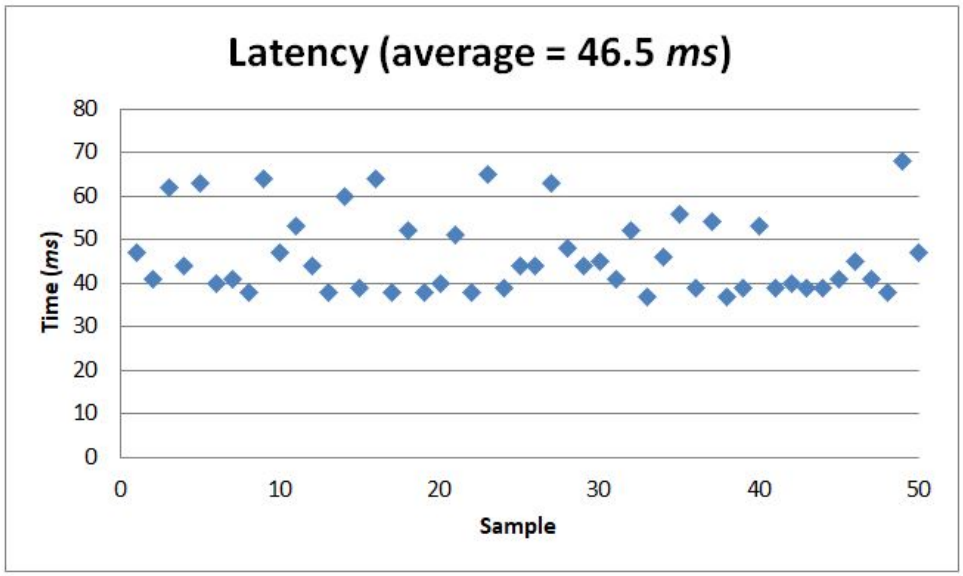

Figure 4.32: Latency test result from 50 samples. The average 46.5 ms latency is suitable for haptics. It is significantly less than the 600 ms tolerable delay that a surgeon would accept in the absence of haptic feedback, according to Tavakoli and Patel [165].

small solenoid motors are replaced by mini-servo motors in Prototype 2, which are low-power devices as shown in Figure 4.30. The current rating of a mini servo is around 100 mA at 4.8V. There are two micro-servos for each retractable ID badge holder, as shown in Figure 4.30(a).

Moreover, the resistance of the retractable wire was measured ten times for each angle of 0°, 30°, 60°, and 90°, respectively. The result of force vs. angle is shown in Figure 4.31.

The fine-grained haptic wearable's microcontroller Arduino Nano 33 IoT has a built-in WiFi Nina chip for wireless connectivity. Aside from WiFi connectivity, this microcontroller can connect via Classic Bluetooth, enabling the fine-grained haptic hand wearable to interface with the VR Quest 2 headset wirelessly. The classic Bluetooth was successfully activated, running at a 115,200 baud rate.

Fifty samples of data communication were recorded using the haptic wearable. Using a Bluetooth connection, an average latency of 46.5 ms was recorded with a standard deviation (SD) of 9.06 ms, as shown in Figure 4.32. The latency is slightly higher than the 42.38 ms PC-Arduino USB serial communication latency reported in [191]. However, the setup is wireless with 46.5 ms latency, much lower than the

600 ms tolerable delay acceptable by a surgeon in the absence of haptic feedback in teleoperated surgery reported by Tavakoli and Patel [165]. There is a larger SD of 9.06 ms compared to the 1.29 ms SD in USB serial communication reported [191] because the latency was tested using Bluetooth communication.

4.10 Chapter Summary

This chapter presented the development of a unified multimodal haptic hand wearable with haptic primary colours and fine-grained cutaneous feedback that could be used to complement the HaptiTemp sensor. Different haptic wearables were discussed to form the unified hand wearable. Prototype 1 is an untethered multimodal haptic wearable with haptic primary colours *(force, vibration, and temperature)* feedback. The force feedback comes from the retractable ID badge holders that could restrict finger movements. There are minivibration motors on each fingertips that could give vibration feedback to user. Aside from the minivibration motor at the index finger, there is an annular Peltier device that could give temperature feedback. The minivibration motor together with the Peltier device form a thermo-vibro feedback. On the other hand, Prototype 2 has fine-grained cutaneous feedback made from commercially available Metec P20 Braille cells. It has 80 tactile pins that can be controlled individually. The hand wearable is untethered, lightweight, portable, modular, and can be wirelessly connected using classic Bluetooth or WiFi. The components for the prototype are commercially available, and the software application was developed using open-source software. The device has a maximum power consumption of 830 mW and a total weight of 204 g. The fine-grained wearable can be fed with predetermined patterns such as Braille or tapping patterns. It can also be used to scan surfaces and detect the edges of images using the Canny edge detection algorithm.

Moreover, experiments involving human participants were conducted. In the spatial test, participants were able to recognise different patterns related to corners, diagonals, perimeters, or boundaries of the tactile matrix with 92.22% accuracy for patterns activated once and 93.33% accuracy for patterns activated three times.

In general, it has been noticed that tapping three times or a single time does not affect the responses. In the temporal test, where the index finger only was used, participants were able to recognise patterns vibrating at different frequencies moving in different directions with 92.96% accuracy, but the combination of index and thumb helped to increase the accuracy from 92.96% to 95.80%. In the 2D scanning test, participants achieved 100% accuracy in recognising empty/blank boxes, vertical lines, and horizontal lines. Participants in the 2D scanning test achieved a detection rate of 89% and 78% in detecting plane and edge square, respectively. The lowest accuracy is 56% for edge triangles confused mostly with edge squares. A 56% average accuracy was obtained in recognising plane circles that were confused mostly with the plane square, not with vertical or horizontal lines or blank squares. These 2D scanning test results show that the prototype can be used as a vision substitution device.

The communication delay, which results in instability and divergence, is one of the major problems with haptic-enabled telerobotic systems, according to Mehrdad et al. [164]. The average latency of the fine-grained cutaneous haptic hand wearable in this thesis is 46.5 ms, which is significantly less than the 600 ms tolerable delay that a surgeon would accept in the absence of haptic feedback, according to Tavakoli and Patel [165]. One of the biggest obstacles to integrating haptic feedback into surgical telerobotic systems is stability [164]. The effectiveness and performance of teleoperation and immersive systems can be increased by adding high-resolution cutaneous feedback in the form of a fine-grained tactile matrix actuator on a haptic hand wearable.

Furthermore, this chapter presented how to combine Prototype 1 and Prototype 2 to form Prototype 3, a unified untethered multimodal haptic hand wearable with haptic primary colours *(force, vibration, and temperature)* and fine-grained cutaneous feedback.

5

Integrated Visuotactile System and VR Application

5.1 Abstract

Visual information about the things we see, such as shape and colour, comes to our eyes in a non-contact manner. On the other hand, touch information, such as texture and temperature, is received directly in contact with the object of interest. If touch information can be combined with visual information that can be sent to us from a distance in a non-contact manner, we can feel things beyond our reach if only we could actuate the touch information we receive. Moreover, if we combine touch information with virtual objects in a VR environment, we can perceive these virtual objects, not as an illusion but as if they exist.

This chapter demonstrates how the haptic primary colours *(force, vibration, and temperature)* from the HaptiTemp sensor can be actuated using the unified hand wearable. The integration of the HaptiTemp sensor and the unified multimodal fine-grained haptic hand wearable forms a visual-haptic system that could enable the user to feel the tactile information, such as an object's shape, texture, and temperature, beyond reach. The HaptiTemp sensor is for sensing haptic primary colours. The haptic information is then transmitted to an untethered multimodal haptic hand wearable with haptic primary colours feedback to actuate the force,

vibration, and temperature feedback mechanisms. Furthermore, this chapter demonstrates that haptic primary colours information can also be incorporated in a Virtual Reality (VR) environment. The unified haptic hand wearable can then be used in a VR environment to actuate the haptic primary colours to enhance the immersive experience.

5.2 Introduction

An integrated visuotactile system for sensing and actuating haptic primary colours, as shown in Figure 5.1 can be developed by combining the HaptiTemp sensor and the untethered multimodal fine-grained haptic hand wearable with haptic primary colours *(force, vibration, and temperature)* and fine-grained cutaneous feedback, as shown in Fig. 5.2. The HaptiTemp sensor presented in this thesis is a unified visuotactile GelSight-like sensor that can sense not only force and vibration but also temperature, making it a visuotactile haptic primary colours sensor. Moreover, the HaptiTemp sensor can simultaneously do temperature sensing and image classification, which no tactile sensor has done before. Using the HaptiTemp sensor, tactile information of a distant object can be captured and embed in a tactile images which can be retrieve and actuated making it possible to have an estimate or approximate tactile perception on the things beyond reach.

This thesis developed a unified untethered fine-grained haptic hand wearable with force, vibration, and temperature feedback to complement the HaptiTemp sensor, giving the user a perception of what the sensor is touching. The tactile images captured by the HaptiTemp sensor can be converted to lines or edges using the Canny edge detection algorithm, which can then be used to actuate the tactile matrices of the fine-grained haptic hand wearable.

Moreover, research and development on haptics and tactile feedback applied to virtual reality (VR) have been very active in providing an immersive experience [97, 126]. The COVID-19 pandemic has changed our lives forever. It has accelerated Research and Development (R & D) in various fields of our society creating new technological landscapes for the future. Virtual meetings for online learning, online

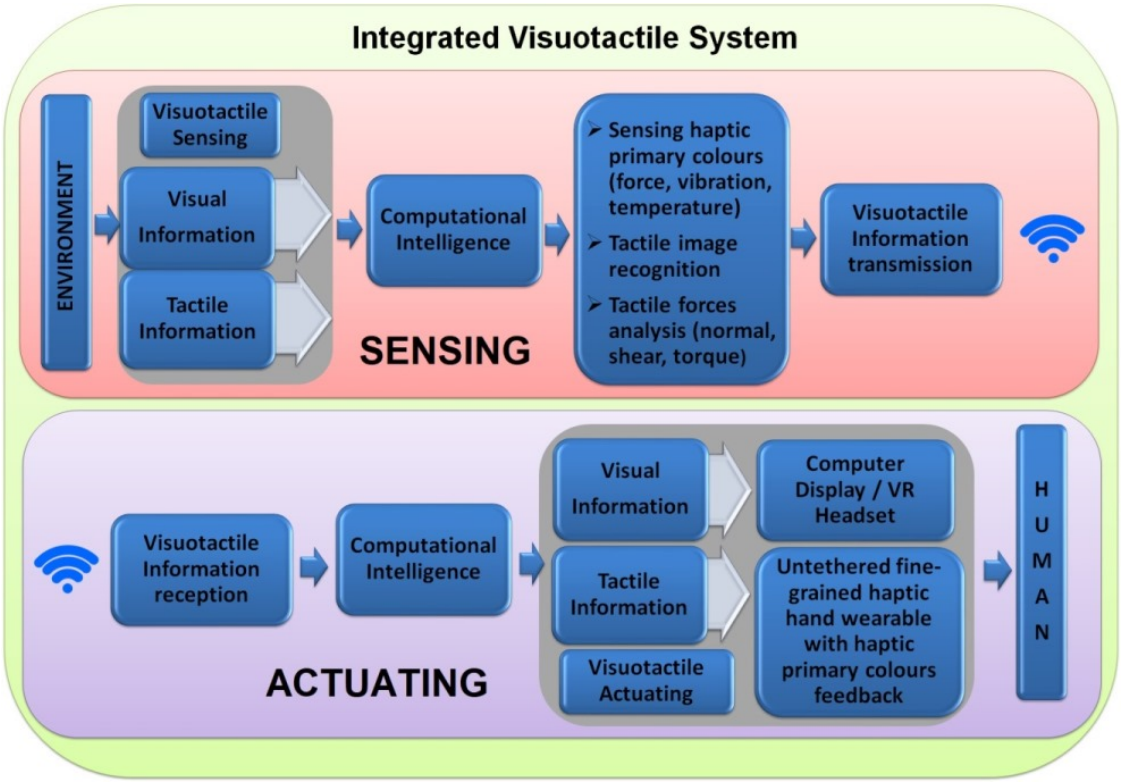

Figure 5.1: Integrated visuotactile system from sensing to actuating.

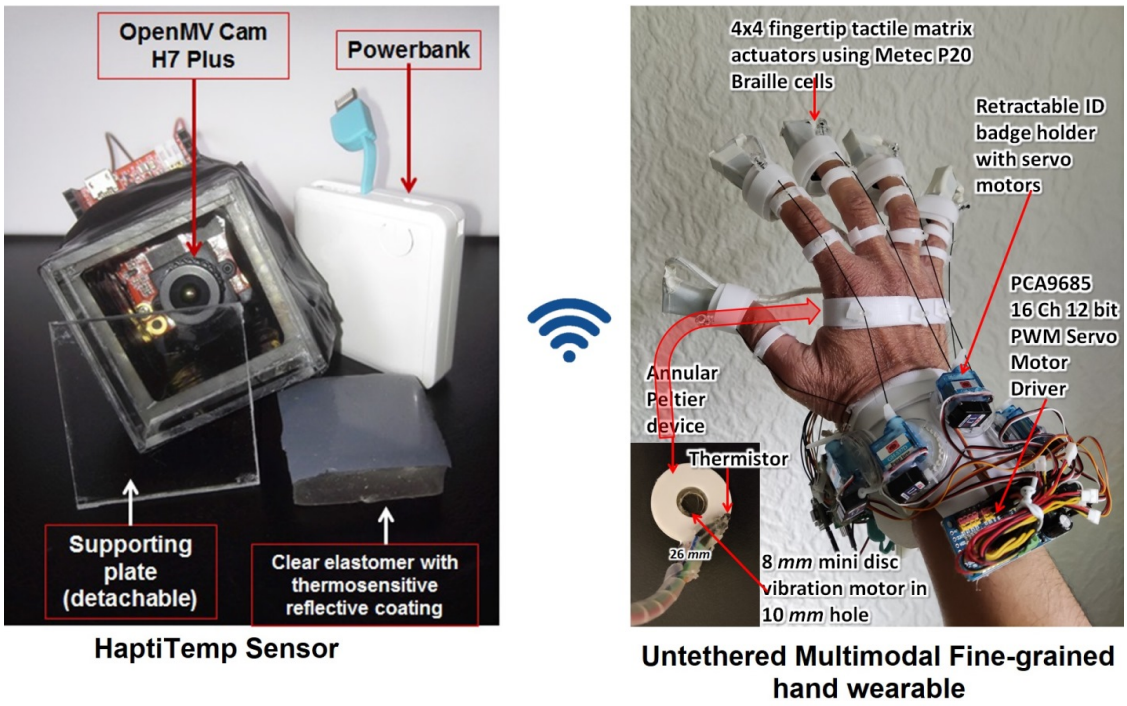

Figure 5.2: Combining the HaptiTemp sensor and the untethered multimodal fine-grained haptic wearable.

conferences, and online work have become prevalent during the pandemic and will continue even post-pandemic. Furthermore, the Metaverse is now gaining a lot of public attention.

Many believe that the Metaverse is the future digital world that may co-exist with the real world. It may encapsulate the whole internet, Spatial A.I., Embodied A.I., Brain Computer Interface (BCI), and eXtended Realities (XR), such as Virtual Reality (VR), Augmented Reality (AR), and Mixed Reality (MR). Many companies such as Microsoft, Sony, and Meta are doing a lot of R & D related to the realisation of the Metaverse by investing a lot in computational intelligence, spatial computing, and producing various XR-related devices for interoperability and seamless connectivity to produce a high degree of immersive experience in a digital world or virtual reality environment. XR devices in the form of VR/AR headsets are the popular devices that can be considered "digital gateways" to the Metaverse. When people wear a VR headset for the first time, the user's natural tendency is to grasp virtual objects. VR headsets may give audio-visual representations of virtual reality, but the immersive experience breaks down as soon as the user tries to grasp a virtual object without haptic feedback to sustain the immersive experience initially produced by the audio-visual effects. No matter how elegant and colourful a VR world is, if there is no haptic feedback, the VR environment will just be a 3D movie, and the VR objects will just be considered digital phantoms by the user. Because of the necessity of haptic feedback to enhance immersive experience, haptic wearables are being developed together with VR headsets.

Aside from integrating with the HaptiTemp sensor, the unified untethered fine-grained haptic hand wearable developed in this thesis can also be integrated into a VR environment using a VR headset such as the Oculus Quest 2 to enhance the immersive experience. It has been tested to work not only in 2D actuation of images but also in a 3D VR environment, making it possible for the user to feel the texture information such as shapes, surfaces, and edges on all the sides and surfaces of a 3D object, giving the user an impression of touching a real object.

Figure 5.3: Integration of HaptiTemp sensor with the unified fine-grained haptic hand wearable.

5.3 Testing and Validation: Integration of the Unified Fine-grained Multimodal Hand Wearable and the HaptiTemp Sensor

The unified multimodal haptic hand wearable discussed in Chapter 4 can be integrated with the HaptiTemp sensor to give the user an approximate sensation of the haptic primary colours *(force, vibration, and temperature)*, and can also be used to feel or actuate the edges of a 2D tactile image captured by the HaptiTemp sensor. The setup showing the integration of the HaptiTemp sensor with the fine-grained haptic wearable is shown in Figure 5.3.

5.3.1 Force

It has been reported and demonstrated by Headley and Pawluk [188] in 2010 that the Metec Braille cell can be activated at varying amplitudes by varying the supply voltage of the piezoelectric bimorph. Using a digital potentiometer such as X9C103 [189] that can be controlled using Arduino and the blob detection algorithm in the OpenCV library [145], the supply voltage for the fingertip tactile matrix can be varied automatically relative to the area of the bounding box of the detected blob, producing different tactile pin heights. If the bounding box area increases with force, the change in the area can be translated to varying amplitudes of the fingertip tactile matrix actuators to give the user a perception of varying force detected by the HaptiTemp sensor. Variations in the area of bounding boxes caused by variations in the detected force can also be translated or actuated as variations in the ID badge holder's wire resistance restricting finger movements.

5.3.2 Vibration

As discussed in Chapter 4, the P20 Braille cells used in the fine-grained wearable can be actuated to produce tapping vibrations. Using the blob detection [145], the fingertip tactile matrix actuator can be activated whenever a blob is detected, as shown in Figure 5.3. By doing this, vibration can be sensed by the user.

5.3.3 Temperature

The temperature data, or the "hot signal," discussed in Chapter 3, that triggers the Dobot robotic arm to retract can also be sent to an annular TEG at the palm area of the unified multimodal haptic hand wearable to give "hot" temperature feedback to the user by warming up the TEG. Moreover, a "cold" signal from the HaptiTemp sensor when it touches an object that has less than 31°C can also be sent to the annular TEG to make it cold.

5.3.4 2D Tactile Image Scanning

The tactile images captured by the HaptiTemp sensor can be converted into edges using the Canny edge detection algorithm as discussed in Chapter 4 and be used to actuate the fine-grained haptic wearable. Because the tactile matrix simulator is activated by black pixels, the Canny edge should be inverted using the Hough transform function of the OpenCV library. After thickening the black lines, the resulting tactile image can now be combined as the background image of the tactile matrix simulator.

5.4 Results and Discussion: Integration of the Unified Fine-grained Multimodal Hand Wearable and the HaptiTemp Sensor

One-to-one mapping between sensing and actuating haptic primary colours is shown in Fig. 5.4. Fine-grained actuation of the edges of a high-resolution tactile image captured by the HaptiTemp sensor is also shown in Fig. 5.4.

5.4.1 Force

When an object is pushed against the HaptiTemp sensor with varying force, the bounding box's area changes, which can be translated to different wire resistances of the ID badge holder, as shown in Fig. 5.4v, or varying amplitude of the fingertip tactile matrix actuators to give the user a perception of varying force detected by the HaptiTemp sensor, as shown in Figure 5.5.

5.4.2 Vibration

Using the blob detection algorithm in OpenCV [145], the fingertip tactile matrix actuator can be activated whenever a blob is detected, as shown in Figure 5.5. The vibrations detected by the HaptiTemp sensor, as shown in Fig. 5.4ii, can be actuated as tapping vibrations using the P20 Braille cells in Fig. 5.4i or minivibration motor, as shown in Fig. 5.4vii.a. By doing this, vibration can be sensed by the user.

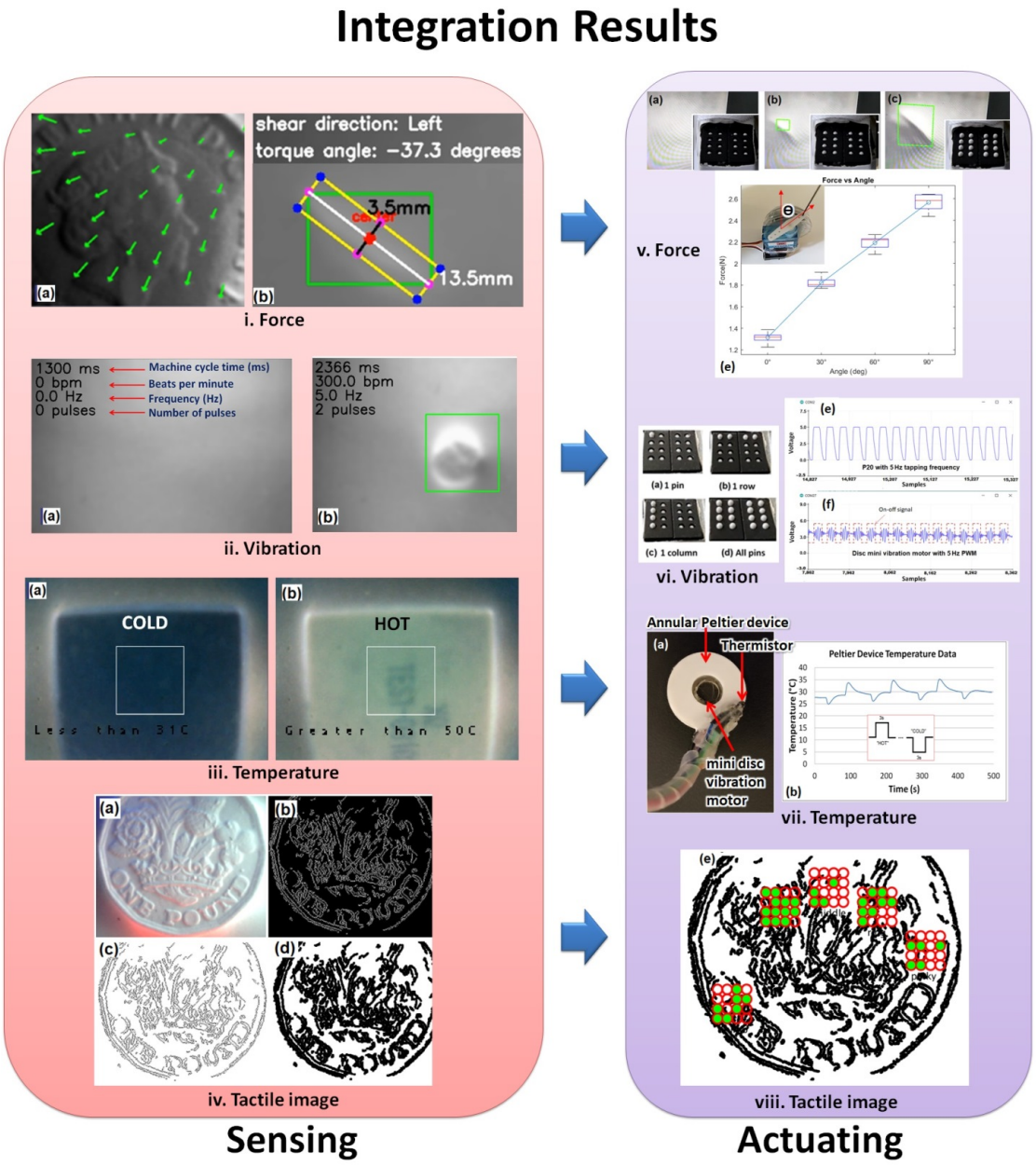

Figure 5.4: Integration Results. The tactile parameters detected by the HaptiTemp sensor can be sent wirelessly to the unified haptic wearable. The force estimation from the HaptiTemp sensor is shown in Fig. 5.4i can be actuated by a varying tactile pin height or different wire resistance of the ID badge holder, as shown in Fig. 5.4v. The vibrations detected by the HaptiTemp sensor, as shown in Fig. 5.4ii, can be actuated as tapping vibrations using the P20 Braille cells in Fig. 5.4i or minivibration motor, as shown in Fig. 5.4vii.a. The "hot" and "cold" signals from the HaptiTemp sensor can be used to trigger the annular Peltier device, as shown in Fig. 5.4vii, to make it "hot" or "cold". The tactile image captured by the HaptiTemp sensor can be transformed into edges, as shown in Fig. 5.4iv, and be actuated using the tactile matrix simulator, as shown in Fig. 5.4viii, that will activate the corresponding tactile pins in the haptic wearable.

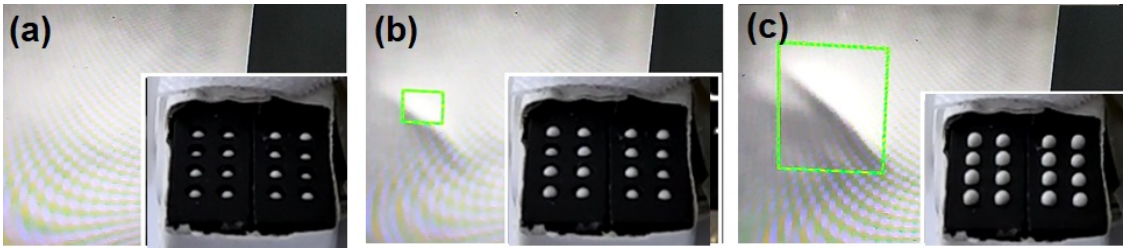

Figure 5.5: (a) no blob detected, fingertip tactile matrix is not activated, (b) small blob detected causing the fingertip tactile matrix to move up a little as compared to (c) where in there is a big blob detected which fully activated the tactile pins.

5.4.3 Temperature

The annular TEG, as shown in Figure 5.4vii, was used to produce hot and cold sensations. The hot and cold trigger signal is sent by the HaptiTemp sensor. Three cycles with 2 *Hz* sampling time were presented in Chapter 4. The ambient temperature is around 29°C. It was observed that once the Peltier device was heated up for 3 seconds, the cooling time from hot temperature to ambient temperature was twice as long as the warming up from cold to ambient temperature.

5.4.4 2D Tactile Image Scanning

The tactile image captured by the HaptiTemp sensor is converted into edges using the Canny edge detection algorithm, as shown in Figure 5.6. The actual one UK pound coin, as shown in Figure 5.6(a), is converted to Canny edges as shown in Figure 5.6(b). Since the tactile matrix simulator is activated by a black pixel, the Canny edge is inverted as shown in Figure 5.6(c), and the lines are thickened as shown in Figure 5.6(d) using the Hough transform function of the OpenCV library. The scaled-up image of the edges of one UK pound coin is shown in Figure 5.6(e), and the tactile matrix simulator is then applied to it so that the user of the fine-grained haptic hand wearable can feel the edges of the tactile image of the coin.

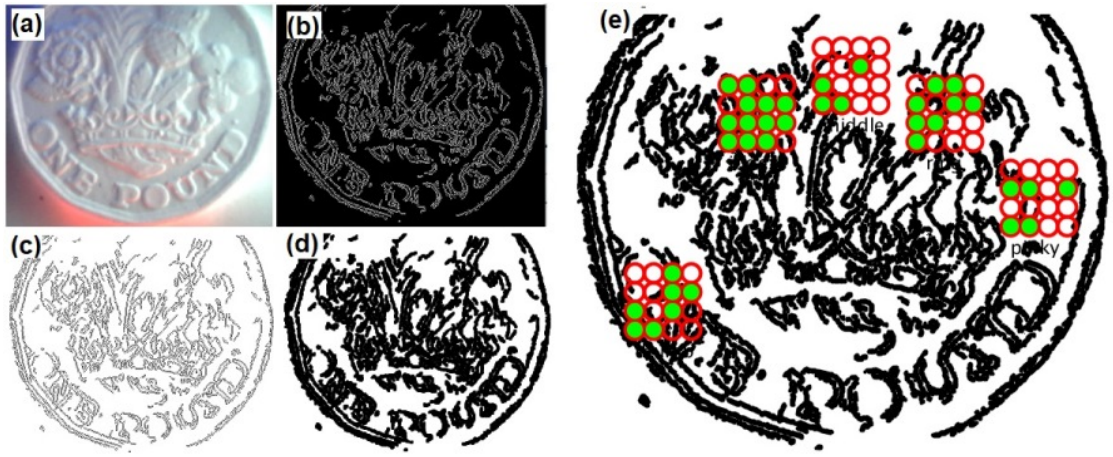

Figure 5.6: Canny edge detection on a tactile image. (a) tactile image of one UK pound coin, (b) canny edge, (c) invert image, (d) thickened lines, and (e) tactile simulator on the thickened lines.

5.5 Testing and Validation: Haptic Primary Colours *(force, vibration, and temperature)* in a Virtual Reality (VR) Environment

Haptic primary colours *(force, vibration, and temperature)* can be embedded in a VR environment that can be actuated by the haptic wearable developed in this thesis. The unified haptic wearable can be activated by the collision detection script embedded in the fingertips and palm area of the VR hand avatar. Each fingertip has sixteen collision detectors forming a 4x4 matrix corresponding to the 4x4 fingertip tactile matrix actuator. Different 3D VR objects can be assigned with different trigger signals for actuation. For example, different VR push button switches can have different spring resistance that can be changed in the physical property setting in Unity 3D software. Vibrations can be felt when scanning VR horizontal bars or VR rain drops. Moreover, temperature signals, such as "hot" or "cold", the can trigger the TEG or annular Peltier device at the palm area can be embedded on different 3D VR objects. When these objects are touched by the hand avatar in the VR environment, aside from collision detection signals, temperature signals are also sent to the unified haptic hand wearable.

Hand tracking devices are vital component in a VR environment. A leap

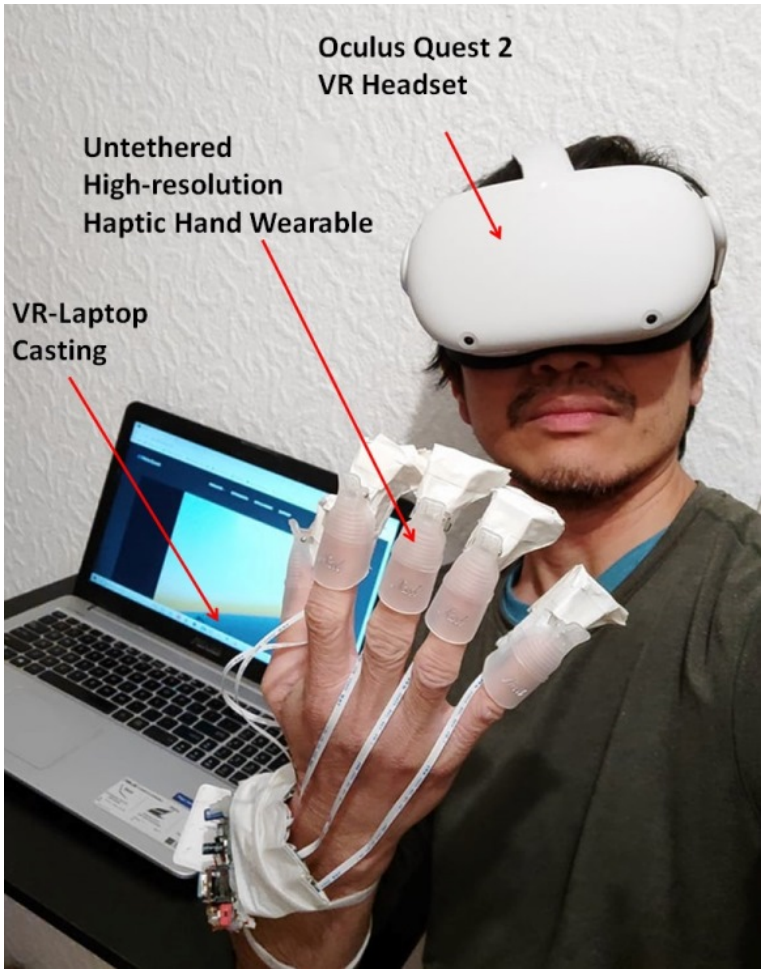

Figure 5.7: Setup for 3D surface scanning of VR objects using Oculus Quest 2 VR headset.

motion controller and VR headset Oculus Quest 2 with builtin hand tracking system were used in this thesis.

5.5.1 VR Setup Using Oculus Quest 2 VR Headset

The open-palm and open-backhand designs of the unified untethered wearable make it possible to connect to a Leap Motion Controller as a hand-tracking device, as discussed in Chapter 4, or connect to an Oculus Quest 2 VR headset using a Bluetooth connection. Oculus Quest 2 has a built-in hand-tracking capability. The 3D virtual objects are developed using Unity 2019 software. The VR environment can be cast on a laptop, as shown in Figure 5.7. The position of the control circuit of the untethered haptic hand wearable was placed on the wrist so that the Oculus

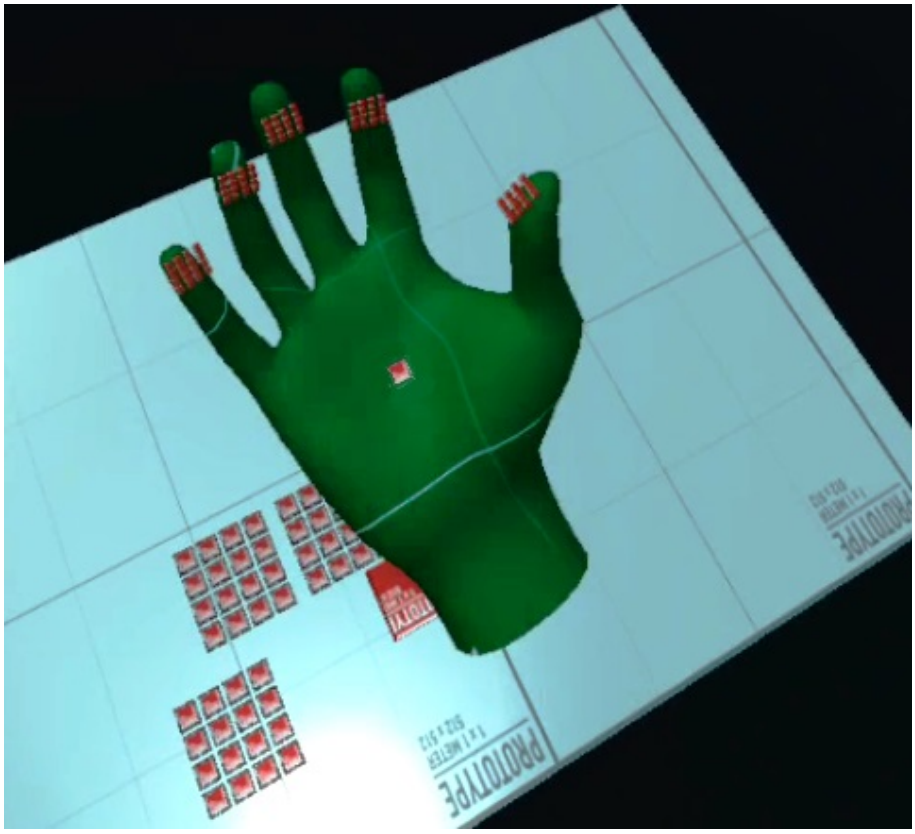

Figure 5.8: 4x4 collision detectors on each fingertip and one temperature detector on the palm area.

Quest 2 VR headset could track the back of the hand.

Similar to the 2D tactile matrix simulator, a 3D tactile matrices simulator has been created, as shown in Figure 5.8. The basic idea is to create a group of 4 × 4 button switches and attach it to each of the fingertips of the VR hand avatar. Scaling down the switches to fit on the fingertip is not a good option because the trigger point will collapse, and the button will not work. The workaround is to increase the OVRCameraRig scale to 10. A 3D environment was developed, as shown in Figure 5.9, where the shapes and edges of 3D VR objects can be explored. Each button switch on the fingertip of the 3D VR hand has a script that sends a signal to the corresponding hardware actuator during VR object collision.

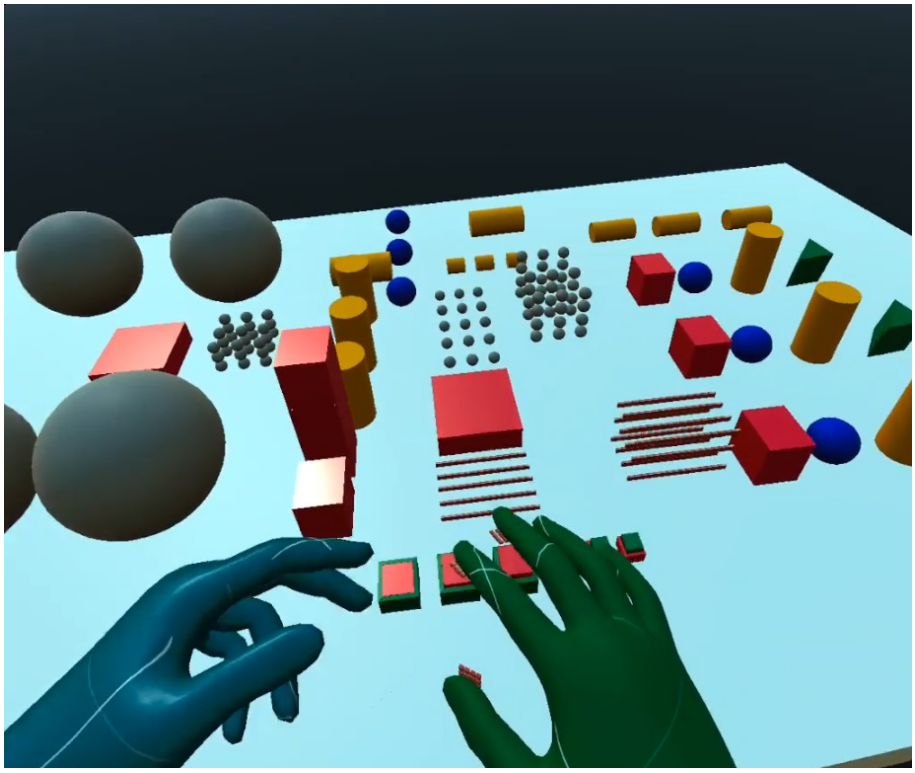

Figure 5.9: 3D VR environment where shapes and edges of 3D VR objects can be explored.

5.6 Results and Discussion: Haptic Primary Colours *(force, vibration, and temperature)* in a Virtual Reality (VR) Environment

One-to-one mapping between sensing and actuating haptic primary colours in a VR environment is shown in Fig. 5.10.

During VR object collision, the activated fingertip tactile detector of the VR hand avatar sends a signal to activate the corresponding tactile pin in the fingertip tactile matrices of the unified multimodal haptic hand wearable, as demonstrated in Figure 5.11. The binary scale of either high or low pin actuation was presented and demonstrated to feel the texture of 3D VR objects illustrated in Figure 5.9. Using the 3D scene as shown in Figure 5.9, when the palm of the avatar hand touches the red square, a "hot" signal is sent to the TEG controller to make it hot. In contrast, when the blue sphere is touched, it will send a "cold" signal making the TEG device cold. Moreover, the user can feel the basic texture information, such

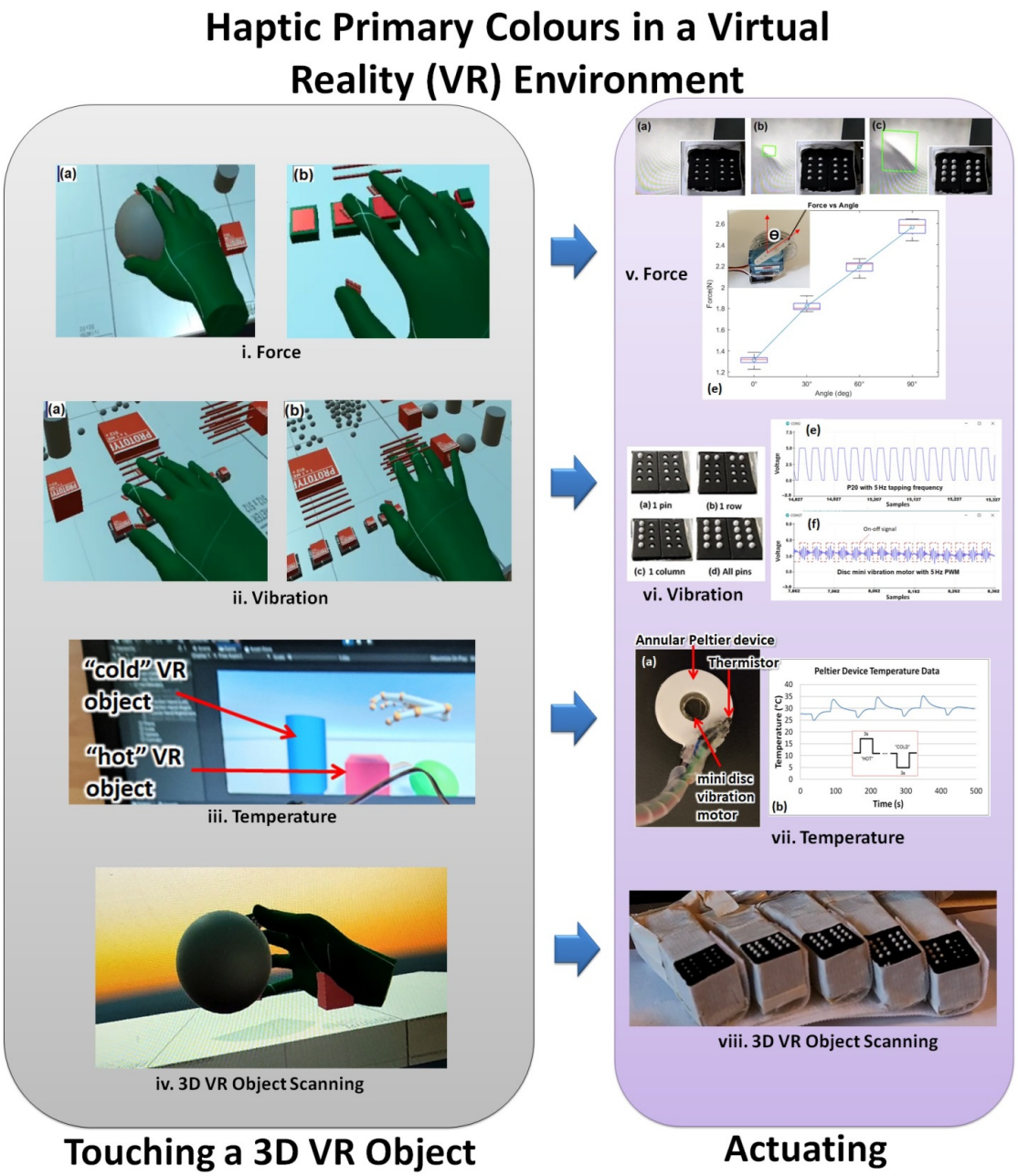

Figure 5.10: Actuating Haptic Primary Colours *(force, vibration, and temperature)* in a 3D VR environment. i.a) gripping a sphere with an embedded resistance signal to the retractable ID badge holder, as shown in Fig. 5.10v, can simulate a squeeze ball, i.b) different VR buttons with different push resistance can be implemented by assigning different spring resistance in the physics of the 3D object that will send varying actuation resistance to the ID badge holder or to the different tactile heights, ii.a) scanning horizontal ridges like rumble strips on a highway produces vibration sensation, or ii.b) scanning floating horizontal strips similar to window blinds can also produce vibration sensation that can be actuated either by the tapping tactile pins or the minivibration motor, as shown in Fig. 5.10vi, iii) cold and hot signal can be embedded different VR objects that can trigger the annular Peltier device, as shown in Fig. 5.10vii, and iv) touching the surface of a 3D VR object can be produce different tactile patterns in the cutaneous feedback, as shown in Fig. 5.10viii.

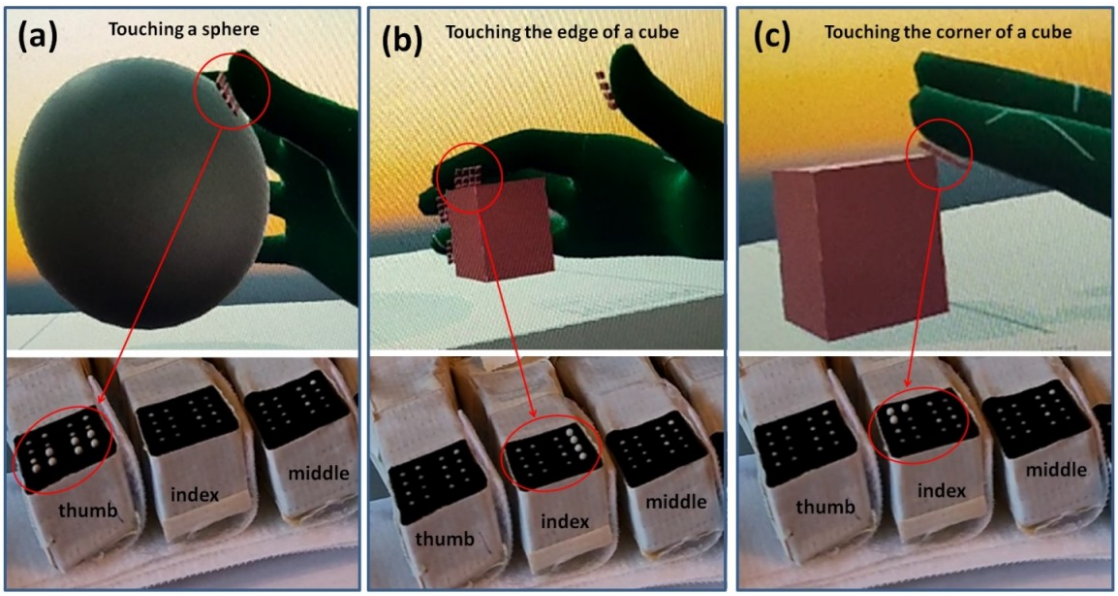

Figure 5.11: Touching 3D VR objects. (**a**) Touching a sphere's surface, (**b**) touching a cube's edge, and (**c**) touching a cube's corner.

as a sphere, edge, and corner of a cube on the 3D screen, as shown in Figure 5.11, while using the Oculus Quest 2 VR Headset. The user can also feel the contours or edges at the back of a 3D VR object, even if they are not visible on the 2D screen. This feeling of touching the back of a 3D VR object that is not visible on a 2D screen creates the illusion of touching a real 3D object in the VR world. The actual 3D VR test videos can be found at this link: [181].

5.7 Chapter Summary

This chapter discussed the visuotactile system that has the HaptiTemp sensor as its input device and the untethered multimodal haptic hand wearable with fine-grained cutaneous feedback as its actuating device. It presented how the unified haptic hand wearable with haptic primary colours *(force, vibration, and temperature)* and fine-grained cutaneous feedback can be used to actuate the haptic primary colours detected by the HaptiTemp sensor. The force estimated by the HaptiTemp sensor can be actuated as a varying tactile pin height of the fingertip tactile matrix or the wire resistance of the ID badge holder. The vibrations detected by the sensor can be actuated as tapping vibrations from the tactile pins or buzzing vibrations

from the minivibration motor inside the annular Peltier device at the palm area of the unified haptic wearable. The vibration motor is inserted in an annular Peltier device to form a thermo-vibro haptic feedback. A thermistor is attached to the annular TEG or Peltier device as a feedback mechanism. “Hot” and “cold” signals from the HaptiTemp sensor can trigger the annular Peltier device. Aside from the tactile sensing and actuating, the unified hand wearable was used scan a 2D tactile image captured by the HaptiTemp sensor.

Moreover, the chapter discussed how the haptic primary colours can be incorporated in a VR environment. A VR application was developed using Unity 2019, and a Leap Motion Controller or Oculus Quest 2 VR headset could be used as hand tracking device. Collision detection scripts were developed to activate the tactile pins and the thermo-vibro feedback whenever the hand avatar in the 3D environment touches a 3D VR object. Vibration motor and servo motors were activated whenever the VR hand finger touched a VR object. The unified haptic hand wearable can be used in extended realities such as VR, augmented reality, and mixed reality to enhance the immersive experience.

6
Conclusion and Future Work

6.1 Summary of Results

This thesis developed the HaptiTemp sensor, a unified visuotactile sensor that can detect haptic primary colours *(force, vibration, and temperature)*, and can do tactile image classification. The HaptiTemp sensor has novel switchable UV markers that mitigate the negative effects of permanent markers that may conceal important image features that might be helpful for object classification, especially if these markers are more significant than the image features. It is the first GelSight-like sensor that has temperature detection capability with a rapid response of 643 *ms* similar to the human withdrawal reflex. It can detect temperatures from 31°C to 50°C. The HaptiTemp can do temperature sensing and tactile image recognition simultaneously. This capability has not been demonstrated by any tactile sensors. Moreover, this thesis also developed an untethered haptic hand wearable with haptic primary colours *(force, vibration, and temperature* and fine-grained cutaneous feedback that can correspond with the HaptiTemp sensor, forming a visuotactile system. This multimodal wearable could also be used in a VR environment and could be used in telerobotics and telemedicine.

Chapter 2 presented an overview of the human skin's tactile properties in terms of its mechanoreceptors and thermoreceptors. It covers a comprehensive

review of previous works, gaps, and challenges in the field of visuotactile sensing and perception, with emphasis on the GelSight sensor. The concept of haptic primary colours was also discussed. This chapter also presented related literature about the development of different tactile matrix actuators and haptic hand wearables that can be used in vision substitution, tactile augmentation, telerobotics, and VR applications. It covers tactile matrix displays from the OpTaCon device in the 1960s, to the advanced and sophisticated haptic VR hand wearables from Meta and Haptx.

Chapter 3 presented the development of the HaptiTemp sensor, a visuotactile sensor that can sense haptic primary colours *(force, vibration, and temperature)* and can do tactile image classification. The HaptiTemp sensor has novel switchable UV markers on the reflective coating that can be made visible using UV LEDs. These UV markers can be tracked using an optical flow algorithm and vector arrows to visualise slip, shear, and torsion inferred from gel deformation. The UV are invisible without UV light and the HaptiTemp sensor can capture high-resolution images. The switchable markers feature is a real novelty of the HaptiTemp because it can be used in the analysis of tactile information from gel deformation without impairing the ability to classify or recognise images. The HaptiTemp sensor can also measure vibrations by counting the number of blobs or pulses detected per unit time using blob detection algorithm. Moreover, the HaptiTemp has a novel thermosensitive reflective layer made from different layers of thermochromic pigments with different colours and temperature thresholds. The HaptiTemp is capable of very rapid detection of temperature changes (19°C/s). A response time of 643 ms for cold-to-hot and hot-to-cold that covers 31°C to 50°C was recorded. This is unique in that it provides a system that parallels the withdrawal reflex of the human autonomic system to extreme heat. Furthermore, the HaptiTemp sensor can do simultaneous temperature sensing and tactile image classification using the OpenMV Cam H7 Plus machine vision camera. This novel capability of simultaneous sensing and image classification was not reported in any literature about tactile sensors.

Chapter 4 presented three haptic hand wearables. Prototype 1 is an untethered multimodal haptic wearable with haptic primary colours *(force, vibration, and*

temperature) feedback. The force feedback comes from the retractable ID badge holders that could restrict finger movements. There are minivibration motors on each fingertip that could give vibration feedback to the user. Aside from the minivibration motor at the index finger, there is an annular Peltier device that could give temperature feedback. The minivibration motor together with the Peltier device form a thermo-vibro feedback. Prototype 2 has fine-grained cutaneous feedback made from commercially available Metec P20 Braille cells. It has 80 tactile pins that can be controlled individually. The hand wearable is untethered, lightweight, portable, modular, and can be wirelessly connected using classic Bluetooth or WiFi. The fine-grained wearable can be fed with predetermined patterns such as Braille or tapping patterns. It can also be used to scan surfaces and detect the edges of images using the Canny edge detection algorithm. Moreover, three experiments involving human participants were carried out. Experiment 1 is a spatial test to determine how well a person can distinguish between tactile patterns that are activated at various positions on the fingertip. In Experiment 2, a temporal test is used to determine how well humans can distinguish between various vibrating patterns travelling in various directions on the fingertip. In Experiment 3, a 2D image identification test is used to examine how well humans can identify edges, lines, and basic geometric shapes. Furthermore, this chapter discussed how to combine Prototype 1 and Prototype 2 to form Prototype 3, a unified untethered multimodal haptic hand wearable with haptic primary colours *(force, vibration, and temperature)* and fine-grained cutaneous feedback.

Chapter 5 presented a visuotactile system that has the HaptiTemp sensor as its input device and the untethered multimodal haptic hand wearable with fine-grained cutaneous feedback as its actuating device. This chapter presented how the unified haptic hand wearable with haptic primary colours *(force, vibration, and temperature)* and fine-grained cutaneous feedback could be used to actuate the haptic primary colours detected by the HaptiTemp sensor. A one-to-one mapping on sensing and actuating haptic primary colours was presented in this chapter. Aside from the tactile sensing and actuating, the unified hand wearable was used to scan a 2D

tactile image captured by the HaptiTemp sensor. Moreover, this chapter discussed how the haptic primary colours can be incorporated into a VR environment that can be actuated using the unified multimodal haptic hand wearable. A VR application was developed using Unity 2019, and a Leap Motion Controller or Oculus Quest 2 VR headset could be used as a hand tracking device.

6.2 Future Work

Spatial Computing and Spatial AI go hand-in-hand with the development of the Metaverse in mapping the real world to create a digital copy that can be used in XR environments. The HaptiTemp sensor created in this thesis can record high-resolution tactile images and may one day be utilised to create 3D images for virtual reality applications. It is possible to investigate 3D image reconstruction using a monochrome LED for the HaptiTemp sensor. Aside from the simultaneous temperature testing and tactile image recognition presented in this thesis, the HaptiTemp sensor could also be used for simultaneous tactile sensing (force and vibration), temperature sensing, and tactile image recognition in the near future. A fingertip-sized HaptiTemp sensor, like the Digit [192], could also be developed and be put on the fingertip of a robotic hand. The HaptiTemp sensor's capability to sense temperature could also be utilised to incorporate temperature data into tactile images. The use of the HaptiTemp sensor in fingerprint or hand-print scanning systems that consider body temperature as an additional security measure is possible. The HaptiTemp sensor could be used as a skin model to study how the interaction of different objects with different textures and temperatures affects the skin. It could also be used for palpation and lump detection. In the future, it might possibly be included in robotic hands or robotic fingertips as artificial skin. Delicate soft robots can also use the rapid temperature response to respond swiftly to abrupt changes in the environment's temperature.

On the other hand, the unified untethered multimodal haptic hand wearable developed in this thesis will enable the user to feel the shapes, surfaces, edges, and temperatures of VR objects. The users will feel the coldness of VR ice or the heat

of a burning VR flame. In the future, users will be able to shake hands with others in a virtual meeting wherever they are on the planet, in space, on the moon, or on Mars. In exploring the VR world, the untethered feature of the prototype will enable users to physically move freely in a broader space compared to the tethered wearables, which are limited by the length of their wires or pneumatic air tubing. The haptic hand wearable in this thesis is not only for the VR environment or the Metaverse. It can be used in online shopping, where users can feel the things in online shops before buying them. People generally touch things before buying them. This activity has been lost in online shopping. Moreover, the untethered fine-grained wearable could be used in teleoperation, especially in telerobotics, and telemedicine, to give fine-grained cutaneous feedback to the user. Furthermore, the haptic wearable could be used to touch a hologram in the near future.

Bibliography

[1] J. R. Anshel, "Visual ergonomics in the workplace," Aaohn Journal 55, 10 (2007), 414–420

[2] What happens to humans when we can't touch? | BBC Ideas, https://www.youtube.com/watch?v=ErWfdjdOah8, Accessed: 23 June 2022

[3] Bresciani JP, Dammeier F, Ernst MO. Vision and touch are automatically integrated for the perception of sequences of events. J Vis. 2006 Apr 20;6(5):554-64. doi: 10.1167/6.5.2. PMID: 16881788.

[4] A. Ranasinghe, N. Sornkarn, P. Dasgupta, K. Althoefer, J. Penders, T. Nanayakkara, "Salient Feature of Haptic-Based Guidance of People in Low Visibility Environments Using Hard Reins," IEEE Transactions on Cybernetics, vol. 46, no. 2, pp. 568-579, 2016.

[5] D. G. Myers, "Sensation and Perception," in Psychology (9th Edition), Worth Publishers, 2010, ch. 6, pp. 228-290.

[6] J. A. Perrone, "Sensation and perception," In A. Weatherall, M. Wilson, D. Harper & J. McDowall (Eds), Psychology in Aotearoa/New Zealand, 2007, ch. 4, pp.20-25, Auckland, New Zealand: Pearson Education New Zealand.

[7] M. J. Morgan, "Molyneux's Question: Vision, Touch and the Philosophy of Perception," Cambridge: Cambridge University Press, 1977.

[8] Ferreira, Mafalda. (2017). The Information Visualization Thematic, Head to Head with Color Blindness. https://www.researchgate.net/publication/313657827_The_Information_Visualization_Thematic_Head_to_Head_with_Color_Blindness (Accessed on 30 June 2022)

[9] S. Tachi, K. Mlnamlzawa, M. Furukawa and C. L. Fernando, "Haptic media construction and utilization of human-harmonized "tangible" information environment," 2013 23rd International Conference on Artificial Reality and Telexistence (ICAT), 2013, pp. 145-150, doi: 10.1109/ICAT.2013.6728921.

[10] Haptic Primary Colors, Available online: `https://tachilab.org/en/about/hpc.html` (Accessed on 30 June 2022)

[11] Hiroyuki Kajimoto, Masahiko Inami, Naoki Kawakami and Susumu Tachi, SmartTouch: Electric Skin to Touch the Untouchable, IEEE Computer Graphics & Applications Magazine, Vol.23, No.1, pp.36-43 (2004.1)

[12] S. J. Lederman, R. L. Klatzky, "Haptic perception: A tutorial," Attention, Perception, & Psychophysics, 2009, 71(7), 1439-1459. doi: 10.3758/APP.71.7.1439.

[13] Sreelakshmi M.; Subash T.D. Haptic technology: A comprehensive review on its applications and future prospects. *Mater. Today* **2017**, *4*, 4182–4187.

[14] Giri, G.S.; Maddahi, Y.; Zareinia, K. An Application-Based Review of Haptics Technology. *Robotics* **2021**, *10*, 29. https://doi.org/ 10.3390/robotics10010029.

[15] Pacchierotti, C.; Prattichizzo, D. Sensory subtraction via cutaneous feedback: A novel technique to improve the transparency of robotic surgery. In Proceedings of the 4th Joint Workshop on Computer/Robot Assisted Surgery, Genova, Italy, 14–16 October 2014.

[16] Pacchierotti, C.; Meli, L.; Chinello, F.; Malvezzi, M.; Prattichizzo, D. Cutaneous haptic feedback to ensure the stability of robotic teleoperation systems. *Int. J. Robot. Res.* **2015**, *34*, 1773–1787. https://doi.org/10.1177/0278364915603135.

[17] Pacchierotti, C.; Sinclair, S.; Solazzi, M.; Frisoli, A.; Hayward, V.; Prattichizzo, D . Wearable haptic systems for the fingertip and the hand: Taxonomy review and perspectives. *IEEE Trans. Haptics* **2017**, *10*, 580–600.

[18] Wang, D.; Song, M.; Naqash, A.; Zheng, Y.; Xu, W.; Zhang, Y. Toward Whole-Hand Kinesthetic Feedback: A Survey of Force Feedback Gloves. *IEEE Trans. Haptics* **2019**, *12*, 189–204. https://doi.org/10.1109/TOH.2018.2879812.

[19] Secco, E.L.; Maereg, A.T.; Reid, D.; Nagar, A.K. An integrated haptic system combining VR, a markerless motion capture system and tactile actuators. *ICST Trans. Ambient. Syst.* **2018**, *5*, 154375. https://doi.org/10.4108/eai.23-3-2018.154375.

[20] Abad, A. C.; Ormazabal, M.; Reid D.; Ranasinghe, A. An Untethered Multimodal Haptic Hand Wearable. In Proceedings of the 2021 IEEE Sensors, Sydney, Australia, 31 October–3 November 2021; pp. 1–4, https://doi.org/10.1109/SENSORS47087.2021.9639526.

[21] I. Nurutdinova, R. Hänsch, V. Mühler, S. Bourou, A. I. Papadaki, O. Hellwich, "Specularity, Shadow, and Occlusion Removal for Planar Objects in Stereo Case", VISIGRAPP (4: VISAPP) 2017, pp. 98-106.

[22] Hiroyuki Kajimoto, Naoki Kawakami and Susumu Tachi: "Electro-Tactile Display with Tactile Primary Color Approach,"in the workshop of International Conference on Intelligent Robots and Systems(IROS2004), Sendai, Tokyo (2004.10)

[23] Molyneux's Problem, `https://plato.stanford.edu/entries/molyneux-problem/` (Accessed on 30 June 2022)

[24] M. M. Zhang, "Tactile Perception and Visuotactile Integration for Robotic Exploration," PhD Dissertation, University of Pennsylvania, 2019. Dissertations available from ProQuest. AAI13808064. `https://repository.upenn.edu/dissertations/AAI13808064`

[25] F. Kato, Y. Inoue,S. Tachi, "Soft Finger-tip Sensing Probe Based on Haptic Primary Colors," International Conference on Artificial Reality and Telexistence

and Eurographics Symposium on Virtual Environments, ICAT-EGVE 2018, Limassol, Cyprus, November 7-9, 2018 107-114 2018.

[26] THE FUTURE OF MACHINE TOUCH, Biotac Sensor, `https://syntouchinc.com/wp-content/uploads/2017/01/BioTac-Brochure.pdf` (Accessed on 30 June 2022)

[27] Fumihiro Kato, Charith Lasantha Fernando, Yasuyuki Inoue, Susumu Tachi: Classification Method of Tactile Feeling using Stacked Autoencoder Based on Haptic Primary Colors, Proceedings of IEEE Virtual Reality 2017, Los Angeles, California, pp.391-–392, 2017.3

[28] F. Kato, Y. Inoue and S. Tachi, "Haptic Display Glove Capable of Force/Vibration/Temperature," 2019 IEEE International Symposium on Measurement and Control in Robotics (ISMCR), 2019, pp. D2-2-1-D2-2-5, doi: 10.1109/ISMCR47492.2019.8955735.

[29] M. K. Johnson and E. Adelson, "Retrographic sensing for the measurement of surface texture and shape," in Computer Vision and Pattern Recognition (CVPR), 2009 IEEE Conference on. IEEE, 2009, pp. 1070-–1077.

[30] J. Chodera, "Examination methods of standing in man," FU CSA VPraha., 1957, vols. I-III.

[31] J. Chodera, "Pedobarograph - apparatus for the visual demonstration of the clinging surfaces of the irregularly shaped objects," 1960, Czs Patent 104 514 30d.

[32] L. Klenerman, B. Wood, "The Measurement of Footprints (Pedobarography)," In: The Human Foot. Springer, London, 2006.

[33] T. G. Strickler, "Design of an Optical Touch sensing system for a remote manipulator," MIT Mechanical Engineering Masters Thesis, June, 1966. `https://dspace.mit.edu/handle/1721.1/13413`

[34] S. Begej, "Planar and finger-shaped optical tactile sensors for roboticapplications," IEEE J. Robotics Autom., vol. 4, no. 5, pp. 472-484, Oct. 1988.

[35] H. Maekawa, K. Tanie, K. Komoriya, "A Finger-Shaped Tactile Sensor Using an Optical Waveguide," Proc. of IEEE Int. Conf. on Systems Man and Cybernetics, vol. 5, pp. 403-408, 1993.

[36] D. F. Gomes, Z. Lin, S. Luo, GelTip: A finger-shaped optical tactile sensor for robotic manipulation, IEEE International Conference on Intelligent Robots and Systems (2020) 9903–9909doi:10.1109/IROS45743. 2020.9340881.

[37] K. Tanie, K. Komoriya, M. Kaneko, S. Tachi, and A. Fujikawa, "A high resolution tactile sensor," Proceedings of the 4th International Conference on Robot Vision and Sensory Controls, pp.251-260.,0ctober 1984.

[38] M. Ohka, Y. Mitsuya, S. Takeuchi, O. Kamekawa, "A Three-axis Optical Tactile Sensor (FEM Contact Analyses and Sensing Experiments Using a Large-sized Tactile Sensor)," Proc. 1995 IEEE Int. Conf. on Robotics Automation, pp. 817-824, 1995.

[39] M. Ohka, Y. Mitsuya, K. Hattori, I. Higashioka, "Data Conversion Capability of Optical Tactile Sensor Featuring an Array of Pyramidal Projections," Proc. 1996 IEEE/SICE/RJS Proc. Int. Conf. on Multisensor Fusion and Integration for Intelligent Systems, pp. 573-580, 1996.

[40] C. Chorley, C. Melhuish, T. Pipe, and J. Rossiter, "Development of a Tactile Sensor Based on Biologically Inspired Edge Encoding," Design, 2008.

[41] B. Winstone, G. Griffiths, C. Melhuish, T. Pipe, J. Rossiter, "TACTIP-tactile fingertip device challenges in reduction of size to ready for robot hand integration," 2012 IEEE International Conference on Robotics and Biomimetics (ROBIO) 2012.

[42] K. Kumagi, K. Shimonomura, "Event-based Tactile Image Sensor for Detecting Spatio-Temporal Fast Phenomena in Contacts," 2019 IEEE World Haptics Conference (WHC), Tokyo, Japan, 9-12 July 2019

[43] K. Sato, K. Kamiyama, K. Nii, H. Kawakami, N. Tachi, S., "Measurement of force vector field of robotic finger using vision-based haptic sensor," International Conference on Intelligent Robots and Systems, 2008.

[44] K. Sato, K. Kamiyama, N. Kawakami et al., "Finger-shaped Gelforce: sensor for measuring surface traction fields for robotic hand," Trans. Haptics, vol. 3, no. 1, pp. 37-47, 2010.

[45] K. Sato, H. Shinoda, S. Tachi, "Vision-based cutaneous sensor to measure both tactile and thermal information for telexistence," Proc. 2011 IEEE International Symposium on VR Innovation, pp. 119-122, 2011.

[46] X. Lin, M. Wiertlewski , "Sensing the Frictional State of a Robotic Skin via Subtractive Color Mixing," IEEE Robotics and Automation Letters (RAL) paper presented at the 2019 International Conference on Robotics and Automation (ICRA) Palais des congres de Montreal, Montreal, Canada, May 20-24, 2019.

[47] C. Sferrazza, R. D'Andrea, "Design, Motivation and Evaluation of a Full-Resolution Optical Tactile Sensor," Sensors 2019, 19, 928.

[48] D. Hristu, N. Ferner, R.W. Brockett, "The performance of a deformable-membrane tactile sensor: basic results on geometrically-defined tasks." Proc. IEEE Int'l Conf. on Robotics and Automation, 2000.

[49] A. Yamaguchi, C. G. Atkeson, "Implementing Tactile Behaviors Using FingerVision," Proc. of 2017 IEEE-RAS 17th International Conference on Humanoid Robotics, pp. 241-248, 2017.

[50] C. G. A. A. Yamaguchi, "Combining finger vision and optical tactile sensing: Reducing and handling errors while cutting vegetables," in 2016 IEEE-RAS 16th International Conference on Humanoid Robots (Humanoids), Nov 2016, pp. 1045–1051.

[51] S. Dong, W. Yuan, and E. Adelson, "Improved GelSight tactile sensor for measuring geometry and slip," IROS, 2017.

[52] X. Jia, R. Li, M. A. Srinivasan, and E. H. Adelson, "Lump detection with a gelsight sensor," in World Haptics Conference (WHC), 2013. IEEE, 2013, pp. 175–179.

[53] M. K. Johnson, F. Cole, A. Raj, and E. H. Adelson, "Microgeometry capture using an elastomeric sensor," in TOG, vol. 30, no. 4. ACM, 2011, p. 46.

[54] R. Li and E. Adelson, "Sensing and recognizing surface textures using a gelsight sensor," in Proceedings of the IEEE Conference on Computer Vision and Pattern Recognition, 2013, pp. 1241-–1247.

[55] R. Li, R. Platt, W. Yuan, A. ten Pas, N. Roscup, M. A. Srinivasan, and E. Adelson, "Localization and manipulation of small parts using gelsight tactile sensing," in Intelligent Robots and Systems (IROS 2014), 2014 IEEE/RSJ International Conference on. IEEE, 2014, pp. 3988–3993.

[56] W. Yuan, S. Dong, and E. H. Adelson, "GelSight: High resolution robot tactile sensors for estimating geometry and force," Sensors, vol. 17, no. 12, p. 2762, 2017.

[57] E. Donlon, S. Dong, M. Liu, J. Li, E. Adelson, A. Rodriguez, "GelSlim: A High-Resolution, Compact, Robust, and Calibrated Tactilesensing Finger," IROS 2018: 1927–1934.

[58] D. Ma, E. Donlon, S. Dong, A. Rodriguez, "Dense Tactile Force Estimation using GelSlim and inverse FEM," 2019 International Conference on Robotics

and Automation (ICRA) Palais des congres de Montreal, Montreal, Canada, May 20-24, 2019, pp. 5418-5424.

[59] Sandra Q. Liu, Edward H. Adelson, GelSight Fin Ray: Incorporating Tactile Sensing into a Soft Compliant Robotic Gripper, 2022 IEEE 5th International Conference on Soft Robotics (RoboSoft) `https://doi.org/10.48550/arXiv.2204.07146`

[60] W. Yuan, "Tactile measurement with a gelsight sensor," Master's thesis, MIT, Cambridge, MA, USA, 2014.

[61] R. Li, "Touching Is Believing: Sensing and Analyzing Touch Information with GelSight," Ph.D. Thesis, Massachusetts Institute of Technology, Cambridge, MA, USA, 2015.

[62] W. Li, J. Konstantinova, Y. Noh, A. Alomainy, K. Althoefer, "Camerabased force and tactile sensor." Towards Autonomous Robotic Systems: 19th Annual Conference, TAROS 2018, Bristol, UK July 25-27, 2018, Proceedings. Vol. 10965 LNAI, pp. 438–450.

[63] K. Takahashi, J. Tan, "Deep Visuo-Tactile Learning: Estimation of Tactile Properties from Images," 2019 International Conference on Robotics and Automation (ICRA) Palais des congres de Montreal, Montreal, Canada, May 20-24, 2019, pp. 8951-8957.

[64] M. Bauza, O. Canal and A. Rodriguez, "Tactile Mapping and Localization from High-Resolution Tactile Imprints," 2019 International Conference on Robotics and Automation (ICRA) Palais des congres de Montreal, Montreal, Canada, May 20-24, 2019, pp. 3811-3817.

[65] W. Yuan, R. Li, M. A. Srinivasan, and E. H. Adelson, "Measurement of shear and slip with a gelsight tactile sensor," in Robotics and Automation (ICRA), 2015 IEEE International Conference on. IEEE, 2015, pp. 304—311.

[66] W. Yuan, M. A. Srinivasan, and E. Adelson, “Estimating object hardness with a gelsight touch sensor,” in Intelligent Robots and Systems (IROS 2016), 2016 IEEE/RSJ International Conference on. IEEE, 2016.

[67] W. Li, Y. Noh, A. Alomainy, I. Vitanov, Y. Zheng, P. Qi, K. Althoefer, "F-TOUCH Sensor for Three-Axis Forces Measurement and Geometry Observation," 2020 IEEE SENSORS, 2020, pp. 1-4, doi: 10.1109/SENSORS47125.2020.9278600.

[68] Liquid Crystal Thermochromic Colour Changing Sheet. Available online: `https://www.sfxc.co.uk/products/lc-liquid-crystal-thermochromic-sheets?variant=6780064833` (Accessed on 30 June 2022)

[69] SFXC® SPRAYABLE LIQUID CRYSTAL INK. Available online: `https://www.sfxc.co.uk/products/sprayable-liquid-crystal-inks` (Accessed on 30 June 2022)

[70] K. Sato, H. Shinoda and S. Tachi, "Finger-shaped thermal sensor using thermo-sensitive paint and camera for telexistence," 2011 IEEE International Conference on Robotics and Automation, 2011, pp. 1120-1125, doi: 10.1109/ICRA.2011.5980271.

[71] COLOUR CHANGING THERMOCHROMIC PIGMENT TRIAL PACK - COLOUR TO COLOUR. Available online: `https://www.sfxc.co.uk/collections/thermochromatic-thermochromic-pigments-ink-paint/products/colour-changing-thermochromic-pigment-trial-pack` (Accessed on 30 June 2022)

[72] HALI Thermochromic pigment. Available online: `https://www.aliexpress.com/store/2071018?spm=a2g0o.detail.1000002.2.2ef28326dujrbt` (Accessed on 30 June 2022)

[73] GelSight. Available online: `https://www.youtube.com/watch?v=aKoKVA4Vcu0` (accessed on 30 June 2022)

[74] S. Leutenegger, M. Chli, and R. Siegwart, "Brisk: Binary robust invariant scalable keypoints," in IEEE Int'l Conf. on Computer Vision, 2011.

[75] M. Fischler and R. Bolles, "Random sample consensus: A paradigm for model fitting with applications to image analysis and automated cartography," Communications of the ACM, vol. 24, pp. 381–395, 1981.

[76] Optical Flow, Available online: `https://docs.opencv.org/3.4/d4/dee/tutorial_optical_flow.html` (accessed on 30 June 2022).

[77] B. D. Lucas, T. Kanade, "An iterative image registration technique with an application to stereo vision," In IJCAI, volume 81, pages 674-679, 1981.

[78] S. Baker, I. Matthews, "Lucas-kanade 20 years on: A unifying framework," International journal of computer vision, 56(3):221-255, 2004.

[79] W. Yuan, C. Zhu, A. Owens, M. A. Srinivasan, and E. Adelson, "Shape-independent hardness estimation using deep learning and a gelsight tactile sensor," in Robotics and Automation (ICRA), 2017 IEEE International Conference on. IEEE, 2017.

[80] W. Yuan, S. Wang, S. Dong, and E. Adelson, "Connecting look and feel: Associating the visual and tactile properties of physical materials," in IEEE Conference on Computer Vision and Pattern Recognition (CVPR), July 2017.

[81] J. Li, S. Dong, E. Adelson, "Slip Detection with Combined Tactile and Visual Information," ICRA 2018: 7772-7777, arXiv:1802.10153.

[82] W. Yuan, Y. Mo, S. Wang, E. H. Adelson, "Active Clothing Material Perception Using Tactile Sensing and Deep Learning," ICRA 2018: 1–8.

[83] J. C. Bliss, M. H. Katcher, C. H. Rogers, and R. P. Shepard, "Optical-to-tactile image conversion for the blind," IEEE Trans. Man-Mach. Sys., vol. 11, no. 1,pp. 58–65, Mar. 1970.

[84] S. F. Frisken-Gibson, P. Bach-Y-Rita, W. J. Tompkins, and J. G., Webster, "A 64-Solenoid, Four-Level Fingertip Search Display for the Blind," IEEE Transactions on Biomedical Engineering, VOL.BME-34, NO. 12, 1987.

[85] M. Ide, A. Yaguchi, M. Sano, R. Fukatsu, M. Wada, "Higher Tactile Temporal Resolution as a Basis of Hypersensitivity in Individuals with Autism Spectrum Disorder," Journal of Autism and Developmental Disorders (2019) 49:44–53, https://doi.org/10.1007/s10803-018-3677-8

[86] Yu Xie, Chuhao Chen, Dezhi Wu, Wenming Xi, and Houde Liu, "Human-Touch-Inspired Material Recognition for Robotic Tactile Sensing," Applied Sciences, June 2019, 9(12):2537, DOI:10.3390/app9122537

[87] Dong-Soo Kwon, Tae-Heon Yang, JoonYeon Cho, "Trend & prospects of haptic technology in mobile devices," Symposium on Industrial Electronics (ISIE), IEEE, pp.3778–3783, July 2010.

[88] Z. Kappassov, J.-A. Corrales, V. Perdereau„ "Tactile sensing in dexterous robot hands - Review," Robotics and Autonomous Systems, Elsevier, 2015, 74, Part A, pp.195-220.

[89] Y. Shen, Y. Liu, and L. Kejie,"Haptic Tactile Feedback in Teleoperation of a Multifingered Robot Hand," Proc. Third World Congress Intelligent Control and Automation, vol. 1, pp. 85-90, 2000.

[90] Y. Visell, "Tactile sensory substitution: Models for enaction in HCI," Interacting with Computers, vol. 21, no. 1–2, pp. 38–53.

[91] C. Collins, "Tactile Television–Mechanical and Electrical Image Projection," IEEE Transactions on Man–Machine Systems, vol. 11, no. 1, pp. 65–71, 1970.

[92] J. G. Linvill and J. C. Bliss, "A direct translation reading aid for the blind," in Proceedings of the IEEE, vol. 54, no. 1, pp. 40-51, Jan. 1966, doi: 10.1109/PROC.1966.4572.

[93] J. C. Bliss, "A Relatively High-Resolution Reading Aid for the Blind," in IEEE Transactions on Man-Machine Systems, vol. 10, no. 1, pp. 1-9, March 1969, doi: 10.1109/TMMS.1969.299874.

[94] P. Kammermeier and G. Schmidt, "Application-specific evaluation of tactile array displays for the human fingertip," IEEE/RSJ International Conference on Intelligent Robots and Systems, 2002, pp. 2937-2942 vol.3, doi: 10.1109/IRDS.2002.1041718.

[95] P. Kammermeier, A. Kron, M. Buss and G. Schmidt, "Towards Intuitive Multifingered Haptic Exploration and Manipulation", Proc. of the 2001 Workshop on Advances in Multimodal Telepresence Systems, pp. 57-70, 2001

[96] Dot pad: tactile graphic & braille display for the visually impaired. `https://www.facebook.com/watch/?v=1633029773479398` (Accessed on 30 June 2022)

[97] M. Benali-Khoudja, M. Hafez, A. Kheddar, “VITAL: An electromagnetic integrated tactile display,” Displays 28(3), 133-144(2007).

[98] M. Rotard, C. Taras, and T. Ertl, “Tactile web browsing for blind people,” Multimedia Tools Appl. 37, 1 (March 2008), 53-69. DOI: http://dx.doi.org/10.1007/s11042-007-0170-3

[99] Y. Ikei, K. Wakamatsu , and S. Fukuda, “Vibratory tactile display of image-based textures,” in IEEE Computer Graphics and Applications. 1997.

[100] J. Wu, J. Zhang, J. Yan, W. Liu, G. Song, “Design of a Vibrotactile Vest for Contour Perception,” International Journal of Advanced Robotic Systems 9, 166 (2012).

[101] Ozioko, O.; Dahiya, R. Smart Tactile Gloves for Haptic Interaction, Communication, and Rehabilitation. *Adv. Intell. Syst.* **2022**, *4*, 2100091. https://doi.org/10.1002/aisy.202100091.

[102] Lee, K.T.; Chee P.S.; Lim, E.H.; Lim, C.C. Artificial intelligence (AI)-driven smart glove for object recognition application. *Mater. Today Proc.* **2022**, ISSN 2214-7853. https://doi.org/10.1016/j.matpr.2021.12.473.

[103] Z. Szabo, E.T. Enikov, "Developement of Wearable Micro-Actuator Array for 3-D Virtual Tactile Display," Journal of Electromagnetic Analysis and Application, v.4, 2012.

[104] Q.Wang and V. Hayward, "Biomechanically optimized distributed tactile transducer based on lateral skin deformation," Int. J. Robot. Res., vol. 29, pp. 323–335, 2009.

[105] I. R. Summers and C. M. Chanter, "A broadband tactile array on the fingertip," J. Acoust. Soc. Amer., vol. 112, pp. 2118–2126, 2002.

[106] N. Besse, S. Rosset, J. J. Zárate, E. Ferrari, L. Brayda, and H. Shea, "Understanding Graphics on a Scalable Latching Assistive Haptic Display Using a Shape Memory Polymer Membrane," Haptics IEEE Transactions on, vol. 11, no. 1, pp. 30-38, 2018.

[107] H. Sawada, "Tactile Display Using the Micro-vibration of Shape-Memory Alloy Wires and Its Application to Tactile Interaction Systems," In: Kajimoto H., Saga S., Konyo M. (eds) Pervasive Haptics. Springer, Tokyo, 2016.

[108] H. Kajimoto, L. Jones, "Wearable Tactile Display Based on Thermal Expansion of Nichrome Wire," IEEE Transaction on Haptics (accepted), 2019, DOI: 10.1109/TOH.2019.2912960

[109] Y. Shimizu, "Tactile display terminal for visually handicapped," Displays, 7(3):116-120, 1986.

[110] A. Russomanno, Z. Xu, S. O'Modhrain, and B. Gillespie, "A pneu shape display: Physical buttons with programmable touch response," In 2017 IEEE World Haptics Conference (WHC). IEEE, New York, NY, USA, 641–646. DOI: http://dx.doi.org/10.1109/WHC.2017.7989976

[111] A. A. Stanley, K. Hata, A. M. Okamura, "Closed-loop shape control of a Haptic Jamming deformable surface", Robotics and Automation (ICRA) 2016 IEEE International Conference on, pp. 2718-2724, 2016.

[112] Braibook, `https://braibook.com/` (Accessed on 30 June 2022)

[113] Wall, S.A. and Brewster, S. 2006. Sensory substitution using tactile pin arrays: Human factors, technology and applications. Signal Processing. 86, 12 (Dec. 2006), 3674–3695. DOI:https://doi.org/10.1016/J.SIGPRO.2006.02.048.

[114] Tactile Mouse by Watanabe et al. `http://www.nise.go.jp/research/kogaku/twatanab/Tactile/TactileMouse/TactileMouseEn.html` (Accessed on 30 June 2022)

[115] Owen, J. M.; Petro, J. A.; Souza, S. M. D.; Rastogi, R.; & Pawluk, D. T. V.; "An Improved, Low-cost Tactile "Mouse" for Use by Individuals Who are Blind and Visually Impaired." Proceedings of the 11th international ACM SIGACCESS conference on Computers and accessibility (Assets'09), October(25-28), 223–224.

[116] C. -H. King et al., "Tactile Feedback Induces Reduced Grasping Force in Robot-Assisted Surgery," in IEEE Transactions on Haptics, vol. 2, no. 2, pp. 103-110, April-June 2009, doi: 10.1109/TOH.2009.4.

[117] King, C.-H.; Culjat, M.O.; Franco, M.L.; Bisley, J.W.; Dutson, E.; Grundfest, W.S. Optimization of a Pneumatic Balloon Tactile Display for Robot-Assisted Surgery Based on Human Perception. *IEEE Trans. Biomed. Eng.* **2008**, *55*, 2593–2600. https://doi.org/10.1109/TBME.2008.2001137.

[118] McMahan, W.; Gewirtz, J.; Standish, D.; Martin, P.; Kunkel, J.A.; Lilavois, M.; Wedmid, A.; Lee, D.I.; Kuchenbecker, K.J. Tool Contact Acceleration Feedback for Telerobotic Surgery. *IEEE Trans. Haptics* **2011**, *4*, 210–220. https://doi.org/10.1109/TOH.2011.31.

[119] Meli, L.; Pacchierotti, C.; Prattichizzo, D. Sensory Subtraction in Robot-Assisted Surgery: Fingertip Skin Deformation Feedback to Ensure Safety and Improve Transparency in Bimanual Haptic Interaction. *IEEE Trans. Biomed. Eng.* **2014**, *61*, 1318–1327. https://doi.org/10.1109/TBME.2014.2303052.

[120] Pacchierotti, C.; Prattichizzo, D.; Kuchenbecker, K.J. Cutaneous Feedback of Fingertip Deformation and Vibration for Palpation in Robotic Surgery. *IEEE Trans. Biomed. Eng.* **2016**, *63*, 278–287. https://doi.org/10.1109/TBME.2015.2455932.

[121] Haptx Microfluidic skin, `https://haptx.com/technology/` (Accessed on 30 June 2022)

[122] Li M, Konstantinova J, Althoefer K (2018) Haptic feedback modalities for minimally invasive surgery. In: Soft and Stiffness-controllable Robotics Solutions for Minimally Invasive Surgery: The STIFF-FLOP Approach. River Publishers, p. 229.

[123] Konstantinova J, Jiang A, Althoefer K, Dasgupta P, Nanayakkara T (2014) Implementation of tactile sensing for palpation in robot-assisted minimally invasive surgery: A review. IEEE Sensors Journal 14(8): 2490–2501.

[124] Li M, He B, Liang Z, Zhao C-G, Chen J, Zhuo Y, Xu G, Xie J and Althoefer K (2019) An Attention-Controlled Hand Exoskeleton for the Rehabilitation of Finger Extension and Flexion Using a Rigid-Soft Combined Mechanism. Front. Neurorobot. 13:34. doi: 10.3389/fnbot.2019.00034

[125] Meta pneumatic actuators, `https://www.facebook.com/TechatMeta/videos/265370998894023/` (Accessed on 30 June 2022)

[126] Caeiro-Rodríguez, M.; Otero-González, I.; Mikic-Fonte, F.A.; Llamas-Nistal, M. A Systematic Review of Commercial Smart Gloves: Current Status and Applications. Sensors 2021, 21, 2667. https://doi.org/10.3390/s21082667

[127] Inside Reality Labs Research: Bringing Touch to the Virtual World, `https://about.fb.com/news/2021/11/reality-labs-haptic-gloves-research/` (Accessed on 30 June 2022)

[128] Jeff Bezos operates a Tactile Telerobot, `https://www.youtube.com/watch?v=uwYtwQtoOh0` (Accessed on 30 June 2022)

[129] A. C. Abad and A. Ranasinghe, "Visuotactile Sensors with Emphasis on GelSight Sensor: A Review", IEEE Sensors Journal, DOI: 10.1109/JSEN.2020.2979662

[130] J. M. Castellote and J. Valls-Solé, "Temporal relationship between perceptual and physiological events triggered by nociceptive heat stimuli," Sci. Rep., vol. 9, Feb. 2019, Art. no. 3264. [Online]. Available: `https://doi.org/10.1038/s41598-019-39509-3`

[131] S. Luo, W. Yuan, E. Adelson, A. Cohn and R. Fuentes, "ViTac: Feature Sharing between Vision and Tactile Sensing for Cloth Texture Recognition", IEEE International Conference on Robotics and Automation (ICRA), 2018

[132] J. Lee, D. Bollegala, S. Luo, " "Touching to See" and "Seeing to Feel": Robotic Cross-modal Sensory Data Generation for Visual-Tactile Perception," 2019 International Conference on Robotics and Automation (ICRA) Palais des congres de Montreal, Montreal, Canada, May 20-24, 2019, pp. 4276-4282.

[133] J. Li, S. Dong, E. H. Adelson, "End-to-end pixelwise surface normal estimation with convolutional neural networks and shape reconstruction using GelSight sensor," International Conference on Robotics and Biomimetics, 2018, Kuala Lumpur, Malaysia, December 12-15, 2018, ROBIO 2018: 1292-1297.

[134] Psycho Paint: Available online: https://www.smooth-on.com/products/psycho-paint/ (Accessed on 30 June 2022)

[135] Silc Pigments: Available online: https://www.smooth-on.com/products/silc-pig/ (Accessed on 30 June 2022)

[136] Novocs: Available online: https://www.smooth-on.com/products/novocs/ (Accessed on 30 June 2022)

[137] OpenMV Cam H7 Plus. Available online: https://openmv.io/products/openmv-cam-h7-plus (Accessed on 30 June 2022)

[138] M5StickV. Available online: https://m5stack.com/products/stickv (Accessed on 30 June 2022)

[139] Sipeed MAix Go. Available online: https://www.seeedstudio.com/Sipeed-MAix-GO-Suit-for-RISC-V-AI-IoT-p-2874.html (Accessed on 30 June 2022)

[140] Jevois Smart Machine Vision Camera. Available online: http://jevois.org/ (Accessed on 30 June 2022)

[141] Kittenbot KOI AI. Available online: https://www.kittenbot.cc/products/kittenbot-koi-artificaial-intelligence-module (Accessed on 30 June 2022)

[142] Google AIY Vision Kit. Available online: https://aiyprojects.withgoogle.com/vision (Accessed on 30 June 2022)

[143] HUSKYLENS: AI Camera with Kendryte K210. Available online: https://community.dfrobot.com/makelog-308252.html (Accessed on 30 June 2022)

[144] OpenCV AI Kit: OAK—1. Available online: https://store.opencv.ai/products/oak-1 (Accessed on 30 June 2022)

[145] Blob Detection, Available online: https://www.learnopencv.com/blob-detection-using-opencv-python-c/ (Accessed on 30 June 2022)

[146] OpenMV IDE. Available online: https://openmv.io/pages/download (Accessed on 30 June 2022)

[147] Edge Impulse. Available online: https://www.edgeimpulse.com/ (Accessed on 30 June 2022)

[148] Smile Detection with OpenMV IDE and Edge Impulse. Available online: https://www.youtube.com/watch?v=YKwVope5RsU&feature=youtu.be (Accessed on 30 June 2022)

[149] Adding sight to your sensors. Available online: https://docs.edgeimpulse.com/docs/image-classification (Accessed on 30 June 2022)

[150] Y. She, S. Wang, S. Dong, N. Sunil, A. Rodriguez, and E. Adelson, "Cable manipulation with a tactile-reactive gripper," Robotics: Science and Systems (2020)

[151] M. Samii, "Understanding, Measuring, And Using Thermistor Thermal Time Constants", Feb 24, 2017. Available online: https://www.fierceelectronics.com/components/understanding-measuring-and-using-thermistor-thermal-time-constants (accessed on 2 August 2021)

[152] "AlexNet", https://ww2.mathworks.cn/help/deeplearning/ref/alexnet.html (Accessed on 30 June 2022)

[153] OpenMV WiFi Shield. Available online: https://openmv.io/products/wifi-shield-1 (Accessed on 30 June 2022)

[154] SingTown - OpenMV Cam video tutorial 12 - WiFi Shield. Available online: https://www.youtube.com/watch?v=wIwJhw2rBkQ&t=329s (Accessed on 30 June 2022)

[155] HaptiTemp videos. Available online: https://drive.google.com/drive/u/1/folders/1fS1P-nl0cHBa3WUswQFPRBCXzJ9TW59p (Accessed on 30 June 2022)

[156] OpenMV MicroPython libraries. Available online: `https://docs.openmv.io/library/omv.image.html` (Accessed on 30 June 2022)

[157] A. Delazio, A. Israr and R. L. Klatzky, "Cross-modal correspondence between vibrations and colors," 2017 IEEE World Haptics Conference (WHC), 2017, pp. 219-224, doi: 10.1109/WHC.2017.7989904.

[158] OpenMV class Servo – 3-wire hobby servo driver, `https://docs.openmv.io/library/pyb.Servo.html` (accessed on 13 June 2022)

[159] OpenMV Tutorial: Control DC Motors with the L298N driver module, `https://www.youtube.com/watch?v=N6xXUvtEGF0&t=327s` (Accessed on 30 June 2022)

[160] Ranasinghe, A.; Althoefer, K.; Dasgupta, P.; Nagar, A.; Nanayakkara, T.; "Wearable haptic based pattern feedback sleeve system." In: Proceedings of the 6th international conference on soft computing for problem solving, Thapar University, Patiala, India, 23–24 December 2016

[161] Scalera, L.; Seriani, S.; Gallina, P.; Di Luca, M.; and Gasparetto, A. "An experimental setup to test dual-joystick directional responses to vibrotactile stimuli." 2017 IEEE World Haptics Conference (WHC). 2017, pp. 72-77, doi: 10.1109/WHC.2017.7989879.

[162] Yunus, R.; Ali, S.; Ayaz, Y.; Khan, M.; Kanwal, S.; Akhlaque, U.; and Nawaz, R. "Development and Testing of a Wearable Vibrotactile Haptic Feedback System for Proprioceptive Rehabilitation." in IEEE Access. vol. 8, pp. 35172-35184, 2020, doi: 10.1109/ACCESS.2020.2975149.

[163] van der Putten, E.P.W.; van den Dobbelsteen, J.J.; Goossens, R.H.M.; Jakimowicz, J.J.; Dankelman, J. The Effect of Augmented Feedback on Grasp Force in Laparoscopic Grasp Control. *IEEE Trans. Haptics* **2010**, *3*, 280–291. https://doi.org/10.1109/TOH 2010.23.

[164] Mehrdad, S.; Liu, F.; Pham, M.T.; Lelevé, A.; Atashzar, S.F. Review of Advanced Medical Telerobots. *Appl. Sci.* **2021**, *11*, 209. https://doi.org/10.3390/app11010209.

[165] Tavakoli, M.; Patel, R.V. "Haptics in Telerobotic Systems for Minimally Invasive Surgery." Telesurgery. pp. 113-124,(2008).

[166] Metec P20 Braille cell Datasheet, `https://www.metec-ag.de/downloads/p20.pdf` (accessed on 06 February 2022)

[167] Malvezzi, M.; Chinello, F.; Prattichizzo, D.; and Pacchierotti, C. "Design of Personalized Wearable Haptic Interfaces to Account for Fingertip Size and shape," in IEEE Transactions on Haptics, vol. 14, no. 2, pp. 266-272, 1 April-June 2021, doi: 10.1109/TOH.2021.3076106.

[168] weart TouchDIVER, `https://www.weart.it/touchdiver/` (Accessed on 30 June 2022)

[169] Hands-on: Dexmo Haptic Force-feedback Gloves are Compact and Wireless, `https://www.roadtovr.com/dexta-dexmo-vr-gloves-force-feedback-haptic-hands-on/` (Accessed on 30 June 2022)

[170] BeBop Forte Data Gloves, `https://bebopsensors.com/arvr/` (Accessed on 30 June 2022)

[171] HaptX Gloves DK2 haptic VR gloves with 133 tactile sensors per hand, `https://www.geeky-gadgets.com/haptic-vr-gloves-28-01-2021/` (Accessed on 30 June 2022)

[172] Dot Incorporated, Korea, `https://www.dotincorp.com/` (Accessed on 30 June 2022)

[173] ARDUINO NANO 33 IOT, `https://store.arduino.cc/arduino-nano-33-iot` (Accessed on 30 June 2022)

[174] Abad, A.C.; Swarup, D.; Reid, D.; Ranasinghe, A. 4 × 4 Fingertip Tactile Matrix Actuator with Edge Detection Scanning ROI Simulator. In *2020 IEEE SENSORS*; IEEE; Rotterdam, Netherlands; 2020 ; pp. 1–4. https://doi.org/10.1109/SENSORS47125.2020.9278765.

[175] Arduino Nano 33 BLE same as ESP32?, `https://forum.arduino.cc/index.php?topic=659059.0` (Accessed on 30 June 2022)

[176] Arduino NINA-W102 firmware, `https://github.com/arduino/nina-fw` (Accessed on 30 June 2022)

[177] Metec DC-DC 5V-200V boost converter, `https://www.metec-ag.de/downloads/dcdc-converter-5to200v.pdf` (Accessed on 30 June 2022)

[178] Leap Motion Controller, `https://www.ultraleap.com/datasheets/Leap_Motion_Controller_Datasheet.pdf` (Accessed on 30 June 2022)

[179] Watanabe, T.; Kume, Y.; and Ifukube, T. "Shape discrimination with a tactile mouse." Journal of the Institute of Image Information and Television Engineers. Vol.54, No.6, pp.840-847, 2000 (in Japanese).

[180] Hribar, V. E.; Deal, L. G.; Pawluk, D. T. V. "Displaying braille and graphics with a "tactile mouse"." ASSETS '12: Proceedings of the 14th international ACM SIGACCESS conference on Computers and accessibility. October 2012. pp. 251–252. doi: 10.1145/2384916.2384978.

[181] High Resolution Haptic Glove Database, `https://drive.google.com/drive/u/1/folders/1jBfT5-lH9-dx2a5O3dPrMOJ_ZvB8WX5z` (Accessed on 30 June 2022)

[182] Which Haptic Effects Should You Use?, Available online: `https://www.precisionmicrodrives.com/content/which-haptic-effects-should-you-use/` (Accessed on 30 June 2022)

[183] J.W. Van Strien, "Classificatie van links- en rechtshandige proefpersonen. [Classification of left- and right-handed research participants]," Nederlands, 1992, Tijdschrift voor de Psychologie, 47, 88-92.

[184] T. Fukuda, H. Morita., F. Arai, H. Ishihara and H. Matsuura, "Micro Resonator Using Electromagnetic Actuator for Tactile Display," 1997 International Symposium on Micromechatronics and Human Science, Nagoya, Japan.

[185] M. Nakatani, K. Sato, K. Sato, Y. Kawana, D. Takai, K. Minamizawa, et al.,(2016).A novel multimodal tactile module that can provide vibro-thermal feedback. in International AsiaHaptics conference, pp. 437-443.

[186] Lucas VRTech, "I made $22 Virtual Reality Gloves.", `https://www.youtube.com/watch?v=nmP8iGaPbeI` (Accessed on 30 June 2022)

[187] Adafruit PCA9685 16-Channel Servo Driver, `https://learn.adafruit.com/16-channel-pwm-servo-driver/hooking-it-up` (Accessed on 30 June 2022)

[188] Headley, P.; and Pawluk, D. "A Low-Cost, Variable Amplitude Haptic Distributed Display for Persons who are Blind and Visually Impaired." ACM Assets, Orlando, Florida, October 25-27, 2010.

[189] Digital Potentiometer X9C103s Arduino Circuit and Programming, `https://www.electroniclinic.com/digital-potentiometer-x9c103s-arduino-circuit-and-programming/`

[190] K. Sato, T. Maeno, "Presentation of rapid temperature change using spatially divided hot and cold stimuli", Journal of Robotics and Mechatronics 25(3), 497-505 (6 2013)

[191] Schubert, T.W.; D'Ausilio, A.; Canto, R.; "Using Arduino microcontroller boards to measure response latencies." Behav Res Methods. 2013 Dec;45(4):1332-46. doi: 10.3758/s13428-013-0336-z. PMID: 23585023.

[192] Digit, `https://digit.ml/` (Accessed on 24 December 2022)

Appendices

Research Ethics Form

Section 1

Your details

a) Researcher

Alex Abad
(18009297)

b) Title of Proposed Project

Development of a High-Resolution Haptic Hand Wearable using P20 Braille cells with cutaneous and kinaesthetic feedback

c) Programme Title and Level of Study

COMPUTER SCIENCE AND INFORMATICS

d) Research Dates

Start Date:

I confirm that I wiill not start my research before ethical approval has been given

I confirm that I wiill not start my research before ethical approval has been given

End Date:

2022-02-02

e) Department

First Subject

MATHEMATICS, COMPUTER SCIENCE AND ENGINEERING

First Supervisor Name

Dr Anuradha Dissanayake Mudiyanselage

f) Professional Guidelines Referenced

No Guidelines Referenced

Section 2
Who will be taking part in your research?

a) Will other people be taking part in your research?

Human participants

Section 3.1
General

a) Full title of the research project

Development of a High-Resolution Haptic Hand Wearable using P20 Braille cells with cutaneous and kinaesthetic feedback

b) Aims and Objectives

To develop a high-resolution haptic hand wearable using P20 Braille cells with cutaneous and kinaesthetic feedback that can be used for VR applications, telerobotics, and teleoperations.

The experiments on this study aim to gauge or evaluate the participant's virtual reality immersive experience in using the multimodal high-resolution haptic hand wearable. There will be experiments related to tactile pattern recognition tests, warm or cold perception tests, and grasping tests with different levels of stiffness or softness as the participant touches or grabs a virtual object.

c) Please give a brief outline of the research study

This study is a continuation of our previous study in developing Braille-like tactile displays for fingertip haptics with an approved ethics approval form S – 24-06-2019 SEL 087. Aside from using solenoids for one fingertip display, we are

now developing a high-resolution haptic hand wearable with cutaneous and kinaesthetic feedback for Virtual Reality (VR) applications and telerobotics. We will explore the use of P20 Braille-cells that have piezo-based tactile actuators with a small form factor.

The Prototypes

1. Haptic hand wearable with 96 tactile actuators.

The exoskeleton glove is a modular and lightweight Bluetooth and WiFi-enabled high-resolution haptic exoskeleton glove made from commercial off-the-shelf components. The prototype has 96 tactile actuators or tactors, a total weight of 235 grams, including the USB power bank, and operates at a 5V DC supply with a maximum power consumption of 4.84W. A 4x4 miniaturized (9mm x 10mm) tactile matrix consists of piezo-based pin actuators (Metec P20 Braille-cells) is strapped to the fingertips of the exoskeleton glove using Velcro. 16 mini-vibration motors (Jinlong Ltd.) are mounted to the palm of a haptic exoskeleton glove. 96 tactile actuators or tactors can be controlled by an 18mm x 45mm mini-microcontroller (Arduino Nano 33 IoT). Application software was developed using Processing to demonstrate the real-time actuation of the haptic exoskeleton glove. It is possible to feel a 2D binary image by emphasizing the edges in that image using Canny edge detection
and the Hough transform algorithm. In this demonstration, five 4x4 matrices of small circles corresponding to the 16 piezo-based tactile pins of P20 Braille cells are used, along with a Leap Motion Controller, to feel regions of interest on the screen. The Leap Motion Controller may be replaced by a VR headset such as Oculus Quest 2 for a 3D VR experience.

Though the haptic hand wearable uses 5V DC supply, there is a DC-DC converter circuit that steps up to 200V DC for the commercially available piezo-based P20 Braille cells. The P20 Braille-cells use 200V DC but they consume very little current in the range of micro-Amperes (uA). The use of 200V DC with low-current devices is safe. The P20 Braille cells are commercially available and being used as a Braille display for the visually impaired. We covered our power supply device by
insulative material to make sure there will be no conduction in current. This has been tested.

2. Haptic wearables with cutaneous and kinaesthetic Feedback

The novel untethered hand wearable can be used to extract haptic primary

colors of temperature, vibration, and force feedback. It used 5V DC supply and was made
from low-cost and commercial off-the-shelf components. To mimic cutaneous feedback, a 26mm annular Peltier element (TES1- 04903 Thermoelectric Peltier) with a 10mm hole is coupled to an 8mm disc vibration motor, forming vibro-thermal tactile feedback for the user. A 10K NTC thermistor is attached to the annular Peltier element as a temperature feedback device. All the other fingertips have an 8mm disc vibration motor strapped on them using Velcro. Kinesthetic feedback extracted from a retractable ID badge holder with a small solenoid stopper is used as force feedback that restricts the fingers' movement. Moreover, servos can be used as solenoid replacements for gradient force feedback. Hand and finger tracking is done using Leap Motion Controller interfaced to a virtual setup with different geometric figures developed using Unity software.

Perception test

This study will recruit ten to thirty sighted healthy individuals, age between 18 to 55 years old, but can be extend the number of participants to cover visually impaired or blind participants in the future. The participants are seated and wore hand wearable. The tactile pin actuation generates patterns such as rows, columns, diagonal, and random tactile patterns. The participants will be asked how they perceive the patterns. Those patterns can be static or vibrations. The vibration frequency will be 5Hz, 10Hz, 15Hz, and 20Hz which are within the range of frequencies that triggers fingertip's tactile mechanoreceptors: Meissner's corpuscles and Merkel's cells that are sensitive to edge pressure and flutter tap as reported by Visell [1], and Lederman & Klatzky [2]. It has been proven that humans can feel frequencies from 0.4Hz to 800Hz by previous research on haptics [1,2]. Aside from pre-defined tactile patterns, they may be asked if they can perceive the edges of an image in the edge-detection test in the VR environment using the LeapMotion controller as a hand tracking device. Moreover, they may be asked to wear a VR headset such as Oculus Quest2 in exploring the VR environment.

[1] Y. Visell, "Tactile sensory substitution: Models for enaction in HCI," Interacting with Computers, vol. 21, no. 1–2, pp. 38-53, Jan. 2009.

[2] S. J. Lederman, R. L. Klatzky, "Haptic perception: A tutorial," Attention, Perception, & Psychophysics, 2009, 71(7), 1439-1459. doi:10.3758/APP.71.7.1439

Moreover, aside from the tactile pattern perception test, we will also do an integration test that includes temperature and force feedback tests.

Integration test

This study will use the hand wearable with the combination of cutaneous and kinaesthetic feedback. The participant will be asked not only to feel the tactile patterns but also to change in temperature on the palm area as well as change in stiffness/softness of the retractable string as the participant touches a virtual object.

This study will use a small Peltier device or Thermoelectric Generator (TEG) to be strapped on a fingertip using Velcro. The participant in this test will tell if the TEG is hot or cold when he touches a virtual object in the VR simulator. The temperature of the virtual hot object will not exceed 40°C and the cold will not be lower than 10°C. There will be a temperature controller that will ensure our prototype will not exceed these temperatures. Before starting the experiment, participants are asked to feel lower and upper-temperature thresholds to make sure participants are ready for experiments. If participants feel uncomfortable with this training, they can withdraw without taking part in experiments. Our prototype has an emergency switchable mode to turn it off in any case of emergency and the Velcro straps can easily be removed.

This study will use the hand wearable that has gradient force feedback using retractable ID badge holder and servos. The participant will be asked to feel the change in tension on the string of the retractable ID badge holder as the angle of the servo lever changes. This test aims to simulate hardness or softness in touching virtual objects.

d) Some types of research must be referred (by the Faculty Ethics Research Sub-Committee) to the University Research Ethics Sub-Committee. Therefore, please state here if your research involves or may involve deception, the use of covert methods, matters involving national security, illegal activity or might endanger the University's reputation. Please also highlight the key aspects which cause it to fall into one or more of these categories.

This study will not involve deception. Only the tactile patterns are held secret to the participants. Prototype mechanisms will be explained thoroughly to the participants before the tests. No security risk or any illegal activity in this study.

e) Where will the study take place and in what setting? If in a workplace, or if the participants are from a workplace (e.g. a school), identify what your connections are with that workplace

All the experiments will be carried out at the Robotics Lab (FML401) in FML Building, Liverpool Hope University.

The researcher will not use any friends, colleagues, and students he knows. He will choose participants from other groups or schools.

Data will be stored in a password-protected computer in a password-protected folder at the university.

f) Give a brief description of your target sample (e.g. age, occupation, gender)

Age: greater than 18 years old

Number of participants: ten (10) to thirty (30) sighted individuals

Gender: any

Occupation: any

g) Is the participation individual or as part of a group?

Individual participant

j) How will participants be selected, approached and recruited? Identify clearly and analyse fully any issues of power relations that might arise, and say what steps you will take to alleviate them. This applies particularly if the location of the research is a place of the researcher's own employment, or if they have other strong links with the participants.

Any consenting adult can be part of the perception tests.

This will be advertised at the department notice board and circulate via Science bulletin to find volunteers for the experiments.

k) Is written consent to be obtained?

Yes

Please complete the appropriate sections of the standard Consent Form(s) and the accompanying Research Information Sheet(s) that can be found at the end of this documentation

How will the participants' right to withdraw be ensured?

Before starting the experiment, participants are introduced to the setup and will have training such as feeling the tactile training patterns, the tension on the retractable string during finger movements, and the lower and upper temperature thresholds to make sure participants are ready for the experiments. If participants feel uncomfortable with the training, they can withdraw without taking part in experiments.

Participants are given breaks every 10 minutes if they feel fatigued. However, they are free to ask for a break or withdraw whenever they feel uncomfortable.

Participants can withdraw anytime during the experiment (not only if they feel uncomfortable), and the researcher will delete or erase whatever data he got from the participant who wishes to withdraw.

Section 3.2

Risk & Ethical Procedures

a) What potential risks are there of physical harm to participants? Please specify, and explain any steps you will take to address them.

- Since tapping is involved, participants might feel uncomfortable. Therefore, participants are given breaks every 10 minutes if they feel fatigued. However, they are free to ask for a break or withdraw whenever they feel uncomfortable.

- Though the haptic hand wearables use a 5V DC supply, there is a DCDC converter circuit that steps up to 200V DC for the piezo-based commercially available P20
Braille-cells. The P20 Braille cells use 200V DC, but they consume very little current in the range of micro-amperes. The use of 200V DC with low-current devices is safe. The P20 Braille cells are commercially available and being used as a Braille display for the visually impaired. We covered our power supply device with an insulative material to make sure there will be no conduction in current. This has been tested.

- This study will use a small Peltier device or Thermoelectric Generator (TEG) to be fitted on a fingertip. The participant in this test will tell if the TEG is hot or cold

when it touches a virtual object in the VR simulator. The temperature of the virtual hot object will not be greater than 40°C, and the cold will not be lower than 10°C. There will be a temperature controller that will ensure our prototype will not exceed these temperatures. Before starting the experiment, participants are asked to feel lower and upper-temperature thresholds to make sure participants are ready for experiments. If participants feel uncomfortable with this training, they can withdraw without taking part in experiments. Our prototype has an emergency switchable mode to turn it off in any case of emergency, and the Velcro straps can easily be removed.

- Government and NHS guidelines listed in such as frequent washing of hands (or using hand sanitiser), social distancing, wearing face-covering, and opening the windows in the lab to let fresh air in will be followed during the experiments. Our hardware is compatible with disinfected solutions. Therefore, hardware will be disinfected after each of the participants. We can maintain social distancing during testing because our hand wearable and VR headset are wirelessly connected to a laptop/computer. Aside from disinfecting the VR headset, we will also use disposable universal sanitary cover mask for VR headset that can be replaced after every use.

- The researcher will strictly follow the General Data Protection Regulation (GDPR) in handling personal data. We will only collect the name, gender, age, and handedness of each participant. The personal data of participants in this study will be encrypted or encoded. The data will be stored in a password-protected computer in a secure folder at the university.

b) What potential psychological risks are there to participants? In particular, how might participation in this research cause discomfort or distress to participants? Please specify, and explain any steps you will take to address these issues.

- Participants are given a five-minute break in every 10 minutes to avoid fatigue and discomfort. However, participants can ask for a break anytime if they feel uncomfortable. Moreover, participants can withdraw from the experiment at any time (not only f they feel uncomfortable), and the data collected will be erased as soon the participant who wishes to withdraw informs the researcher.

c) Are there any risks to you as the researcher (and / or your co-researchers, if you have any) in this project? If so, outline the steps you will take to minimise them.

All the wires in the circuit are properly insulated. There might be a little

discomfort in the mounting of the haptic glove and VR headset due to fatigue. The researcher can take a rest or take a break.

d) How might participants benefit from taking part in this research?

-Participants will be given a final report upon request to highlight main findings.

e) Does any aspect of your research require that participants be naïve (i.e. they are not given full or exact information about the aims of the research)? Please explain why and give details of the debriefing procedures you would use when the need for the naiveté is over

Before starting the experiment, participants are introduced to the setup and will have training such as feeling the tactile training patterns, the tension on the retractable string during finger movements, and the lower and upper temperature thresholds to make sure participants are ready for the experiments. If participants feel uncomfortable with the training, they can withdraw without taking part in experiments. Moreover, participants can withdraw from the experiment at any time (not only if they feel uncomfortable), and the data collected will be erased as soon the participant who wishes to withdraw informs the researcher.

Section 3.3

Data Security, Confidentiality, Anonymity and Destruction

a) Where and how do you intend to store any data collected from this research? Give details of steps you will take to ensure the security of any data you collect.

- The researcher will strictly follow the General Data Protection Regulation (GDPR) in handling personal data. We will only collect the name, gender, age, and handedness of each participant. The personal data of participants in this study will be encrypted or encoded. The data will be stored in a password-protected computer in a secure folder at the university.

- The data to be collected will be aggregated or converted into statistics making it impossible to identify individuals from the collected data.

- Participants can withdraw anytime during the experiment (not only if they feel

uncomfortable), and the researcher will delete or erase whatever data he got from the participant who wishes to withdraw.

- All the experiments will be carried out at the Robotics Lab (FML401) in FML Building, Liverpool Hope University.

- Data will be stored in a password-protected computer in a password-protected folder at the university.

b) What steps will you take to safeguard the anonymity and confidentiality of personal records?

- The researcher will strictly follow the General Data Protection Regulation (GDPR) in handling personal data. We will only collect the name, gender, age, and handedness of each participant. The personal data of participants in this study will be encrypted or encoded. The data will be stored in a password-protected computer in a secure folder at the university.

- The data to be collected will be aggregated or converted into statistics making it impossible to identify individuals from the collected data.

- All the experiments will be carried out at the Robotics Lab (FML401) in FML Building, Liverpool Hope University.

- Participants can withdraw anytime during the experiment (not only if they feel uncomfortable), and the researcher will delete or erase whatever data he got from the participant who wishes to withdraw.

c) Will this research require the use of any of the following?

Video Recordings

No

Audio Recordings

No

Photos

No

Observation of participants

No

d) Deletion of personal data

I will destroy all personal data recorded by the end of my degree programme

You should NOT make this point dependent on a successful outcome of your studies.

Date you will delete the data

February 02, 2022

Section 4

Consent Forms, Research Information Sheet and Additional Documentation

a) Consent Form

Uploaded Files:

- AbAdA_research_consent_form.docx

c) Research Information Sheet

Uploaded Files:

- AbAdA_research_information_sheet_v2.docx

d) Additional Documentation

Uploaded Files:

- AbAdA_Application for Ethical Clearance Research with NON vulnerable human groups_v2.pdf

Uploaded Documenation

The following pages are copies of the supporting documentation for this ethics form.

Section 3. INFORMATION ABOUT PROPOSED RESEARCH STUDY.

3.1 GENERAL

a) Full title of the research project:
"**Development of a High-Resolution Haptic Hand Wearable using P20 Braille cells with cutaneous and kinaesthetic feedback"**

b) Aims and objectives:
To develop a high-resolution haptic hand wearable using P20 Braille cells with cutaneous and kinaesthetic feedback that can be used for VR applications, telerobotics, and teleoperations.

The experiments on this study aim to gauge or evaluate the participant's virtual reality immersive experience in using the multimodal high-resolution haptic hand wearable. There will be experiments related to tactile pattern recognition tests, warm or cold perception tests, and grasping tests with different levelsof stiffness or softness as the participant touches or grabs a virtual object.

c) Brief outline of the research study. Please ensure that you include details of the **design** (qualitative/quantitative, etc) as well as the **methods and procedures** (questionnaire, interviews, experimental trial, observation, etc).

This study is a continuation of our previous study in developing Braille-like tactile displays for fingertip haptics with an approved ethics approval form **S – 24-06-2019 SEL 087**. Aside from using solenoids for one fingertip display, we are now developing a high resolution haptic hand wearable with cutaneous and kinaesthetic feedback for Virtual Reality (VR) applications, and telerobotics. We will explore the use of P20 Braille cells that have piezo-based tactile actuators with small form factor.

The Prototypes

1. Haptic hand wearable with 96 tactile actuators.

The exoskeleton glove is a modular and lightweight Bluetooth and WiFi-enabled high-resolution haptic exoskeleton glove made from commercial off-the-shelf components. The prototype has 96 tactile actuators or tactors, a total weight of 235 grams, including the USB power bank, and operates at a 5V DC supply with a maximum power consumption of 4.84W. A 4x4 miniaturized (9mm x 10mm) tactile matrix consists of piezo-based pin actuators (Metec P20 Braille cells) are strapped to the fingertips of the exoskeleton glove using Velcro. 16 mini-vibration motors (Jinlong Ltd.) are mounted to the palm of a haptic exoskeleton glove. 96 tactile actuators or tactors can be controlled by an 18mm x 45mm mini-microcontroller (Arduino Nano 33 IoT). Application software was developed using Processing to demonstrate the real-time actuation of the haptic exoskeleton glove. It is possible to feel a 2D binary image by emphasizing the edges in that image using Canny edge detection and the Hough transform algorithm. In this demonstration, five 4x4 matrices of small circles corresponding to the 16 piezo-based tactile pins of P20 Braille cells are used, along with a Leap Motion Controller, to feel regions of interest on the screen. The Leap Motion Controller may be replaced by a VR headset such as Oculus Quest 2 for 3D VR experience. The integrated experimental setup is shown in Fig. 1.

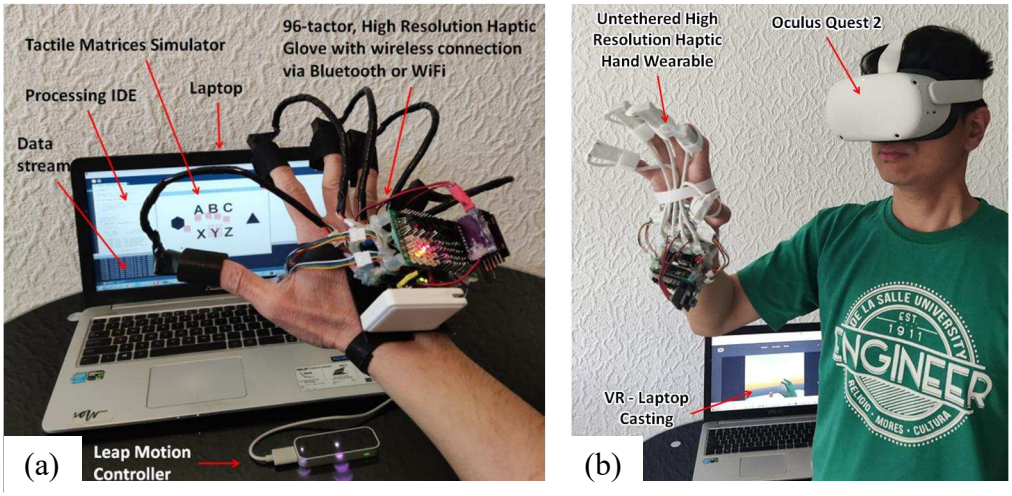

Figure 1. The integrated experimental setup. (a) Using Leap Motion Controller and haptic glove, and (b) using VR headset and haptic glove

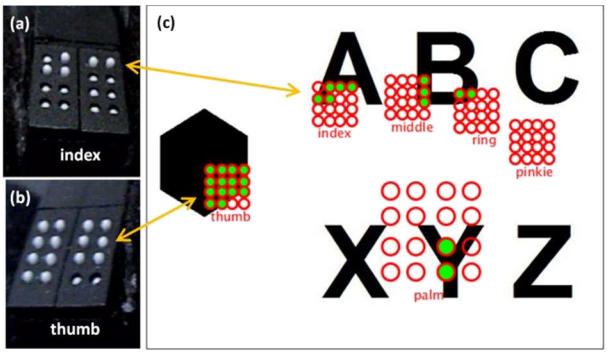

Figure 2. Fingertip tactile matrices, and Graphical User Interface (GUI).

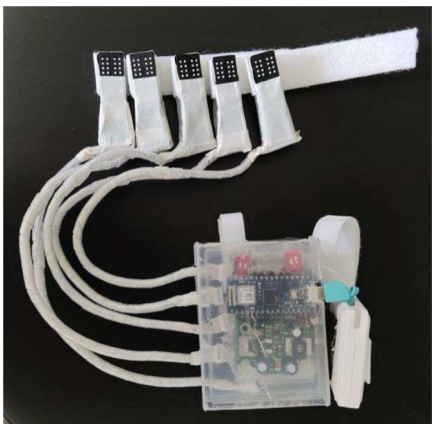

Figure 3. Haptic hand wearable with enclosed electronic parts.

Though the haptic hand wearable uses 5V DC supply, there is a DC-DC converter circuit that steps up to 200V DC for the commercially avaible piezo-based P20 Braille cells. The P20 Braille cells uses 200V DC but they consume very little current in the range of micro-Amperes (uA). The use of 200V DC with low-current

devices is safe. The P20 Braille cells are commercially available and being used as a Braille display for the visually impaired. We covered our power supply device by insulative material to make sure there will be no conduction in current. This has been tested.

2. Haptic wearables with cutaneous and kinaesthetic Feedback

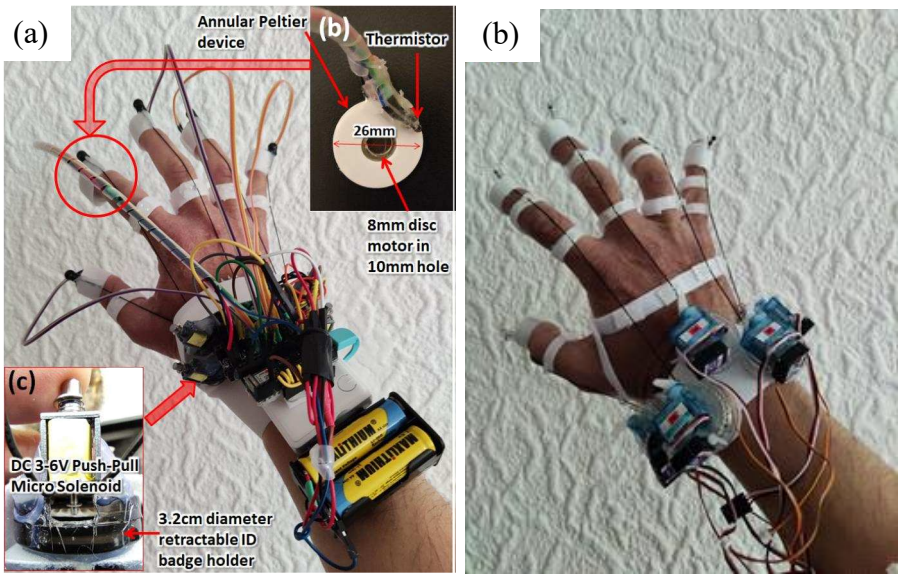

Figure 4. Untethered haptic hand wearable with haptic primary colors feedback. (a) The hand wearable haptic has cutaneous and kinesthetic haptic feedbacks. Each fingertip has mini vibration motor. Aside from mini vibration motor, the index fingertip has an annular Peltier device making it a vibro-thermal haptic feedback as shown in Fig. 4(b). The force feedback that can restrict the movement of each finger is formed by combining a retractable ID badge holder and small solenoid stopper as shown in Fig. 4(c). Fig. 4(d) uses servo motors instead of solenoid for gradient force feedback.

The novel untethered hand wearable shown in Fig. 4 can be used to extract haptic primary colors of temperature, vibration, and force feedback. It used 5V DC supply and made from low-cost and commercial off-the-shelf components. To mimic cutaneous feedback, a 26mm annular Peltier element (TES1- 04903 Thermoelectric Peltier) with a 10mm hole is coupled to an 8mm disc vibration motor, forming vibro-thermal tactile feedback for the user. A 10K NTC thermistor is attached to the annular Peltier element as a temperature feedback device. All the other fingertips have an 8mm disc vibration motor strapped on them using Velcro. Kinesthetic feedback extracted from a retractable ID badge holder with a small solenoid stopper is used as force feedback that restricts the fingers' movement. Moreover, servos can be used as solenoid replacements for gradient force feedback. Hand and finger tracking is done using Leap Motion Controller interfaced to a virtual setup with different geometric figures developed using Unity software.

Perception test

This study will recruit ten to thirty sighted healthy individuals, age between 18 to 55 years old, but can be extend the number of participants to cover visually impaired

or blind participants in the future. The participants are seated and wore hand wearable. The actuation generates the patterns like those shown in Fig. 5 and participants will be asked how they perceive the patterns. Those patterns can be static or vibrations. The vibration frequency will be 5Hz, 10Hz, 15Hz, and 20Hz which are within the range of frequencies that triggers fingertip's tactile mechanoreceptors: Meissner's corpuscles and Merkel's cells that are sensitive to edge pressure and flutter tap as reported by Visell [1], and Lederman & Klatzky [2] . It has been proven that humans can feel frequencies from 0.4Hz to 800Hz by previous research on haptics [1,2]. Aside from pre-defined tactile patterns, they may be asked if they can perceive the edges of an image in the edge-detection test in the VR environment using the Leap Motion controller as a hand tracking device. Moreover, they may be asked to wear a VR headset such as Oculus Quest2 in exploring the VR environment.

[1] Y. Visell, "Tactile sensory substitution: Models for enaction in HCI," Interacting with Computers, vol. 21, no. 1–2, pp. 38-53, Jan. 2009.
[2] S. J. Lederman, R. L. Klatzky, "Haptic perception: A tutorial," Attention, Perception, & Psychophysics, 2009, 71(7), 1439-1459. doi:10.3758/APP.71.7.1439

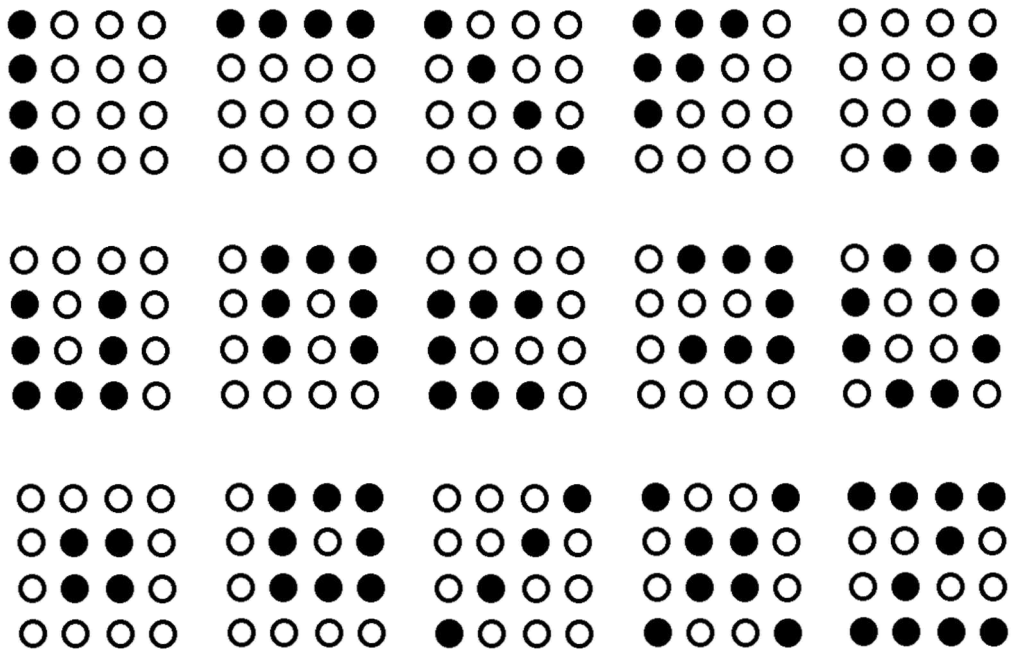

Figure 5. Tactile patterns

Moreover, aside from tactile pattern perception test, we will also do integration test that includes temperature and force feedback tests.

Integration test

This study will use the combination of hand wearables as shown in Fig. 1 and Fig. 4(d). The combined setup is the combination of cutaneous and kinaesthetic feedback. The participant will be asked not only to feel the tactile patterns but also change in temperature on the palm area as well as change in stiffness/softness of the retractable string as the participant touches a virtual object.

This study will use a small Peltier device or Thermoelectric Generator (TEG) to be strapped on a fingertip using Velcro. The participant in this test will tell if the TEG is

hot or cold when he touches a virtual object in the VR simulator. The temperature of the virtual hot object will not exceed 40°C and the cold will not be lower than 10°C. There will be temperature controller that will ensure our prototype will not exceed these temperatures. Before starting the experiment, participants are asked to feel lower and upper temperature thresholds to make sure participants are ready for experiments. If participants feel uncomfortable on this training, they can withdraw without taking part into experiments. Our prototype has an emergency switchable mode to turn it off in any case of emergency and the Velcro straps can easily be removed.

This study will use the hand wearable as shown in Fig. 4(d) that has gradient force feedback using retractable ID badge holder and servos. The participant will be asked to feel the change in tension on the string of the retractable ID badge holder as the angle of the servo lever changes. This test aims to simulate hardness or softness in touching virtual objects.

LIVERPOOL HOPE UNIVERSITY
Est. 1844

LIVERPOOL HOPE UNIVERSITY

RESEARCH CONSENT FORM

Title of research project: "Development of a High-Resolution Haptic Hand Wearable using P20 Braille cells with cutaneous and kinaesthetic feedback"

Name of researcher: Alexander C. Abad

1	I confirm that I have read and understand the information sheet for the above research project and have had the opportunity to ask questions.	Yes / No
2.	I understand that my participation is voluntary and that I am free to withdraw at any time, without giving any reason.	Yes / No
3.	I agree to take part in this research project and for the anonymised data to be used as the researcher sees fit, including publication.	Yes / No

Name of participant:

Signature:

Date:

Research Consent Form

LIVERPOOL HOPE UNIVERSITY
Est. 1844

LIVERPOOL HOPE UNIVERSITY

RESEARCH INFORMATION SHEET

Outline of the research (a couple of sentences in non-specialist language)

-An untethered multimodal high-resolution haptic hand wearable was developed to study tactile pattern perception of humans. This hand wearable can be used to enhance the immersive experience in a virtual reality environment. The prototype is like an exoskeleton glove with 16 tactile pins on each fingertip made from commercially available P20 Braille cells, and 16 mini-vibration motors on the palm area. Aside from the tactile pins and mini-vibration motors, retractable strings are attached to each fingertip that restricts finger movement simulating hardness or softness when the participants touch or grab a virtual object. There is also a small Peltier device on the palm area that gets warm or cold depending on what the participant has touched virtual object.
- The experiments on this study aim to gauge or evaluate the participant's virtual reality immersive experience in using the multimodal high-resolution haptic hand wearable. There will be experiments related to tactile pattern recognition tests, warm or cold perception tests, and grasping tests with different levels of stiffness or softness as the participant touches or grabs a virtual object.

Who is the researcher?

Name: **Alexander C. Abad**

Institution: Liverpool Hope University

Researcher's University email address: 18009297@hope.ac.uk

What will my participation in the research involve?

- **You will be asked to feel a virtual object, described the edges of an image or tactile patterns felt by your fingertips and palm**
- **You will be asked to feel if the Peltier device is warm or cold as you touch a virtual object**
- **You will be asked to describe the change in the gradient force feedback**

Will there be any benefits to me to taking part?

- **You will be given an introduction on aims and objectives of the research. You are eligible to ask main findings of the research at the end of this project on February 02, 2022.**

Will there be any risks to me in taking part?

- **Since a tapping is involved, participants might feel uncomfortable. Therefore, participants are given breaks every 10 minutes if they feel fatigue. However, they are free to ask a break or withdraw whenever they feel uncomfortable.**
- **If you are uncomfortable with the temperature of the Peltier device, you can easily remove the Velcro strap.**

What happens if I decide that I don't want to take part during the actual research study, or decide that the information given should not be used?

- **You can always withdraw anytime you want and we will delete or erase whatever data we got from you as soon as you inform us.**

How will you ensure that my contribution is anonymous?

- **All the experiments will be carried out at the Robotics Lab (FML401) in FML Building, Liverpool Hope University.**

- **The researcher will strictly follow the General Data Protection Regulation (GDPR) in handling personal data. We will only collect the name, gender, age, and handedness (right or left handed) of each participant. The personal data of participants in this study will be encrypted or encoded. The data will be stored in a password-protected computer in a secure folder at the university.**

- **The data to be collected will be aggregated or converted into statistics making it impossible to identify individuals from the collected data.**

Please note that your confidentiality and anonymity cannot be assured if, during the research, it comes to light that you are involved in illegal or harmful behaviours which I may need to disclose to the appropriate authorities.

Liverpool Hope University

Ethical Approval Request only for research involving human participants who are NOT children (below 18) or vulnerable adults

1) For text-based projects not involving human participants, use the designated shorter request form rather than this one.

2) For projects involving children or vulnerable adult, use the designated longer request form rather than this one.

SECTION 1 [TO BE COMPLETED BY THE RESEARCHER]

1.1 Researcher **For staff: Name:** **(For joint research conducted by staff, the names of all the researchers should be given with the Principal Researcher's name given in bold.)** **For students: Name, student ID, name of supervisor:**	Alexander C. Abad ID: 18009297 Dr. Anuradha Ranasinghe
1.2 Title of Proposed Project:	Development of Braille-like Tactile feedback using dot matrix print head, small solenoids, and retractable pens
1.3 For students only: Programme Title and Level of Study (e.g. MA Education; Philosophy and Ethics Level H).	PhD in Informatics and Computer Science
1.4 For staff only: Position held at Hope (e.g. Lecturer).	
1.5 Faculty and Department or equivalent : (*for research involving two Faculties or Departments, please state both. The name first given should be that of the Faculty and*	Department of Mathematics and CS

Department whose DEL is being asked to approve.[1])	
1.6 Start date of proposed research (note: this must be later than the date at which approval may be given)	June 25th, 2019
End date of proposed research	February 02nd, 2022
1.7 Professional guidelines referenced	BPS Code Of Ethics and Conduct BPS Code of Human Research Ethics General Data Protection Regulations (GDPR)

SECTION 2

NOTES ON ALL RESEARCH INVOLVING HUMAN PARTICIPANTS

Approval will be given by

(a) The University Research Ethics Sub-committee for
- research that may involve deceptive or covert activity
- empirical research into illegal activities
- research that may be connected to any aspect of national security
- and/or research deemed to pose a significant risk to the University's reputation.

The researcher should identify all such cases and refer them to their supervisor, who in turn will contact their Departmental Research Ethics Lead (DEL) for suggestions. The DEL will forward the application to the Faculty Research Ethics Sub-committee for consideration and, if necessary, for referral to the University Research Ethics Sub-committee

OR

(b) The Faculty Research Ethics Sub-committee for research involving children (under 18) or vulnerable adults and recommended by a Departmental Research Ethics Lead (DEL)

OR

(c) The DEL for research involving human participants but NOT children (under 18) or vulnerable adults.

[1] The University does not require double approval for shared research. Where the research is cross-Faculty, the researcher should seek advice from an appropriate person about which Faculty should be asked to approve.

OR

(d) An authorized staff who for good reason cannot refer the request to a supervisor

NOTE: For projects not involving human participants, use the designated shorter request form rather than this one.

In all cases, initial scrutiny will be carried out by the supervisor or DEL, as appropriate.

Initial scrutiny consists of a careful reading of the request coupled with ensuring completion of the checklist given at the end of this form. This process may need to be iterative with the researcher*. When ALL responses are satisfactory, the initial scrutineer should complete the last section of the checklist and should send this form (and any associated documentation) on to the next stage of the process as explained at the end of the checklist.

*If ANY prompt cannot be given an acceptable response, the initial scrutineer should return the form to the researcher, clearly explaining the remedial action needed, and advising of a deadline for the form to be returned to the initial scrutineer.

Section 3. INFORMATION ABOUT PROPOSED RESEARCH STUDY.

Note: the checklist given at the end of this document should be completed by the researcher. The initial scrutineer may either add to it, or simply endorse it as agreed. A supervisor or DEL receiving a form without the checklist having been completed will return it to the supervisor (for student research) or the researcher (for staff research) for completion.

3.1 GENERAL
a) Full title of the research project: **Development of Braille-like Tactile sensor using dot matrix print head, small solenoids, and retractable pens**
b) Aims and objectives: **To develop a low-cost, scalable, easy to assemble, and can be fully latching tactile sensor using different prototypes such as dot matrix print head, small solenoids, and retractable pens.**
c) Brief outline of the research study. Please ensure that you include details of the **design** (qualitative/quantitative, etc) as well as the **methods and procedures** (questionnaire, interviews, experimental trial, observation, etc). **The Prototypes** This study will develop three types of braille-like tactile sensors. The first prototype is based from dot matrix print head. The pin arrangement is modified to form a square or 3x3 matrix. It is powered by 9V dc supply. The pin pitch is

around 1mm – 2mm. There is a finger platform that will hold the fingertip. The finger platform will prevent the finger to push the pins but will support the finger to feel the presence of an activated pin. When actuated, the pins rise to about 0.5mm from its resting position. Each pin can be controlled individually. Please see the prototype set-up shown in Figure 1. Aside from 9-pin print head, 24-pin and 48-pin print head will also be explored.

The second prototype is based on retractable pen driven by small solenoid. The solenoid will latch and de-latch the tip of the pen. Figure 2(a) shows the assembly of retractable pens forming a 4x4 matrix. Figure 2(b) shows the top of the tactile display showing only the tip of the latch pens. The small solenoid for this prototype will use 5V dc supply. Each pin can be controlled individually. The pen tip protrusion on the surface will be around 0.5mm with 0.4mm-0.5mm pitch. Ink was removed from the pens.

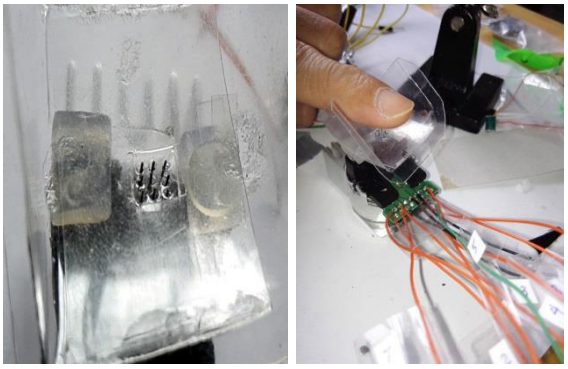

(a) (b)

Figure 1. Fingertip tactile set-up using dot matrix print head

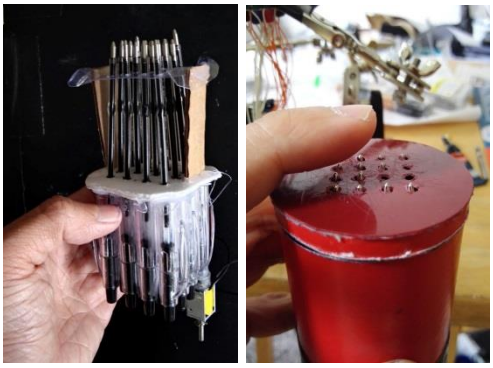

(a) (b)

Figure 2. Fingertip tactile set-up using retractable pens

The third protoype shown in Figure 3 is based on small solenoids that are group together to form a 3x4 martix. When activated, the pins go up to about 0.5mm with 3 mm pitch. The pins can stay up if the there is a continous power or can be made to vibrate or tap at different frequencies using pulse with modulation (PWM) technique. Each pin can be controlled individually. 5V dc supply is used to activate each small solenoid.

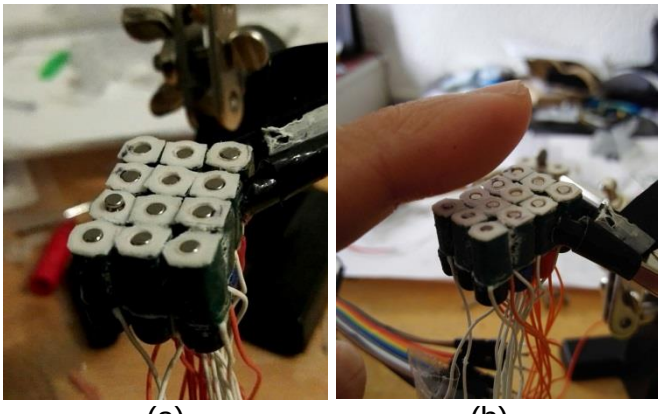

(a) (b)

Figure 3. Fingertip tactile set-up using small solenoids

Stable platform will be made to ensure that no fingertip will be hurt in this study.

Perceptions tests

This study will recruit thirty sighted adult individuals but can be extend the number of subjects to cover visually impaired or blind subjects in the future. The sighted subjects will be blindfolded and will try to recognize different patterns that will emerge from the fingertip tactile feedback prototype. They will use the index finger of their dominant hand in the perception tests. Some of the patterns that will be used in perception tests are shown in Figure 4.

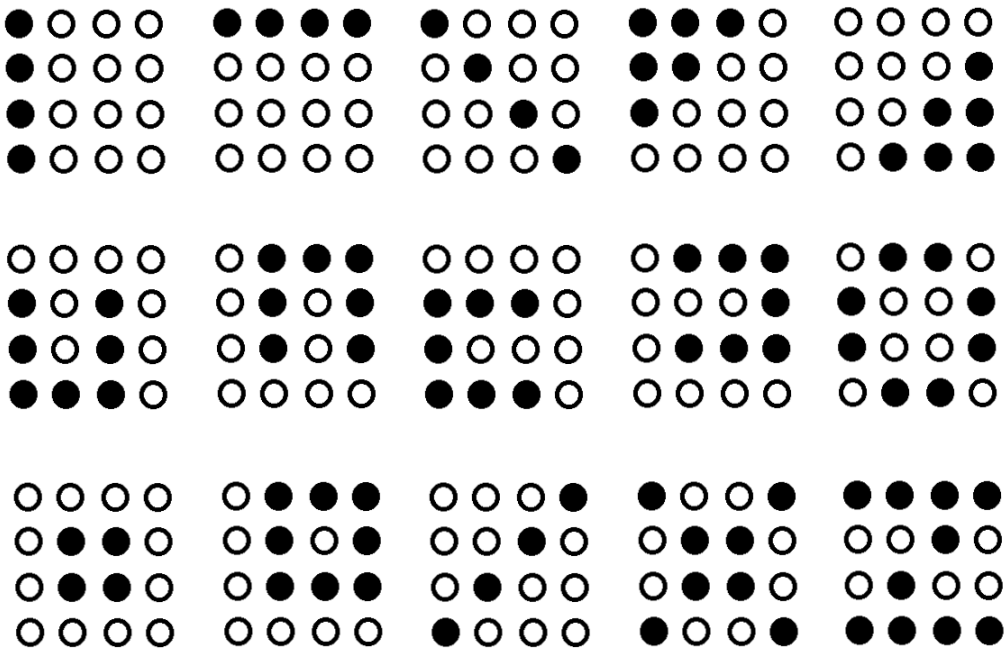

Figure 4. Tactile patterns

d) As mentioned under Section 2 (a), some types of research must be referred (by the Faculty Ethics Research Sub-Committee) to the University Research Ethics Sub-Committee. Therefore, please state here if your research involves or may involve deception, the use of covert methods, is into matters involving national security, is into illegal activity or might endanger the University's reputation. Please also highlight the key aspects which cause it to fall into one or more of these categories.

This study will not involve deception. Only the tactile patterns are held secret to the participants. Prototype mechanisms will be explained thoroughly to the participants before the tests. No security risk or any illegal activity in this study.

e) Where will the study take place and in what setting? If in a workplace, or if the participants are from a workplace, identify what your connections are with that workplace.

All the experiments will be carried out at the Robotics Lab (HS/106) in Health Science Building, Liverpool Hope University.

Data will be stored in password protected computer in a password protected folder at the university.

f) Give a brief description of your target sample (e.g. age, occupation, gender).

Age: greater than 18 years old
Number of participants: thirty (30) sighted individuals
Gender: any
Occupation: any

g) Is the participation individual or as part of a group?

individual

h) How will participants be selected, approached and recruited?
Clearly identify and fully analyse any issues of power relations that might arise, and say what steps will be taken to alleviate them. This applies particularly if the location of the research is a place of the researcher's employment, or if they have other strong links with the participants.

Any consenting adult can be part of the perception tests.
This will be advertised at the department notice board and circulate via Science bulletin to find volunteers for the experiments.

i) Free and informed consent and the right to withdraw at any time are indispensable.

Is written consent to be obtained? Please delete as appropriate **YES**

If **YES**, please complete the appropriate sections of the standard Consent Form(s) and the accompanying Research Information Sheet(s) that can be found at the end of this documentation.

If **NO**, please state *why*. As free and informed consent is essential, you need to give strong and convincing reasons for not obtaining informed consent.

How will the participants' right to withdraw be ensured?

Participants will be informed via written consent form and email before the experiments.

3.2 Risk & Ethical Procedures

Please note: all studies with human participants have the potential to create a level of risk. “No risk” is thus not an acceptable answer, although “Minimal risk” is. You are fully responsible for the protection of both yourself and your research participants. Please try to anticipate the context and perspective of your participants when completing this section.

a) What potential risks are there of physical harm to participants? Please specify, and explain any steps you will take to address them.

- Since a tapping is involved, participants might feel uncomfortable. Therefore, participants are given breaks every 10 minutes if they feel fatigue. However, they are free to ask a break or withdraw whenever they feel uncomfortable.

b) What potential risks are there of psychological harm to participants? In particular, how might participation in this research cause discomfort or distress to participants? Please specify, and explain any steps you will take to address these issues.

- Participants are given five minute break in every 10 minutes to avoid fatigue and discomfort.

c) Are there any risks to you as the researcher (and / or your co-researchers, if you have any) in this project? If so, outline the steps you will take to minimise them.

- None

d) How might participants benefit from taking part in this research?

-Participants will be given a final report upon request to highlight main findings.

e) Does any aspect of your research require that participants be naïve *(i.e. they are not given full or exact information about the aims of the research)*? Please explain why and give details of the debriefing procedures you would use when the need for the naiveté is over.

- Not Applicable

3.3 Data Security, Confidentiality, Anonymity and Destruction

a) Where and how do you intend to store any data collected from this research? Give details of steps you will take to ensure the **security** of any data you collect.

Note that data protection regulations stipulate that data must be stored securely and not be accessible or interpretable by individuals outside of the project. Hence, data should be stored in a password-protected file on a password-protected device such as a desktop or laptop, and not on easily movable devices such as USB keys or CD ROMs.

- **All the experiments will be carried out at the Robotics Lab (HS/106) in Health Science Building, Liverpool Hope University.**

- **Data will be stored in password protected computer in a password protected folder at the university.**

b) What steps will you take to safeguard the **confidentiality and anonymity** of personal records?

- **Data will be stored in password protected computer in a password protected folder at the university.**
- **Participants will be anonymous**

c) Will this research require the use of any of the following (please delete as appropriate):

Video recordings	NO
Audio recordings	NO
Photos	NO
Observation of participants	NO

If you answered YES to any of the above, please provide a more detailed explanation of how you will ensure confidentiality and anonymity.

d) Please confirm that you will destroy all personal data and indicate at which point you will do so.

For students: A date should be provided. This should normally be no later than the end of their degree programme. Students should NOT make this point dependent on a successful outcome of their studies.

- **February 02nd, 2022**

For staff: A date should be provided. For certain types of research, it is acceptable for destruction of anonymised data to be indefinitely deferred. This must be clearly declared in the Research Information Sheet.

- **N/A**

4 For students only: Supervisor's comments
(Please note that applications submitted without supervisor's comments will not be considered.) **Alex discussed with me the design of experiments with me. Therefore, I have confirmed that I have gone through research ethics form prior to submission.** **Supervisor's name: Dr. Anuradha Ranasinghe** **Date: 14.06.2019**

Blank Research Consent Form and Research Information Sheets are appended. Please ensure you complete the relevant forms, and delete any that are not required.

Note 1

The question of when childhood is deemed to end, such that mentally capable young people can themselves give free and informed consent without needing parental consent, is much discussed, and to some extent depends on the reason why the consent is being sought. As a precaution the University takes the age of personal consent for research participation as being 18, and this should be applied throughout. Only if ALL participants in this research are over 18 should this form be used.

LIVERPOOL HOPE UNIVERSITY

RESEARCH CONSENT FORM

Title of research project: "Development of Braille-like Fingertip Tactile feedback using dot matrix print head, small solenoids, and retractable pens"

Name of researcher: Alexander C. Abad

I confirm that I have read and understand the information sheet for the above research project and have had the opportunity to ask questions.	Yes	No
I understand that my participation is voluntary and that I am free to withdraw at any time, without giving any reason.	Yes	No
I agree to take part in this research project and for the anonymised data to be used as the researcher sees fit, including publication.	Yes	No

Name of participant:

Signature:

Date:

LIVERPOOL HOPE UNIVERSITY

RESEARCH INFORMATION SHEET

Outline of the research (a couple of sentences in non-specialist language):

This study focus to develop a low-cost, scalable, easy to assemble, and fully latching tactile fingertip tactile feedback using dot matrix print head, small solenoids, and retractable pens. Perception tests will be carried out with at least 30 adult participants to recognize at least 12 different patterns or tactile dictionary.

Who is the researcher?

Name: **Alexander C. Abad**

Institution: **Liverpool Hope University**

Researcher's University email address: **18009297@hope.ac.uk**

What will my participation in the research involve?

- **You will be asked to described the tactile patterns felt by your fingertip**

Will there be any benefits to me to taking part?

- **You will be given an introduction on aims and objectives of the research. You are eligible to ask main findings of the research at the end of this project on February 02, 2022.**

Will there be any risks to me in taking part?

- **Since a tapping is involved, participants might feel uncomfortable. Therefore, participants are given breaks every 10 minutes if they feel fatigue. However, they are free to ask a break or withdraw whenever they feel uncomfortable.**

What happens if I decide that I don't want to take part during the actual research study, or decide that the information given should not be used?

- **You can always withdraw anytime you want and we can always delete whatever that we got from you as soon as you withdraw.**

How will you ensure that my contribution is anonymous?

- **All the experiments will be carried out at the Robotics Lab (HS/106) in Health Science Building, Liverpool Hope University.**

- **Data will be stored in password protected computer in a secure folder at the university.**

- **We do not collect personal data such as name, gender, and age.**

Please note that your confidentiality and anonymity cannot be assured if, during the research, it comes to light that you are involved in illegal or harmful behaviours that I may need to disclose to the appropriate authorities.

CHECKLIST FOR RESEARCH ETHICS APPROVAL REQUESTS (STAFF OR STUDENT)

Name of researcher: Alexander C. Abad

Name of Supervisor (if student): Dr. Anuradha Ranasinghe

Date completed: June 14, 2019

For use by staff or students to help improve the Ethics Approval request before submission

For use by supervisors before completing the Supervisor comments section of the form. If you cannot answer 'Yes' to every prompt, please discuss with, or return the form to, the student.

Checklist completed by: Alexander C. Abad

Date: June 14, 2019

PROMPT	See form:	Yes/ No
1 Start-date is after date of scrutiny	1.6	**Yes**
2 Appropriate professional guidelines are identified	1.7	**Yes**
3 Informed consent is being sought from ALL relevant parties and Consent Form(s) and Research Information Sheet(s) are included.	3.1.i, end of document – Research Information Sheet(s) and Consent Forms. Check that they match.	**Yes**
4 Power relations are clearly defined and discussed and appropriate steps to address any issues are set out	3.1 e and 3.1. h	**Yes**

5 Risk to research subjects is adequately discussed and addressed. 'No risk' is not an acceptable response, although 'minimal' is. *Note that if questionnaires or interviews are involved, part of the assessment of risk is linked to the questions to be asked. It is therefore helpful if these can be attached, or at least if there can be as full information about them as possible.*	3.2 a–c	**Yes**
6 Risk to the researcher is adequately discussed and addressed	3.2 d	**Yes**
7 The right to withdraw is explicit and fully thought through in this Request Form. The Inform Consent Forms the Research Information Sheet(s) contain further information. It might be necessary for the researcher to give quite detailed information about HOW participants can withdraw and how possible psychological harm could be avoided.	Often discussed under 3.1 i	**Yes**
8 Anonymity is adequately dealt with in the Request Form and is confirmed in the Research Information Sheet(s)	3.3	**Yes**
9 Confidentiality is adequately dealt with in the Request Form and is confirmed in the Research Information Sheet(s)	3.2 b	**Yes**
10 Security of information is adequately dealt with in the Consent Form and is confirmed in the Research Information Sheet(s)	3.3 a	**Yes**
11 Destruction of information is adequately dealt with in the Request Form and Research Information Sheet(s) For students: destruction of the data should not be be made dependent on **successful** completion of the research project. An expression such as 'when my studies are complete' covers all eventualities. For staff: it is acceptable for staff research to have a 'never destroyed' statement, but this must be transparent in the Research Information Sheet(s) and Consent Form(s).	3.3 d	**Yes**
12 The research is NOT into illegal activities	2.a & 3.1. d Likely to be buried in the narrative	**Yes**

13 The research does NOT employ deceptive or covert methods, such as to negate or impede the ability of the participants to give informed consent.	2.a & 3.1. d Likely to be buried in the narrative	**Yes**
14 The research HAS NO interaction with issues of national security	2.a & 3.1. d	**Yes**

Note that if any of the last three prompts indicates that the problem scenario is present, the request will not necessarily be refused, but it will need to be sent (by the Faculty Sub-committee) to the University Sub-committee. Please flag this up when sending the form to the Faculty Sub-committee, but it would be helpful if you also completed the rest of the checklist.

APPROVAL

Please select A or B, as appropriate. Delete the other.

A: For STUDENT RESEARCH – to be completed by the DEL:

I APPROVE the research and it may begin immediately. Any improvements listed below (or as communicated – please make clear) should be made and incorporated in your completed work.

Name: Emanuele Lindo Secco

Role (i.e. supervisor or a different DEL acting in lieu of supervisor): **DEL**

Date (must be earlier than proposed start date): June the 24th, 2019

B For STAFF RESEARCH – to be completed by the DEL:

I APPROVE the research and it may begin immediately. Any improvements listed below (or as communicated – please make clear) should be made and incorporated in your completed work.

Name:

Role – Departmental Ethics Lead

Date (must be earlier than proposed start date):

Application number: **S – 24-06-2019 SEL 087**

Ethical Approval Request for research not involving human participants Note: For research projects that do involve human participants, there are two other forms, one of which should be used as appropriate.	
SECTION 1 *[TO BE COMPLETED BY THE RESEARCHER]*	
1.1 Researcher **For staff: Name:** **(For joint research conducted by staff the names of all the researchers should be given with the Principal Researcher's name given in bold.)** **For students: Name, student ID, name of supervisor:**	Name: Alexander C. Abad ID: 18009297 Supervisor: Dr. Anuradha Ranasinghe
1.2 Title of Proposed Project:	Development of Braille-like Tactile feedback sensor using Nitinol wires and a low-cost GelSight sensor using Silicone Sponge
1.3 For students only: Programme Title and Level of Study (e.g. MA Education; Philosophy and Ethics Level H)	PhD in Informatics and Computer Science
1.4 For staff only: Position held at Hope (e.g. Lecturer)	
1.5 Faculty and Department or equivalent: (for research involving two, please identify both)	Department of Mathematics and CS
1.6 Start date of proposed research (Note: this must be later than the date at which approval may be given)	April, the 1st, 2019
End date of proposed research:	January, the 31st, 2021
1.7 Professional guidelines referenced	

PLEASE CONFIRM THE FOLLOWING [by placing an x in the relevant box]		
2.1	The research does NOT involve human participants:	X
2.2	The research involves no risk to me as the researcher OR	X
	The research could involve risk to me as the researcher, and a separate statement is appended defining this and saying how I propose to address it.	

SUMMARY OF RESEARCH PROJECT

3.1 Students: Please provide a brief but clear 200-word summary of project, and if appropriate (see 2.2) provide a brief statement about risk.

"Development of Braille-like Tactile feedback sensor using Nitinol wires and a low-cost GelSight sensor using Silicone Sponge"

This project is about the development of a Braille-like tactile feedback using Nitinol wires or Shape Memory Alloys (SMA). I will develop an electronically controlled matrix of small pins or bumps that can move up and down. I will use small Nitinol spring in each pin or bump that will expand when heated and contract when cooled down. The Nitinol springs can be purchased online but can also be created using nitinol wire. Using commercially available Nitinol wires and springs do not pose any health risk. They are being used in magic tricks for kids because they can be deformed and can return to original "programmed" shape upon heating. A nitinol spring can return to its programmed shaped using warm water (around 45-60 °C). Nitinol wires are also being used in the medical field, called NiTi wires/mesh, for teeth braces and stents. In this study, I will explore the activation of nitinol spring using the heat (around 45-60 °C) from super bright light emitting diode (LED), small thermoelectric generator (TEG), and electric current. I will also explore on how to make the Nitinol wire contracts faster using coolants such as silicone gel and thermal paste use in heatsink of computer microprocessor.

On the other hand, I will also develop a low-cost GelSight sensor. It was proven that it is worth to explore in many haptics and tactile sensing applications. Elastomer, reflective coating, lighting, and camera were the main challenges of making a GelSight sensor within a short period. In this study, I will explore on the possibility of using a clear silicone cosmetic sponge as the elastomeric slab. This will skip the degassing process and hours of curing time in making a clear elastomeric slab need in GelSight sensor. I will use Psycho paint used by visual effects artists, Light Emitting Diodes (LEDs), and Logitech C270 webcam. I will also try to use UV marker pen for a new type of GelSight Marker. UV ink markers are invisible using ordinary LED but can be made visible using UV LED lighting. I will use mask in painting the silicone sponge. GelSight sensor poses no health risk aside from the fume from the painting of silicone

sponge. Data gathering will be on based on digital image processing using computer. Data will be stored in password protected computer in a secure folder at the university.

All the experiments will be carried out at the Robotics Lab in Health Science Building, Liverpool Hope University.

All these projects will not involve any human participants.

3.2 Staff: Please provide a brief but clear 200-word summary of project, and if appropriate (see 2.2) provide a brief statement about risk. In addition to this, if appropriate, please provide information about any other researchers involved.

ETHICS APPLICATION PROCEDURE:
Submit this form (and any other relevant documents) electronically to your supervisor (students) or to your designated Departmental Ethics Lead (staff).

Note: students who cannot submit this form to a supervisor should declare this in an appended statement and forward the form to the appropriate DEL of their Department instead.

FOR USE ONLY BY SUPERVISOR OR DEPARTMENTAL ETHICS LEAD

PROJECTS NOT INVOLVING HUMAN PARTICIPANTS

The above project is APPROVED on the basis that (please say YES for each).

If NO, please liaise with the researcher or their supervisor, as necessary, for appropriate action and resubmission.

The research DOES NOT involve human participants. It EITHER raises no issues of risk OR issues of risk have been fully addressed by the researcher.	**X**
The research DOES NOT represent a risk to the University's reputation.	**X**

Approved By (name): Emanuele Lindo Secco

Role (i.e. Supervisor or DEL acting as Supervisor): DEL

Date: March the 29th 2019

NOTE:
1) This date must be earlier than proposed start date of the research project.

2) Please ensure that your approval is communicated to the researcher in a trackable form (e.g., email), in accordance with the manner agreed in your Faculty.

Application number: **S – 29-03-2019 SEL 083**